t No. FHWA-RD-77-57

NVESTIGATION OF THE EFFECTIVENESS OF STING BRIDGE DESIGN METHODOLOGY IN PROVIDING ADEQUATE STRUCTURAL RESISTANCE TO SEISMIC DISTURBANCES.

Phase V: Correlative Investigations on Theoretical and Experimental Dynamic Behavior of a Model Bridge Structure

July 1976

Final Report

This document is available to the public through the National Technical Information Service, Springfield, Virginia 22161

Prepared for

FEDERAL HIGHWAY ADMINISTRATION
Offices of Research & Development
Washington, D.C. 20590

FOREWORD

This report is the fourth in a series to result from research being conducted at the University of California, Berkeley, for the Federal Highway Administration (FHWA), Office of Research, under Contract DOT-FH-11-7798. The report will be of interest to structural researchers concerned with earthquake resistant design of highway bridges. It outlines correlations between analytical and experimental seismic response of a highway bridge modeled to incorporate features of typical high curved highway structures.

Copies of the report are being distributed by FHWA transmittal memorandum. Additional copies may be obtained from the National Technical Information Service, 5285 Port Royal Road, Springfield, Virginia 22161.

Charles F. Scheffey
Director, Office of Research
Federal Highway Administration

DISCLAIMER NOTICE

Technical Report Documentation Page

1. Report No.	2. Government Accession No.	3. Recipient's Catalog No.
FHWA-RD-77-57		

4. Title and Subtitle An Investigation of the Effectiveness of Existing Bridge Design Methodology in Providing Adequate Structural Resistance to Seismic Disturbances. Phase V : Correlative Investigations on Theoretical and Experimental Dynamic Behavior of a Model Bridge Structure.

5. Report Date July 1976

6. Performing Organization Code

7. Author(s)

Kazuhiko Kawashima and Joseph Penzien

8. Performing Organization Report No. EERC-76-29

9. Performing Organization Name and Address

University of California
Campus Research Office
118 California Hall
Berkeley, California 94720

10. Work Unit No. (TRAIS)

11. Contract or Grant No. DOT-FH-11-7798

12. Sponsoring Agency Name and Address

Office of Research and Development
Federal Highway Administration
U.S. Department of Transportation
Washington, D.C. 20590

13. Type of Report and Period Covered Phase V Final Report

14. Sponsoring Agency Code

15. Supplementary Notes

FHWA Contract Manager: James D. Cooper, HRS-11

16. Abstract

This report is one in a series to result from the investigation, "An Investigation of the Effectiveness of Existing Bridge Design Methodology in Providing Adequate Structural Resistance to Seismic Disturbances," sponsored by the U. S. Department of Transportation, Federal Highway Administration. Descriptions are given of the correlations between analytical and experimental seismic responses of a model bridge structure which was constructed to have the same features as the typical full-scale high curved highway bridge structure.

Modifications of the previously reported mathematical procedures for simulating the nonlinear behavior of expansion joints are presented. These include subdividing the time interval of integration and applying an equilibrium correction at the end of each interval and each subinterval.

Correlations of displacement response of the bridge model carried out for three different excitations are described. Parameter studies conducted to assist in the interpretation of correlation results are presented and the characteristics of the dynamic behavior of the bridge model are discussed.

Finally, based on the correlation results presented, general conclusions are deduced and summarized.

17. Key Words	18. Distribution Statement
Earthquake, Bridges, Seismic Analysis, Structural Analysis, Dynamic Behavior	No restrictions. This document is available through the National Technical Information Service, Springfield, Virginia 22161

19. Security Classif. (of this report)	20. Security Classif. (of this page)	21. No. of Pages	22. Price
Unclassified	Unclassified	228	

Form DOT F 1700.7 (8-72) Reproduction of completed page authorized

ACKNOWLEDGMENT

The authors wish to express their sincere thanks and appreciation to Dr. D. Williams, Mr. S. Howe and Professor W. G. Godden for providing the experimental test data of the bridge model structure studied in the investigation and to Dr. W. S. Tseng, Bechtel Power Corporation, San Francisco, for his assistance in modifying the computer programs and his encouragement throughout the study. Special thanks are also extended to the Public Works Research Institute, Ministry of Construction, Government of Japan, for allowing the senior author to work at Earthquake Engineering Research Center, University of California, Berkeley, during the period of the investigation reported herein.

TABLE OF CONTENTS

Page

ABSTRACT i

ACKNOWLEDGMENT ii

LIST OF TABLES v

LIST OF FIGURES vi

I. INTRODUCTION 1

A. STATEMENT OF PROBLEM 1

B. OBJECTIVES AND SCOPE 3

II. ANALYTICAL MODEL OF EXPANSION JOINTS 6

A. PIECEWISE LINEAR EXPANSION JOINT STIFFNESS 6

B. COLLISIONS 11

C. COULOMB FRICTION FORCE 13

III. DYNAMIC ANALYSIS PROCEDURE 21

A. INCREMENTAL EQUATION OF MOTION 21

B. STEP-BY-STEP INTEGRATION 23

C. ACCURACY OF SOLUTION 25

D. SUBDIVISION OF TIME INTERVAL 26

E. EQUILIBRIUM ITERATION 27

IV. EXPERIMENTAL MODEL STUDY AND TEST RESULTS 33

A. EXPERIMENTAL MODEL 33

B. TEST PROCEDURES AND TEST RESULTS 36

V. FORMULATION OF A BASIC ANALYTICAL MODEL 79

A. IDEALIZATION OF EXPERIMENTAL MODEL 79

B. BASIC ANALYTICAL MODEL 79

Page

VI. ANALYTICAL PREDICTION OF SEISMIC RESPONSES 89

A. LOW INTENSITY SEISMIC EXCITATION (TEST H1) 89

B. HIGH INTENSITY SEISMIC EXCITATION (TEST HV2) 94

C. HIGH INTENSITY SEISMIC EXCITATION (TEST H3). 99

VII. DISCUSSION OF CORRELATION RESULTS 136

A. JOINT RESTRAINER TIE BARS 136

B. COLLISIONS 137

C. COULOMB FRICTION FORCE 137

D. VERTICAL EXCITATION 138

E. IMPACT SPRING STIFFNESS 139

VIII. CONCLUSIONS 145

BIBLIOGRAPHY 147

APPENDIX

A. LONGITUDINAL COLLINEAR COLLISION OF TWO RODS A-1

B. FREE VIBRATION OF A SINGLE SPRING-MASS SYSTEM WITH COULOMB FRICTION B-1

C. COMPUTER LISTING OF NEABS C-1

LIST OF TABLES

Page

TABLE 4.1 PRINCIPAL FEATURES OF SEISMIC EXCITATION IN SERIES IV 49

TABLE 5.1 STIFFNESS PROPERTIES AND BOUNDARY CONDITIONS OF EXPERIMENTAL MODEL 84

TABLE 5.2 EFFECTS OF EXPANSION JOINT CONSTRAINTS ON CALCULATED LOW FREQUENCY CHARACTERISTICS OF BRIDGE MODEL 86

TABLE A.1 EFFECTS OF VARIOUS PARAMETERS ON PREDICTED RESPONSE OF COLLIDING RODS A-8

LIST OF FIGURES

Page

FIG. 2.1 IDEALIZED EXPANSION JOINT 18

FIG. 2.2 COORDINATE SYSTEM FOR EXPANSION JOINT 19

FIG. 2.3 RIGID-PLASTIC HYSTERETIC MODEL FOR COULOMB FRICTION . . 20

FIG. 2.4 ELASTOPLASTIC HYSTERETIC MODEL FOR COULOMB FRICTION . . 20

FIG. 4.1 EXPERIMENTAL MODEL BRIDGE STRUCTURE 50

FIG. 4.2 MEASUREMENTS OF RESPONSE DISPLACEMENT 51

FIG. 4.3 EXPANSION JOINT OF BRIDGE MODEL 52

FIG. 4.4.1 ESTIMATED FORCE VS. RELATIVE DISPLACEMENT RELATION OF EXPANSION JOINT; EFFECT OF RUBBER PAD AND SLIPPAGES 53

FIG. 4.4.2 ESTIMATED FORCE VS. RELATIVE DISPLACEMENT RELATION OF EXPANSION JOINT; EFFECT OF TIE BARS AND COLLISIONS 54

FIG. 4.5 TYPICAL FORCE VS. DEFORMATION RELATION OF TIE BAR . . . 55

FIG. 4.6 TYPICAL FORCE VS. DEFORMATION RELATION OF RUBBER PAD 56

FIG. 4.7 STATIC LOAD-DEFORMATION TEST FOR SIDE SUBASSEMBLAGE . . 57

FIG. 4.8 RESONANT CURVE OF BRIDGE MODEL IN TRANSVERSE EXCITATION 58

FIG. 4.9 ACCELERATION RESPONSE SPECTRUM OF TABLE MOTION (TESTS H1, H3 AND HV2). 59

FIG. 4.10 RELATION BETWEEN MAXIMUM HORIZONTAL TABLE ACCELERATION AND MAXIMUM HORIZONTAL RESPONSE AT CENTER OF BRIDGE MODEL 60

FIG. 4.11 HORIZONTAL TABLE ACCELERATION TIME HISTORY; TEST H1 61

FIG. 4.12.1 MEASURED RESPONSE OF SIDE GIRDER NO. 1; LONGITUDINAL (X) DIRECTION; TEST H1 62

FIG. 4.12.2 MEASURED RESPONSE OF SIDE GIRDER NO. 1; TRANSVERSE (Y) DIRECTION; TEST H1 62

FIG. 4.12.3 MEASURED RESPONSE OF CENTER GIRDER; TRANSVERSE (Y) DIRECTION; TEST H1 63

Page

FIG. 4.12.4 MEASURED RESPONSE OF SIDE GIRDER NO. 2; LONGITUDINAL (X) DIRECTION; TEST H1 63

FIG. 4.12.5 MEASURED RESPONSE OF SIDE GIRDER NO. 2; TRANSVERSE (Y) DIRECTION; TEST H1 64

FIG. 4.12.6 MEASURED RESPONSE OF EXPANSION JOINT NO. 1; INNER SIDE; TEST H1 64

FIG. 4.12.7 MEASURED RESPONSE OF EXPANSION JOINT NO. 1; OUTER SIDE; TEST H1 65

FIG. 4.12.8 MEASURED RESPONSE OF EXPANSION JOINT NO. 2; INNER SIDE; TEST H1 65

FIG. 4.12.9 MEASURED RESPONSE OF EXPANSION JOINT NO. 2; OUTER SIDE; TEST H1 66

FIG. 4.13 HORIZONTAL TABLE ACCELERATION TIME HISTORY; TEST H2 67

FIG. 4.14.1 MEASURED RESPONSE OF SIDE GIRDER NO. 1; LONGITUDINAL (X) DIRECTION; TEST H2 68

FIG. 4.14.2 MEASURED RESPONSE OF SIDE GIRDER NO. 1; TRANSVERSE (Y) DIRECTION; TEST H2 68

FIG. 4.14.3 MEASURED RESPONSE OF CENTER GIRDER; TRANSVERSE (Y) DIRECTION; TEST H2 69

FIG. 4.14.4 MEASURED RESPONSE OF SIDE GIRDER NO. 2; LONGITUDINAL (X) DIRECTION; TEST H2 69

FIG. 4.14.5 MEASURED RESPONSE OF SIDE GIRDER NO. 2; TRANSVERSE (Y) DIRECTION; TEST H2 70

FIG. 4.14.6 MEASURED RESPONSE OF EXPANSION JOINT NO. 1; INNER SIDE; TEST H2 70

FIG. 4.14.7 MEASURED RESPONSE OF EXPANSION JOINT NO. 1; OUTER SIDE; TEST H2 71

FIG. 4.14.8 MEASURED RESPONSE OF EXPANSION JOINT NO. 2; INNER SIDE; TEST H2 71

FIG. 4.14.9 MEASURED RESPONSE OF EXPANSION JOINT NO. 2; OUTER SIDE; TEST H2 72

FIG. 4.15.1 HORIZONTAL TABLE ACCELERATION TIME HISTORY; TEST HV2 73

FIG. 4.15.2 VERTICAL TABLE ACCELERATION TIME HISTORY; TEST HV2 73

Page

FIG. 4.16.1 MEASURED RESPONSE OF SIDE GIRDER NO. 1; LONGITUDINAL (X) DIRECTION; TEST HV2 74

FIG. 4.16.2 MEASURED RESPONSE OF SIDE GIRDER NO. 1; TRANSVERSE (Y) DIRECTION; TEST HV2 74

FIG. 4.16.3 MEASURED RESPONSE OF CENTER GIRDER; TRANSVERSE (Y) DIRECTION; TEST HV2 75

FIG. 4.16.4 MEASURED RESPONSE OF SIDE GIRDER NO. 2; LONGITUDINAL (X) DIRECTION; TEST HV2 75

FIG. 4.16.5 MEASURED RESPONSE OF SIDE GIRDER NO. 2; TRANSVERSE (Y) DIRECTION; TEST HV2 76

FIG. 4.16.6 MEASURED RESPONSE OF EXPANSION JOINT NO. 1; INNER SIDE; TEST HV2 76

FIG. 4.16.7 MEASURED RESPONSE OF EXPANSION JOINT NO. 1; OUTER SIDE; TEST HV2 77

FIG. 4.16.8 MEASURED RESPONSE OF EXPANSION JOINT NO. 2; INNER SIDE; TEST HV2 77

FIG. 4.16.9 MEASURED RESPONSE OF EXPANSION JOINT NO. 2; OUTER SIDE; TEST HV2 78

FIG. 5.1 ANALYTICAL MODEL OF BRIDGE MODEL 87

FIG. 5.2.1 CALCULATED LOWEST VIBRATION MODE; LONGITUDINAL (X) DIRECTION 87

FIG. 5.2.2 CALCULATED LOWEST VIBRATION MODE; TRANSVERSE (Y) DIRECTION 88

FIG. 5.2.3 CALCULATED LOWEST VIBRATION MODE; VERTICAL (Z) DIRECTION 88

FIG. 6.1.1 LINEAR CORRELATION FOR TEST H1; SIDE GIRDER NO. 1; LONGITUDINAL (X) DIRECTION 101

FIG. 6.1.2 LINEAR CORRELATION FOR TEST H1; SIDE GIRDER NO. 1; TRANSVERSE (Y) DIRECTION 101

FIG. 6.1.3 LINEAR CORRELATION FOR TEST H1; CENTER GIRDER; TRANSVERSE (Y) DIRECTION 102

FIG. 6.1.4 LINEAR CORRELATION FOR TEST H1; SIDE GIRDER NO. 2; LONGITUDINAL (X) DIRECTION 102

FIG. 6.1.5 LINEAR CORRELATION FOR TEST H1; SIDE GIRDER NO. 2; TRANSVERSE (Y) DIRECTION 103

Page

FIG. 6.1.6 LINEAR CORRELATION FOR TEST H1; EXPANSION JOINT NO. 1; INNER SIDE 103

FIG. 6.1.7 LINEAR CORRELATION FOR TEST H1; EXPANSION JOINT NO. 1; OUTER SIDE 104

FIG. 6.1.8 LINEAR CORRELATION FOR TEST H1; EXPANSION JOINT NO. 2; INNER SIDE 104

FIG. 6.1.9 LINEAR CORRELATION FOR TEST H1; EXPANSION JOINT NO. 2; OUTER SIDE 105

FIG. 6.2.1 NONLINEAR CORRELATION FOR TEST H1; SIDE GIRDER NO. 1; LONGITUDINAL (X) DIRECTION 106

FIG. 6.2.2 NONLINEAR CORRELATION FOR TEST H1; SIDE GIRDER NO. 1; TRANSVERSE (Y) DIRECTION 106

FIG. 6.2.3 NONLINEAR CORRELATION FOR TEST H1; CENTER GIRDER; TRANSVERSE (Y) DIRECTION 107

FIG. 6.2.4 NONLINEAR CORRELATION FOR TEST H1; SIDE GIRDER NO. 2; LONGITUDINAL (X) DIRECTION 107

FIG. 6.2.5 NONLINEAR CORRELATION FOR TEST H1; SIDE GIRDER NO. 2; TRANSVERSE (Y) DIRECTION 108

FIG. 6.2.6 NONLINEAR CORRELATION FOR TEST H1; EXPANSION JOINT NO. 1; INNER SIDE 108

FIG. 6.2.7 NONLINEAR CORRELATION FOR TEST H1; EXPANSION JOINT NO. 1; OUTER SIDE 109

FIG. 6.2.8 NONLINEAR CORRELATION FOR TEST H2; EXPANSION JOINT NO. 2; INNER SIDE 109

FIG. 6.2.9 NONLINEAR CORRELATION FOR TEST H1; EXPANSION JOINT NO. 2; OUTER SIDE 110

FIG. 6.3.1 PREDICTED TIE BAR FORCE FOR TEST H2; EXPANSION JOINT NO. 1 111

FIG. 6.3.2 PREDICTED TIE BAR FORCE FOR TEST H1; EXPANSION JOINT NO. 2 111

FIG. 6.4.1 LINEAR CORRELATION FOR TEST HV2; SIDE GIRDER NO. 1; LONGITUDINAL (X) DIRECTION 112

FIG. 6.4.2 LINEAR CORRELATION FOR TEST HV2; SIDE GIRDER NO. 1; TRANSVERSE (Y) DIRECTION 112

FIG. 6.4.3 LINEAR CORRELATION FOR TEST HV2; CENTER GIRDER; TRANSVERSE (Y) DIRECTION 113

Page

FIG. 6.4.4 LINEAR CORRELATION FOR TEST HV2; SIDE GIRDER NO. 2; LONGITUDINAL (X) DIRECTION 113

FIG. 6.4.5 LINEAR CORRELATION FOR TEST HV2; SIDE GIRDER NO. 2; TRANSVERSE (Y) DIRECTION 114

FIG. 6.4.6 LINEAR CORRELATION FOR TEST HV2; EXPANSION JOINT NO. 1; INNER SIDE 114

FIG. 6.4.7 LINEAR CORRELATION FOR TEST HV2; EXPANSION JOINT NO. 1; OUTER SIDE 115

FIG. 6.4.8 LINEAR CORRELATION FOR TEST HV2; EXPANSION JOINT NO. 2; INNER SIDE 115

FIG. 6.4.9 LINEAR CORRELATION FOR TEST HV2; EXPANSION JOINT NO. 2; OUTER SIDE 116

FIG. 6.5.1 NONLINEAR CORRELATION FOR TEST HV2; SIDE GIRDER NO. 1; LONGITUDINAL (X) DIRECTION 117

FIG. 6.5.2 NONLINEAR CORRELATION FOR TEST HV2; SIDE GIRDER NO. 1; TRANSVERSE (Y) DIRECTION 117

FIG. 6.5.3 NONLINEAR CORRELATION FOR TEST HV2; CENTER GIRDER; TRANSVERSE (Y) DIRECTION 118

FIG. 6.5.4 NONLINEAR CORRELATION FOR TEST HV2; SIDE GIRDER NO. 2; LONGITUDINAL (X) DIRECTION 118

FIG. 6.5.5 NONLINEAR CORRELATION FOR TEST HV2; SIDE GIRDER NO. 2; TRANSVERSE (Y) DIRECTION 119

FIG. 6.5.6 NONLINEAR CORRELATION FOR TEST HV2; EXPANSION JOINT NO. 1; INNER SIDE 119

FIG. 6.5.7 NONLINEAR CORRELATION FOR TEST HV2; EXPANSION JOINT NO. 1; OUTER SIDE 120

FIG. 6.5.8 NONLINEAR CORRELATION FOR TEST HV2; EXPANSION JOINT NO. 2; INNER SIDE 120

FIG. 6.5.9 NONLINEAR CORRELATION FOR TEST HV2; EXPANSION JOINT NO. 2; OUTER SIDE 121

FIG. 6.6.1 PREDICTED TIE BAR FORCE AND YIELD LENGTH FOR TEST HV2; EXPANSION JOINT NO. 1 122

FIG. 6.6.2 PREDICTED TIE BAR FORCE AND YIELD LENGTH FOR TEST HV2; EXPANSION JOINT NO. 2 122

FIG. 6.7.1 PREDICTED CONTACT FORCE FOR TEST HV2; EXPANSION JOINT NO. 1 123

Page

FIG. 6.7.2 PREDICTED CONTACT FORCE FOR TEST HV2; EXPANSION JOINT NO. 2 123

FIG. 6.8.1 LINEAR CORRELATION FOR TEST H3; SIDE GIRDER NO. 1; LONGITUDINAL (X) DIRECTION 124

FIG. 6.8.2 LINEAR CORRELATION FOR TEST H3; SIDE GIRDER NO. 1; TRANSVERSE (Y) DIRECTION 124

FIG. 6.8.3 LINEAR CORRELATION FOR TEST H3; CENTER GIRDER; TRANSVERSE (Y) DIRECTION 125

FIG. 6.8.4 LINEAR CORRELATION FOR TEST H3; SIDE GIRDER NO. 2; LONGITUDINAL (X) DIRECTION 125

FIG. 6.8.5 LINEAR CORRELATION FOR TEST H3; SIDE GIRDER NO. 2; TRANSVERSE (Y) DIRECTION 126

FIG. 6.8.6 LINEAR CORRELATION FOR TEST H3; EXPANSION JOINT NO. 1; INNER SIDE 126

FIG. 6.8.7 LINEAR CORRELATION FOR TEST H3; EXPANSION JOINT NO. 1; OUTER SIDE 127

FIG. 6.8.8 LINEAR CORRELATION FOR TEST H3; EXPANSION JOINT NO. 2; INNER SIDE 127

FIG. 6.8.9 LINEAR CORRELATION FOR TEST H3; EXPANSION JOINT NO. 2; OUTER SIDE 128

FIG. 6.9.1 NONLINEAR CORRELATION FOR TEST H3; SIDE GIRDER NO. 1; LONGITUDINAL (X) DIRECTION 129

FIG. 6.9.2 NONLINEAR CORRELATION FOR TEST H3; SIDE GIRDER NO. 1; TRANSVERSE (Y) DIRECTION 129

FIG. 6.9.3 NONLINEAR CORRELATION FOR TEST H3; CENTER GIRDER; TRANSVERSE (Y) DIRECTION 130

FIG. 6.9.4 NONLINEAR CORRELATION FOR TEST H3; SIDE GIRDER NO. 2; LONGITUDINAL (X) DIRECTION 130

FIG. 6.9.5 NONLINEAR CORRELATION FOR TEST H3; SIDE GIRDER NO. 2; TRANSVERSE (Y) DIRECTION 131

FIG. 6.9.6 NONLINEAR CORRELATION FOR TEST H3; EXPANSION JOINT NO. 1; INNER SIDE 131

FIG. 6.9.7 NONLINEAR CORRELATION FOR TEST H3; EXPANSION JOINT NO. 1; OUTER SIDE 132

FIG. 6.9.8 NONLINEAR CORRELATION FOR TEST H3; EXPANSION JOINT NO. 2; INNER SIDE 132

Page

FIG. 6.9.9 NONLINEAR CORRELATION FOR TEST H3; EXPANSION JOINT NO. 2; OUTER SIDE 133

FIG. 6.10.1 PREDICTED TIE BAR FORCE AND YIELD LENGTH FOR TEST H3; EXPANSION JOINT NO. 1 134

FIG. 6.10.2 PREDICTED TIE BAR FORCE AND YIELD LENGTH FOR TEST H3; EXPANSION JOINT NO. 2 134

FIG. 6.11.1 PREDICTED CONTACT FORCE FOR TEST H3; EXPANSION JOINT NO. 1 135

FIG. 6.11.2 PREDICTED CONTACT FORCE FOR TEST H3; EXPANSION JOINT NO. 2 135

FIG. 7.1.1 EFFECT OF LONGITUDINAL RESTRAINER TIE BARS ON RESPONSE OF CENTER GIRDER; TEST HV2 140

FIG. 7.1.2 EFFECT OF LONGITUDINAL RESTRAINER TIE BARS ON RELATIVE RESPONSE OF EXPANSION JOINT NO. 2 (OUTER SIDE); TEST HV2 140

FIG. 7.2.1 EFFECT OF COLLISIONS ON RESPONSE OF CENTER GIRDER; TEST HV2 141

FIG. 7.2.2 EFFECT OF COLLISIONS ON RELATIVE RESPONSE OF EXPANSION JOINT NO. 2 (OUTER SIDE); TEST HV2 141

FIG. 7.3.1 EFFECT OF COULOMB FRICTION ON RESPONSE OF CENTER GIRDER; TEST HV2 142

FIG. 7.3.2 EFFECT OF COULOMB FRICTION ON RELATIVE RESPONSE OF EXPANSION JOINT NO. 2 (OUTER SIDE); TEST HV2 . . . 142

FIG. 7.4.1 EFFECT OF VERTICAL EXCITATION ON RESPONSE OF CENTER GIRDER; TEST HV2 143

FIG. 7.4.2 EFFECT OF VERTICAL EXCITATION ON RELATIVE RESPONSE OF EXPANSION JOINT NO. 2 (OUTER SIDE); TEST HV2 . . . 143

FIG. 7.5.1 EFFECT OF IMPACT SPRING STIFFNESS ON RESPONSE OF CENTER GIRDER; TEST HV2 144

FIG. 7.5.2 EFFECT OF IMPACT SPRING STIFFNESS ON RELATIVE RESPONSE OF EXPANSION JOINT NO. 2 (OUTER SIDE); TEST HV2 144

FIG. A.1 LONGITUDINAL COLINEAR COLLISION OF TWO RODS A-9

FIG. A.2 ANALYTICAL MODEL FOR COLLISION OF RODS A-10

FIG. A.3 EXACT SOLUTION OF RELATIVE DISPLACEMENT AND RELATIVE VELOCITY A-11

Page

FIG. A.4.1 EFFECT OF IMPACT SPRING STIFFNESS ON RELATIVE RESPONSE OF RODS (k_I = 10, 10^2 and 10^3) A-12

FIG. A.4.2 EFFECT OF IMPACT SPRING STIFFNESS ON RELATIVE RESPONSE OF RODS (k_I = 10^4 and 10^5) A-13

FIG. A.5 EFFECT OF TIME INTERVAL ON RELATIVE RESPONSE OF RODS A-14

FIG. A.6 EFFECT OF ELEMENT NUMBER ON RELATIVE RESPONSE OF RODS A-15

FIG. A.7 PREDICTED PARTICLE VELOCITY AND STRESS OF RODS A-16

FIG. B.1 FREE VIBRATION OF A BLOCK WITH COULOMB FRICTION B-6

FIG. B.2 FREE VIBRATION RESPONSE OF A BLOCK WITH COULOMB FRICTION B-7

FIG. B.3 EFFECT OF MAGNITUDE OF u^e ON FREE VIBRATION RESPONSE OF A BLOCK B-8

FIG. B.4 EFFECT OF TIME INTERVAL ON FREE VIBRATION RESPONSE OF A BLOCK B-9

METRIC CONVERSION FACTORS

Approximate Conversions to Metric Measures

Symbol	When You Know	Multiply by	To Find	Symbol
		LENGTH		
in	inches	*2.5	centimeters	cm
ft	feet	30	centimeters	cm
yd	yards	0.9	meters	m
mi	miles	1.6	kilometers	km
		AREA		
in^2	square inches	6.5	square centimeters	cm^2
ft^2	square feet	0.09	square meters	m^2
yd^2	square yards	0.8	square meters	m^2
mi^2	square miles	2.6	square kilometers	km^2
	acres	0.4	hectares	ha
		MASS (weight)		
oz	ounces	28	grams	g
lb	pounds	0.45	kilograms	kg
	short tons (2000 lb)	0.9	tonnes	t
		VOLUME		
tsp	teaspoons	5	milliliters	ml
Tbsp	tablespoons	15	milliliters	ml
fl oz	fluid ounces	30	milliliters	ml
c	cups	0.24	liters	l
pt	pints	0.47	liters	l
qt	quarts	0.95	liters	l
gal	gallons	3.8	liters	l
ft^3	cubic feet	0.03	cubic meters	m^3
yd^3	cubic yards	0.76	cubic meters	m^3
		TEMPERATURE (exact)		
°F	Fahrenheit temperature	5/9 (after subtracting 32)	Celsius temperature	°C

*1 in = 2.54 (exactly). For other exact conversions and more detailed tables, see NBS Misc. Publ. 286, Units of Weights and Measures, Price $2.25, SD Catalog No. C13.10:286.

Approximate Conversions from Metric Measures

Symbol	When You Know	Multiply by	To Find	Symbol
		LENGTH		
mm	millimeters	0.04	inches	in
cm	centimeters	0.4	inches	in
m	meters	3.3	feet	ft
m	meters	1.1	yards	yd
km	kilometers	0.6	miles	mi
		AREA		
cm^2	square centimeters	0.16	square inches	in^2
m^2	square meters	1.2	square yards	yd^2
km^2	square kilometers	0.4	square miles	mi^2
ha	hectares (10,000 m^2)	2.5	acres	
		MASS (weight)		
g	grams	0.035	ounces	oz
kg	kilograms	2.2	pounds	lb
t	tonnes (1000 kg)	1.1	short tons	
		VOLUME		
ml	milliliters	0.03	fluid ounces	fl oz
l	liters	2.1	pints	pt
l	liters	1.06	quarts	qt
l	liters	0.26	gallons	gal
m^3	cubic meters	35	cubic feet	ft^3
m^3	cubic meters	1.3	cubic yards	yd^3
		TEMPERATURE (exact)		
°C	Celsius temperature	9/5 (then add 32)	Fahrenheit temperature	°F

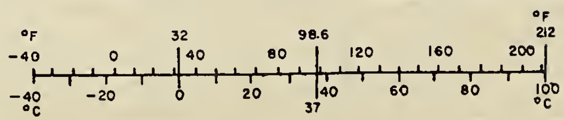

I. INTRODUCTION

A. STATEMENT OF THE PROBLEM

In the past, numerous highway bridges have suffered extensive damages due to strong motion earthquake [1]*. The older bridges, consisting of single or multiple simple truss or girder spans supported on massive piers and abutments, were particularly vulnerable to the action of strong ground motions. Seismic damages were most commonly caused by foundation failures resulting from excessive ground deformation and/or loss of stability and bearing capacity of the foundation soils. As a direct result, the substructures often tilted, settled, slid, or even overturned; thus severe cracking or complete failure was often experienced. These large support displacements also caused relative shifting of and damage to the superstructures, induced failures within the bearing supports, and even caused spans to fall off their supports. It is significant to note that very little damage occurred to these older structures as a direct result of structural vibration effects.

Certain types of modern highway bridges may, on the other hand, be quite susceptible to damage from strong ground vibration effects. This fact became very evident during the San Fernando earthquake of February 9, 1971, when numerous reinforced concrete highway bridges which were designed by the traditional elastic approach; i.e., by the equivalent static seismic coefficient method similar to that previously adopted for buildings, suffered severe damages. Because of this experience, it was immediately apparent that the seismic requirements used were inadequate and that the design methodology should be critically examined. Action was quickly taken following the earthquake to correct certain design

---

* Numbers in brackets refer to bibliography numbers.

deficiencies; however, the basic static approach to design still remains in effect.

Recognizing the urgent need for both theoretical and experimental research related directly to seismic effects on bridge structures, an investigation entitled "An Investigation Of The Effectiveness of Existing Bridge Design Methodology in Providing Adequate Structural Resistance to Seismic Disturbances" was initiated in 1971 within the Earthquake Engineering Research Center, University of California, Berkeley, under the sponsorship of the U.S. Department of Transportation, Federal Highway Administration. This investigation consists of the following six phases:

(1) A thorough review of the world's literature on seismic effects on highway bridge structure including damages to bridges during the San Fernando earthquake of February 9, 1971.

(2) An analytical investigation of the dynamic response of long, multiple-span, highway overcrossings of the type which suffered heavy damages during the 1971 San Fernando earthquake.

(3) An analytical investigation of the dynamic response of short, single and multiple span highway overcrossings of the type which suffered heavy damages during the 1971 San Fernando earthquake.

(4) Detailed model experiments on a shaking table to provide dynamic response data similar to prototype behavior which can be used to verify the validity of theoretical response predictions.

(5) Correlation of dynamic response data obtained from shaking table experiments with theoretical response and modification of analytical procedures as found necessary.

(6) Preparation of recommendations for changes in seismic design specifications and methodology as necessary to provide adequate protection of reinforced concrete highway bridges against future earthquakes.

Final reports coverning Phases 1, 2, and 3 have been published [1,2,6] and the final report coverning Phase 4 is now nearing completion. The present final report covers Phase 5 and the final report on Phase 6 will be completed during summer and fall of 1977.

B. OBJECTIVES AND SCOPE

The primary objectives of the investigation in Phase 5 are to correlate the dynamic responses of the experimental model measured during shaking table tests conducted in Phase 4 with the corresponding responses determined using the analytical model and numerical procedures developed in Phase 2.

To achieve these objectives, the analytical model and numerical procedures defined and developed in Phase 2 have been re-examined for use in predicting the seismic response of the experimental model structure. Modifications of the analytical model simulating nonlinear dynamic behavior of expansion joints and the analytical procedure for numerical integration of equations of motion have been found necessary. These changes have been incorporated into the nonlinear response analysis computer program NEABS.

Experimental test results obtained in Phase 4 were reviewed to select suitable excitation tests for correlation purposes. Since it was found that the model structure is more susceptible to damage when the excitation is oriented in the transverse direction, test results obtained under transverse and under simultaneous transverse and vertical excitations were used for correlation purposes.

Correlation of the measured experimental displacement response with the corresponding response predicted by linear and nonlinear analyses has been performed for three types of seismic excitation (Series IV excitation tests), namely, (1) low intensity excitation in the transverse direction, (2) high intensity excitation in the transverse direction, and (3) high intensity excitation in both the transverse and vertical directions. The linear response analysis computer program BSAP and the nonlinear response analysis computer program NEABS as revised have been used for these correlations.

Finally, a parameter study of the dynamic response was conducted using the nonlinear analytical model and analysis procedures.

Chapter II of this report discribes the modifications introduced into the nonlinear analytical model of expansion joints which allow proper simulations of the impact phenomenon, slippage with Coulomb type friction, and separation under the action of elastoplastic joint restrainer tie bars acting in tention only. Chapter III describes certain modification to the analytical procedures including an equilibrium correction introduced through iteration and subdivision of time intervals into a specified number of equal sub-intervals. Chapter IV describes the experimental model and test results which were used to formulate the analytical model used in the correlation study. Chapter V describes the procedure used to formulate a basic analytical model which reproduces the observed dynamic characteristics of the experimental model under the initial low intensity excitations. Chapter VI presents the correlation results for the three seismic excitations having various intensities of table motion. Chapter VII gives a discussion of the correlation results and Chapter VIII summarizes the conclusions drawn from the investigation.

Finally, numerical results obtained from the parameter studies of impact and Coulomb friction are presented in order to show the applicability of the analytical model and numerical procedures defined in Chapters II and III.

II. ANALYTICAL MODEL OF EXPANSION JOINTS

A nonlinear analytical model for simulating the dynamic behavior of expansion joints was formulated by Tseng and Penzien [2,4]. It includes relative translational and rotational degrees of freedom, elastoplastic joint restrainer tie bars acting in tension, impact, and Coulomb type friction with slippage. Although the original analytical model of expansion joints was basically correct, certain modifications were needed to make it fully reproduce the characteristics of the model bridge structure. The modifications introduced into the original analytical model and into the nonlinear analysis computer program NEABS [2] were the following:

(1) The impact spring was modified in such a way that it approximates elastic collisions.

(2) The Coulomb type friction force was approximated by an elastoplastic hysteretic model.

The subsequent discussion in this chapter concentrates on the above modifications to the analytical model of the expansion joints with some mention of the basic equations needed to characterize their nonlinear behavior.

A. PIECEWISE LINEAR EXPANSION JOINT STIFFNESS [2,4]

The force vs. displacement relation of the idealized expansion joint as shown in Fig. 2.1 can be characterized using an expansion joint coordinate system as defined in Fig. 2.2, i.e.,

$$\Delta \underline{\bar{S}} = \underline{\bar{k}}_t^{EJ} \; \Delta \underline{\bar{r}} \qquad (1)$$

where

$$\Delta\bar{\underline{S}} = \begin{Bmatrix} \Delta\bar{\underline{S}}_I \\ \Delta\bar{\underline{S}}_J \end{Bmatrix}, \quad \Delta\bar{\underline{S}}_K = \begin{Bmatrix} \Delta S_{Ax} \\ \Delta S_y \\ \Delta S_{AZ} \\ \Delta S_{Bx} \\ \Delta M_s \\ \Delta S_{Bz} \end{Bmatrix}_K \quad (K = I,J) \tag{2}$$

$$\Delta\bar{\underline{r}} = \begin{Bmatrix} \Delta\bar{\underline{r}}_I \\ \Delta\bar{\underline{r}}_J \end{Bmatrix}, \quad \Delta\bar{\underline{r}}_K = \begin{Bmatrix} \Delta r_{Ax} \\ \Delta r_y \\ \Delta r_{Az} \\ \Delta r_{Bx} \\ \Delta\theta_s \\ \Delta r_{Bz} \end{Bmatrix}_K \quad (K = I,J) \tag{3}$$

Matrix $\bar{\underline{k}}_t^{EJ}$ is a tangent stiffness matrix at time t which relates the expansion joint force increment $\Delta\bar{\underline{S}}$ with the expansion joint displacement increment $\Delta\bar{\underline{r}}$.

The expansion joint coordinate system can be related to the local nodal coordinate system defined by

$$\underline{r} = \begin{Bmatrix} \underline{r}_I \\ \underline{r}_J \end{Bmatrix}, \quad \underline{r}_K = \begin{Bmatrix} r_x \\ r_y \\ r_z \\ \theta_x \\ \theta_y \\ \theta_z \end{Bmatrix}_K \quad (K = I,J) \tag{4}$$

$$\underline{S} = \begin{Bmatrix} \underline{S}_I \\ \underline{S}_J \end{Bmatrix}, \quad \underline{S}_K = \begin{Bmatrix} S_x \\ S_y \\ S_z \\ M_x \\ M_y \\ M_z \end{Bmatrix}_K \quad (K = I,J) \tag{5}$$

through the transformations

$$\bar{\underline{r}} = \begin{Bmatrix} \bar{\underline{r}}_I \\ \bar{\underline{r}}_J \end{Bmatrix} = \begin{bmatrix} \underline{a} & \underline{0} \\ \underline{0} & \underline{a} \end{bmatrix} \begin{Bmatrix} \underline{r}_I \\ \underline{r}_J \end{Bmatrix} \equiv \underline{A}\,\underline{r} \tag{6}$$

and

$$\underline{S} = \begin{Bmatrix} \underline{S}_I \\ \underline{S}_J \end{Bmatrix} = \begin{bmatrix} \underline{a}^T & \underline{0} \\ \underline{0} & \underline{a}^T \end{bmatrix} \begin{Bmatrix} \bar{\underline{S}}_I \\ \bar{\underline{S}}_J \end{Bmatrix} \equiv \underline{A}^T \bar{\underline{S}} \tag{7}$$

where matrix $\underline{a}$ is given by

$$\underline{a} = \begin{bmatrix} 1 & 0 & 0 & 0 & 0 & d/2 \\ 0 & 1 & 0 & 0 & 0 & 0 \\ 0 & 0 & 1 & -d/2 & d/2 \cdot \tan\psi & 0 \\ 1 & 0 & 0 & 0 & 0 & -d/2 \\ 0 & 0 & 0 & 0 & 1/\cos\psi & 0 \\ 0 & 0 & 1 & d/2 & -d/2 \cdot \tan\psi & 0 \end{bmatrix} \tag{8}$$

in which ψ represents the skew angle of the deck.

It is convenient to define the stiffness coefficients of $\bar{\underline{k}}_t^{EJ}$ in terms of the relative expansion joint displacements $\bar{\underline{u}}$ defined by

$$\underline{\bar{u}} = \begin{Bmatrix} u_{Ax} \\ u_y \\ u_{Az} \\ u_{Bx} \\ u_s \\ u_{Bz} \end{Bmatrix} \equiv \begin{Bmatrix} r_{Ax} \\ r_y \\ r_{Az} \\ r_{Bx} \\ \theta_s \\ r_{Bz} \end{Bmatrix}_J - \begin{Bmatrix} r_{Ax} \\ r_y \\ r_{Az} \\ r_{Bx} \\ \theta_s \\ r_{Bz} \end{Bmatrix}_I = \underline{\bar{r}}_J - \underline{\bar{r}}_I \tag{9}$$

and the corresponding expansion joint force $\underline{\bar{F}}$ defined by

$$\underline{\bar{F}} = \begin{Bmatrix} F_{Ax} \\ F_y \\ F_{Az} \\ F_{Bx} \\ M_s \\ F_{Bz} \end{Bmatrix} = \begin{Bmatrix} S_{Ax} \\ S_y \\ S_{Az} \\ S_{Bx} \\ M_s \\ S_{Bz} \end{Bmatrix}_J = \underline{\bar{S}}_J = - \underline{\bar{S}}_I \tag{10}$$

Thus, the idealized expansion joint can be characterized by a stiffness matrix $\underline{\bar{k}}$ relating $\Delta\underline{\bar{F}}$ to $\Delta\underline{\bar{u}}$, i.e.,

$$\Delta\underline{\bar{F}} = \underline{\bar{k}}\ \Delta\underline{\bar{u}} \tag{11}$$

Using Eqs. (9) and (10), the stiffness matrix $\underline{\bar{k}}_t^{EJ}$ can be expressed as

$$\underline{\bar{k}}_t^{EJ} = \begin{bmatrix} \underline{\bar{k}} & -\underline{\bar{k}} \\ -\underline{\bar{k}} & \underline{\bar{k}} \end{bmatrix} \tag{12}$$

The stiffness matrix $\underline{\bar{k}}_t^{EJ}$ must be transformed to the local nodal coordinate system using Eqs. (6) and (7). This transformation results in the relation

$$\Delta \underline{S} = \underline{k}_t^{EJ} \, \Delta \underline{r} \quad , \quad \underline{k}_t^{EJ} = \underline{A}^T \, \bar{\underline{k}}_t^{EJ} \, \underline{A} \tag{13}$$

Matrix $\underline{k}_t^{EJ}$ is the stiffness matrix which relates the vector of local nodal force increments $\Delta \underline{S}$ to the vector of local nodal displacement increments $\Delta \underline{r}$ at time t, and which, after local to global coordinate transformation, can be used to assemble the total stiffness matrix $\underline{K}_t$ for the complete structural system.

Stiffness matrix $\bar{\underline{k}}$ defined in Eq. (11) represents contributions from two sources. One contribution is a stiffness matrix $\bar{\underline{k}}_1$ of the idealized joint without collisions and another contribution is matrix $\bar{\underline{k}}_2$ that represents the effect of collisions, i.e.,

$$\bar{\underline{k}} = \bar{\underline{k}}_1 + \bar{\underline{k}}_2 \tag{14}$$

The stiffness coefficients of $\bar{\underline{k}}_1$ can be written in the form

$$\bar{\underline{k}}_1 = \begin{bmatrix} k_{AA} & 0 & 0 & k_{AB} & 0 & 0 \\ 0 & k_S & 0 & 0 & 0 & 0 \\ 0 & 0 & k_V & 0 & 0 & 0 \\ k_{AB} & 0 & 0 & k_{BB} & 0 & 0 \\ 0 & 0 & 0 & 0 & 0 & 0 \\ 0 & 0 & 0 & 0 & 0 & k_V \end{bmatrix} \tag{15}$$

where k_S is the elastic stiffness of the spring which resists the relative transverse displacement, k_V is the elastic stiffness of the springs which resists the relative vertical displacement at points A and B, and

$$k_{AA} = \sum_{i=1}^{N_T} k_{Ti} \left(\frac{1}{2} - \frac{y_i}{d}\right)^2$$

$$k_{BB} = \sum_{i=1}^{N_T} k_{Ti} \left(\frac{1}{2} + \frac{y_i}{d}\right)^2 \qquad (16)$$

$$k_{AB} = \sum_{i=1}^{N_T} k_{Ti} \left(\frac{1}{2} - \frac{y_i}{d}\right)\left(\frac{1}{2} + \frac{y_i}{d}\right)$$

in which N_T is the number of tie bars and k_{Ti} is the instantaneous stiffness of the ith tie bar at time t.

The stiffness coefficients of $\bar{\underline{k}}_2$ is described in the following paragraph.

B. COLLISIONS

Longitudinal collisions are defined to take place at points A and B when the relative displacement between the two end diaphrams close the joint gap Δ_G with a nonzero relative velocity. At the instant collision takes place, the longitudinal impact springs having large stiffness k_I which are attached to one end diaphram leaving a small gap Δ_G with the other end diaphram start to resist the motion. A collision is completed when rebound occurs and the relative displacement between the two diaphrams becomes equal to the joint gap Δ_G.

The contact forces acting at points A and B can be written as

$$P_{AI} = k_I < u_{Ax} + \Delta_G > (u_{Ax} + \Delta_G)$$

$$P_{BI} = k_I < u_{Bx} + \Delta_G > (u_{Bx} + \Delta_G) \qquad (17)$$

where

$$
< u_{Ax} + \Delta_G > = \begin{cases} 1 & u_{Ax} + \Delta_G < 0 \\ 0 & u_{Ax} + \Delta_G \geq 0 \end{cases}
$$

$$
< u_{Bx} + \Delta_G > = \begin{cases} 1 & u_{Bx} + \Delta_G < 0 \\ 0 & u_{Bx} + \Delta_G \geq 0 \end{cases} \tag{18}
$$

If it is assumed that $(u_{Ax} + \Delta_G)$ and $(u_{Bx} + \Delta_G)$ do not change sign during a time interval Δt, the change of contact force during a time interval can be expressed as

$$
\begin{aligned} \Delta P_{AI} &= k_I < u_{Ax} + \Delta_G > \Delta u_{Ax} \\ \Delta P_{BI} &= k_I < u_{Bx} + \Delta_G > \Delta u_{Bx} \end{aligned} \tag{19}
$$

Let $\Delta \underline{\bar{F}}^I$ represent the incremental contact force vector in the relative expansion joint coordinate system during a time interval Δt as defined by

$$
\Delta \underline{\bar{F}}^I = \begin{Bmatrix} \Delta P_{AI} \\ 0 \\ 0 \\ \Delta P_{BI} \\ 0 \\ 0 \end{Bmatrix} \tag{20}
$$

Then, $\Delta \underline{\bar{F}}^I$ can be expressed as

$$
\Delta \underline{\bar{F}}^I = \underline{\bar{k}}_2 \, \Delta \underline{\bar{u}} \tag{21}
$$

in which

$$\bar{\underline{k}}_2 = \begin{bmatrix} k_I < u_{Ax} + \Delta_G > & 0 & 0 & 0 & 0 & 0 \\ 0 & 0 & 0 & 0 & 0 & 0 \\ 0 & 0 & 0 & 0 & 0 & 0 \\ 0 & 0 & 0 & k_I < u_{Bx} + \Delta_G > & 0 & 0 \\ 0 & 0 & 0 & 0 & 0 & 0 \\ 0 & 0 & 0 & 0 & 0 & 0 \end{bmatrix} \quad (22)$$

C. COULOMB FRICTION FORCES

Coulomb friction forces are developed at contact points A and B when the expansion joint undergoes longitudinal relative displacement and when the vertical contact forces are compressive. The friction at each point A and B always acts in the direction opposite to the relative velocity as a pair of self equilibrating forces. When the expansion joint does not undergo longitudinal relative displacement, each friction force can have a magnitude anywhere between its maximum and minimum values. The magnitude of a friction force depends on the magnitude of other forces acting on the expansion joint. Such characteristics can be represented by a rigid-plastic hysteretic force-relative displacement model as shown in Fig. 2.3. It should be noted here that the model of the Coulomb friction force represented in Fig. 2.3 is mathematically the same as the model of a rigid-plastic restoring force. Plastic deformations in the latter model correspond to slippages in the former model. In order to avoid numerical instability caused by a sudden change in the Coulomb friction force at zero relative velocity, the force is modeled by the elastoplastic hysteretic force-relative displacement model shown in Fig. 2.4. If the slope of OA in Fig. 2.4 is taken large enough, then both models of Figs. 2.3 and 2.4 are practically the same.

According to the assumption described, the Coulomb friction forces acting at points A and B at time t can be expressed as

$$
C_{Ax} = \begin{cases} -\nu < F_{Az} > \left|F_{Az}\right| & \text{for} \quad u_{Ax} \leq u^S_{Ax} - u^E_{Ax} \\ k^C < F_{Az} > (u_{Ax} - u^S_{Ax}) & \text{for} \quad u^S_{Ax} - u^E_{Ax} < u_{Ax} < u^S_{Ax} + u^E_{Ax} \\ \nu < F_{Az} > \left|F_{Az}\right| & \text{for} \quad u_{Ax} \geq u^S_{Ax} + u^E_{Ax} \end{cases}
$$

(23)

$$
C_{Bx} = \begin{cases} -\nu < F_{Bz} > \left|F_{Bz}\right| & \text{for} \quad u_{Bx} \leq u^S_{Bx} - u^E_{Bx} \\ k^C < F_{Bz} > (u_{Bx} - u^S_{Bx}) & \text{for} \quad u^S_{Bx} - u^E_{Bx} < u_{Bx} < u^S_{Bx} + u^E_{Bx} \\ \nu < F_{Bz} > \left|F_{Bz}\right| & \text{for} \quad u_{Bx} \geq u^S_{Bx} + u^E_{Bx} \end{cases}
$$

where ν is a constant coefficient of Coulomb friction, u^S_{Ax} and u^S_{Bx} are the current slippages at points A and B, respectively, and u^E_{Ax} and u^E_{Bx} are the elastic deformations at points A and B, respectively, as given by

$$
u^E_{Ax} = \nu \left|F_{Az}\right|/k_C \quad , \quad u^E_{Bx} = \nu \left|F_{Bz}\right|/k_C \tag{24}
$$

where

$$
< F_{Az} > = \begin{cases} 1 & F_{Az} < 0 \\ 0 & F_{Az} \geq 0 \end{cases}
$$

(25)

$$
< F_{Bz} > = \begin{cases} 1 & F_{Bz} < 0 \\ 0 & F_{Bz} \geq 0 \end{cases}
$$

If it is assumed that the vertical compressive contact forces F_{Az} and F_{Bz} are constant and deformations $(u_{Ax} - u^S_{Ax} \pm u^E_{Ax})$ and $(u_{Bx} - u^S_{Bx} \pm u^E_{Bx})$

do not change signs during a time interval Δt, then the changes of Coulomb friction force during the time interval can be expressed as

$$\Delta C_{Ax} = \begin{cases} k^C < F_{Az} > \Delta u_{Ax} & \text{for} \quad u^S_{Ax} - u^E_{Ax} < u_{Ax} < u^S_{Ax} + u^E_{Ax} \\ 0 & \text{for} \quad u_{Ax} \leq u^S_{Ax} - u^E_{Ax} \quad \text{or} \\ & \phantom{\text{for}} \quad u_{Ax} \geq u^S_{Ax} + u^E_{Ax} \end{cases}$$

$$\Delta C_{Bx} = \begin{cases} k^C < F_{Bz} > \Delta u_{Bx} & \text{for} \quad u^S_{Bx} - u^E_{Bx} < u_{Bx} < u^S_{Bx} + u^E_{Bx} \\ 0 & \text{for} \quad u_{Bx} \leq u^S_{Bx} - u^E_{Bx} \quad \text{or} \\ & \phantom{\text{for}} \quad u_{Bx} \geq u^S_{Bx} + u^E_{Bx} \end{cases} \tag{26}$$

Let $\Delta \bar{\underline{P}}^C$ represent the incremental Coulomb friction force vector in the expansion joint coordinate system during the time interval Δt; then, $\Delta \bar{\underline{P}}^C$ can be expressed as

$$\Delta \bar{\underline{P}}^C = \begin{Bmatrix} \Delta \bar{\underline{P}}^C_I \\ \Delta \bar{\underline{P}}^C_J \end{Bmatrix}, \quad \Delta \bar{\underline{P}}^C_I = \begin{Bmatrix} -\Delta C_{Ax} \\ 0 \\ 0 \\ -\Delta C_{Bx} \\ 0 \\ 0 \end{Bmatrix} \quad \Delta \bar{\underline{P}}^C_J = \begin{Bmatrix} \Delta C_{Ax} \\ 0 \\ 0 \\ \Delta C_{Bx} \\ 0 \\ 0 \end{Bmatrix} \tag{27}$$

Thus $\Delta \bar{\underline{P}}^C$ can be related to the vector of incremental expansion joint displacement $\Delta \bar{\underline{r}}$ by a matrix $\bar{\underline{k}}^C_t$ in the form

$$\Delta \bar{\underline{P}}^C = \bar{\underline{k}}^C_t \; \Delta \bar{\underline{r}} \tag{28}$$

where $\bar{\underline{k}}^C_t$ is a function of $\bar{\underline{r}}$ at time t.

From Eqs. (9) and (10), $\bar{\underline{k}}_t^C$ can be written in the form

$$\bar{\underline{k}}_t^C = \begin{bmatrix} \bar{\underline{k}}_3 & -\bar{\underline{k}}_3 \\ -\bar{\underline{k}}_3 & \bar{\underline{k}}_3 \end{bmatrix} \tag{29}$$

in which $\bar{\underline{k}}_3$ is a matrix defined in the relative expansion joint coordinate system which relates the change of Coulomb friction force vector during a time interval Δt to the change of relative expansion joint displacement $\Delta\bar{\underline{u}}$. From Eqs. (26) and (27), $\bar{\underline{k}}_3$ can be written as

$$\bar{\underline{k}}_3 = \begin{bmatrix} k_A^C & 0 & 0 & 0 & 0 & 0 \\ 0 & 0 & 0 & 0 & 0 & 0 \\ 0 & 0 & 0 & 0 & 0 & 0 \\ 0 & 0 & 0 & k_B^C & 0 & 0 \\ 0 & 0 & 0 & 0 & 0 & 0 \\ 0 & 0 & 0 & 0 & 0 & 0 \end{bmatrix} \tag{30}$$

where

$$k_A^C = \begin{cases} k^C < F_{Az} > & \text{for} \quad u_{Ax}^S - u_{Ax}^E < u_{Ax} < u_{Ax}^S + u_{Ax}^E \\ 0 & \text{for} \quad u_{Ax} \leq u_{Ax}^S - u_{Ax}^E \quad \text{or} \\ & \qquad\;\; u_{Ax} \geq u_{Ax}^S + u_{Ax}^E \end{cases}$$

$$k_B^C = \begin{cases} k^C < F_{Bz} > & \text{for} \quad u_{Bx}^S - u_{Bx}^E < u_{Bx} < u_{Bx}^S + u_{Bx}^E \\ 0 & \text{for} \quad u_{Bx} \leq u_{Bx}^S - u_{Bx}^E \quad \text{or} \\ & \qquad\;\; u_{Bx} \geq u_{Bx}^S + u_{Bx}^E \end{cases} \tag{31}$$

Finally, the matrix $\bar{\underline{k}}_t^C$ must be transformed to the local coordinate system using Eqs. (6) and (7). This transformation results in the relation

$$\Delta \underline{P}^C = \underline{k}_t^C \, \Delta \underline{r} \quad , \quad \underline{k}_t^C = \underline{A}^T \, \bar{\underline{k}}_t^C \, \underline{A} \tag{32}$$

Matrix $\underline{k}_t^C$ relates the vector of local nodal Coulomb friction force increment $\Delta \underline{P}^C$ to the vector of local nodal displacement increment $\Delta \underline{r}$. After local to global coordinate transformation, it can be used to assemble the total stiffness matrix $\underline{K}_t$ together with the stiffness matrix $\underline{k}_t^{EJ}$ defined in Eq. (13).

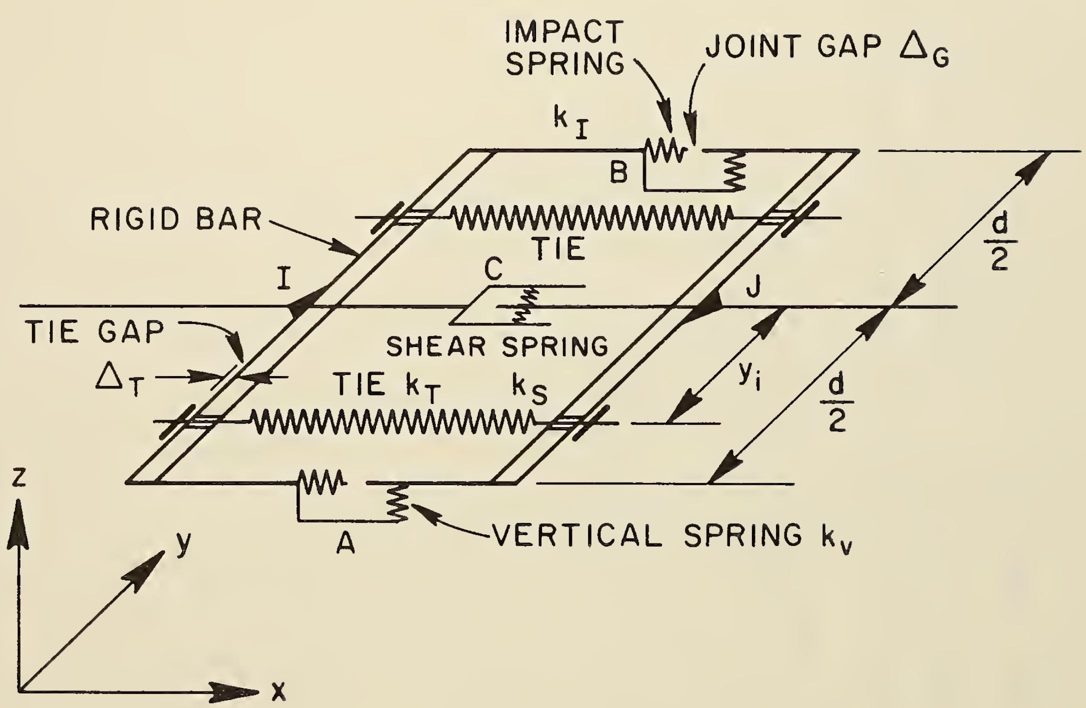

FIG. 2.1 IDEALIZED EXPANSION JOINT [2]

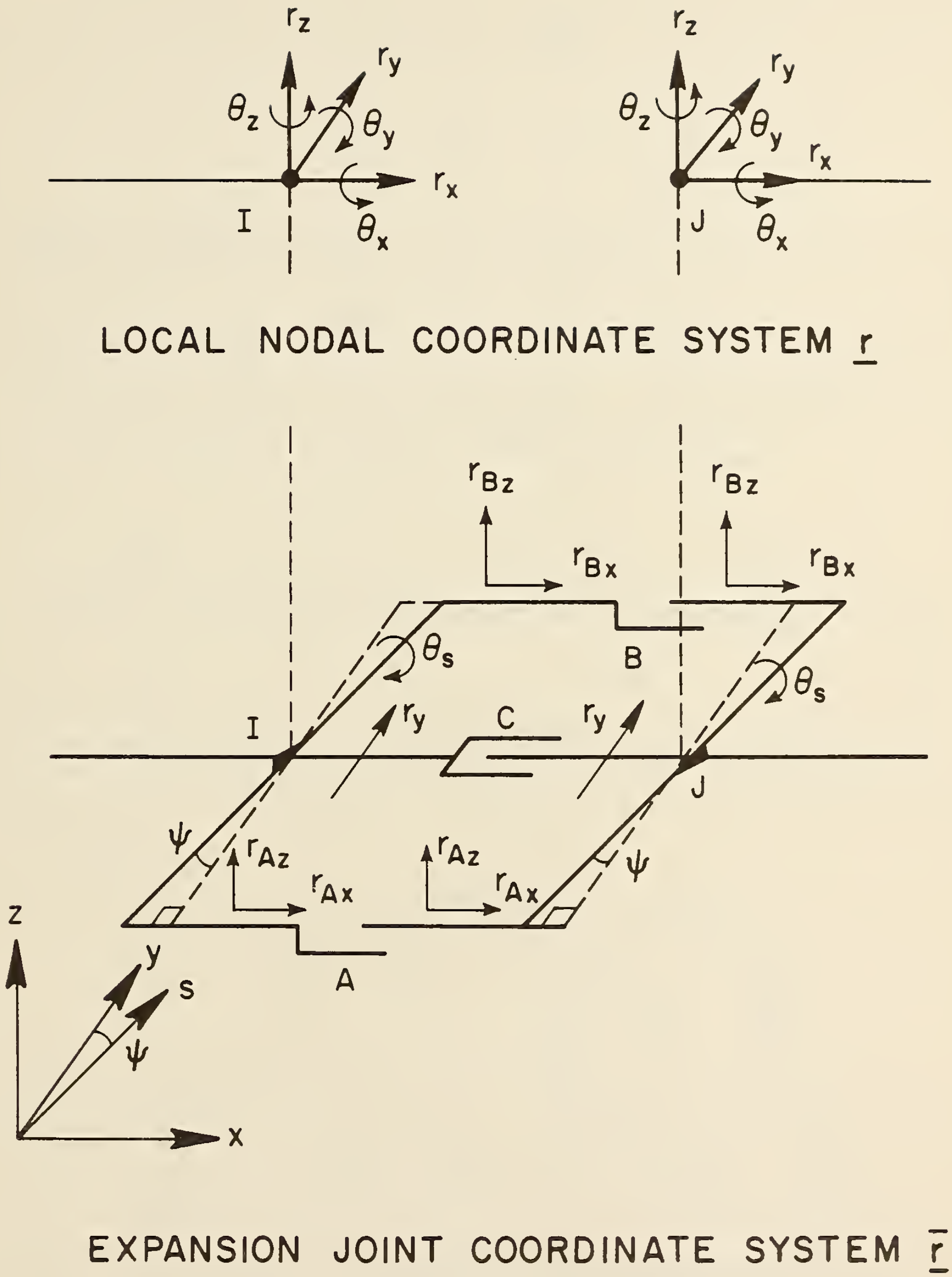

FIG. 2.2 COORDINATE SYSTEM FOR EXPANSION JOINT [2]

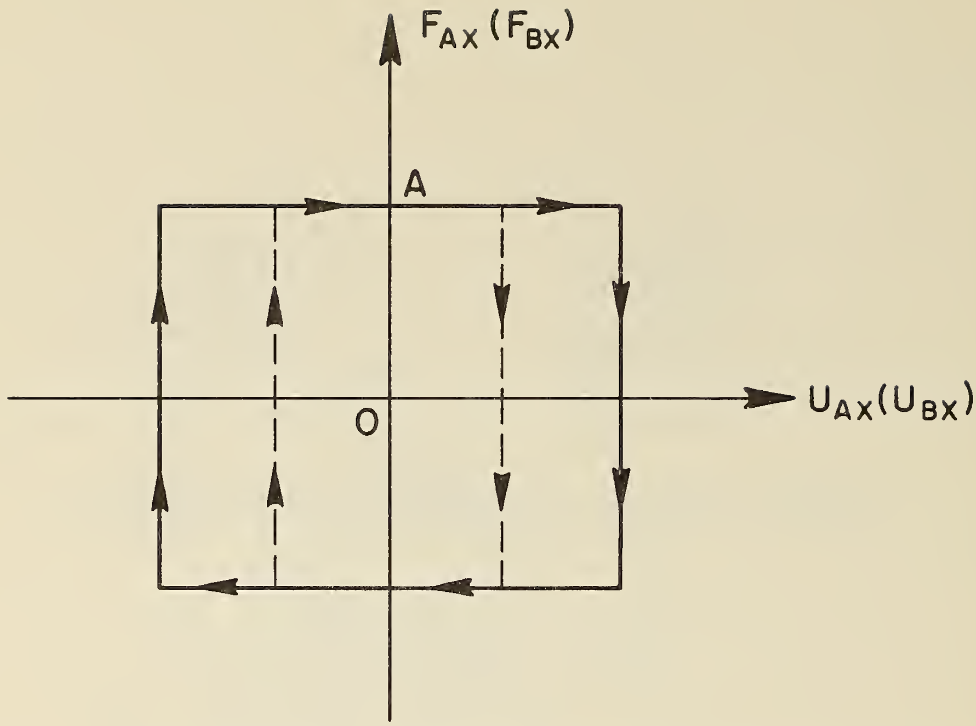

FIG. 2.3 RIGID-PLASTIC HYSTERETIC MODEL FOR COULOMB FRICTION

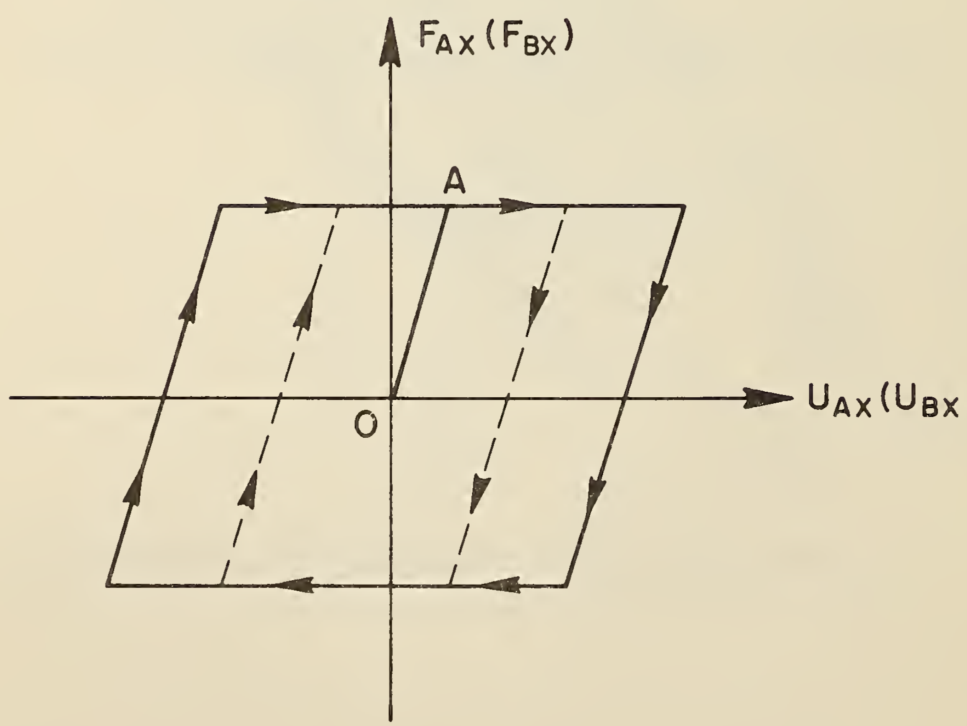

FIG. 2.4 ELASTOPLASTIC HYSTERETIC MODEL FOR COULOMB FRICTION

III. DYNAMIC ANALYSIS PROCEDURE

A. INCREMENTAL EQUATION OF MOTION

The equation of motion for an n degree of freedom system representing dynamic equilibrium at time t can be expressed as

$$\underset{\sim}{F}_t^I + \underset{\sim}{F}_t^D + \underset{\sim}{F}_t^S = \underset{\sim}{R}_t \tag{33}$$

where, $\underset{\sim}{F}_t^I$, $\underset{\sim}{F}_t^D$, $\underset{\sim}{F}_t^S$ and $\underset{\sim}{R}_t$ are the nodal inertia force vector, nodal damping force vector, nodal restoring force vector and nodal external force vector at time t, respectively. When the structure is nonlinear, Eq. (33) is written for time $t + \Delta t$ in the form

$$\left(\underset{\sim}{F}_t^I + \Delta\underset{\sim}{F}_t^I\right) + \left(\underset{\sim}{F}_t^D + \Delta\underset{\sim}{F}_t^D\right) + \left(\underset{\sim}{F}_t^S + \Delta\underset{\sim}{F}_t^S\right) = \underset{\sim}{R}_{t+\Delta t} \tag{34}$$

where, $\Delta\underset{\sim}{F}_t^I$, $\Delta\underset{\sim}{F}_t^D$ and $\Delta\underset{\sim}{F}_t^S$ are the changes of the nodal inertia forces, nodal damping forces and nodal restoring forces during a time interval Δt, respectively. These changes of the forces are assumed to be given by

$$\Delta\underset{\sim}{F}_t^I = \underset{\sim}{M}\,\Delta\ddot{\underset{\sim}{u}}_t \,;\; \Delta\underset{\sim}{F}_t^D = \underset{\sim}{C}\,\Delta\dot{\underset{\sim}{u}}_t \,;\; \Delta\underset{\sim}{F}_t^S = \underset{\sim}{K}_t\,\Delta\underset{\sim}{u}_t \tag{35}$$

where, $\underset{\sim}{M}$, $\underset{\sim}{C}$ and $\underset{\sim}{K}_t$ represent the constant mass matrix, constant viscous damping matrix and tangent stiffness matrix at time t, respectively. Vectors $\Delta\ddot{\underset{\sim}{u}}_t$, $\Delta\dot{\underset{\sim}{u}}_t$ and $\Delta\underset{\sim}{u}_t$ are the changes of nodal accelerations, nodal velocities and nodal displacements during time interval Δt as defined by

$$\Delta \ddot{\underline{u}}_t = \ddot{\underline{u}}_{t+\Delta t} - \ddot{\underline{u}}_t$$

$$\Delta \dot{\underline{u}}_t = \dot{\underline{u}}_{t+\Delta t} - \dot{\underline{u}}_t \tag{36}$$

$$\Delta \underline{u}_t = \underline{u}_{t+\Delta t} - \underline{u}_t$$

Substituting Eq. (35) into Eq. (34), one can obtain the equation of motion in incremental form as

$$\underline{M}\, \Delta \ddot{\underline{u}}_t + \underline{C}\, \Delta \dot{\underline{u}}_t + \underline{K}_t\, \Delta \underline{u}_t = \underline{R}_{t+\Delta t} - \underline{M}\, \ddot{\underline{u}}_t - \underline{C}\, \dot{\underline{u}}_t - \underline{F}_t^S \tag{37}$$

The nodal external force vector $\underline{R}_{t+\Delta t}$ is assumed to be derived from two types of loading [2]; an applied dynamic force $\underline{P}_{t+\Delta t}$ and an inertia force due to ground motion $\ddot{\underline{u}}_{g(t+\Delta t)}$, i.e.,

$$\underline{R}_{t+\Delta t} = \underline{P}_{t+\Delta t} - \underline{M}\, \underline{B}\, \ddot{\underline{u}}_{g(t+\Delta t)} \tag{38}$$

in which $\underline{B}$ is a matrix of ground motion influence coefficients.

The tangent stiffness matrix $\underline{K}_t$ consists of time independent coefficients $\underline{K}^L$ which are assembled before excitation based on the initial stress stage and time-dependent coefficients $\underline{K}_t^N$ which change in each time internal, i.e.,

$$\underline{K}_t = \underline{K}^L + \underline{K}_t^N \tag{39}$$

where

$$\underline{K}^L = \sum_{j=1}^{LEL} \underline{k}_{(j)} + \sum_{j=1}^{NEL} \underline{k}_{(j)}$$

$$\underline{K}_t^N = \sum_{j=1}^{NEL} \underline{k}_{t(j)}^N, \quad \underline{k}_{t(j)}^N = \underline{k}_{t(j)} - \underline{k}_{(j)} \tag{40}$$

in which LEL and NEL represent numbers of linear and nonlinear elements in the system. Matrices $\underline{k}_{(j)}$ and $\underline{k}_{t(j)}$ represent time independent stiffness coefficients for the jth linear or nonlinear element and time dependent stiffness coefficients for the jth nonlinear element, respectively. From Eq. (39), $\underline{F}_t^S$ can be written as

$$\underline{F}_t^S = \underline{F}_t^{SL} + \underline{F}_t^{SN} = \underline{K}^L \underline{u}_t + \sum_{j=1}^{NEL} \underline{f}_{t(j)}^{SN} \tag{41}$$

in which $\underline{f}_{t(j)}^{SN}$ represents time dependent nodal restoring forces for the jth nonlinear element. It is desirable to calculate $\underline{f}_{t(j)}^{SN}$ $(j \in NEL)$ directly from current element deformations in order to avoid accumulating errors during the numerical computation [16].

The damping matrix is assumed to be of the form

$$\underline{C} = \alpha \underline{M} + \beta \underline{K}^L \tag{42}$$

showing one part proportional to the mass distribution and the other part proportional to the initial stiffness distribution before excitation.

B. STEP-BY-STEP INTEGRATION

Newmark's generalized acceleration method assumes the following approximations for the nodal velocities and displacements [12]

$$\begin{aligned} \dot{\underline{u}}_{t+\Delta t} &= \dot{\underline{u}}_t + \left[(1 - \delta)\, \ddot{\underline{u}}_t + \delta\, \ddot{\underline{u}}_{t+\Delta t}\right] \Delta t \\ \underline{u}_{t+\Delta t} &= \underline{u}_t + \dot{\underline{u}}_t \Delta t + \left[\left(\frac{1}{2} - \sigma\right) \ddot{\underline{u}}_t + \sigma\, \ddot{\underline{u}}_{t+\Delta t}\right] \Delta t^2 \end{aligned} \tag{43}$$

where parameters δ and σ can be chosen to give the required integration stability and accuracy. When $\delta = 1/2$ and $\sigma = 1/6$, the approximations correspond to the linear acceleration method and when

$\delta = 1/2$ and $\sigma = 1/4$, they correspond to the constant acceleration method.

Using Eq. (36), the approximations given by Eq. (43) can be expressed in the incremental form

$$\begin{aligned} \Delta\ddot{\underline{u}}_t &= C_1\,\Delta\underline{u}_t - C_2\,\dot{\underline{u}}_t - C_3\,\ddot{\underline{u}}_t \\ \Delta\dot{\underline{u}}_t &= C_4\,\Delta\underline{u}_t - C_5\,\dot{\underline{u}}_t - C_6\,\ddot{\underline{u}}_t \end{aligned} \tag{44}$$

where

$$\begin{aligned} C_1 &= \frac{1}{\sigma\Delta t^2}, \quad C_2 = \frac{1}{\sigma\Delta t}, \quad C_3 = \frac{1}{2\sigma} \\ C_4 &= \frac{\delta}{\sigma\Delta t}, \quad C_5 = \frac{\delta}{\sigma}, \quad C_6 = \left(\frac{\delta}{2\sigma} - 1\right)\Delta t \end{aligned} \tag{45}$$

Substituting Eqs. (41) and (44) into Eq. (37), one can obtain

$$\begin{aligned} \left[C_1\,\underline{M} + C_4\,\underline{C} + \underline{K}_t\right]\Delta\underline{u}_t &= \underline{R}_{t+\Delta t} - \underline{M}\,\ddot{\underline{u}}_t - \underline{C}\,\dot{\underline{u}}_t - \underline{K}^L\,\underline{u}_t - \underline{F}_t^{NS} \\ &\quad + \underline{M}\left[C_2\,\dot{\underline{u}}_t + C_3\,\ddot{\underline{u}}_t\right] + \underline{C}\left[C_5\,\dot{\underline{u}}_t + C_6\,\ddot{\underline{u}}_t\right] \end{aligned} \tag{46}$$

Using Eq. (42), i.e., $\underline{C} = \alpha\,\underline{M} + \beta\,\underline{K}^L$, and introducing the following normalized constants.

$$\begin{aligned} C_7 &= C_1 + \alpha\,C_4, \quad & C_8 &= \beta\,C_4, \quad & C_9 &= C_2 + \alpha\,C_5 - \alpha \\ C_{10} &= 1 - C_3 - \alpha\,C_6, \quad & C_{11} &= \beta(C_5 - 1), \quad & C_{12} &= \beta\,C_6 \end{aligned} \tag{47}$$

Eq. (46) can be written in the form

$$\bar{\underline{K}}_t\,\Delta\underline{u}_t = \Delta\bar{\underline{R}}_t \tag{48}$$

where

$$\bar{\underline{K}}_t = \underline{K}_t + C_7 \underline{M} + C_8 \underline{K}^L$$

$$\Delta\bar{\underline{R}}_t = \underline{R}_{t+\Delta t} - \underline{M} [C_{10} \ddot{\underline{u}}_t - C_9 \dot{\underline{u}}_t] - \underline{K}^L [\underline{u}_t - C_{11} \dot{\underline{u}}_t - C_{12} \ddot{\underline{u}}_t] - \underline{F}_t^{NS} \quad (49)$$

Equation (49) can be solved for $\Delta\underline{u}_t$ at each time step and the nodal accelerations, velocities and displacements at time $t + \Delta t$ can be determined from Eqs. (36) and (44) giving

$$\ddot{\underline{u}}_{t+\Delta t} = \ddot{\underline{u}}_t + C_1 \Delta\underline{u}_t - C_2 \dot{\underline{u}}_t - C_3 \ddot{\underline{u}}_t$$

$$\dot{\underline{u}}_{t+\Delta t} = \dot{\underline{u}}_t + C_4 \Delta\underline{u}_t - C_5 \dot{\underline{u}}_t - C_6 \ddot{\underline{u}}_t \quad (50)$$

$$\underline{u}_{t+\Delta t} = \underline{u}_t + \Delta\underline{u}_t$$

C. ACCURACY OF SOLUTION

Equation (48) is an approximate form of the actual equation of motion to be solved at each time step since it was derived from approximations of the instantaneous linearized stiffness relations between the incremental forces and the incremental displacements. Depending on the nonlinearity of the equation and the magnitude of time interval Δt, the incremental linearization may introduce an instability in the overall solution. A measurement of how well the dynamic equilibrium at time $t + \Delta t$ is being satisfied by the approximate solution of Eq. (48) may be expressed by the residual or unbalanced forces $\delta\underline{R}_{t+\Delta t}$. The correctness of solution using Eq. (48) may then be given by comparing the ratio of the Euclidean norm of the residual forces and the external forces Δ_p with a specified tolerance Δ_{ps} using the relation

$$\Delta_p = \frac{||\delta \underline{R}_{t+\Delta t}||}{||\underline{R}_{t+\Delta t}|| + ||\underline{R}_{t+\Delta t} - \delta \underline{R}_{t+\Delta t}||} \leq \Delta_{ps} \tag{51}$$

where

$$\delta \underline{R}_{t+\Delta t} = \underline{R}_{t+\Delta t} - \underline{M}\, \ddot{\underline{u}}_{t+\Delta t} - \underline{C}\, \dot{\underline{u}}_{t+\Delta t} - \underline{K}^L\, \underline{u}_{t+\Delta t} - \underline{F}^{NS}_{t+\Delta t} \tag{52}$$

When the accuracy of solution is unsatisfactory, it may be improved by using smaller time intervals or by applying an equilibrium correction through an iteration process.

D. SUBDIVISION OF TIME INTERVAL

Although sufficient accuracy of solution can be maintained using small time intervals throughout the period of dynamic response, the computational effort may be excessive. Therefore, it is more efficient to use the smaller intervals only during those intervals of time when they are actually needed and to use longer intervals during the remaining part of the response. When the solution at time t satisfies dynamic equilibrium with the specified accuracy but the solution at time $t + \Delta t$ does not, one can return to the solution at time t and use smaller equidistant sub-intervals between times t and $t + \Delta t$. The accuracy of solution thus obtained by the smaller time intervals can be checked using Eq. (51) at the end of each of the smaller time intervals.

As seen from Eq. (44), the nodal accelerations, nodal velocities and nodal displacements at time $t + \Delta t$ can be reversed to the solution at time t using the relations

$$\begin{aligned} \ddot{\underline{u}}_t &= C_{14}\, \Delta \underline{u}_t - C_{15}\, \dot{\underline{u}}_{t+\Delta t} - C_{16}\, \ddot{\underline{u}}_{t+\Delta t} \\ \dot{\underline{u}}_t &= C_{17}\, \Delta \underline{u}_t - C_{18}\, \dot{\underline{u}}_{t+\Delta t} - C_{19}\, \ddot{\underline{u}}_{t+\Delta t} \\ \underline{u}_t &= \underline{u}_{t+\Delta t} - \Delta \underline{u}_t \end{aligned} \tag{53}$$

where

$$C_{13} = \frac{1}{\delta-\sigma-1/2}, \qquad C_{14} = \frac{C_{13}}{\Delta t^2}, \qquad C_{15} = \frac{C_{13}}{\Delta t}$$

$$C_{16} = C_{13}(\sigma-\delta), \qquad C_{17} = \frac{C_{13}(\delta-1)}{\Delta t}, \qquad C_{18} = C_{13}(\sigma-1/2) \tag{54}$$

$$C_{19} = C_{13}\left(\frac{\delta}{2} - \sigma\right)\Delta t$$

E. EQUILIBRIUM ITERATION

The equation of motion for the ith equilibrium iteration at time t is expressed as

$$\underset{\sim}{M}\,\delta\ddot{\underset{\sim}{u}}_t^{(i)} + \underset{\sim}{C}\,\delta\dot{\underset{\sim}{u}}_t^{(i)} + \underset{\sim}{K}_t^{(i)}\,\delta\underset{\sim}{u}_t^{(i)} = \delta\underset{\sim}{R}_t^{(i)} \tag{55}$$

where, $\underset{\sim}{M}$ and $\underset{\sim}{C}$ are the constant mass and damping matrices, respectively, $\underset{\sim}{K}_t^{(i)}$ is the tangent stiffness matrix at time t for the ith iteration, $\delta\ddot{\underset{\sim}{u}}_t^{(i)}$, $\delta\dot{\underset{\sim}{u}}_t^{(i)}$, and $\delta\underset{\sim}{u}_t^{(i)}$ are the corrective nodal accelerations, nodal velocities and nodal displacements, respectively, for the ith iteration as defined by

$$\begin{aligned}
\delta\ddot{\underset{\sim}{u}}_t^{(i)} &= \ddot{\underset{\sim}{u}}_t^{(i+1)} - \ddot{\underset{\sim}{u}}_t^{(i)} \\
\delta\dot{\underset{\sim}{u}}_t^{(i)} &= \dot{\underset{\sim}{u}}_t^{(i+1)} - \dot{\underset{\sim}{u}}_t^{(i)} \\
\delta\underset{\sim}{u}_t^{(i)} &= \underset{\sim}{u}_t^{(i+1)} - \underset{\sim}{u}_t^{(i)}
\end{aligned} \tag{56}$$

and where $\delta\underset{\sim}{R}_t^{(i)}$ representing the nodal residual forces for the ith iteration is given by

$$\delta\underset{\sim}{R}_t^{(i)} = \underset{\sim}{R}_t - \underset{\sim}{M}\,\ddot{\underset{\sim}{u}}_t^{(i)} - \underset{\sim}{C}\,\dot{\underset{\sim}{u}}_t^{(i)} - \underset{\sim}{K}^L\,\underset{\sim}{u}_t^{(i)} - \underset{\sim}{F}_t^{NS(i)} \tag{57}$$

From the integration scheme of Eq. (44), the corrective accelerations and velocities of Eq. (56) can be written as [22]

$$\delta \ddot{\underline{u}}_t^{(i)} = C_1 \; \delta \underline{u}_t^{(i)}$$
$$\delta \dot{\underline{u}}_t^{(i)} = C_4 \; \delta \underline{u}_t^{(i)} \tag{58}$$

Substituting Eqs. (57) and (58) into Eq. (55), one obtains

$$\bar{\underline{K}}_t^{(i)} \; \delta \underline{u}_t^{(i)} = \delta \bar{\underline{R}}_t^{(i)} \tag{59}$$

where

$$\bar{\underline{K}}_t^{(i)} = \underline{K}_t^{(i)} + C_7 \, \underline{M} + C_8 \, \underline{K}^L$$
$$\delta \bar{\underline{R}}_t^{(i)} = \underline{R}_t - \underline{M} \, [\ddot{\underline{u}}_t^{(i)} + \alpha \dot{\underline{u}}_t^{(i)}] - \underline{K}^L [\underline{u}_t^{(i)} + \beta \dot{\underline{u}}_t^{(i)}] - \underline{F}_t^{NS(i)} \tag{60}$$

Equation (59) can be solved for the ith corrective displacements $\delta \underline{u}_t^{(i)}$ and then the corrected nodal accelerations, nodal velocities and nodal displacements can be calculated using Eqs. (56) and (58), i.e.,

$$\ddot{\underline{u}}_t^{(i+1)} = \ddot{\underline{u}}_t^{(i)} + C_1 \; \delta \underline{u}_t^{(i)}$$
$$\dot{\underline{u}}_t^{(i+1)} = \dot{\underline{u}}_t^{(i)} + C_4 \; \delta \underline{u}_t^{(i)} \tag{61}$$
$$\underline{u}_t^{(i+1)} = \underline{u}_t^{(i)} + \delta \underline{u}_t^{(i)}$$

If convergence occurs, the iteration can be continued until the dynamic equilibrium of the motion is satisfied within the specified accuracy. The convergence of equilibrium iteration may be expressed by comparing the ratio of the Euclidean norm of the corrective displacement to the total displacement Δ_u^I with a specified tolerance Δ_{us}^I in the form

$$\Delta_u^I \equiv \frac{||\delta \underline{u}_t^{(i)}||}{||\underline{u}_t^{(i)}|| + ||\underline{u}_t^{(i+1)}||} \leq \Delta_{us}^I \tag{62}$$

or by comparing the ratio of the Euclidean norm of the residual forces to the total external forces Δ_p^I with a specified tolerance Δ_{ps}^I in the form

$$\Delta_p^I \equiv \frac{||\delta \underline{R}_t^{(i)}||}{||\underline{R}_t|| + ||\underline{R}_t - \delta \underline{R}_t^{(i)}||} \leq \Delta_{ps}^I \tag{63}$$

The step-by-step integration algorithm used herein for non-linear systems including the equilibrium iteration and the subdivision of time intervals may be summarized as follows:

(1) Initial Calculations

(a) Form the initial stiffness matrix $\underline{K}^L$ and the mass matrix $\underline{M}$ for the system.

(b) Solve for the initial displacement and calculate the element forces due to static loads.

(c) Set up the dynamic load and ground excitation time history.

(d) Set initial conditions $\ddot{\underline{u}}_0 = \dot{\underline{u}}_0 = \underline{u}_0 = \underline{0}$, $\underline{f}_0^{NS}(j) = 0$ for $j \in NEL$, $\underline{K}_0 = \underline{K}^L$.

(e) Calculate the step-by-step integration constants C_i ($i = 1,2,....12$) and subdivision control constants C_i ($i = 13,14,....19$).

(2) For Each Time Increment Δt

(f) Form the effective dynamic stiffness matrix $\bar{\underset{\sim}{K}}_t$ and the effective dynamic load vector $\Delta\bar{\underset{\sim}{R}}_t$.

(g) Solve for the displacement increment $\Delta\underset{\sim}{u}_t$.

(h) Compute current accelerations, velocities and displacements $\ddot{\underset{\sim}{u}}_{t+\Delta t}$, $\dot{\underset{\sim}{u}}_{t+\Delta t}$, $\underset{\sim}{u}_{t+\Delta t}$.

(i) Calculate current element forces, check nonlinearity conditions, and compute the new element tangent stiffness matrix $\underset{\sim}{k}^N_{t(j)}$ for $j \in NEL$; determine the inelastic deformation vectors, and current inelastic element nodal restoring force vectors $\underset{\sim}{f}^{SN}_{t(j)}$ for $j \in NEL$.

(j) Compute residual force vector $\delta\underset{\sim}{R}_{t+\Delta t}$ and check the accuracy of solution;

i) if calculated responses are sufficiently accurate, skip to (k).

ii) if subdivision of time interval is needed, go to (3) after reversing the current inelastic element deformations from time $t + \Delta t$ to time t.

iii) if equilibrium iteration is needed, go to (4).

(k) Repeat steps (f) through (j) for the next time increment.

(3) Subdivision of Time Interval

(ℓ) Backspace accelerations, velocities and displacements from time $t + \Delta t$ to time t, and calculate element tangent stiffness matrices and inelastic element nodal restoring forces at time t.

(m) Calculate the dynamic load at time $\hat{t} = t + i\,\hat{\Delta t}$ for $i = 1,2,\ldots.n$ in which $\hat{\Delta t} = \Delta t/n$ and n is a specified number of time interval.

(n) Form the effective dynamic stiffness matrix $\underline{\bar{K}}_{\hat{t}-\Delta\hat{t}}$ and the effective dynamic load vector $\Delta\underline{\bar{R}}_{\hat{t}-\Delta\hat{t}}$.

(o) Solve for the displacement increment $\Delta\underline{u}_{\hat{t}-\Delta\hat{t}}$.

(p) Compute current accelerations, velocities and displacements $\ddot{\underline{u}}_{\hat{t}}$, $\dot{\underline{u}}_{\hat{t}}$, $\underline{u}_{\hat{t}}$.

(q) Calculate current element forces, check nonlinearity conditions, and compute new element tangent stiffness matrices $\underline{k}^{N}_{\hat{t}(j)}$ for j∈NEL; determine the inelastic deformation vectors, and current inelastic element nodal restoring force vector $\underline{f}^{SN}_{\hat{t}(j)}$ for j∈NEL.

(r) Compute residual force vector $\delta\underline{R}_{\hat{t}}$ and check the accuracy of solution;

i) if calculated responses are sufficiently accurate, skip to (s).

ii) if equilibrium iteration is needed, go to (4).

(s) Repeat steps (m) through (r) for next sub-time increment (i = 1,2,....n). If i=n, then go back to (k)

(4) Equilibrium Iteration

(t) Form the effective dynamic stiffness matrix $\underline{\bar{K}}^{(i)}_{t+\Delta t}$ and solve for the corrective displacement vector $\delta\underline{u}^{(i)}_{t+\Delta t}$.

(u) Compute the i+1th corrected accelerations, velocities and displacements $\ddot{\underline{u}}^{(i+1)}_{t+\Delta t}$, $\dot{\underline{u}}^{(i+1)}_{t+\Delta t}$, $\underline{u}^{(i+1)}_{t+\Delta t}$.

(v) Calculate current element forces, check nonlinearity conditions, and compute element tangent stiffness matrices; determine the inelastic deformation vectors, and current element nodal restoring force vectors.

(w) Compute residual force vector $\delta \underset{\sim}{R}_{t+\Delta t}^{(i+1)}$ and check the accuracy of solution;

i) if corrected responses are sufficiently accurate, go back to (k).

ii) if convergence occurs and corrected responses are not yet sufficiently accurate, repeat steps (t) through (w).

IV. EXPERIMENTAL MODEL STUDY AND TEST RESULTS

The purpose of this chapter is to present the characteristics of the model bridge structure, test procedures and test results obtained in the Series IV excitation test program including the results of a number of preliminary component tests used in formulating the analytical model and in interpreting the correlation results of seismic responses with analytical predictions. Detailed information on the experimental phase of the overall program are given in references [23] and [24].

A. EXPERIMENTAL MODEL [23,24]

The bridge model was originally based on a symmetrical simplified version of the east half of the 5/14 South Connector Overcrossing that suffered severe structural damages during the San Fernando earthquake in 1971. It was designed with the aim of providing the primary features of high curved highway bridge structures, namely, deck curvature, expansion joints, and long columns.

Based on size and performance of the shaking table at the University of California, Berkeley [27], scales of the model were established as follows;

$$
\begin{aligned}
L_r &= 30 \\
F_r &= L_r^2 = 900 \qquad\qquad (64) \\
T_r &= \sqrt{L_r} \simeq 1/5.5
\end{aligned}
$$

in which L_r, F_r and T_r represent the geometric, force and time scale factors. In order to bring the inertia forces including gravitational forces into the force scale factor F_r, substantial amount of lead weights were placed on the model. The total weight including the lead weights was approximately 8.5 kips which corresponds to approximately 8.5% of the weight of the shaking table.

The bridge model structure adopted was composed of three subassemblages as shown in Fig. 4.1; a center girder/column system and two side girder/column/abutment systems which were essentially independent of each other having different dynamic characteristics. These subassemblages were tied together by two expansion joints placed in symmetrical positions.

Seismic responses of displacement relative to the shaking table were measured by LVDT at three points of the model as shown in Fig. 4.2, i.e. at the end of side girder No. 1, center of the center girder and end of side girder No. 2. Two horizontal components, namely the longitudinal (X) component and the transverse (Y) component, were measured at each point. In addition to these displacements, relative movements between the two end diaphragms (opening and closing of joint gap) of each expansion joint at both the inner and outer sides were measured. Thus in all, 10 responses of displacement (6 relative to the shaking table and 4 across the expansion joints) were recorded during the periods of seismic excitation. However since the response at the center of the center girder in the longitudinal (X) direction was very small due to the direction of excitation, it was finally disregarded, leaving 9 responses of displacement to be used for the correlation study.

The model was made as a component system allowing repeated experimental data to be derived from one basic model as damaged components were either repaired or replaced. The properties of each component are discribed as follows:

1. <u>Superstructure</u> - The superstructure of the model consisted of

one center girder and two side girders. They were constructed with a rectangular cross section 8.5 inches in width and 2 1/2 inches in thickness. This section was overdesigned by a factor of approximately 2 to insure that the superstructure would behave elastically during all tests [23]. A high strength (8000 psi.) shrinkage resistant, microconcrete was used in constructing the girders to avoid shrinkage cracks which would adversely affect the stiffness and damping characteristics.

2. Columns - Two types of columns having different sections were used in the model; i.e. two weak columns (COL-1B and 2B) having a section 2 1/2 x 1 1/2 inches which supported the center girder and two strong columns (COL-1A and 2A) having a section 2 1/2 x 4 inches which supported the side girders. All columns were constructed using 4500 psi. strength normal Portland cement microconcrete and four #2 (2/8 inch) annealed reinforcing bars having a yield strength of approximately 50 ksi.

The bottoms of the columns were clamped to a base steel frame which was designed with sufficiently high stiffness that essentially full fixty was provided at the base of each column. The top of the columns were attached to the girders.

3. Expansion Joints - Expansion joint element consisted of a hinge seat, a transverse shear key, a rubber pad, a vertical restrainer and a pair of longitudinal joint restrainer tie bars as shown in Fig. 4.3.

The hinge seat and the shear key were constructed of concrete having the same properties as those of the concrete used for the superstructure and they were heavily reinforced to provide high resistance to shear forces and bending moments. The section of the hinge seat was 8.5 inches in width and 0.5 inches in length. The shear key having a section 2.5 inches in width, 0.5 inches in length, and 1.5 inches in height was designed to prevent transverse relative motion between the girders.

A 1/16 inch thickness rubber pad was placed over the entire hinge seat simulating the prototype elastomeric bearing pad.

A pair of vertical stoppers was provided at each expansion joint to prevent up-lift of the girders from the hinge seats.

A pair of longitudinal joint restrainer bars 5 1/2 inches in length and 1/8 of an inch in diameter was used to tie together the superstructure. They were made of annealed mild steels having yield and ultimate strengths (strain) of approximately 650 lbs. (0.2%) and 750 lbs. (20%), respectively. The restrainer tie bars were mounted on each side of the superstructure parallel to the bridge axis. They were designed to resist only opening of the joint gaps when the relative movement exceeded the initial gap Δ_T.

4. Abutments - The abutments were constructed as steel frames to support the outer ends of the side girders. They were originally designed to provide full fixity to the ends of the girders except for allowing rotational freedom around the transverse horizontal (y) axis. However, due to lack of stiffness of the steel cover plate at the abutment, some rotational freedom around the vertical (z) axis was also provided.

B. TEST PROCEDURES AND TEST RESULTS

1. Stiffness Properties of Components - A number of preliminary tests were performed on the components of the model to determine their stiffness properties and their boundary conditions. The test results

obtained are used subsequently in formulating the analytical model of the complete structure.

Columns - Flexural rigidities of columns were determined from the results of static load-deflection tests. The measured load vs. deflection relations were linear up to those levels later produced during the high intensity seismic excitations. The measured flexural rigidities were confirmed by comparing the resulting calculated lowest natural frequencies of the free standing columns with their experimental values. Other column rigidities such as those in the longitudinal and torsional directions were calculated using the known sectional and material properties.

Superstructure - The flexural rigidities of the girders around their strong axes were determined from static load vs. deflection tests. The load vs. deflection relations were linear up to those levels developed during high intensity seismic excitations. The flexural rigidities of the girders around their weak axes, however, could not be determined in the same way since twisting associated with the deck curvature was coupled with bending. Therefore, these rigidities were determined from free vibration tests of the side subassemblage as described in the subsequent paragraph. The longitudinal and torsional rigidities were calculated from their sectional and material properties.

Expansion Joint - The expansion joint is the most complicated component in the entire bridge model. This complexity results from the combined actions of the rubber pad, shear key and tie bars associated with slippages and collisions which take place between girders.

Figure 4.4 shows the force vs. relative displacement relation of the expansion joint in which plus relative displacement corresponds to an opening of the joint gap and minus relative displacement corresponds closing of the joint gap. When the expansion joint undergoes an increasing relative movement in the positive direction, the rubber pad first deforms under shear action providing resistance to the motion. Then, slippage takes place when the applied force reaches the maximum friction force which can be developed on the contact plane of the expansion joint (Fig. 4.4.1). It should be noted here that the difference between dynamic and static frictions is disregarded in this force vs. displacement relation. When the positive relative movement reaches the tie gap Δ_T, the pair of tie bars begin resisting further opening of the joint gap. This resistance builds up linearly with joint separation until the yield strength of the tie bars is reached; then, yielding under constant force takes place (Fig. 4.4.2). When the expansion joint undergoes a relative movement in the negative direction, the rubber pad deforms and resists the motion in the same manner described above for the positive direction. However the tie bars do not resist motion in this direction. If the expansion joint undergoes further negative relative motion reaching the value of the seat gap Δ_G, collision takes place between the girders.

Although the expansion joints have such complex characteristics, a direct measurement of their constraint at the expansion joint was not performed because of difficulties involved in such an experimental test. Therefore the experimental data obtained to formulate the analytical model of the expansion joint were certain element properties.

The stiffness and strength of the tie bar were measured after they were made by annealing mild steel [23]. One typical stress vs. strain relation is displayed in Fig. 4.5. A longitudinal stiffness of

6.47×10^4 lbs/inch and a yield (ultimate) strength of 650 lbs (750 lbs) were determined from the test results.

Preliminary tests were performed on the rubber pad to determine its shearing stiffness [25]. To accomplish this, a specimen of the rubber pad was sandwitched between two steel plates which were then displaced so that pure shear deformation was produced in the pad. The specimen used for this test was 1 inch long and 1/2 inch wide. The test was performed with a changing frequency of cyclic shear load and contact force. Some typical results of the shear force vs. deformation are shown in Fig. 4.6. From the results, it is apparent that the rubber pad has a slight hysteretic type behavior with the average stiffness being significantly affected by contact pressure but less affected by frequency in the range 0-5 Hz. Assuming the stress-strain relation of the rubber pad can be modeled by a linear elastic spring with stiffness proportional to both the contact force and the size of specimen, the effective stiffness of the pad k_x^R was found to be

$$k_x^R = 22800 \text{ lbs/inch} \tag{65}$$

A preliminary tests was also performed to determine the friction coefficient [25]. One of the expansion joint components was subjected to an increasing static force in its longitudinal direction while under compressive contact pressure. The maximum frictional resisting force was measured when slippage first occured. Then, the friction coefficient was obtained by dividing the measured maximum resisting force by the contact pressure. However, due to large variations in the measured data, the test results could only suggest that the friction coefficient was within the range

$$0.3 < \nu^{EJ} < 0.6 \qquad (66)$$

Therefore considering the condition of the contact plane, the friction coefficient was taken as 0.4 for the analytical study. The effect of this assumed value on dynamic response is discussed in Chapter VII.

Finally, combining the measured and estimated data for the expansion joint, its force vs. relative displacement relation was established as shown in Fig. 4.4. Since the vertical contact force at the expansion joint in the bridge model is estimated to be approximately 380 lbs, a friction force of approximately 0.4 x 380 lbs in the longitudinal direction can be developed. Under this force the rubber pad can deform approximately 0.01 inch (0.4 x 380/22,800) before slippages take place. The maximum elastic elongation of the tie bar is approximately 0.01 inch (650/64,700) and the maximum total tie bar force (2 bars) is approximatly 2 x 650 lbs.

2. Static and Dynamic Tests for Side Subassemblage - After one side subassemblage composed of the side girder, column and abutment was fablicated, both a free vibration test and a static load-deflection test were conducted [25]. These test results provided valuable information in determining stiffness properties of the components and also in formulating an analytical model.

The side subassemblage was first excited manually in both horizontal and vertical directions. Since the frequencies decreased slightly with amplitude of vibration, the frequencies corresponding to those amplitudes developed during high intensity seismic excitations were estimated through extrapolation to give

$$F_H^S \simeq 5.8 \text{ Hz} \quad \text{horizontal vibration}$$

$$F_V^S \simeq 9.5 \text{ Hz} \quad \text{vertical vibration} \qquad (67)$$

The side subassemblage was then subjected to an increasing static load up to 400 lbs in the horizontal radial direction and the resulting load vs. deflection relation was measured.

From the test results, the flexural rigidity of the side girder around its weak axis was calculated from the measured natural frequency of vertical vibration. Since the boundary condition of the side girder in that direction was well defined, the flexural rigidity thus determined was considered to be sufficiently reliable.

The natural frequencies of the side subassemblage were then calculated based on the known stiffness properties and boundary conditions and they were compared with the measured results. From these comparisons it was found that the calculated natural frequency in the horizontal direction was approximately 25% higher than the measured result. Because of this discrepancy,the boundary condition of the experimental model was re-examined and it was found that significant flexibility existed in the abutment allowing a rotation to develop around the vertical (z) axis [25]. The abutment steel cover was not sufficiently stiff to provide full fixity to the side girder in that direction. Some flexibility for the rotational component was then introduced into the analytical model so that the calculated natural frequency would match the measured value.

Finally, a static load was applied to the corrected analytical model described above and its static load vs. deflection relation was compared with the measured relations. As shown in Fig. 4.7, both relations are in good agreement.

Based on the good agreement finally achieved in the static load vs. deflection relation, it was felt that the stiffness properties and boundary conditions of the side subassemblage had been determined with sufficient accuracy to be used in formulating the analytical model of the whole bridge model.

3. Small Amplitude Dynamic Properties of the Model - Free vibration tests and forced harmonic excitation tests were conducted to determine the small amplitude dynamic characteristics of the complete model. The free vibration tests were initiated by hand and it was found that the first vibration mode consisted of longitudinal motion of the center girder/column subassemblage combined with antisymmetrical motion of the side subassemblages [23]. The natural frequency of this mode was found to be

$$F_L \simeq 5 \text{ Hz} \tag{68}$$

The second free vibration mode was found to be essentially a symmetric rigid body motion of the superstructure in a horizontal plane. The natural frequency of this mode could not be clearily obtained however since the first free vibrations mode was always excited making it difficult to measure the second mode frequency. This difficulty was encountered even when the test was performed by displacing the structure into essentially a second mode shape and suddenly releasing it by fracturing the tensioned cables attached at three symmetrical points of the model [23]. It should be noted that to excite a particular mode, the excitation should be applied so that a maximum of energy is transferred to this mode with a minimum of energy transferred to its neighboring modes [33]. As described above, the vibration shape of the side subassemblage were similar for both the first and the second modes; thus increasing the difficulty of manually exciting either mode without the other being presented. Furthermore, the second natural frequency is close to the first natural frequency; thus, causing additional difficulty in distinguishing the higher mode from the lower mode.

Forced harmonic excitation tests were conducted by sweeping the frequency of table input motion from 5.5 Hz to 7.5 Hz for transverse vibration and from 8 Hz to 10 Hz for vertical vibration. The table acceleration amplitude was held constant over both frequency ranges. From these tests, it was found that the transverse vibration mode was essentially the same as that observed from the free vibration test and the vertical vibration mode produced vertical motions primarily in the side girders. Resonant curves of response amplitude are shown in Fig. 4.8 for the transverse vibration. The natural frequency and damping ratio determined from this test were

$$\left.\begin{aligned} F_T &\simeq 6.6 \text{ Hz} \\ \xi &\simeq 6\% \text{ of critical} \end{aligned}\right\} \text{ transverse vibration} \qquad (69)$$

For vertical vibrations, the amplitudes could not be easily measured so that only the natural frequency was measured, i.e.,

$$F_V \simeq 9 \sim 10 \text{ Hz} \quad \text{vertical vibration} \qquad (70)$$

4. Seismic Behavior of the Model - The model was subjected to six different earthquake excitations in the Series IV test program. Three of these excitations designated as Tests H1, H2, and H3 consisted of horizontal motion only while the other three excitations designated as Tests HV1, HV2, and HV3 consisted of both horizontal and vertical motions.

The horizontal excitation was prescribed by an artificially generated accelerogram previously defined for post earthquake studies of the Olive View Hospital [28]. The vertical excitation was also prescribed by an artificially generated accelerogram [24]. The peak vertical excitation was chosen to be approximately one half the peak horizontal excitation. Both vertical and horizontal excitations were scaled in time 1/5.5 so as to satisfy the time scale factor T_r. The acceleration response spectra for the motions measured on the shaking table during Tests H1, H3, and HV2 are shown in Fig. 4.9. It is observed that although there are some discrepancies in the amplification factors, the maximum response spectral values occured at approximately 10 Hz for both the horizontal and vertical motions.

Peak table accelerations, maximum horizontal response of center girder, initial tie gaps, and observed damages for the six excitation tests are summarized in Table 4.1. The superstructure and the abutments suffered no visiable structural damages throughout this series of tests. The columns suffered no damage except for one weak column that suffered a slight hair crack at its base. The shear keys of the expansion joints, especially at expansion joint No. 2, suffered severe spalling of concrete during Tests H3 and HV3 requiring that they be replaced after these particular tests. The tie gaps were set at almost zero values before Tests H1 and HV1; however, for the other tests, the initial tie gaps were controlled by the previously accumulated elongations of the tie bars. Collisions occurred in the expansion joints during Test H3, HV1, HV2 and HV3. Sometimes during high intensity excitations, impact at one joint would immediately cause impact to occur at the other joint. Thus, multiple collisions were observed between the center girder and the two side girders. The sounds produced by the impacts were quite severe in intensity.

The relation between peak horizontal table acceleration and maximum horizontal displacement at the deck center is plotted in Fig. 4.10. From this relation, it is observed that the maximum response of the model increases almost linearly with peak table acceleration in the lower intensity range; however, a scatter of maximum response values is observed in the higher intensity range, i.e. for Tests H3, HV2 and HV3. Although Tests H3 and HV2 were conducted using almost the same intensity of horizontal table accelerations, namely 0.5G, the maximum response for Test H3 is approximately 50% larger than that produced in Test HV2. Certainly the presence of the vertical excitation in Test HV2 cannot be credited with this 50% difference. The same discrepancy is observed when comparing the results obtained in Tests HV2 and HV3. Test HV3 followed immediately after the Test HV2 and used almost the same intensities of table motion. To explain this discrepancy, it is necessary to recall that a shear key in expansion joint No. 2 which was undamaged after Test HV2 suffered severe spalling failure during Tests H3 and HV3. Thus, it is believed that failure of the shear key allowed large transverse relative motions to take place between the girders at the expansion joint, which, in turn, resulted in a significant increase in overall response of the complete bridge model. It is of interest to speculate why the shear key failed during Tests H3 and HV3 but did not in the previous Test HV2. The initial and boundary conditions for the superstructure, columns and abutments are the same for all three tests; however, the initial tie gaps were different. For Test HV2 the initial tie gaps were small since little yielding of the tie bars had taken place during Test HV1. Due to yielding of the tie bars which occurred during the previous tests, the initial gaps were reasonably large for Tests H3 and HV3. It should be noted that when superstructure motion takes place in the outward direction, only the tie bars resist the motions at the expansion joints. Hence the large initial tie gaps in Tests H3 and HV3 allowed the model to build up large transverse oscillations before the tie bars became effective. These large oscillations were sufficient to cause failure of the shear key.

Based on the above considerations of model response, three tests were chosen among the six conducted for correlation purposes, namely, Tests H1, H3 and HV2. Test H1 represents a typical response for low intensity excitation. No yielding of tie bars or collisions of girders took place in this test. Tests H3 and HV2 on the other hand represent typical response for high intensity excitations. Yielding of the tie bars and multiple collision did take place in these tests. In addition, a failure of the shear key is believed to have taken during Test H3.

Test H1 - The model was subjected to low intensity excitation with a peak acceleration of 0.11G in the transverse (Y) horizontal direction. The table acceleration and the measured responses of displacement are displayed in Figs. 4.11 and 4.12, respectively.

During this test, collisions of the girders did not occur since the relative response displacements at the expansion joints remained below the initial joint gap of approximately 0.05 inch. The joint restrainer tie bars however resisted the joint separations. It was found by inspection following the test that yielding of the tie bars had not taken place. Since the tie bars resisted only joint separation, the displacement response was small in the outward direction but large for the inward direction. While some non-symmetrical model response was observed, the major response was primarily in a symmetrical mode. This type of response should be expected due to the symmetry conditions of model and seismic loading.

Test H3 - During this test, the model was subjected to high intensity excitation having a peak acceleration of 0.5G in transverse (Y) horizontal direction. The table acceleration and the measured responses of displacement are displayed in Figs 4.13 and 4.14, respectively.

Multiple collisions of the girders together with yieldings of the joint restrainer tie bars took place at the expansion joints. Furthermore, spalling failure of the transverse shear key took place at expansion joint No. 2. Like Test H1, the responses of displacement, especially at the expansion joints, were somewhat unsymmetrical. However they were of a type opposite to that developed in Test H1, i.e. the motions were large in the outward direction and small in the inward direction. This type of response was caused by closure of the joints during inward motion causing stiff arch action to take place between abutments while motion in the outward direction was resisted mainly by the more flexible tie bars. The maximum opening at expansion joint No. 2 equal to approximately 0.35 inch exceeded that of expansion joint No. 1 by a factor of approximately 2. Hence adding the maximum closure (initial joint gap) of approximately 0.05 inch to the maximum opening, the total relative displacement of the joint was approximately 0.4 inch which corresponds to 4/5 of the hinge seat length. This implies that the center girder was supported on only a 0.1 inch hinge seat at the expansion joint. The damages of the rubber pad observed after this test were undoubtedly caused by this severe relative motion.

It was observed from the measured response that substantial drift, especially at expansion joint No. 2, took place during the excitation.

Once this drift developed, the subsequent responses did not return to their original values but simply vibrated the new drifted positions. It should be noted that although the spalling failure of the transverse shear key allowed a large relative transverse movement to take place between the girders, it had essentially nothing to do with the observed drift in response. Most likely this drift was caused by a combination of concrete fractures in the shear key and tearing of the rubber pad in the joint. Obviously, such drift could not be predicted analytically.

Test HV2 - During this test, the model was subjected simultaneously to high intensity horizontal and vertical excitations having peak accelerations of 0.47G and 0.27G, respectively. The table accelerations and the measured responses of displacement are displayed in Figs. 4.15 and 4.16, respectively. The general features of this test are similar to those of Test H3 except that failure of the shear key did not take place. Therefore, the overall response of the model was more symmetrical than the response of Test H3 and drifts in response did not develop.

TABLE 4.1 PRINCIPAL FEATURES OF SEISMIC EXCITATIONS IN SERIES IV TEST

	Peak Table Input Acceleration [G]		Maximum Horizontal Response of Center Girder [inch]	Measured Initial Tie Gap Δ_T [inch]	Observed Features			
	Horizontal	Vertical			Yield of Tie Bars	Collisions	Failure of Shear Key	Permanent Drift of Response
TEST H1	0.11	——	-0.06	set to 0 for both EJs	NO	NO	NO	NO
TEST H2	0.28	——	0.13	0 for both EJs	YES	NO	NO	NO
TEST H3	0.50	——	0.40	0.03 for EJ1 0.04 for EJ2	YES	YES	YES	YES
TEST HV1	0.31	0.16	0.16	set to 0 for both EJs	YES	YES	NO	NO
TEST HV2	0.47	0.27	0.27	0.01 for EJ1 0.02 for EJ2	YES	YES	NO	NO
TEST HV3	0.46	0.25	0.42	0.07 for EJ1 0.17 for EJ2	YES	YES	YES	YES

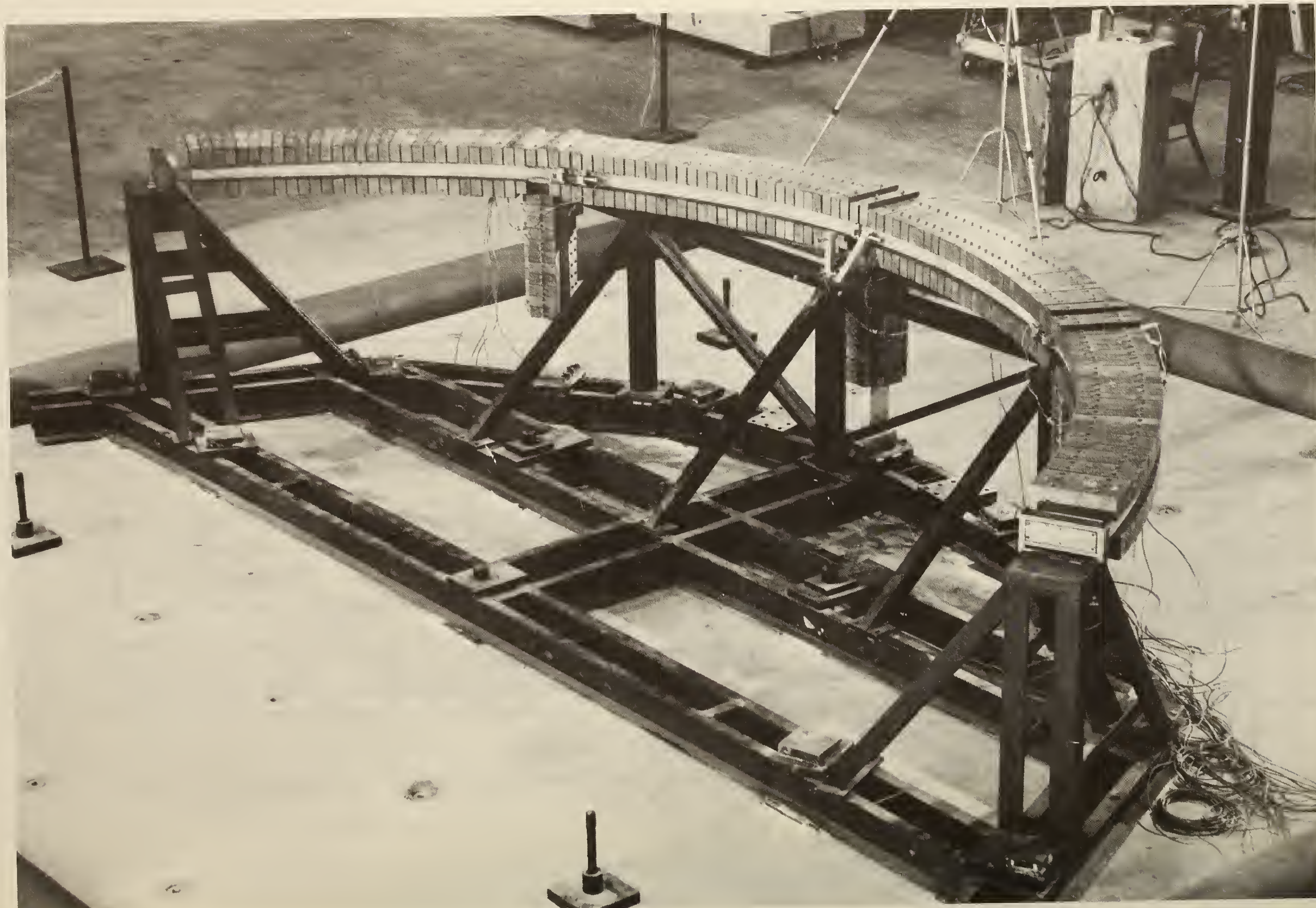

FIG. 4.1 EXPERIMENTAL MODEL BRIDGE STRUCTURE

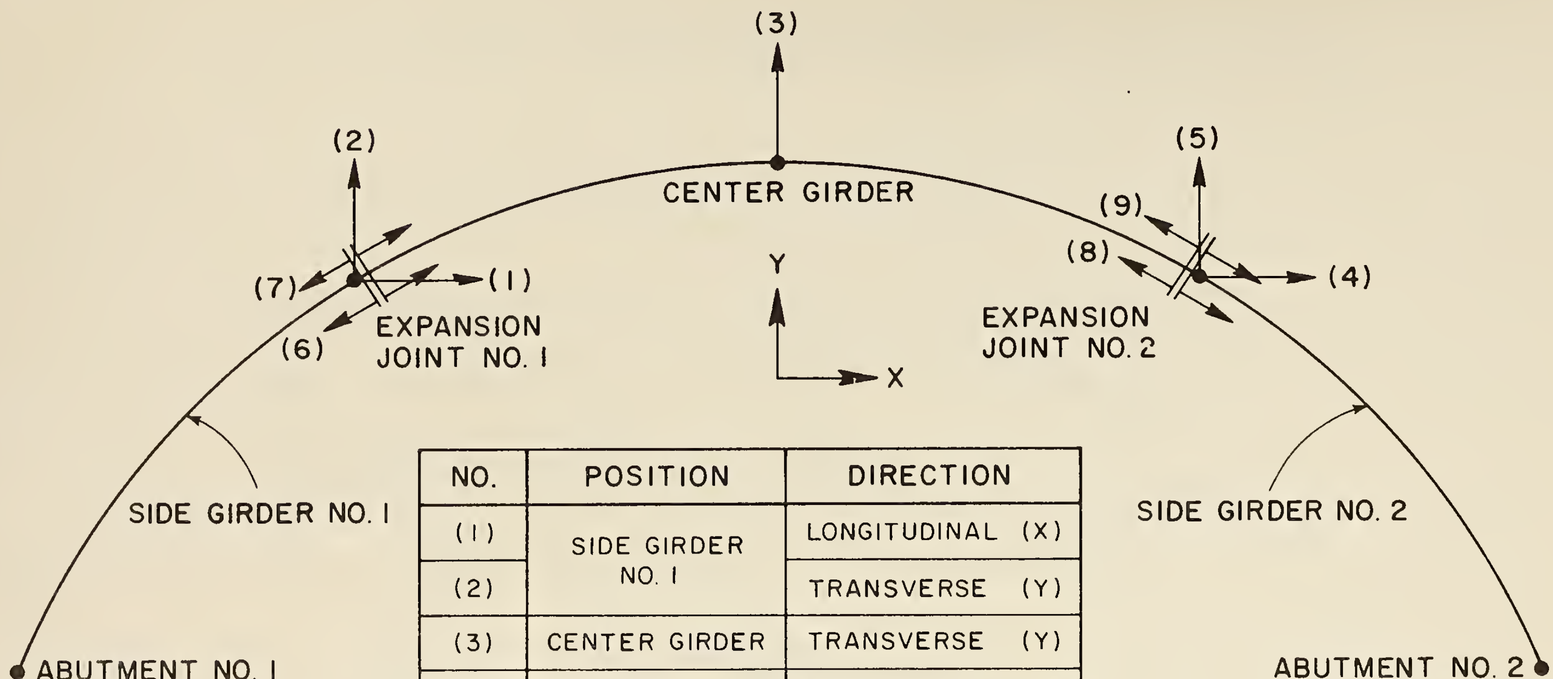

NO.	POSITION	DIRECTION
(1)	SIDE GIRDER NO. 1	LONGITUDINAL (X)
(2)		TRANSVERSE (Y)
(3)	CENTER GIRDER	TRANSVERSE (Y)
(4)	SIDE GIRDER NO. 2	LONGITUDINAL (X)
(5)		TRANSVERSE (Y)
(6)	EXPANSION JOINT NO. 1	INNER SIDE
(7)		OUTER SIDE
(8)	EXPANSION JOINT NO. 2	INNER SIDE
(9)		OUTER SIDE

ARROW (⟶) INDICATES POSITIVE DIRECTION OF RESPONSE

FIG. 4.2 MEASUREMENTS OF RESPONSE DISPLACEMENT

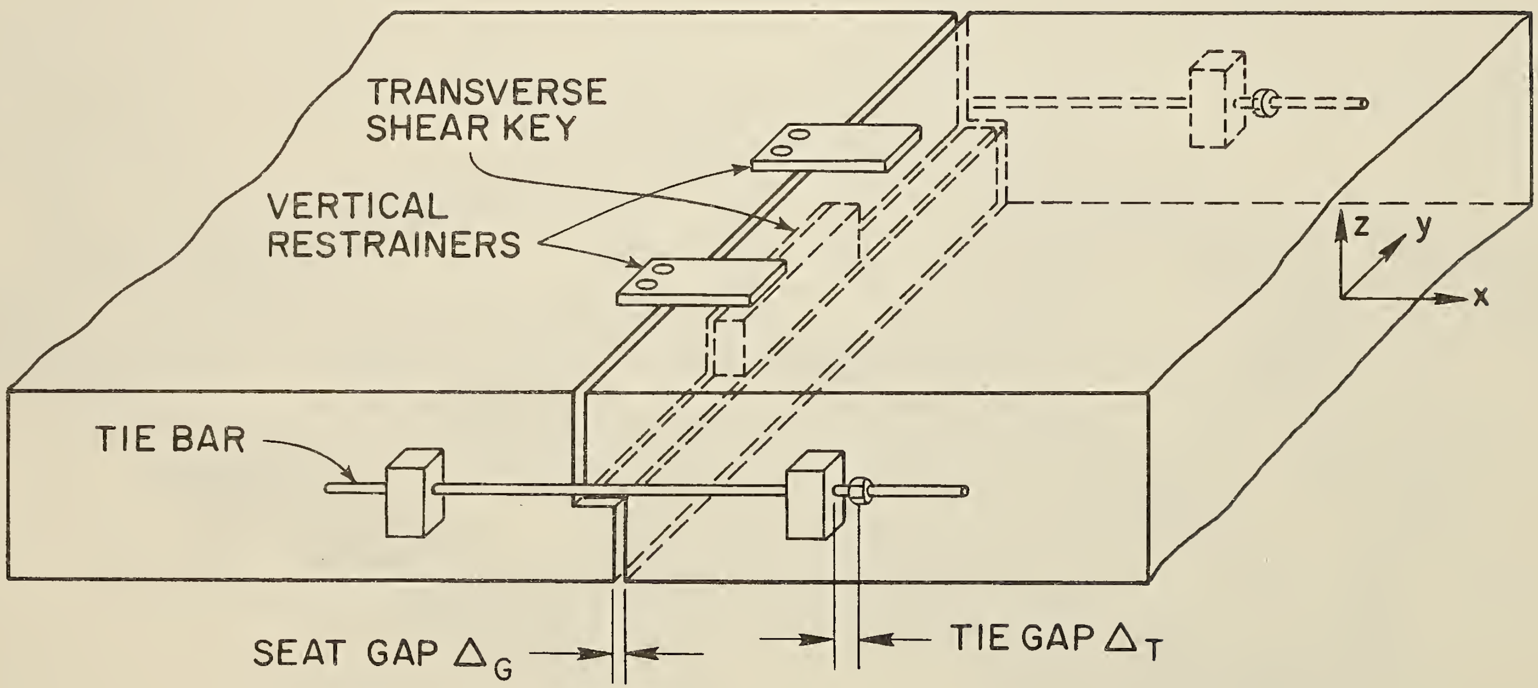

FIG. 4.3 EXPANSION JOINT OF BRIDGE MODEL

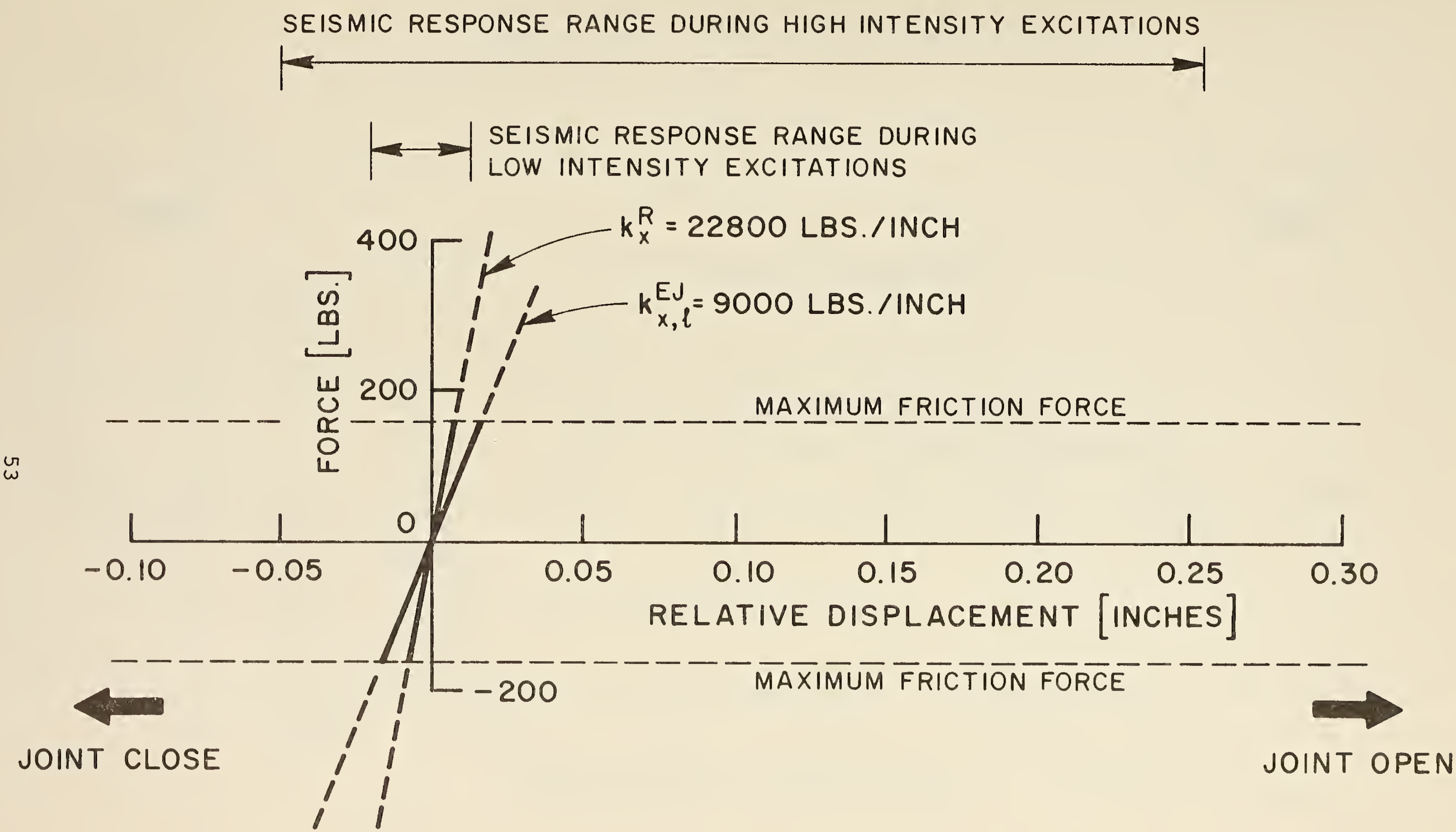

FIG. 4.4.1 ESTIMATED FORCE VS. RELATIVE DISPLACEMENT RELATION OF EXPANSION JOINT; EFFECT OF RUBBER PAD AND SLIPPAGES

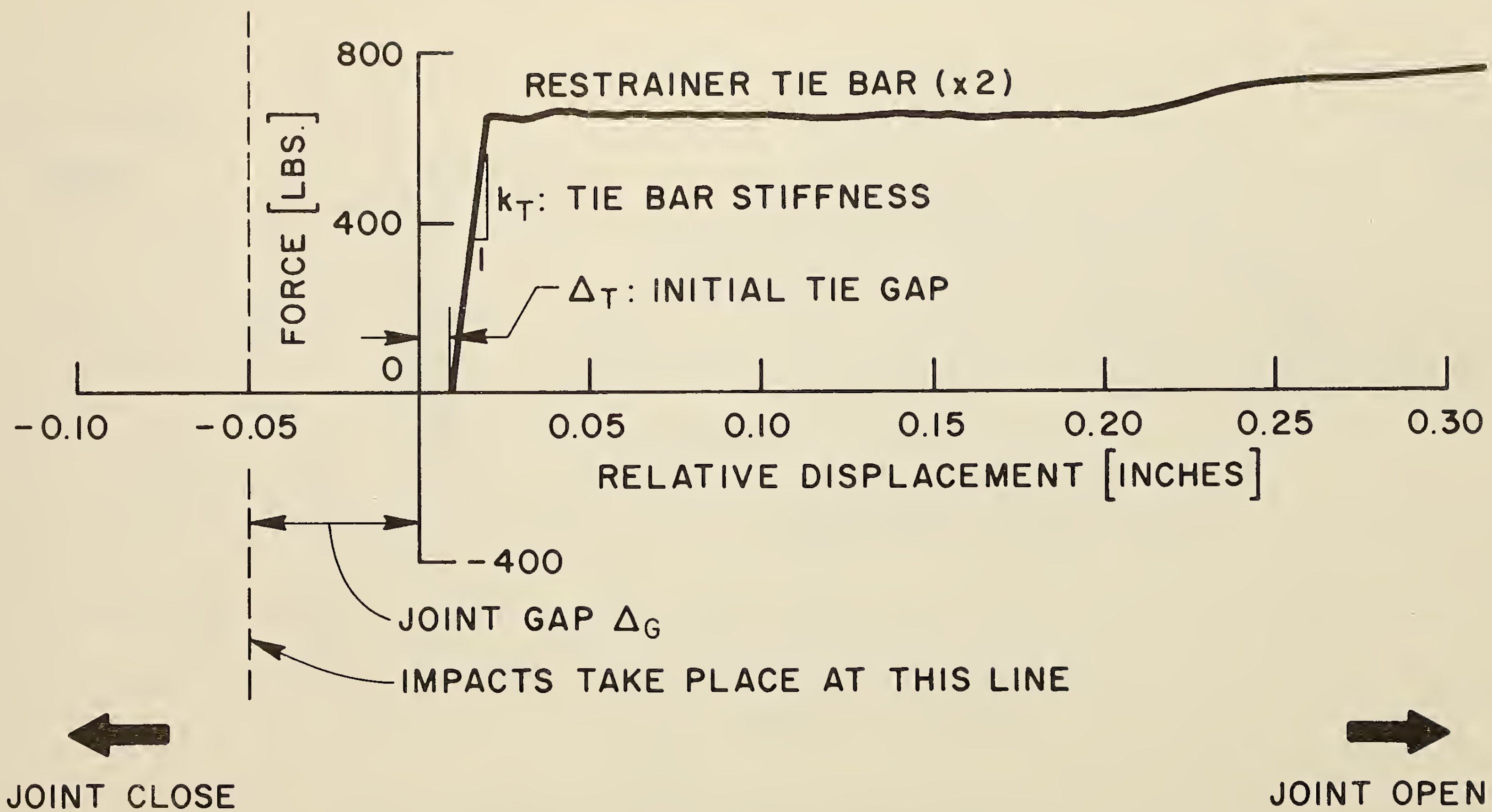

FIG. 4.4.2 ESTIMATED FORCE VS. RELATIVE DISPLACEMENT RELATION OF EXPANSION JOINT; EFFECT OF TIE BARS AND COLLISIONS

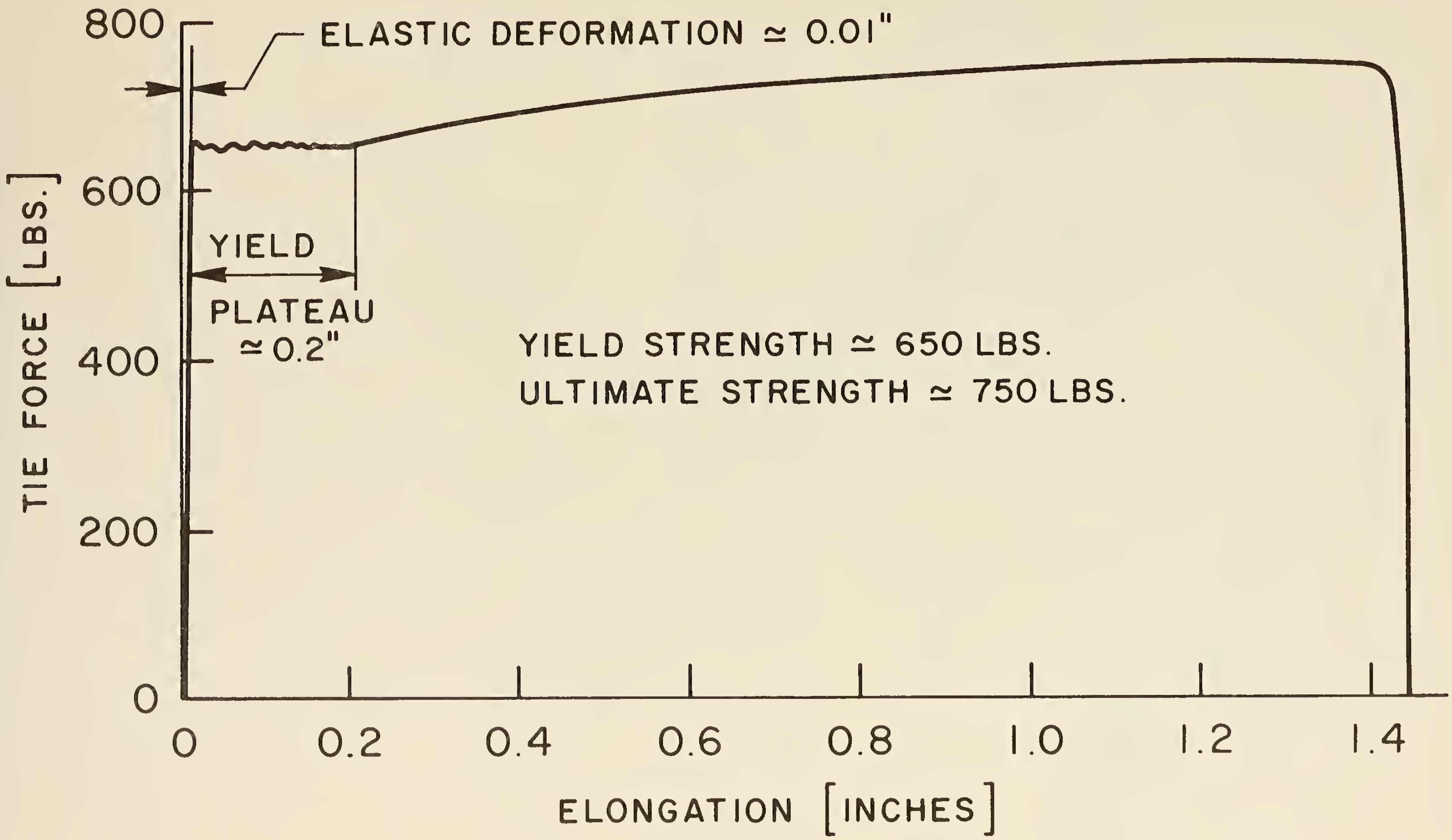

FIG. 4.5 TYPICAL FORCE VS. DEFORMATION RELATION OF TIE BAR [25]

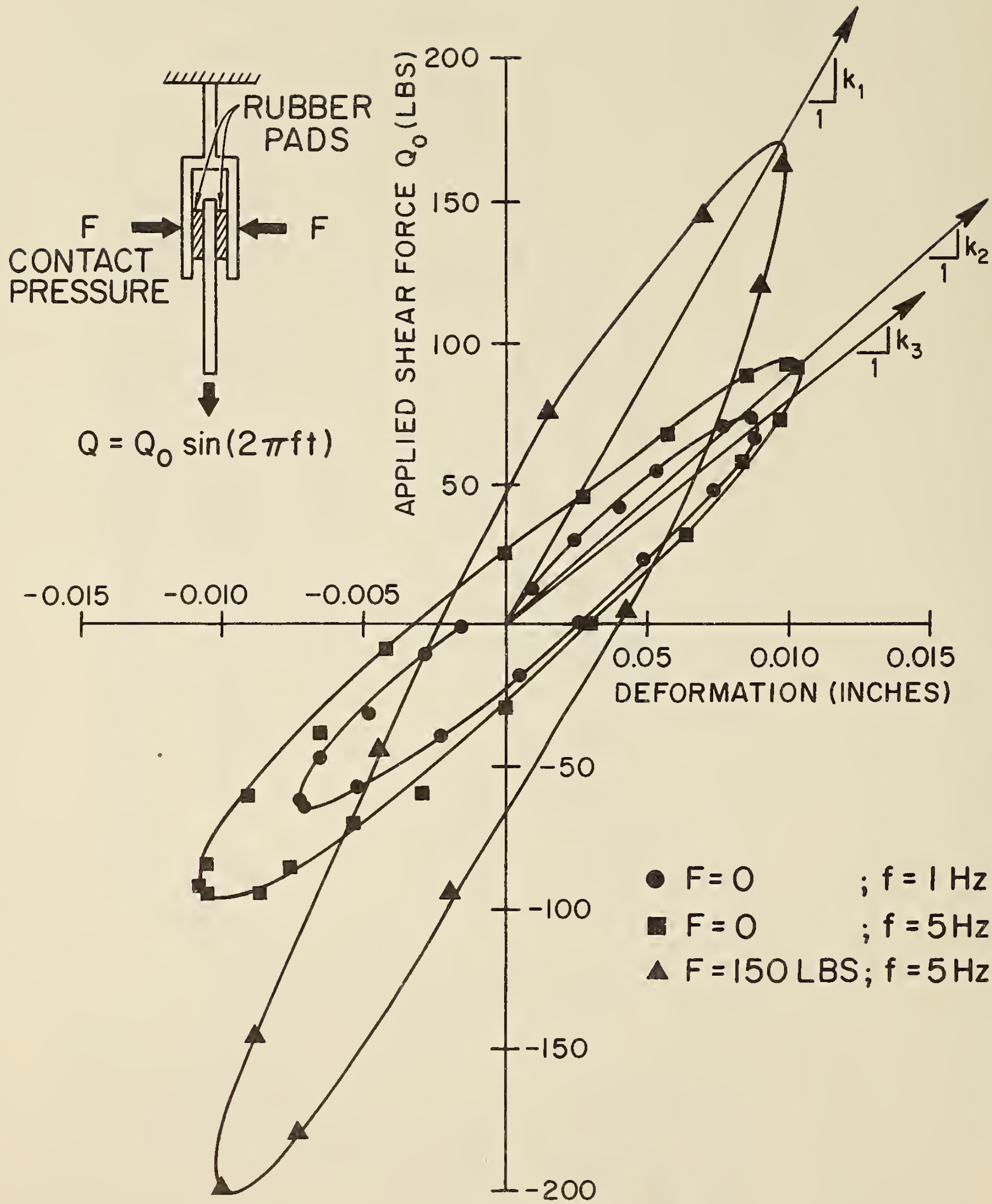

FIG. 4.6 TYPICAL FORCE VS. DEFORMATION RELATION OF RUBBER PAD [25]

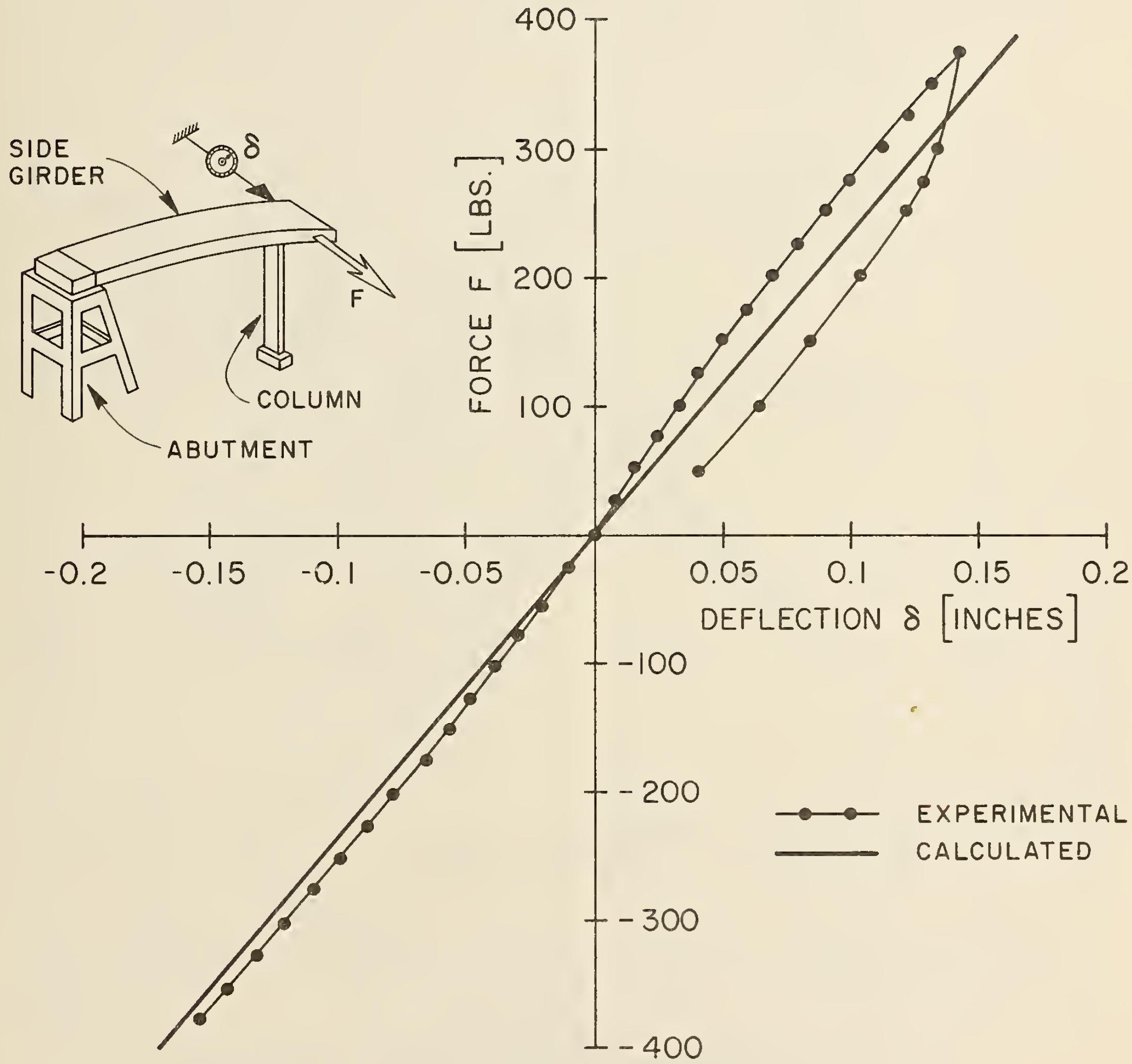

FIG. 4.7 STATIC LOAD-DEFORMATION TEST FOR SIDE SUBASSEMBLAGE [25]

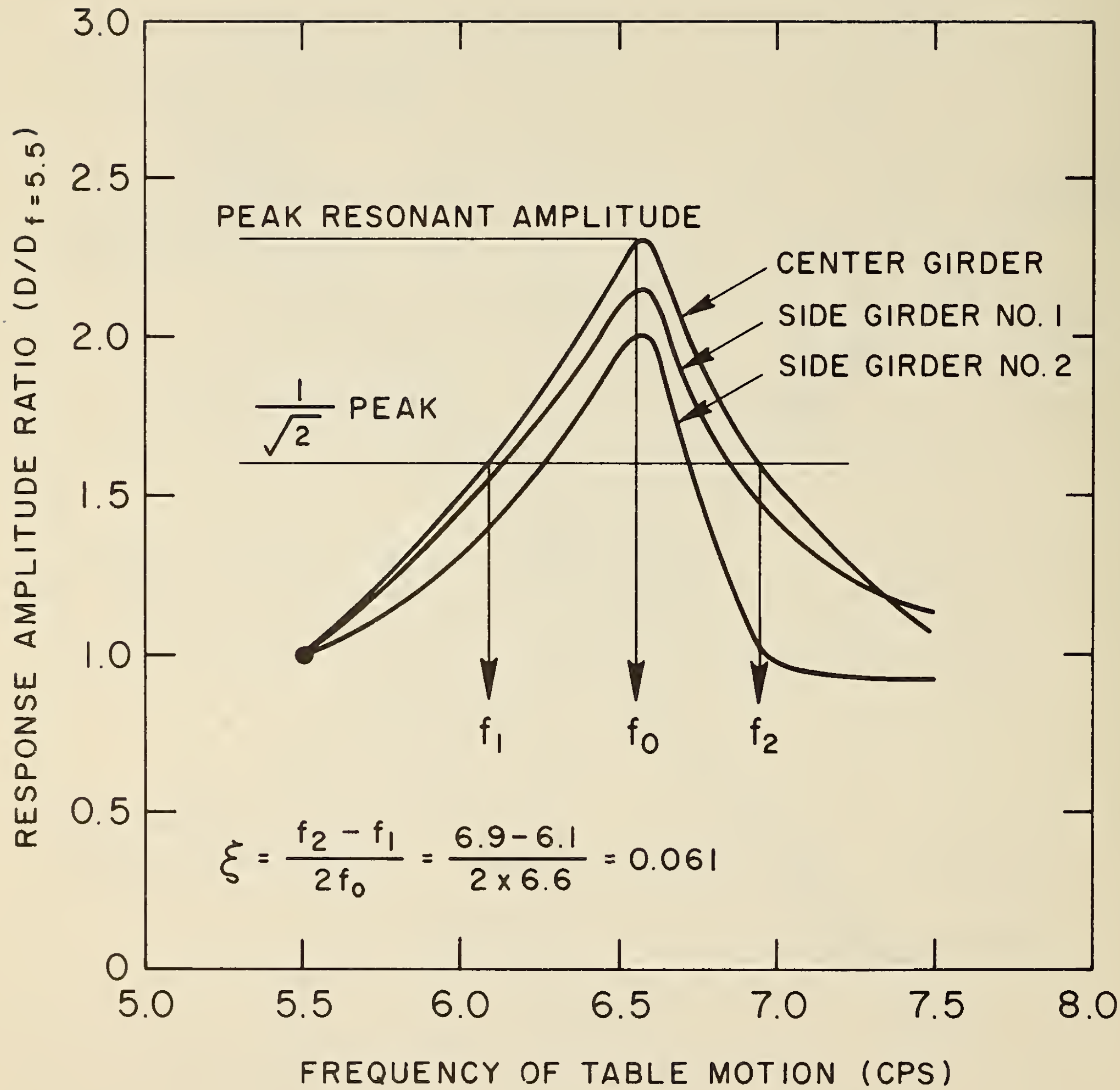

FIG. 4.8 RESONANT CURVE OF BRIDGE MODEL IN TRANSVERSE EXCITATION

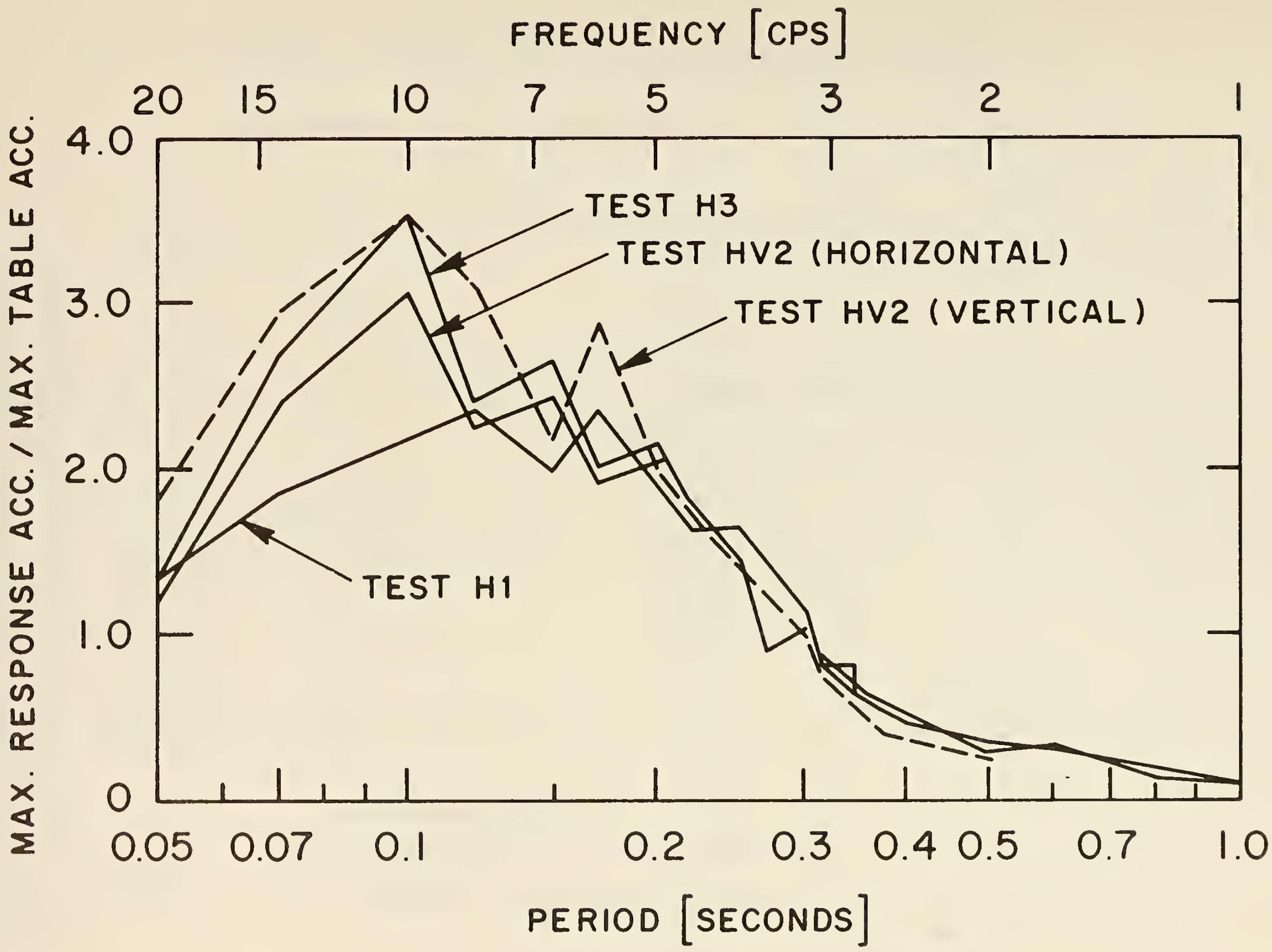

FIG. 4.9 ACCELERATION RESPONSE SPECTRUM OF TABLE MOTIONS
(TESTS H1, H3 AND HV2)

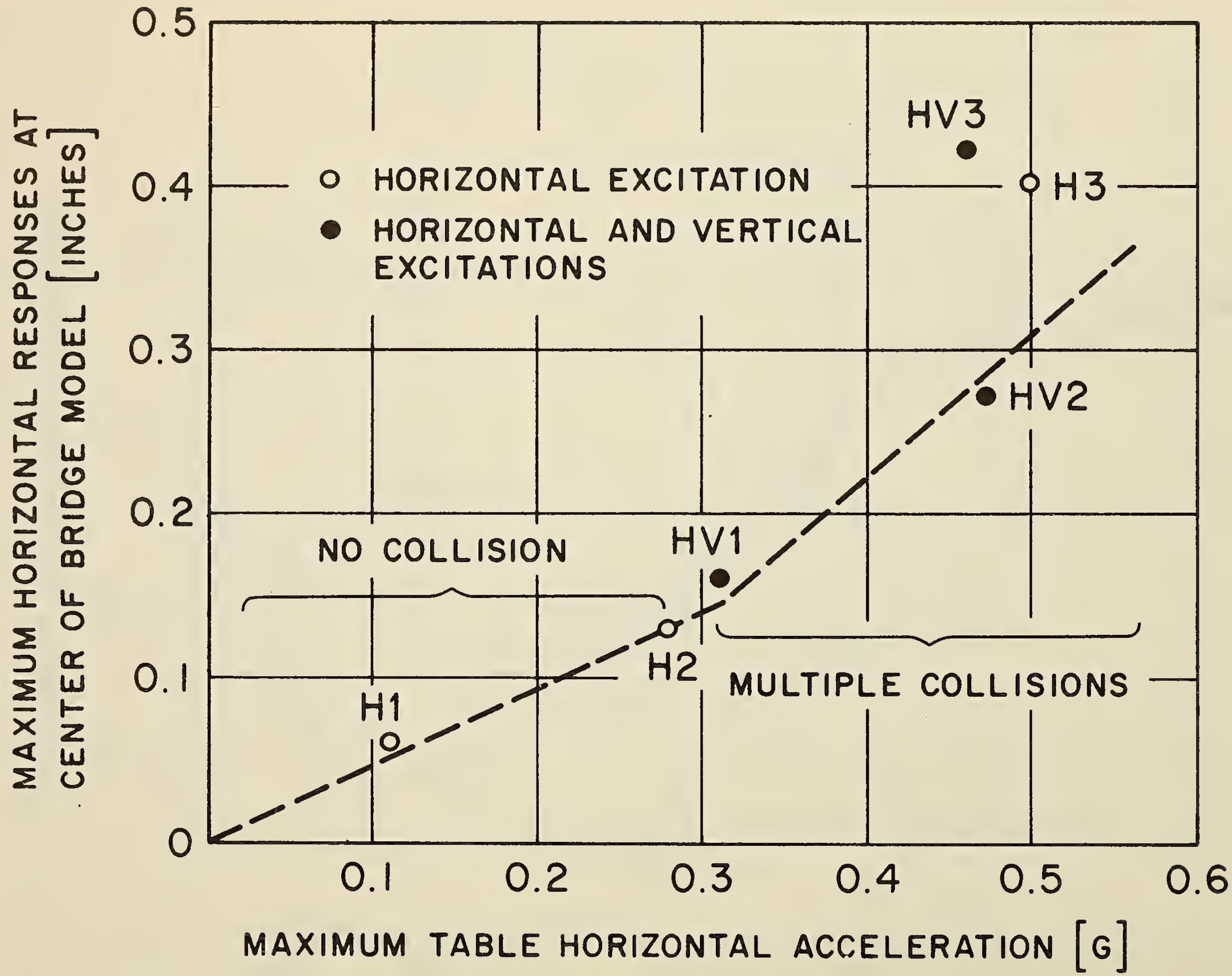

FIG. 4.10 RELATION BETWEEN MAXIMUM HORIZONTAL TABLE ACCELERATION AND MAXIMUM HORIZONTAL RESPONSE AT CENTER OF BRIDGE MODEL

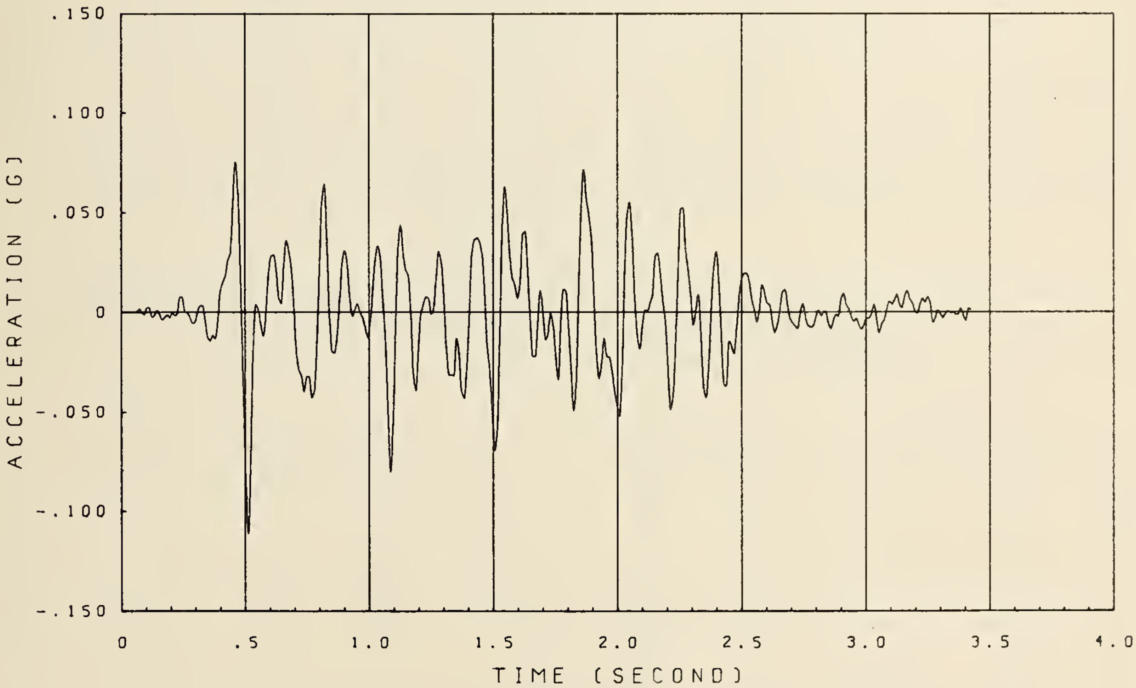

FIG. 4.11 HORIZONTAL TABLE ACCELERATION TIME HISTORY; TEST H1

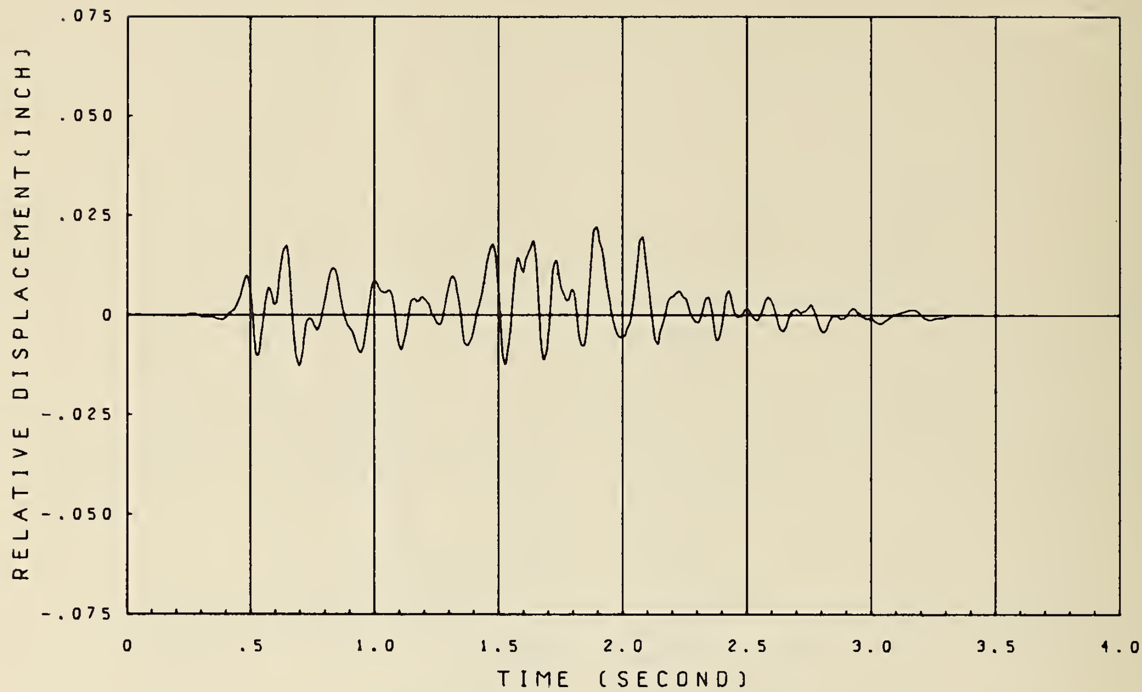

FIG. 4.12.1 MEASURED RESPONSE OF SIDE GIRDER NO. 1; LONGITUDINAL (X) DIRECTION; TEST H1

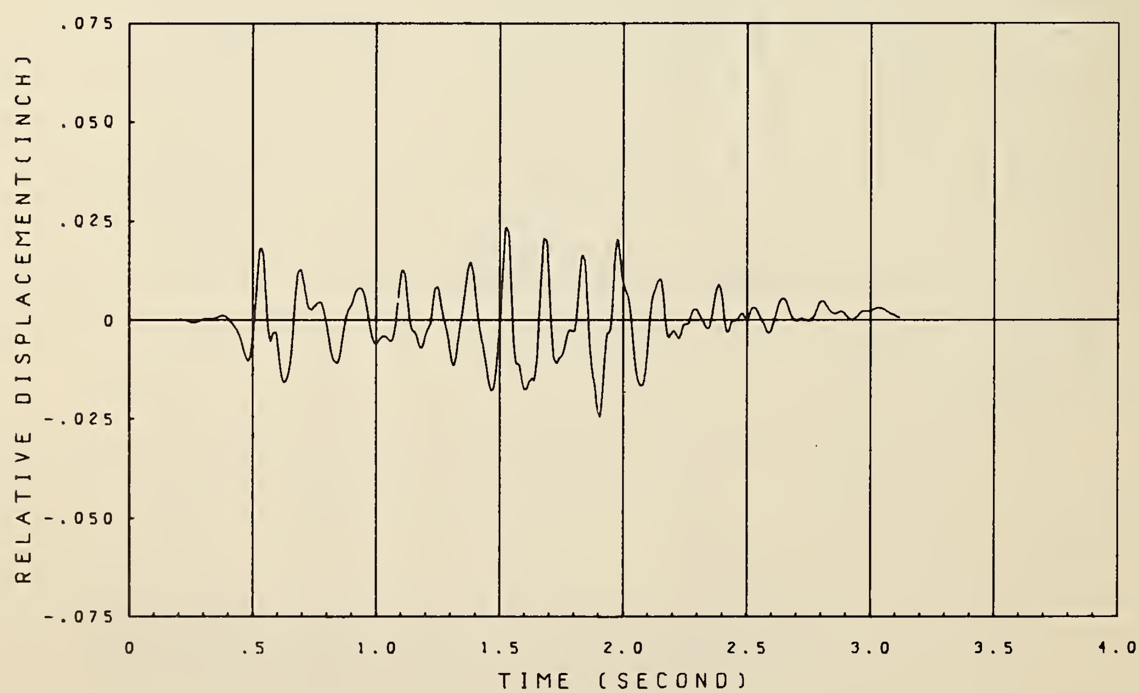

FIG. 4.12.2 MEASURED RESPONSE OF SIDE GIRDER NO. 1; TRANSVERSE (Y) DIRECTION; TEST H1

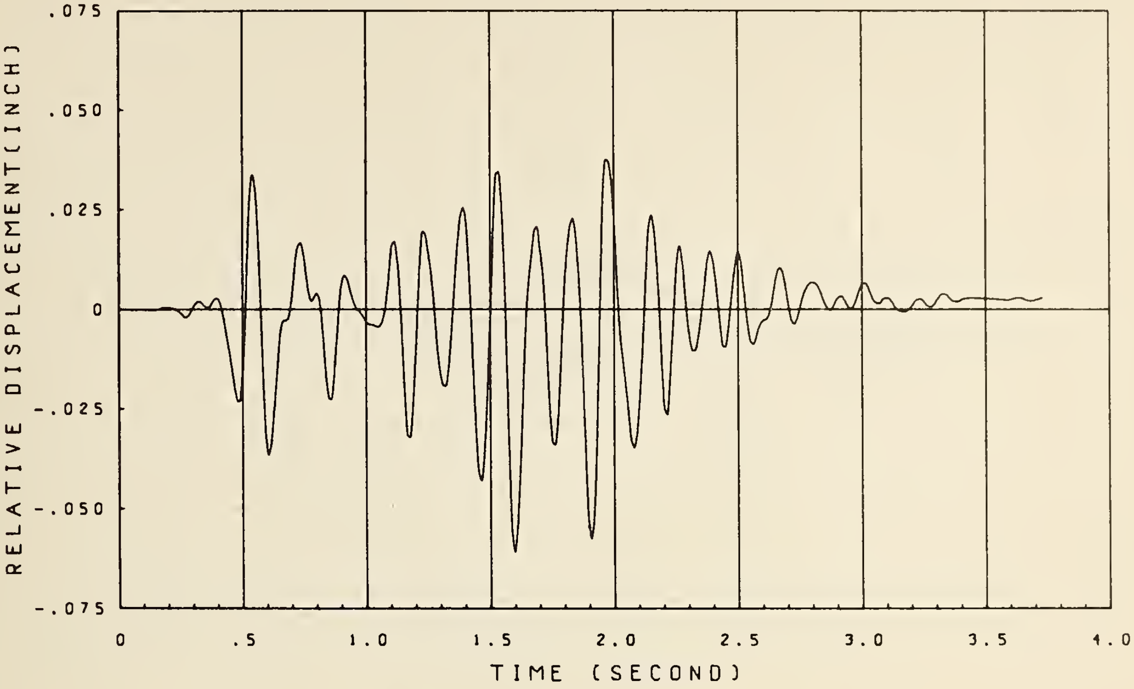

FIG. 4.12.3 MEASURED RESPONSE OF CENTER GIRDER; TRANSVERSE (Y) DIRECTION; TEST H1

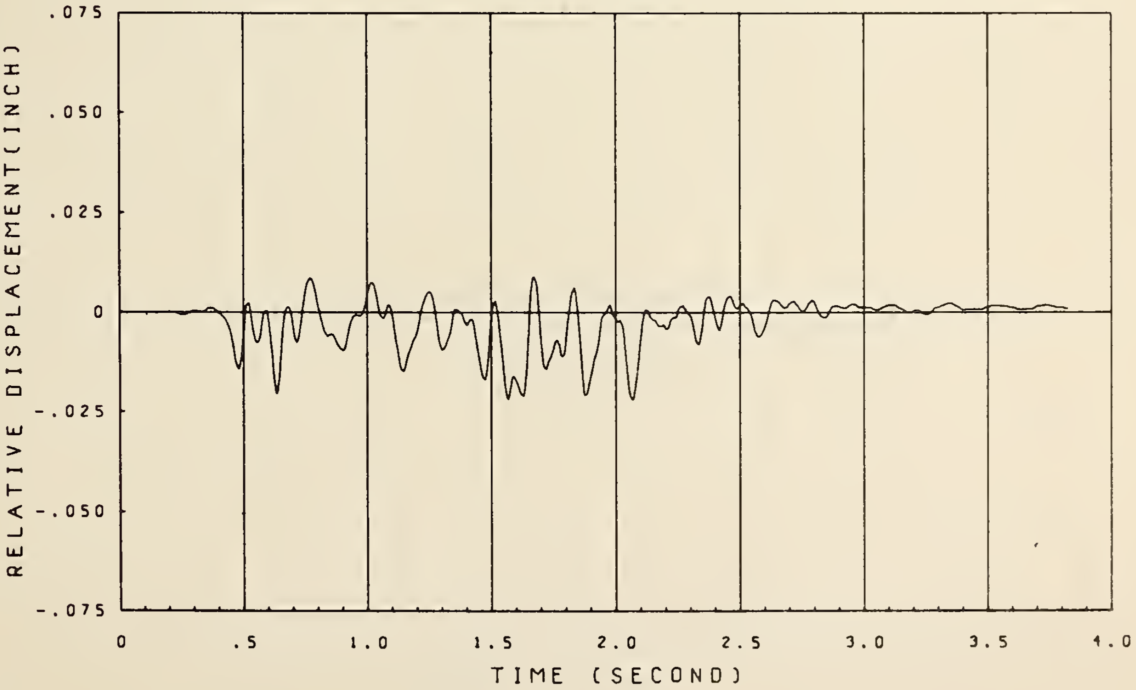

FIG. 4.12.4 MEASURED RESPONSE OF SIDE GIRDER NO. 2; LONGITUDINAL (X) DIRECTION; TEST H1

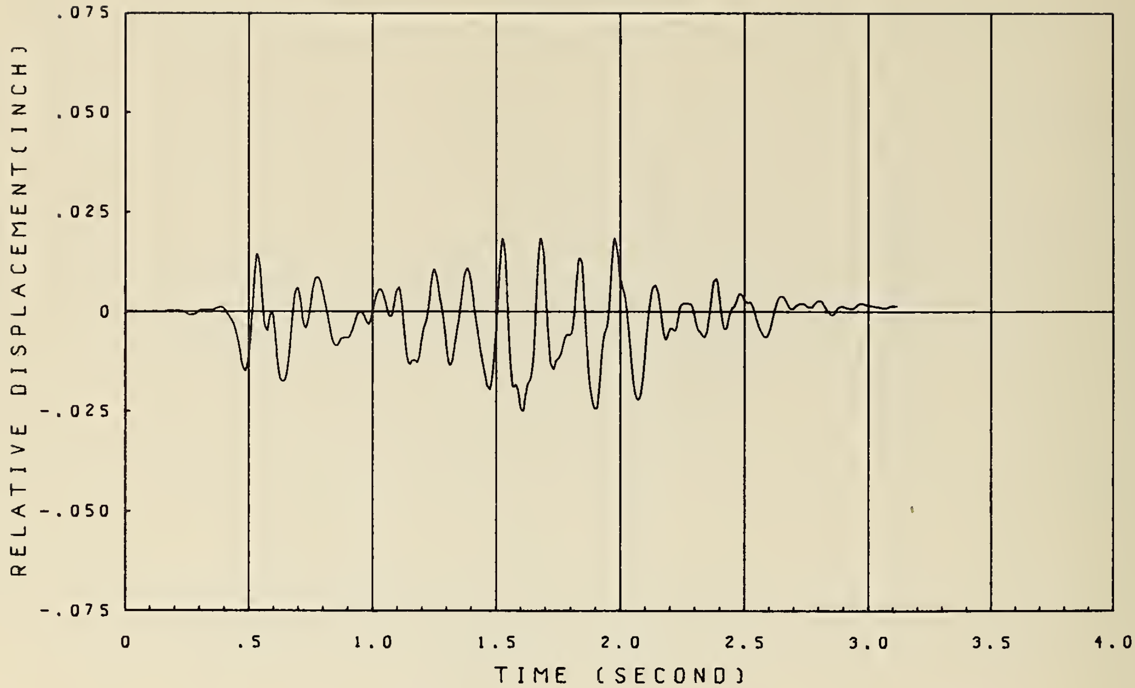

FIG. 4.12.5 MEASURED RESPONSE OF SIDE GIRDER NO. 2; TRANSVERSE (Y) DIRECTION; TEST H1

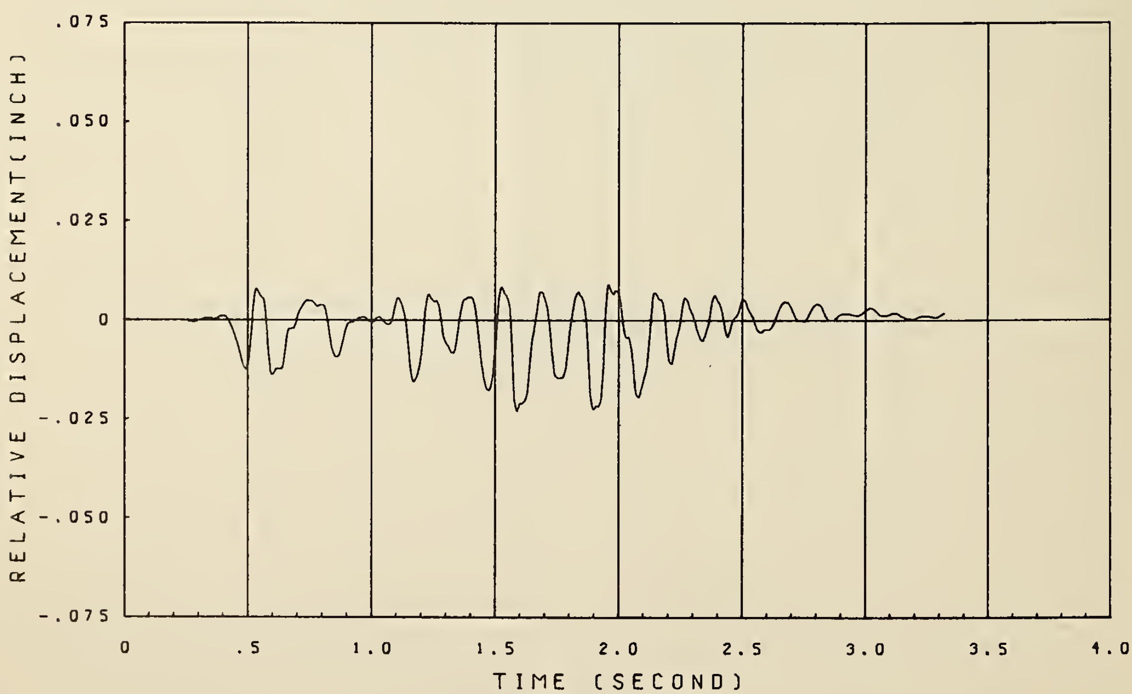

FIG. 4.12.6 MEASURED RESPONSE OF EXPANSION JOINT NO. 1; INNER SIDE; TEST H1

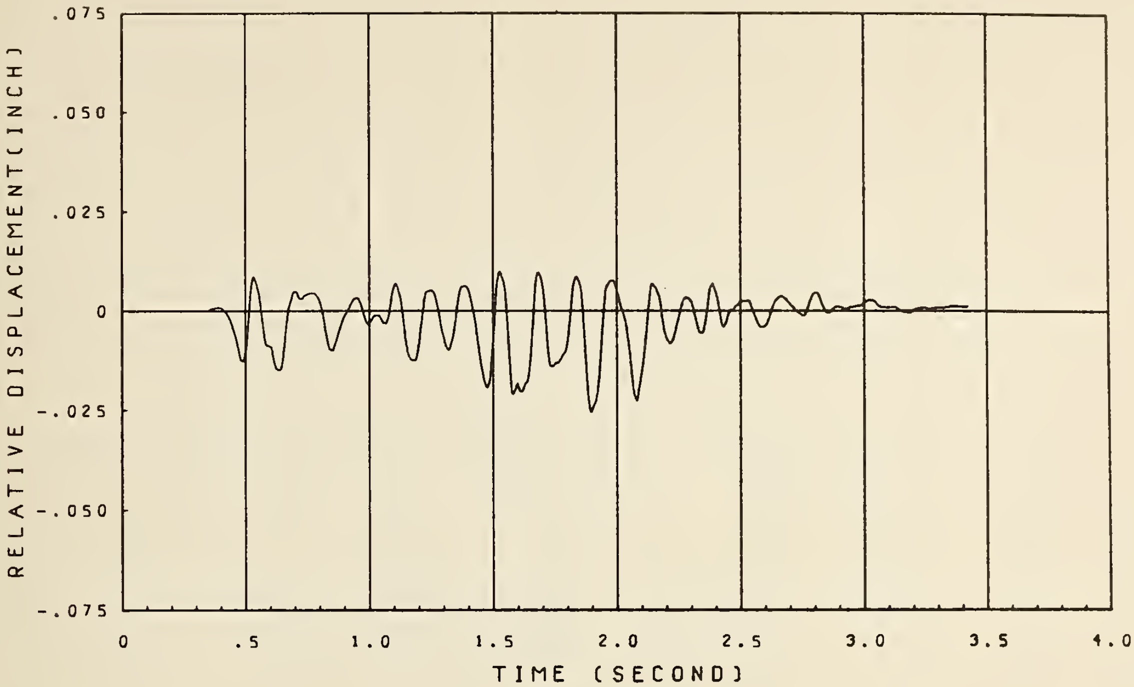

FIG. 4.12.7 MEASURED RESPONSE OF EXPANSION JOINT NO. 1; OUTER SIDE; TEST H1

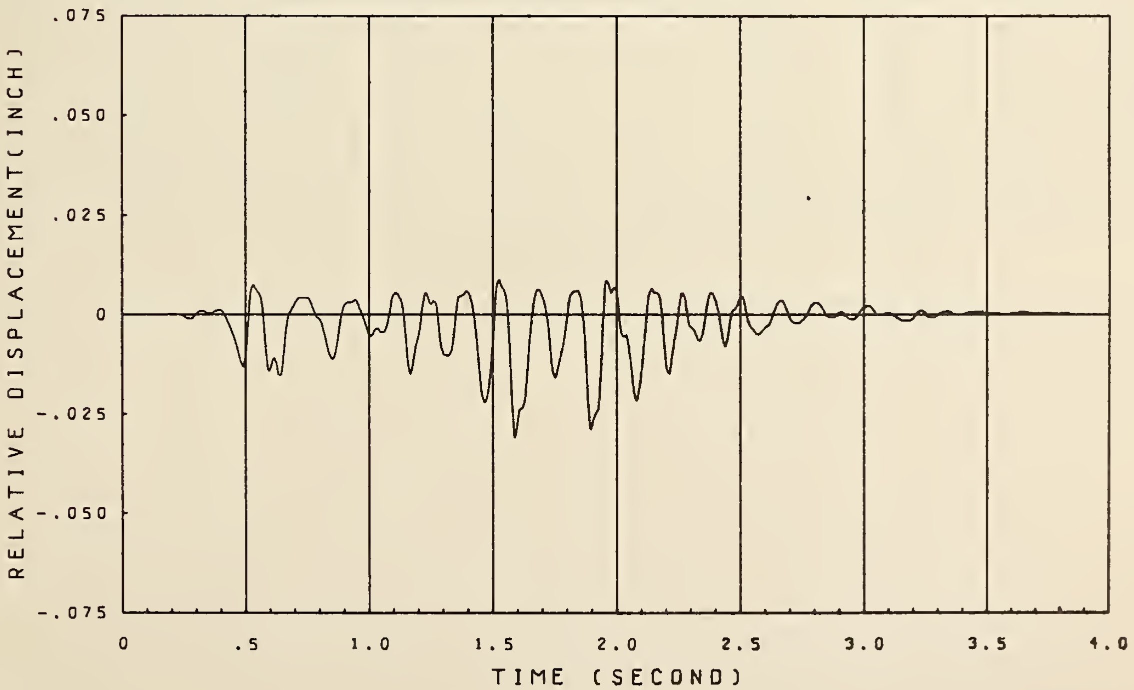

FIG. 4.12.8 MEASURED RESPONSE OF EXPANSION JOINT NO. 2; INNER SIDE; TEST H1

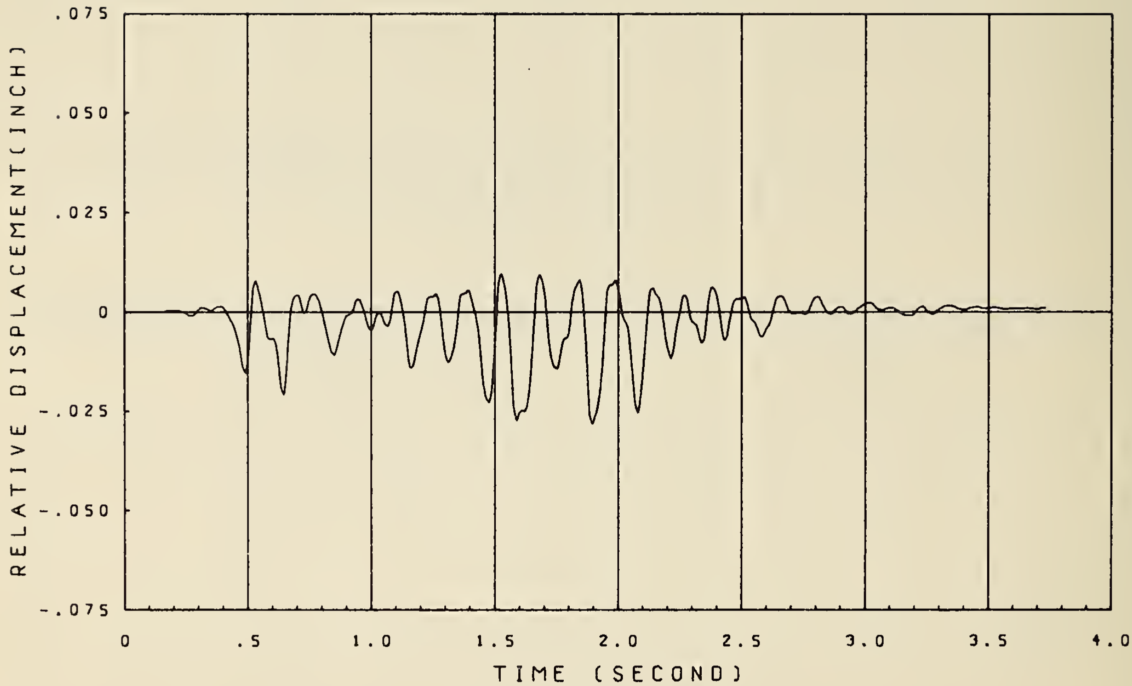

FIG. 4.12.9 MEASURED RESPONSE OF EXPANSION JOINT NO. 2; OUTER SIDE; TEST H1

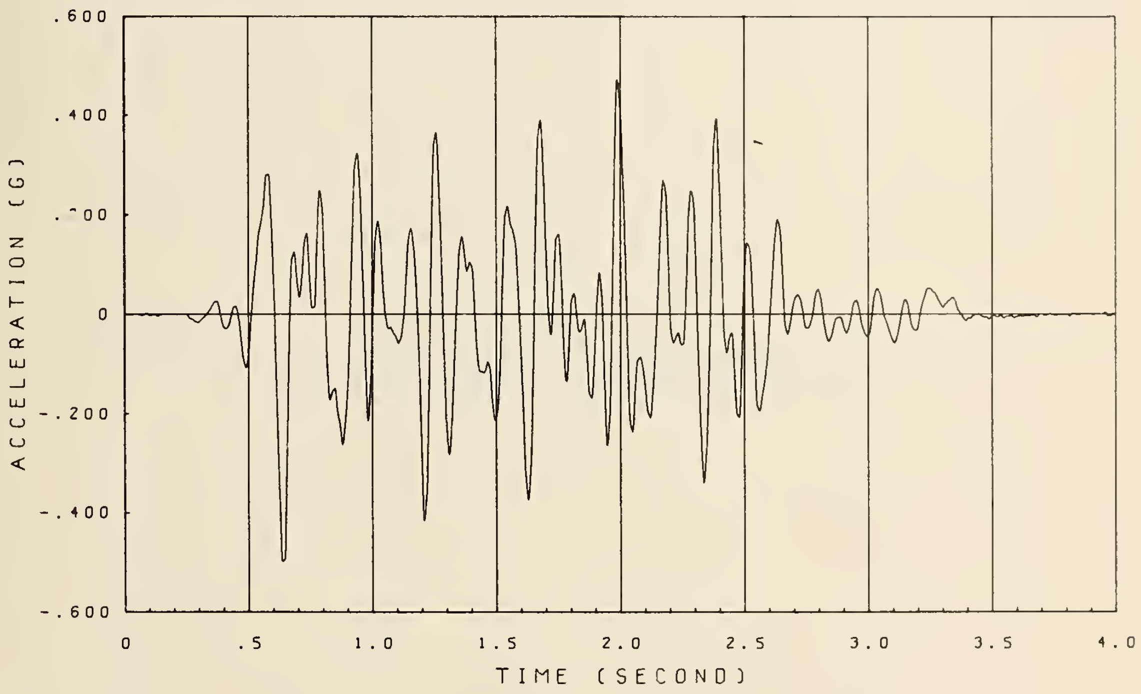

FIG. 4.13 HORIZONTAL TABLE ACCELERATION TIME HISTORY; TEST H2

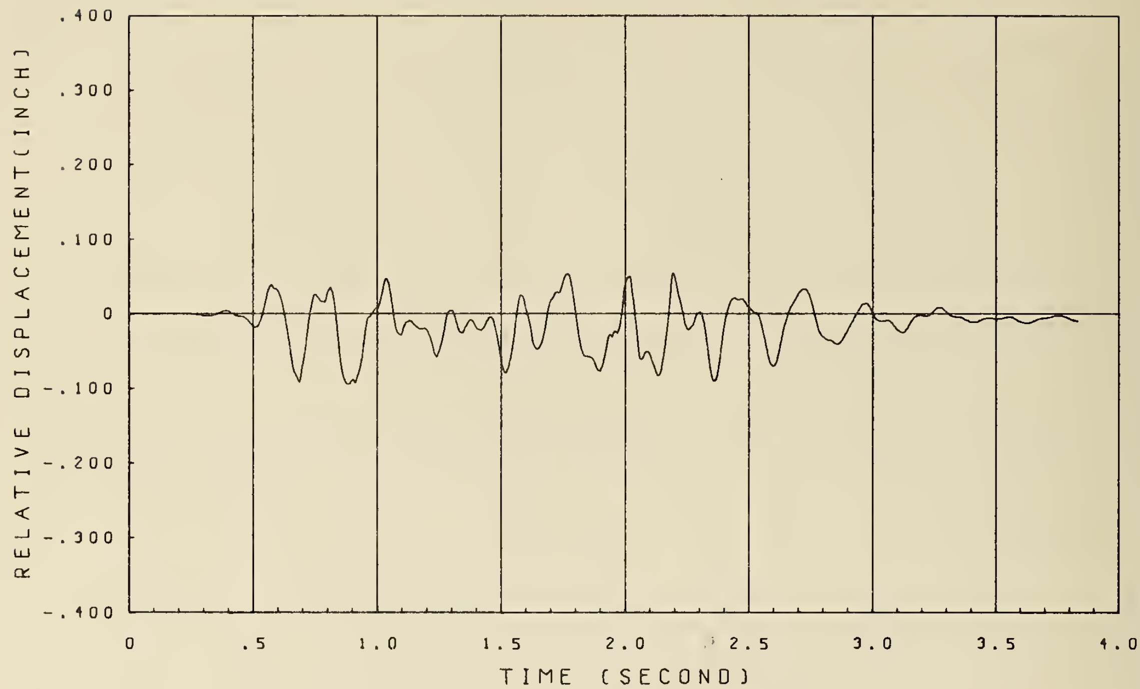

FIG. 4.14.1 MEASURED RESPONSE OF SIDE GIRDER NO. 1; LONGITUDINAL (X) DIRECTION; TEST H2

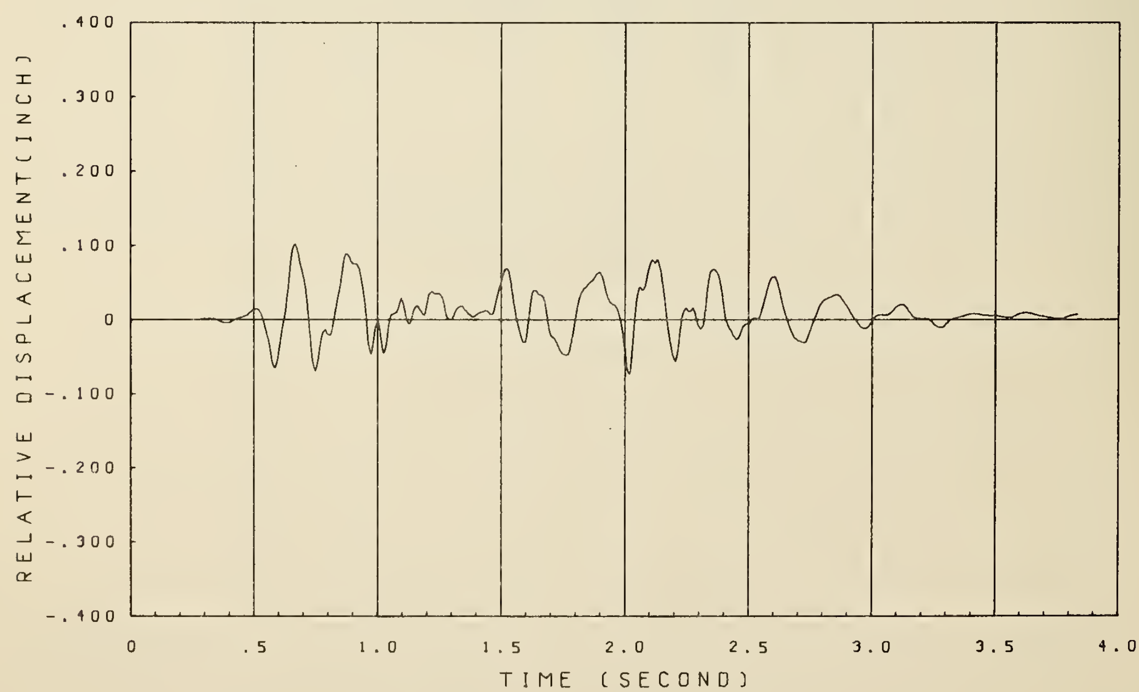

FIG. 4.14.2 MEASURED RESPONSE OF SIDE GIRDER NO. 1; TRANSVERSE (Y) DIRECTION; TEST H2

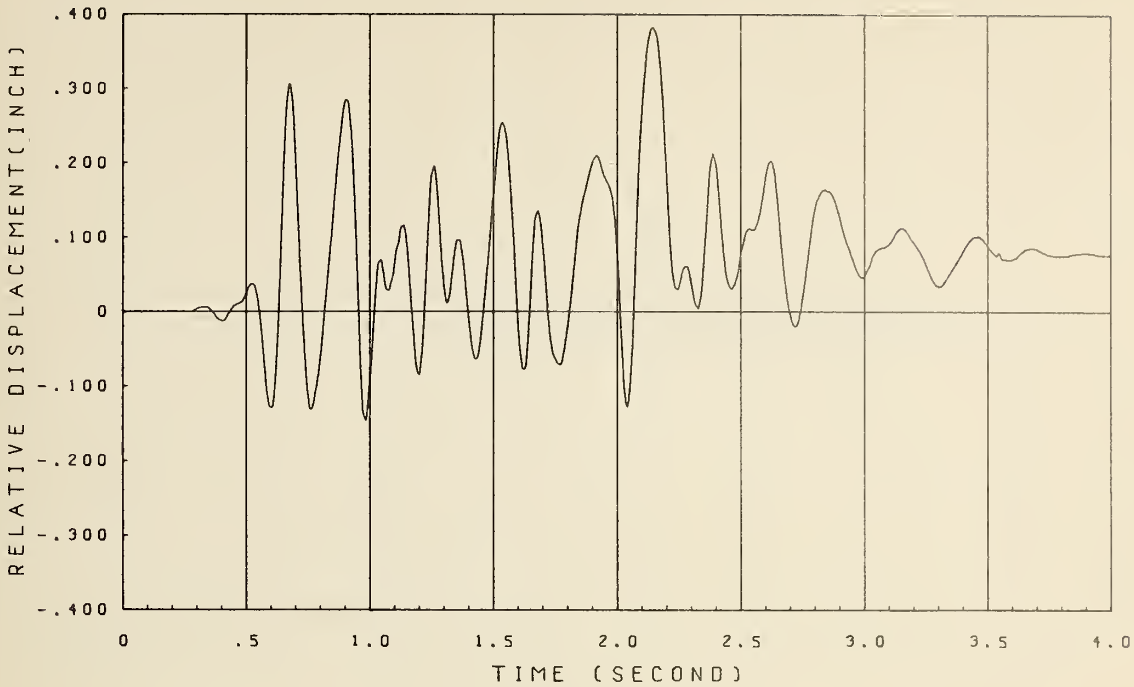

FIG. 4.14.3 MEASURED RESPONSE OF CENTER GIRDER; TRANSVERSE (Y) DIRECTION; TEST H2

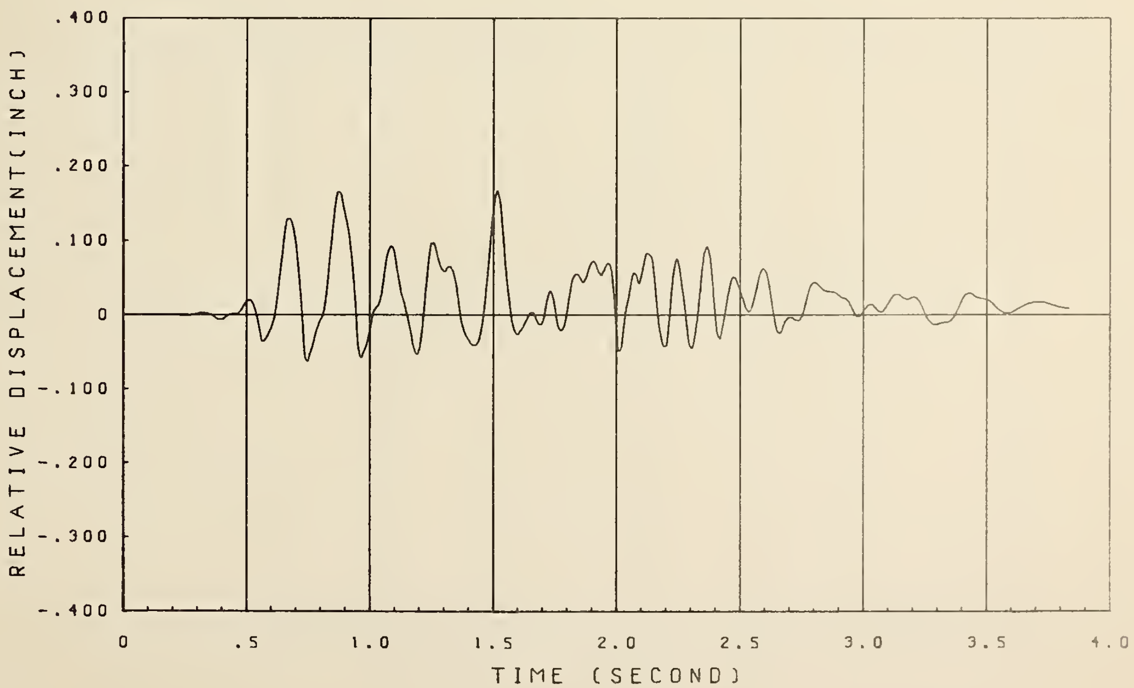

FIG. 4.14.4 MEASURED RESPONSE OF SIDE GIRDER NO. 2; LONGITUDINAL (X) DIRECTION; TEST H2

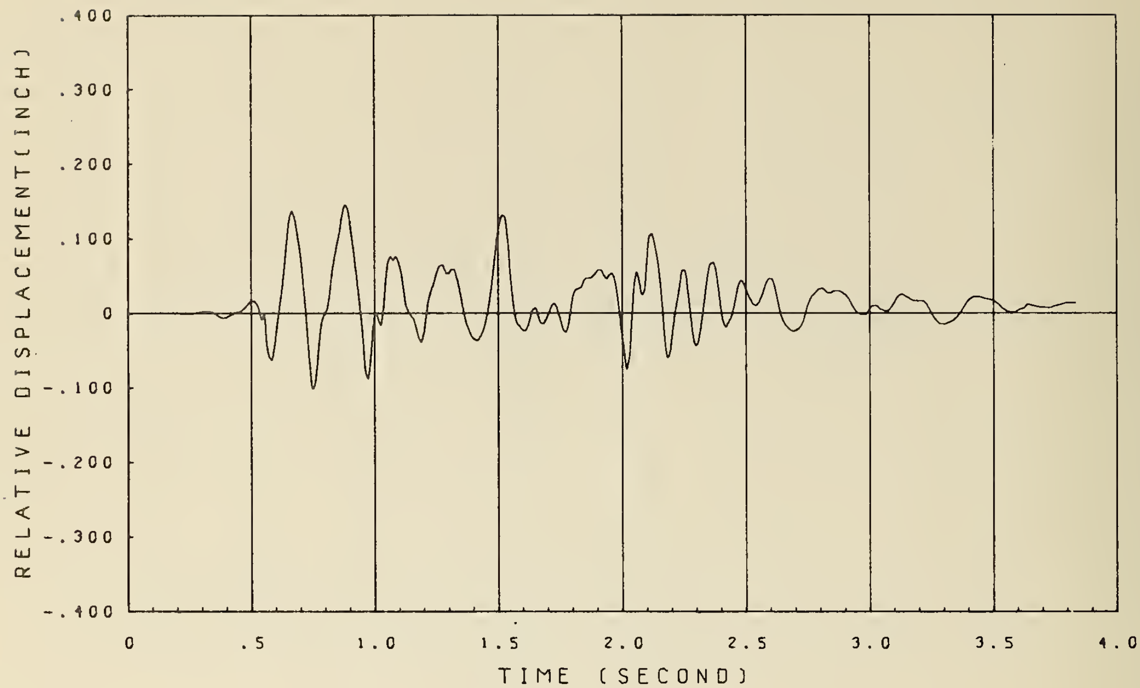

FIG. 4.14.5 MEASURED RESPONSE OF SIDE GIRDER NO. 2; TRANSVERSE (Y) DIRECTION; TEST H2

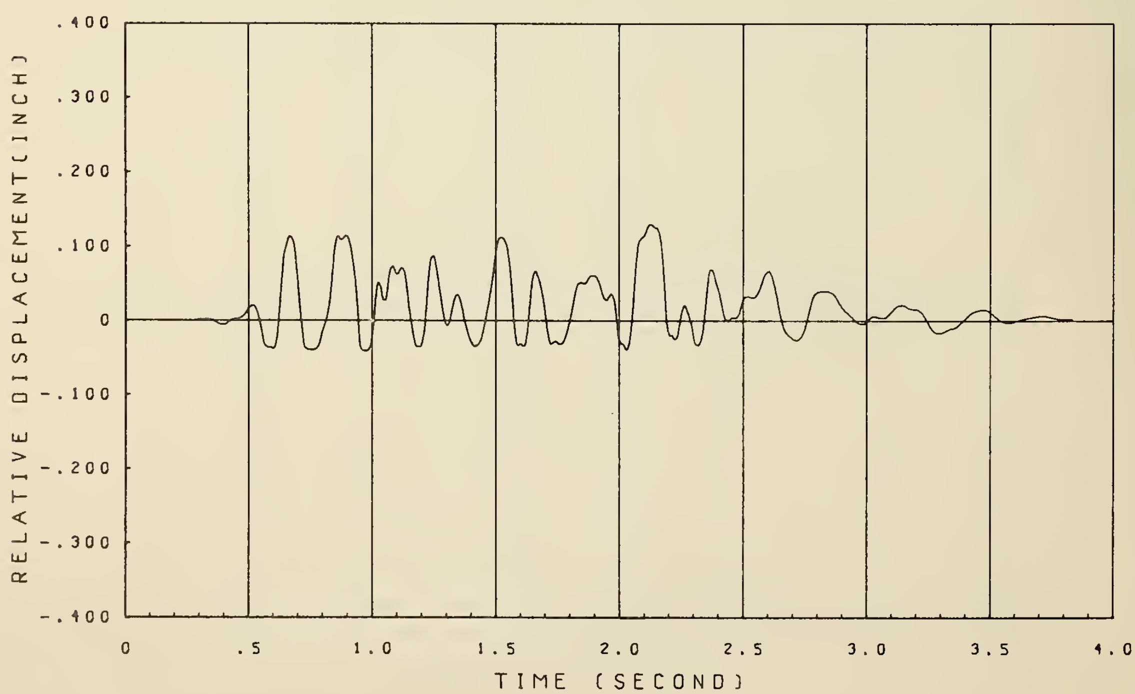

FIG. 4.14.6 MEASURED RESPONSE OF EXPANSION JOINT NO. 1; INNER SIDE; TEST H2

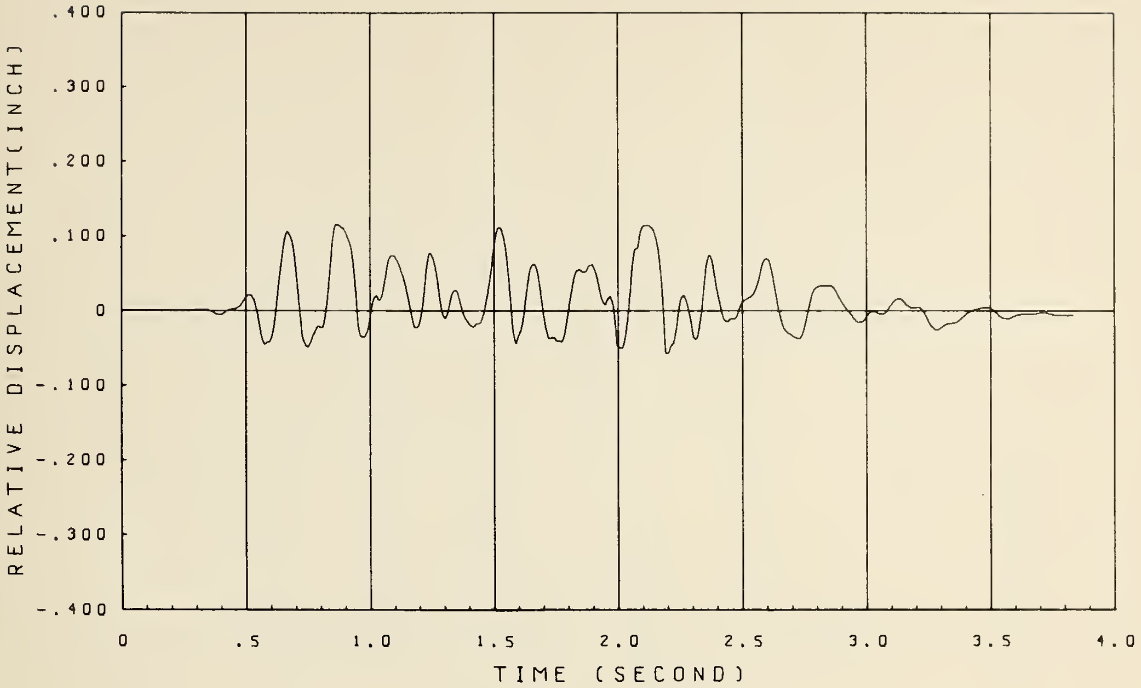

FIG. 4.14.7 MEASURED RESPONSE OF EXPANSION JOINT NO. 1; OUTER SIDE; TEST H2

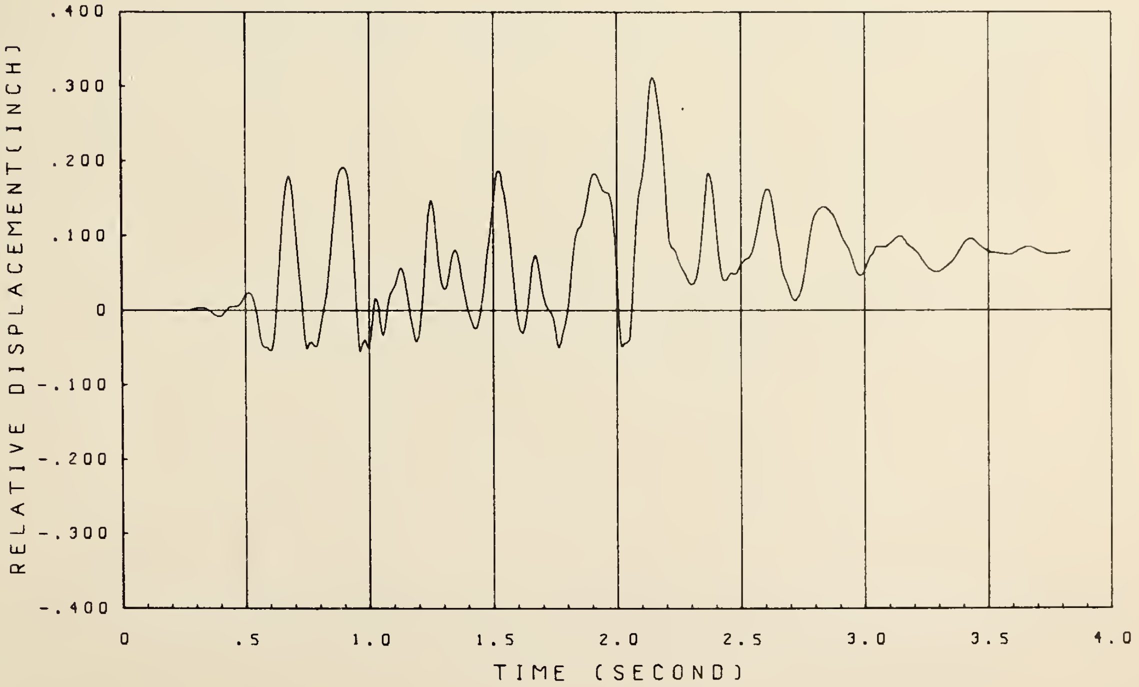

FIG. 4.14.8 MEASURED RESPONSE OF EXPANSION JOINT NO. 2; INNER SIDE; TEST H2

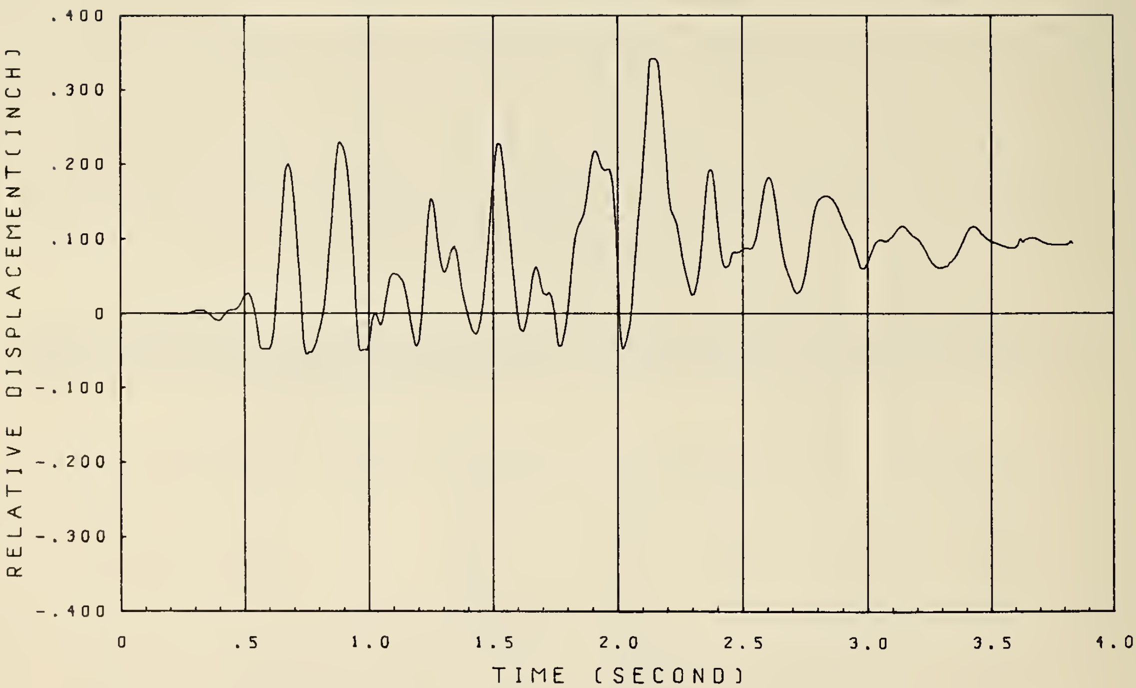

FIG. 4.14.9 MEASURED RESPONSE OF EXPANSION JOINT NO. 2; OUTER SIDE; TEST H2

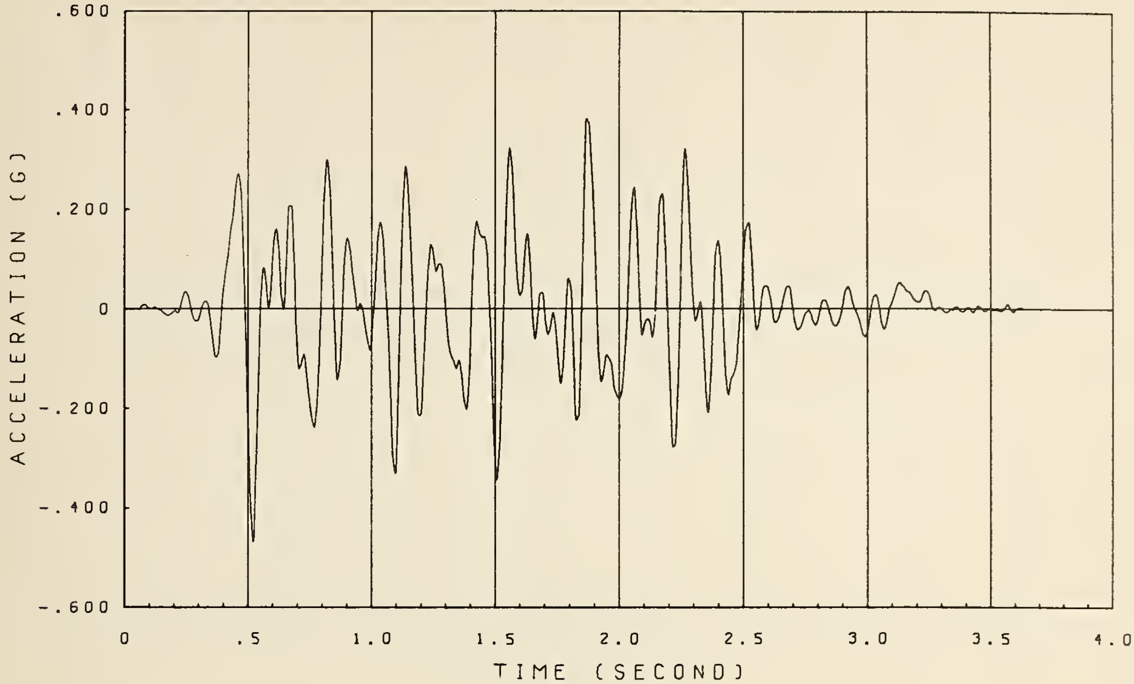

FIG. 4.15.1 HORIZONTAL TABLE ACCELERATION TIME HISTORY; TEST HV2

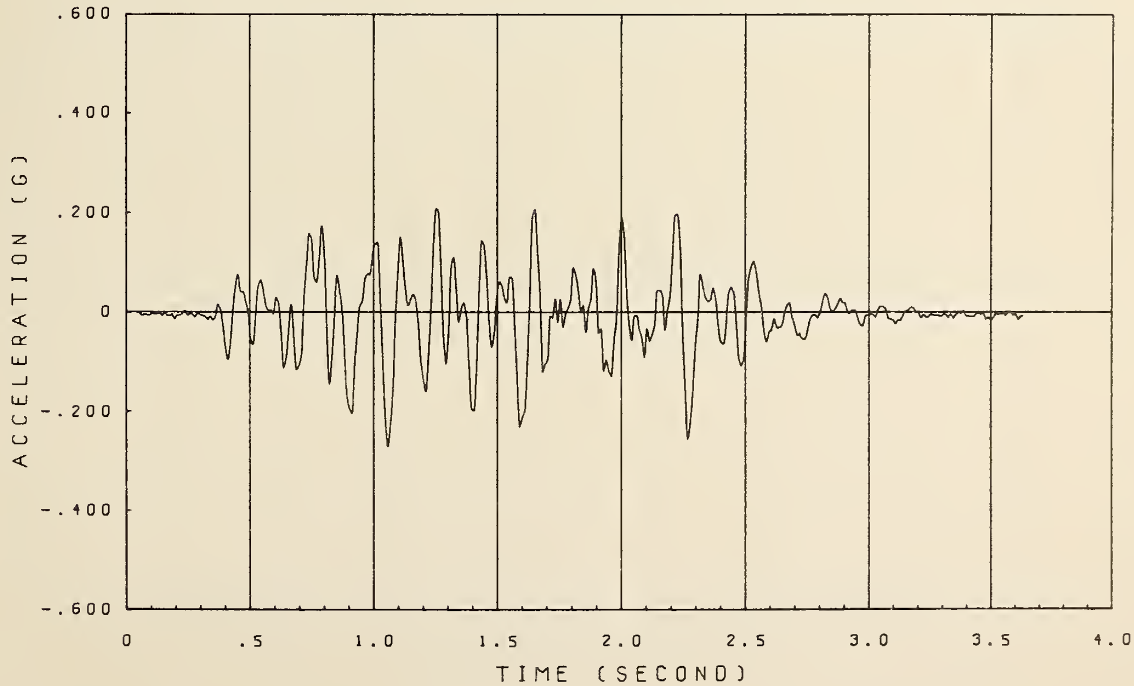

FIG. 4.15.2 VERTICAL TABLE ACCELERATION TIME HISTORY; TEST HV2

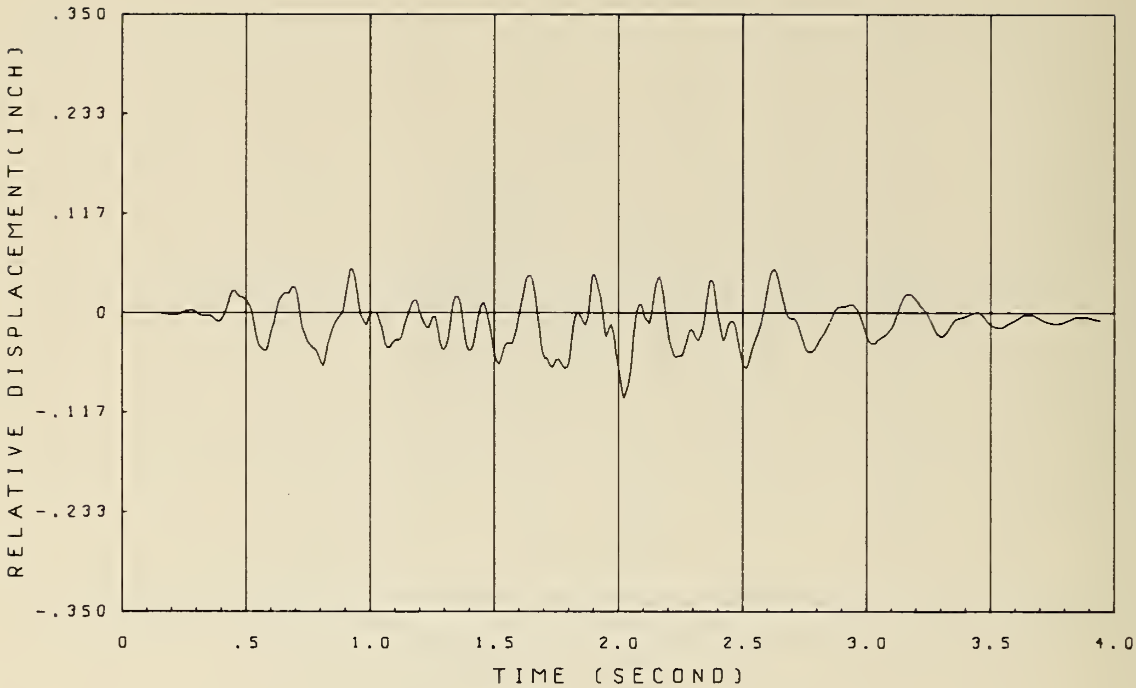

FIG. 4.16.1 MEASURED RESPONSE OF SIDE GIRDER NO. 1; LONGITUDINAL (X) DIRECTION; TEST HV2

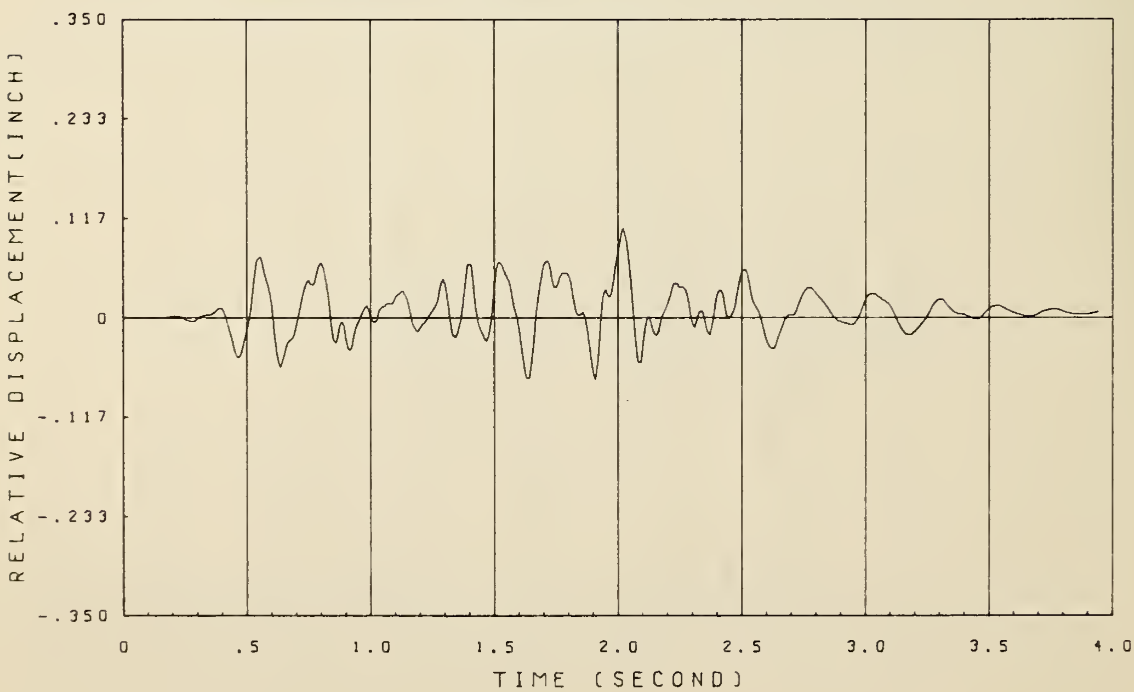

FIG. 4.16.2 MEASURED RESPONSE OF SIDE GIRDER NO. 1; TRANSVERSE (Y) DIRECTION; TEST HV2

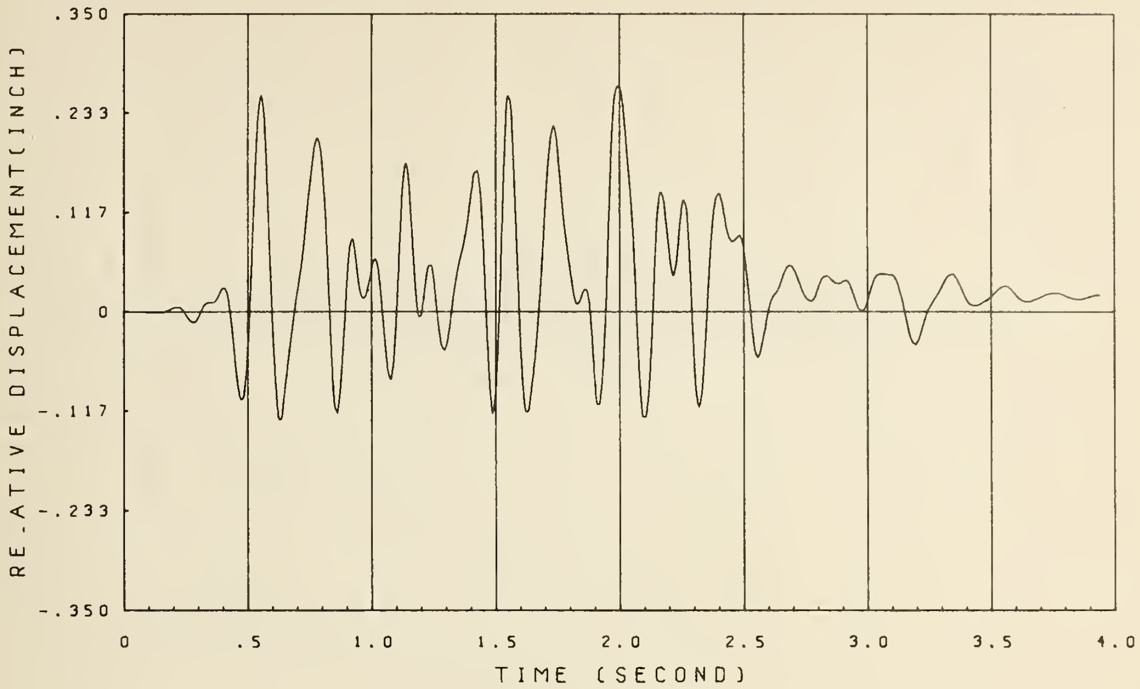

FIG. 4.16.3 MEASURED RESPONSE OF CENTER GIRDER; TRANSVERSE (Y) DIRECTION; TEST HV2

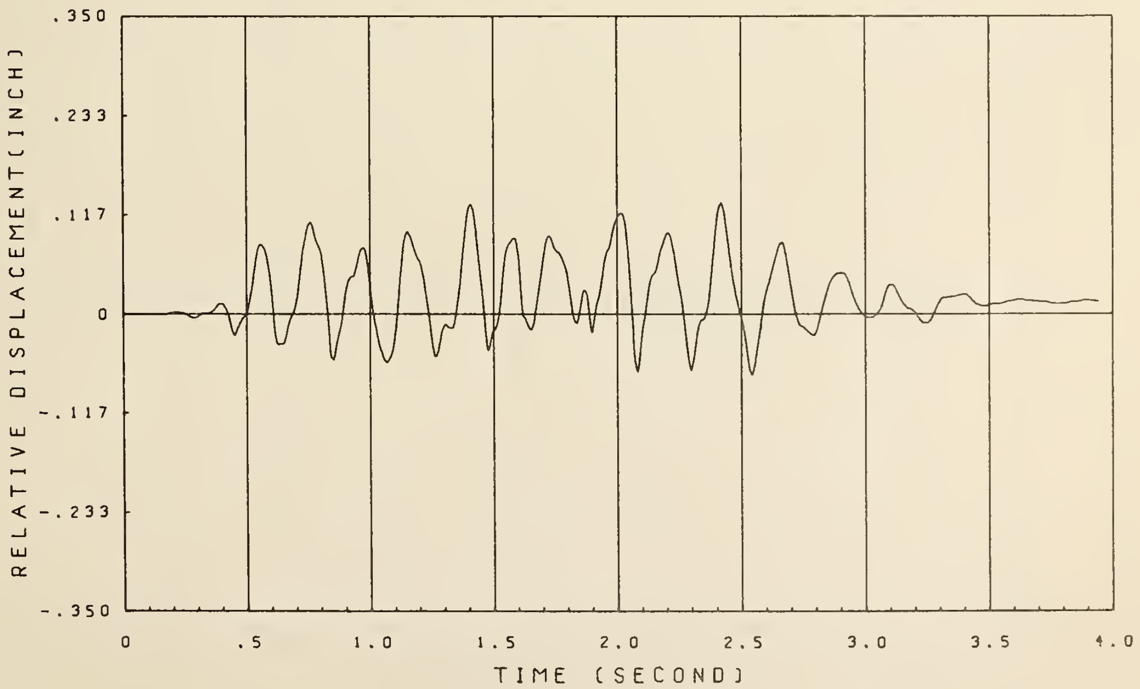

FIG. 4.16.4 MEASURED RESPONSE OF SIDE GIRDER NO. 2; LONGITUDINAL (X) DIRECTION; TEST HV2

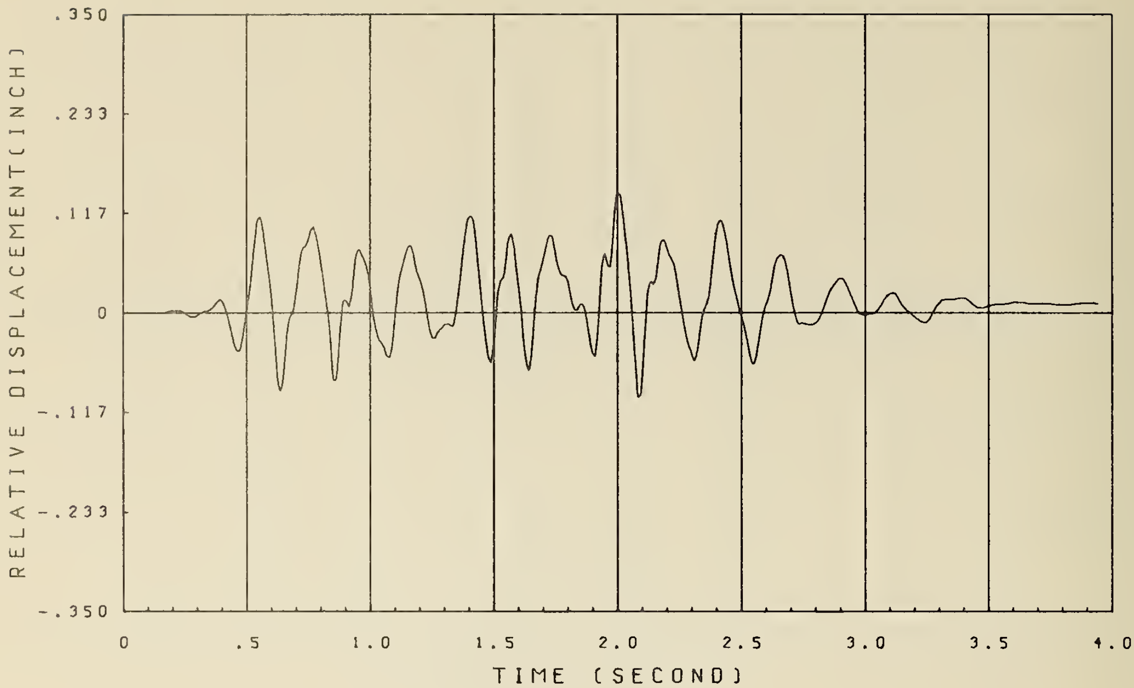

FIG. 4.16.5 MEASURED RESPONSE OF SIDE GIRDER NO. 2; TRANSVERSE (Y) DIRECTION; TEST HV2

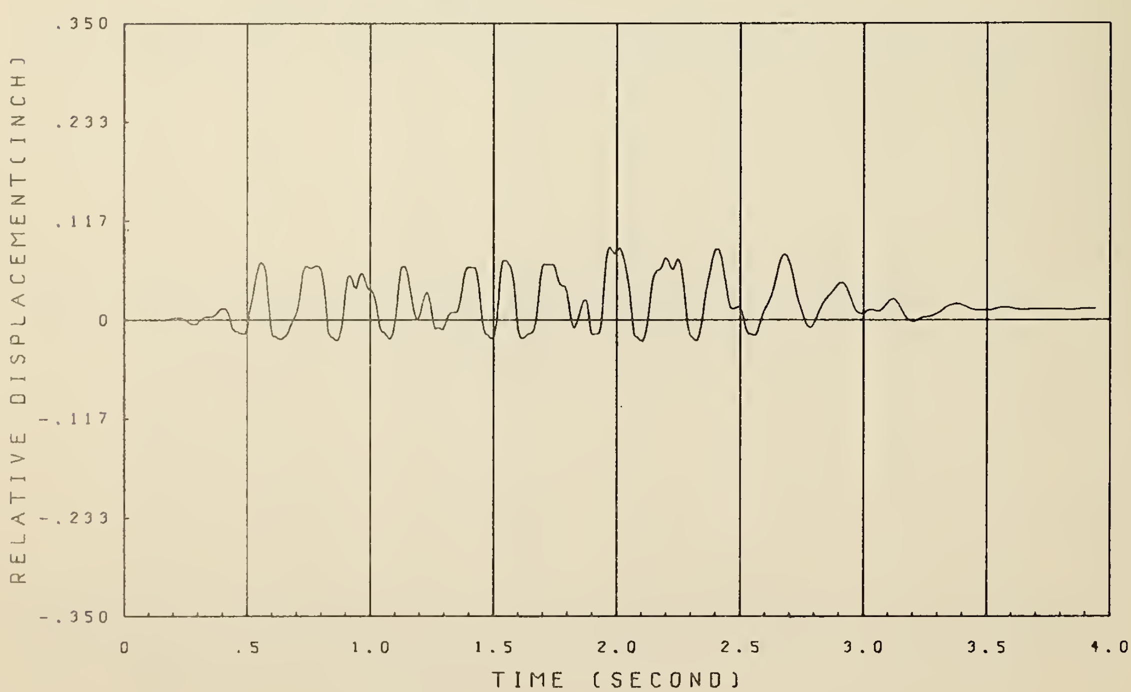

FIG. 4.16.6 MEASURED RESPONSE OF EXPANSION JOINT NO. 1; INNER SIDE; TEST HV2

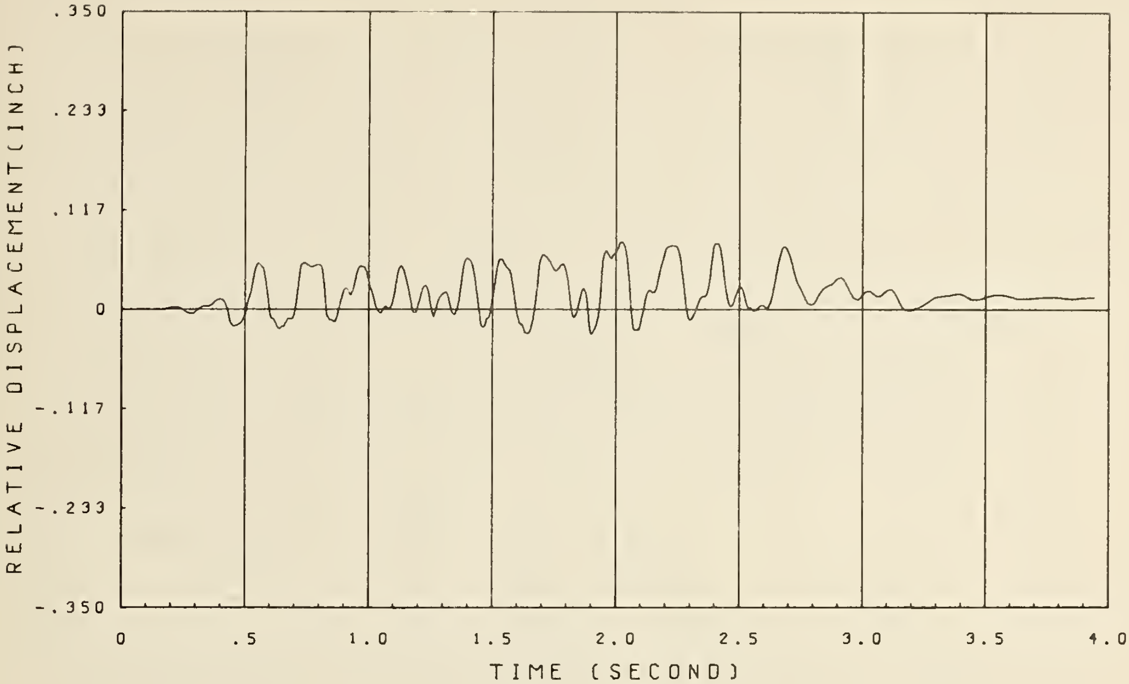

FIG. 4.16.7 MEASURED RESPONSE OF EXPANSION JOINT NO. 1; OUTER SIDE; TEST HV2

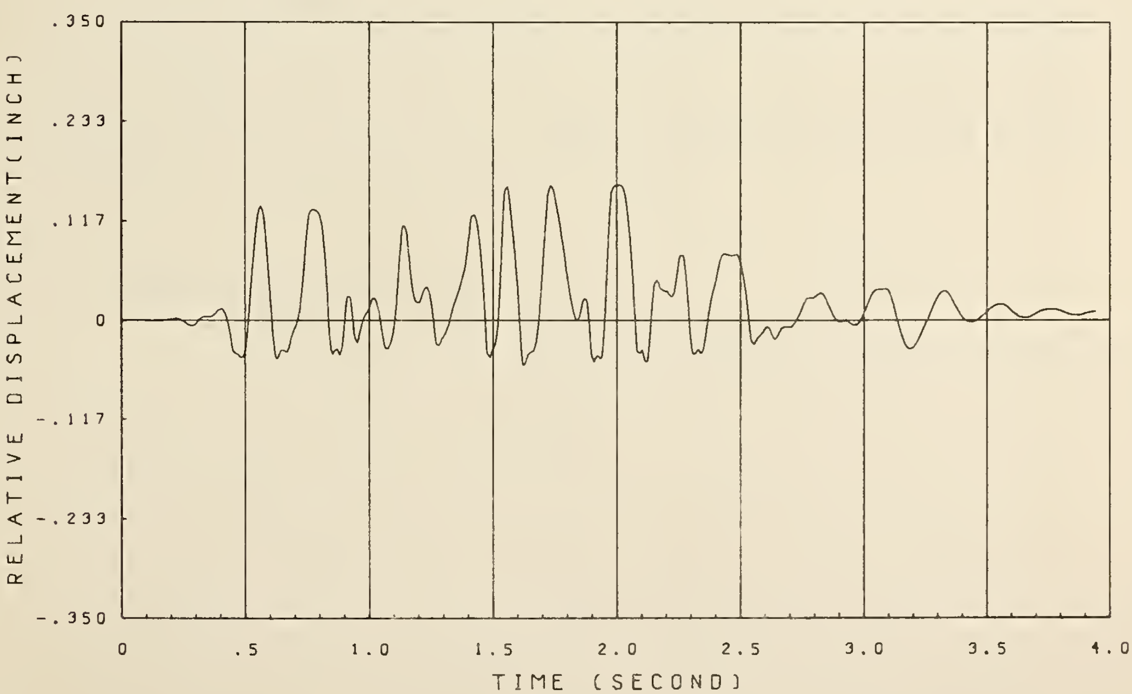

FIG. 4.16.8 MEASURED RESPONSE OF EXPANSION JOINT NO. 2; INNER SIDE; TEST HV2

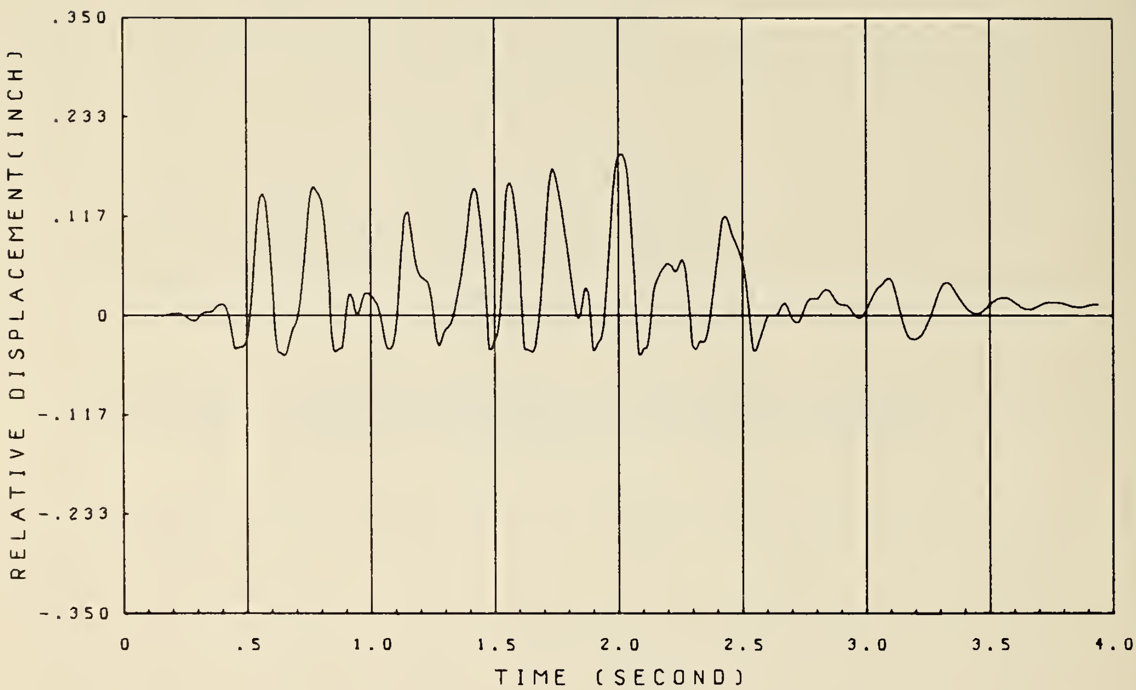

FIG. 4.16.9 MEASURED RESPONSE OF EXPANSION JOINT NO. 2; OUTER SIDE; TEST HV2

V. FORMULATION OF A BASIC ANALYTICAL MODEL

The purpose of this chapter is to integrate the component stiffness properties and boundary conditions previously described into a basic analytical model that satisfies the dynamic characteristics of the experimental model observed under small amplitude free vibration and forced harmonic conditions. These small amplitude characteristics are considered a fundamental requirement of the analytical model to be used in predicting seismic responses of the experimental model.

A. IDEALIZATION OF EXPERIMENTAL MODEL

During the free vibration and forced harmonic excitation tests, all components of the bridge model remained elastic. Therefore, the bridge model was treated as a linear three-dimensional discrete parameter system consisting of 55 nodal points. In this idealization, 24 linear curved beam elements respresenting the superstructure, 24 linear straight beam elements representing the columns, 2 linear elements representing the expansion joints and 2 boundary elements representing the abutments were used as shown in Fig. 5.1.

B. BASIC ANALYTICAL MODEL

The component stiffness properties and boundary conditions previously presented are summarized again in Table 5.1. Except for the expansion joint properties, these characteristics have been fully verified for including in the basic analytical model. The various constraints provided by the expansion joint need further clarification however since they are important factors controlling the dynamic response characteristics of the analytical model. As previously shown in Fig. 4.4, the force vs. relative displacement relation of the expansion joints is very complicated showing numerous changes in stiffness with relative displacement. When the relative displacement is very small, the effects of tie bars are negligible and slippages and collisions do not occur. In such cases, only the transverse shear key, the vertical restrainers and the rubber pad resist the relative movement between girders. Therefore in defining the analytical model, it is necessary that these constraints under small amplitude response be adequately modeled. First, a set of linear elastic springs were selected to resist the relative translational and rotational movements between the girders. The longitudinal stiffness k_x^{EJ} and the rotational stiffness $k_{\theta z}^{EJ}$ around a vertical (z) axis were evaluated considering the shear stiffness of the rubber pad; thus,

$$k_x^{EJ} \simeq k_x^R = 2.28 \times 10^4 \text{ lbs/inch}$$

$$k_{\theta z}^{EJ} \simeq d^2/12 \cdot k_x^R = 1.4 \times 10^5 \text{ lb. inches/rad.} \tag{71}$$

in which d represents width of the superstructure. Next, the vertical restrainers and the transverse shear key were assigned infinite stiffness to prevent vertical and transverse relative motions, respectively. With these prescribed constraints, three degrees of freedom were permitted in the joint, namely, rotations around x and y axes and uniform joint separation. These prescribed conditions (71) together with the stiffness and boundary conditions of Table 5.1 resulted in the following analytically predicted frequencies

$$f_L = 4.1 \text{ Hz} \quad \text{longitudinal vibration}$$

$$f_T = 7.0 \text{ Hz} \quad \text{transverse vibration} \tag{72}$$

$$f_V = 9.2 \text{ Hz} \quad \text{vertical vibration}$$

As described in Chapter IV, the measured natural frequencies of the experimental model were

$$F_L \simeq 5 \text{ Hz} \qquad \text{longitudinal vibration}$$

$$F_T \simeq 6.6 \text{ Hz} \qquad \text{transverse vibration} \tag{73}$$

$$F_V \simeq 9 \sim 10 \text{ Hz} \qquad \text{vertical vibration}$$

Comparing both sets of frequencies, it is apparent that the calculated frequencies are fairly close to their corresponding experimental values. Even so, this discrepancy was judged to be too great to satisfy modelling of the small amplitude dynamic characteristics of the experimental model. The reason for the discrepancy derived from disregarding the effects of tie bars, shear key, etc.

To remove the discrepancy, a parameter study was carried out by changing the pair of expansion joint stiffnesses. First, this study provided information on the effects of each individual stiffness on the low frequency characteristics of the model, and second it indicated the proper combination of stiffnesses to give best agreement of analytical and experimental frequencies. Table 5.2 shows the final results of this parameter study. Clearly, they show that stiffnesses k_x^{EJ}, $k_{\theta z}^{EJ}$ and k_y^{EJ} are more sensitive parameters than are stiffnesses $k_{\theta x}^{EJ}$ and $k_{\theta y}^{EJ}$. The effects of the former three parameters on the calculated natural frequencies may be written as

$$f_L \propto k_{\theta z}^{EJ}$$

$$f_T \propto k_x^{EJ} \text{ and } k_y^{EJ} \tag{74}$$

Further, it was found that the combination of stiffnesses giving best correlations of frequencies was

$$k_x^{EJ} = 1.9 \times 10^4 \text{ lbs/inch}$$
$$k_y^{EJ} = 5 \times 10^4 \text{ lbs/inch} \tag{75}$$
$$k_{\theta z}^{EJ} = 10^7 \text{ lb. inches/rad.}$$

The resulting natural frequencies were

$$f_L = 5.0 \text{ Hz}$$
$$f_T = 6.7 \text{ Hz} \tag{76}$$
$$f_V = 9.3 \text{ Hz}$$

It is interesting to note that the primary changes in stiffnesses given by Eqs. (71) and (75) are the introduction of k_y^{EJ} and a significant change in $k_{\theta z}^{EJ}$. Transverse stiffness k_y^{EJ} which resists relative transverse movement between the girders was incorporated into the analytical model not only to adjust the calculated natural frequencies but also because observations during experimental tests indicated that small transverse relative motions actually took place during high intensity excitations eventhough the transverse shear key prevented large relative motions to occur [26]. The high stiffness of 5×10^4 lbs/inch selected for k_y^{EJ} was considered realistic in allowing small transverse relative motions to develop in the analytical model. The change in stiffness $k_{\theta z}^{EJ}$ can be explained since $k_{\theta z}^{EJ}$ as given by Eq. (71) was derived considering only the shear stiffness of the rubber pad. Actually, however, the transverse shear key gives some contribution to $k_{\theta z}^{EJ}$ since its corners and edges resist rotational movement, and the joint restrainer tie bars also make a contribution; thus, the incremental change in $k_{\theta z}^{EJ}$ from Eq. (71) to Eq. (75) is reasonable.

Finally, the calculated lowest vibration mode shapes in the three major directions, namely, transverse, longitudinal and vertical, were checked against the observed vibration modes of the experimental model. As is shown in Fig. 5.2, it is apparent that all three of the calculated modes are very similar to the corresponding experimental modes.

Based on the discussion above, it is clear that the analytical model having stiffness properties and boundary conditions as shown in Table 5.1 and having the idealized expansion joint constraints as represented by Eq. (75) adequately satisfies the small amplitude dynamic characteristics of the experimental model. It should be noted however that since the spring stiffnesses representing the expansion joint constraints were modeled so that the low frequency characteristics of the analytical model correspond with those of the experimental model, all errors involved in determining the stiffness properties and the boundary conditions of the model are absorbed in the selected set of spring stiffnesses of expansion joints.

TABLE 5.1 STIFFNESS PROPERTIES AND BOUNDARY CONDITIONS OF EXPERIMENTAL MODEL

Component	Stiffnesses	Units	Determined Value	Procedure of Determination		
				Direct Measurement	Undirect Measurement	Calculated or Estimated
Super-Structure	Flexural Rigidity in Transverse Direction	lb. $inches^2$	1.8×10^8 for all girders	0		
	Flexural Rigidity in Vertical Direction	lb. $inches^2$	5.0×10^8 for all girders		0	0
	Axial Rigidity	lbs	1.24×10^7 for all girders			0
	Torsional Rigidity	lb. $inches^2$	3.92×10^7 for all girders			0
Columns	Flexural Rigidity around Strong Axis	lb. $inches^2$	1.90×10^7 for COL-1A 1.90×10^7 for COL-2A 5.59×10^6 for COL-1B 5.41×10^6 for COL-2B	0		
	Flexural Rigidity around Weak Axis	lb. $inches^2$	3.39×10^6 for COL-1A 3.50×10^6 for COL-2A 1.39×10^6 for COL-1B 1.58×10^6 for COL-2B	0		

TABLE 5.1 - CONTINUED -

Component	Stiffnesses	Units	Determined Value	Procedure of Determination		
				Direct Measurement	Undirect Measurement	Calculated or Estimated
Columns	Axial Rigidity	lbs	3.04×10^7 for COL-1A & 2A 1.43×10^7 for COL-1B & 2B			0
	Torsional Rigidity	lb. $inches^2$	6.00×10^6 for COL-1A & 2A 1.46×10^6 for COL-1B & 2B			0
Abutments	Rotational Stiffness around y axis	lb. inches/rad.	0	0		0
	Rotational Stiffness around z axis	lb. inches/rad.	8×10^6		0	0
Expansion Joints	Shear Stiffness of Rubber Pad	lbs/inch	22800	0		
	Coefficient of Friction	——	0.4			0
	Elastic Stiffness of Tie Bar	lbs/inch	6.47×10^4	0		
	Yield Strength of Tie Bar	lbs	650	0		

TABLE 5.2 EFFECT OF EXPANSION JOINT CONSTRAINTS ON CALCULATED LOW FREQUENCY CHARACTERISTICS OF BRIDGE MODEL

No. of Case	Purpose	Stiffnesses Representing EJ Constraints					Calculated Natural Frequencies		
		k_x^{EJ}	k_y^{EJ}	$k_{\theta x}^{EJ}$	$k_{\theta y}^{EJ}$	$k_{\theta z}^{EJ}$	f_L	f_T	f_V
1	EFFECT OF k_x^{EJ}	2.28×10^4	fixed	free	free	1.4×10^5	4.07	6.95	9.23
2		1.9×10^4	fixed	free	free	1.4×10^5	4.06	6.66	9.20
3		1.7×10^4	fixed	free	free	1.4×10^5	4.05	6.47	9.18
4	EFFECT OF $k_{\theta z}^{EJ}$	1.9×10^4	fixed	free	free	10^6	4.35	6.69	9.29
5		1.9×10^4	fixed	free	free	10^7	4.95	6.73	9.33
6		1.9×10^4	fixed	free	free	10^8	5.14	6.74	9.34
7	EFFECT OF k_y^{EJ}	1.9×10^4	10^5	free	free	10^7	4.95	6.71	9.33
8		1.9×10^4	5×10^4	free	free	10^7	4.95	6.68	9.33
9		1.9×10^4	10^4	free	free	10^7	4.93	6.49	9.30
10	EFFECT OF $k_{\theta x}^{EJ}$	1.9×10^4	5×10^4	fixed	free	10^7	5.07	6.74	9.33
11	EFFECT OF $k_{\theta y}^{EJ}$	1.9×10^4	5×10^4	free	fixed	10^7	5.00	6.71	11.39

1) Units - lbs/inch for translational stiffnesses and lb. inches/rad. for rotational stiffnesses

2) f_L: lowest natural frequency (Hz) in longitudinal (X) direction

f_T: lowest natural frequency (Hz) in transverse (Y) direction

f_V: lowest natural frequency (Hz) in vertical (Z) direction

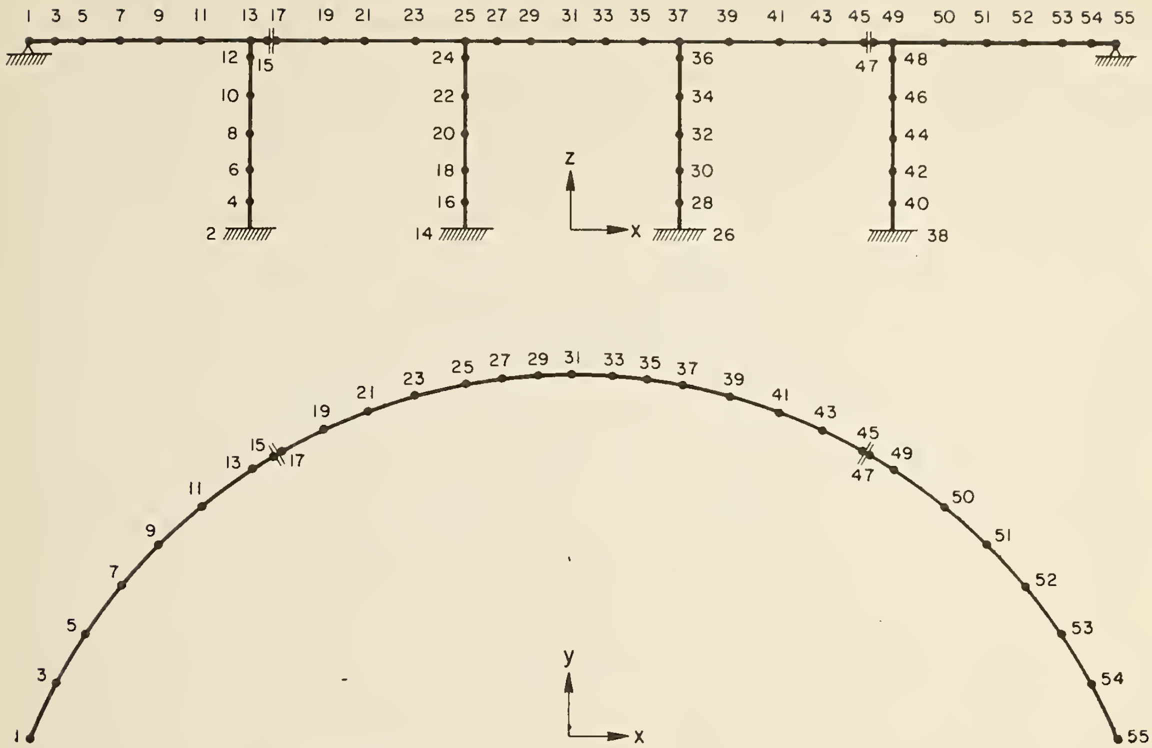

FIG. 5.1 ANALYTICAL MODEL OF BRIDGE MODEL

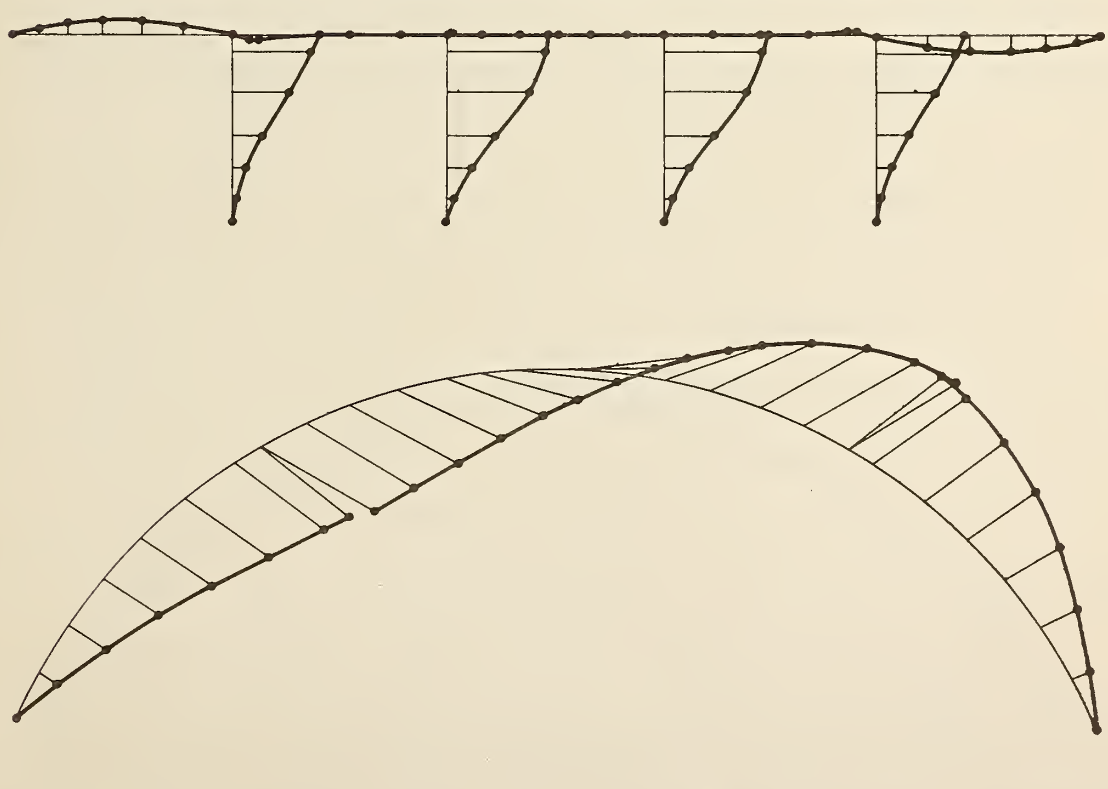

FIG. 5.2.1 CALCULATED LOWEST VIBRATION MODE; LONGITUDINAL (X) DIRECTION

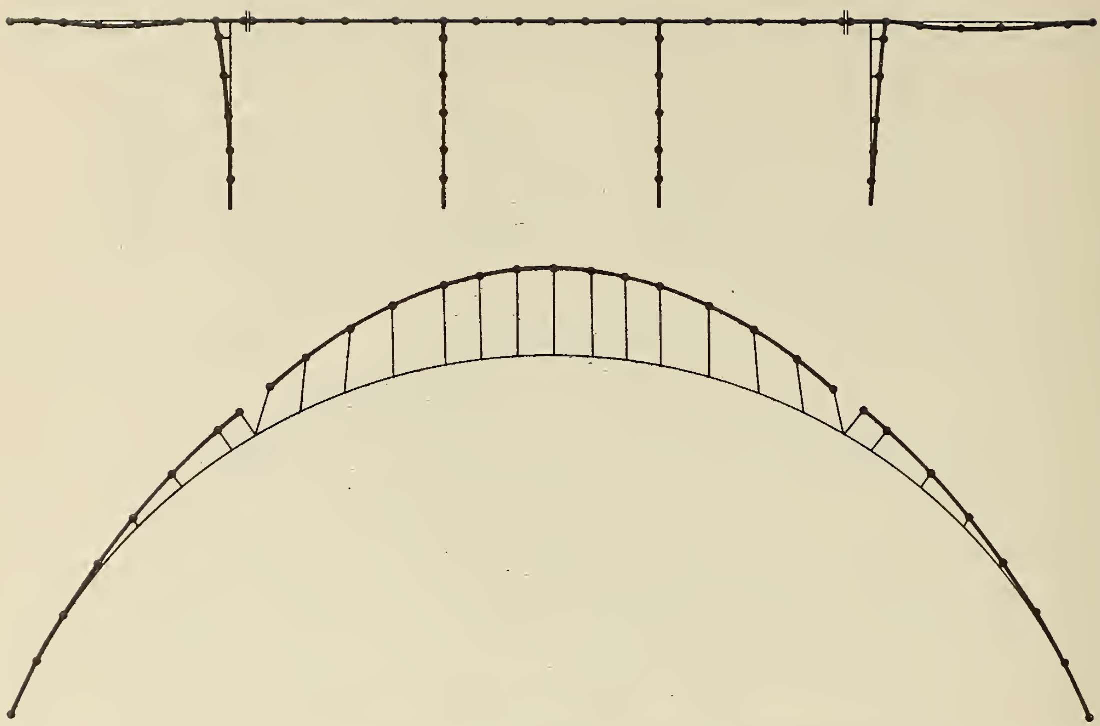

FIG. 5.2.2 CALCULATED LOWEST VIBRATION MODE; TRANSVERSE (Y) DIRECTION

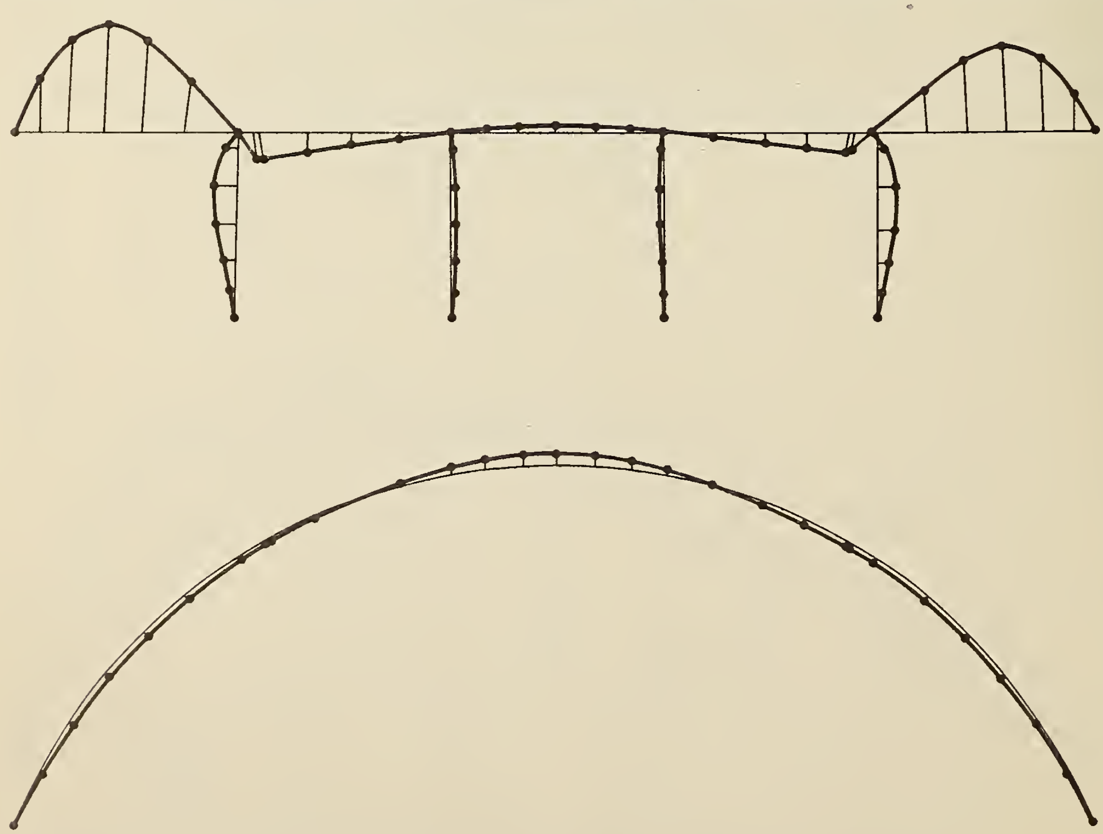

FIG. 5.2.3 CALCULATED LOWEST VIBRATION MODE; VERTICAL (Z) DIRECTION

VI. ANALYTICAL PREDICTION OF SEISMIC RESPONSES

The purpose of this chapter is to correlate the measured responses of displacement of the experimental model with the linear and nonlinear responses determined analytically for the three seismic excitations, i.e. for Tests H1, H3 and HV2. The correlation was initiated with Test H1, since this test represented essentially linear elastic behavior. The correlation derived from this test was basic as it also represented the initial low amplitude behavior of the model during Tests H3, and HV2 which subsequently experienced high amplitude nonlinear behavior.

The correlation was made by comparing predicted and measured responses, paying particular attention to the agreement of maximum responses, phase relations, and the overall dynamic behavior.

A. LOW INTENSITY SEISMIC EXCITATION (TEST H1)

1. Linear Analysis Correlation - The basic analytical model that satisfied the small amplitude dynamic characteristics of the experimental model was used in predicting seismic responses for Test H1. It was subjected to the table acceleration time-history shown in Fig. 4.11 in its transverse direction. A time interval of 0.01025 second was adopted for the numerical integration. A damping ratio of 6% of critical was assumed based on experimental evidence Eq. (69) obtained from low intensity forced harmonic tests at amplitudes of vibration comparable to those developed in the Test H1.

Displacement response time-histories were calculated under these conditions and were compared with the corresponding experimental results. From these comparisons, it was found that although global behavior of the predicted response was similar to the measured response, the correlation of individual peak amplitudes and their phase relations was relatively poor. Further, the predominant frequency of the predicted response was slightly higher than that of the measured response. This implied that the total stiffness of the basic analytical model was slightly higher than that of the experimental model under this particular seismic excitation. It was then decided to modify the stiffness of the analytical model slightly in order to make the phase lag discrepancies as small as possible. The overall stiffness of the expansion joints was chosen for this purpose since it dominated the low frequency characteristics of the model and also since it was the most uncertain property established from experimental evidence. Based on the parameter study represented by Eq. (74), it was apparent that either stiffness k_x^{EJ} or k_y^{EJ} should be changed in order to reduce the natural frequency of vibration in the transverse direction. As described in the previous chapter, k_y^{EJ} was introduced into the basic analytical model to permit some small transverse relative motions to develop at the expansion joints. It was clear therefore that stiffness of k_y^{EJ} should not be decreased from its original value since such a reduction would cause large transverse relative motions to take place. On the other hand, stiffness k_x^{EJ} was derived from the combined effects of the tie bars, slippages, etc.; thus, significant uncertainty was present in setting its numerical value. Hence, k_x^{EJ} was chosen to adjust the frequency and after some calculations, it was set at the value

$$k_x^{EJ} = 18400 \text{ lbs/inch} \tag{77}$$

giving lowest natural frequencies as follows:

$$f_L = 4.9 \text{ Hz} \quad \text{longitudinal vibration}$$

$$f_T = 6.6 \text{ Hz} \quad \text{transverse vibration} \tag{78}$$

$$f_V = 9.3 \text{ Hz} \quad \text{vertical vibration}$$

The resulting predicted response of displacement is shown in Fig. 6.1 together with the measured result. From this comparison it is seen that the predicted response agrees fairly well with that of the experimental model. The amplitudes of the predicted response are very close to those of the response which indicates that the established damping ratio of 6% was appropriate. As one would expect, the predicted response is essentially symmetric both in the outward and inward directions while the measured response is somewhat unsymmetric due to differences in the joint restrainer tie bar properties. This feature can be observed more clearly by comparing the responses of expansion joints.

The above correlation clearily indicates that the measured response during Test H1 could be predicted with fairly good accuracy using a linear analytical model provided its fundamental natural frequency in the direction of excitation agreed well with the experimental value and provided the proper damping factor was introduced into the analysis. It is quite evident however that the unsymmetric response caused by differences in the discontinuous expansion joint constraints cannot be predicted using the linear analytical model.

2. Nonlinear Analysis Correlation - For this correlation study, the linear expansion joint element previously used was replaced by the nonlinear element. It was necessary therefore to change the stiffnesses associated with the tie bars. In the linear analysis correlation, the constraints of the expansion joints were modeled by the following set of linear spring stiffnesses:

$$k_x^{EJ} = 18400 \text{ lbs/inch}, \; k_y^{EJ} = 50000 \text{ lbs/inch}$$
$$k_{\theta z}^{EJ} = 10^7 \text{ lb. inches/rad.} \tag{79}$$

For the present nonlinear analysis correlation, it is not necessary to change k_y^{EJ} since the tie bars do not affect relative transverse motion at the expansion joints. On the other hand, stiffnesses k_x^{EJ} and $k_{\theta z}^{EJ}$ are directly dependent upon the tie bars. Therefore, they must be modified. To accomplish these changes, the force vs. relative displacement relation shown in Fig. 4.4 was used. In Test H1 the maximum relative movements developed at the expansion joints were approximately + 0.01 inch (seperation) and - 0.025 inch (closing). When a Coulomb friction coefficient of 0.4 is prescribed, the elastic shear deformation of the rubber pad is approximately 0.01 inch beyond which slippage takes place between the contact surface of the expansion joint. By comparing the amount of relative movement developed during excitation and the amount of shear deformation possible in the rubber pad, it is clear that maximum slippages of the order of 0.015 inch took place at the expansion joints. Since the amount of slippage in Test H1 was very small, it was decided not to introduce Coulomb type friction force in this analysis. It was then decided to take account of the small slippages approximately by linearlizing the force vs. relative displacement relation. Thus, the longitudinal linearized stiffness $k_{x,\ell}^{EJ}$ was estimated from Fig. 4.4 as

$$k_{x,\ell}^{EJ} \simeq 9000 \text{ lbs/inch} \tag{80}$$

The stiffness $k_{\theta z}^{EJ}$ was also changed for the same reason described above resulting in the value

$$k_{\theta z}^{EJ} = 6 \times 10^{6} \text{ lb. inches/rad.} \tag{81}$$

Damping coefficients α and β were assigned values so that the damping ratio of 6% of critical would be achieved for the first and second normal modes of vibration as calculated by the linear analytical model. The initial tie gaps Δ_T were assigned zero values based on measurements taken just prior to the test which showed that they were very small.

The nonlinear analytical model defined above was subjected to the table acceleration time-history as used in the linear analysis correlation. A time interval of 0.01025 second was adopted for the numerical integration. Equilibrium iteration was used both alone and with the subdivision of time intervals into 3 equidistant sub-time intervals, when needed. The tolerances used to control the equilibrium iteration and the subdivision defined in Eqs. (51) and (62) were

$$\begin{aligned} \Delta_{ps} &= 0.01 \quad \text{equilibrium iteration} \\ \Delta_{ps} &= 0.08 \quad \text{subdivision} \\ \Delta_{us}^{I} &= 0.001 \end{aligned} \tag{82}$$

The predicted displacement response was compared with the experimentally measured result and it was found that the predicted response was substantially improved as compared with the linear analysis correlation although discrepancies were still observed both in the peak amplitudes and their phase relations. The largest discrepancy was seen at the expansion joints where openings of the gaps were excessively suppressed by the tie bars. Because of this discrepancy, it was decided to change the originally assumed zero tie gaps to small realistic values. Hence, both the assumed linearized stiffness of $k^{EJ}_{x,\ell}$ and the initial tie gaps were adjusted; finally, giving good correlation under the conditions

$$\begin{aligned} k^{EJ}_{x,\ell} &= 10000 \text{ lbs/inch} \\ \Delta_T &= 0.05 \text{ inch for both expansion joints} \end{aligned} \tag{83}$$

The comparative plots of predicted and measured responses are shown in Fig. 6.2. Excellent agreement can be seen for these responses at the center point of the model and at both expansion joints, and the unsymmetrical vibration shown by the experimental response is well followed in the analysis. The predicted responses of force induced in the tie bars are shown in Fig. 6.3. Since the maximum value of the predicted tie bar force is approximately 400 lbs, yielding of the tie bar was not indicated by analysis which is consistent with the observed results.

B. HIGH INTENSITY SEISMIC EXCITATION (TEST HV2)

1. Linear Analysis Correlation - To carry out the linear analysis correlation for Test HV2, the same linear model previously described for Test H1 was used. This analytical model was subjected to the measured table accelerations in both the transverse and vertical directions. A time interval of 0.01026 second was used throughout the correlation. Although it was somewhat questionable if the same viscous damping ratio as used in Test H1 should be used for this test due to the high amplitude motion, it was decided to use the same 6% of critical as a first trial.

The responses predicted on this basis were compared with the measured results as shown in Fig. 6.4. As can be seen, the predicted response is significantly different from the measured response both in the magnitude of peak amplitudes and in the frequency characteristics. It soon became apparent from this correlation that several collisions within the joints and yielding of the tie bars do not allow the linear analysis acceptable correlations. Therefore, to obtain reasonable correlation, one must introduce these effects into the analytical model. Thus, further correlation using the lienar analytical model after adjusting parameters was not attempted for Test HV2.

2. Nonlinear Analysis Correlation - In order to introduce the effects of collisions and yielding of tie bars into the analysis, the nonlinear analytical model formulated for the correlation of the Test H1 was further modified.

First, the modeling of constraints in the expansion joint was reviewed. The assumed force vs. relative displacement relation shown in Fig. 4.4 was again used for this purpose. A principal difference in the seismic responses between this test and the Test H1 is the amplitude level. For example, the maximum relative displacements at expansion joint No. 2 are approximately + 0.2 inch (opening) and - 0.05 inch (closing) in this test which are roughly 10 times those values developed during Test H1. It is apparent from these large relative movements that slippages of large amplitude took place during the excitation. Thus, instead of using the linearized stiffness $k^{EJ}_{x,\ell}$ as in Test H1, one must now introduce the Coulomb friction which can be modeled by an elastoplastic hysteretic relation. The initial elastic slope of this Coulomb friction relation was taken equal to the shear stiffness of the rubber pad k^{R}_{x}. By doing so, the assumed relation of Fig. 4.4 can be exactly modeled in the analysis. Stiffnesses k^{EJ}_{y} and $k^{EJ}_{\theta z}$ were unchanged from Test H1 since they do not affect the Coulomb friction force.

Impact springs were incorporated into the analytical model to take account of joint collisions. The stiffness of the impact spring k_I was taken equal to 10^7 lbs/inch which is nearly the same magnitude as the longitudinal stiffnesses of the curved beam elements representing the superstructure. The initial joint gaps Δ_G were determined from the measured experimental responses of expansion joints. Since the joint gaps were changing with each collision and also were not identical between the inner and outer edges, the following joint gaps were obtained by taking averages

$$\begin{aligned} \Delta_G &= 0.025 \text{ inch} \qquad \text{expansion joint No. 1} \\ \Delta_G &= 0.040 \text{ inch} \qquad \text{expansion joint No. 2} \end{aligned} \tag{84}$$

Finally, initial tie gaps Δ_T were prescribed on the basis of measured information as

$$\begin{aligned} \Delta_T &= 0.01 \text{ inch} \qquad \text{expansion joint No. 1} \\ \Delta_T &= 0.02 \text{ inch} \qquad \text{expansion joint No. 2} \end{aligned} \tag{85}$$

Since no experimental data was available to estimate damping factors for the experimental model under high intensity excitations, the same damping coefficients α and β used for the correlation of Test H1 were adopted as a first trial. As before, these values represent 6% viscous damping in the first and second normal modes of vibration.

After introducing these data into the nonlinear analytical model, it was subjected to the table accelerations in the same manner as done previously for the linear analysis correlation. The equilibrium iteration was used both alone and with the subdivision of time intervals into 5 equidistant sub-time intervals, when needed. The tolerances used to control the equilibrium iteration and the subdivision of time interval were

$$\begin{aligned} \Delta_{ps} &= 0.01 \quad \text{equilibrium iteration} \\ \Delta_{ps} &= 0.07 \quad \text{subdivision} \\ \Delta^{I}_{us} &= 0.005 \end{aligned} \qquad (86)$$

From this first correlation, it was found that although the overall response was substantially improved as compared with the linear analysis correlation, it was not satisfactory. The discrepancies were primarily derived from excessive constraint of the tie bars at both expansion joints and from over estimation of the damping force. The former reason indicated that the assumed initial tie gaps were too small; therefore, similar to the correlation of Test H1, the assumed initial tie gaps were increased. In order to interpret the latter reason, all three sources of damping in the analytical model were examined, i.e. the 6% viscous damping which was proportional to both mass distribution and stiffness distribution, Coulomb type damping associated with slippages at the expansion joints, and hysteretic damping associated with yielding of the tie bars. The 6% viscous damping was originally derived from the results of small amplitude forced harmonic excitations. The actual damping in these tests however was probably more in the form of structural damping due to the form of energy dissipation at the expansion joints and abutments. Particularly in view of the fact that damping in the sound microconcrete of the superstructure and columns would be small.

Therefore, when collisions take place and high frequency vibration response is induced, modelling of damping using the same 6% of viscous damping most likely would overestimate this form of energy dissipation.

Thus, changing both the assumed initial tie gaps and the viscous damping ratio, a best correlation was achieved under the conditions

$$\xi = 2\% \text{ of critical for first and second modes of vibration} \tag{87}$$

and

$$\begin{aligned} \Delta_T &= 0.03 \text{ inch} \quad \text{expansion joint No. 1} \\ \Delta_T &= 0.045 \text{ inch} \quad \text{expansion joint No. 2} \end{aligned} \tag{88}$$

Comparative plots of the predicted response with the measured response are shown in Fig. 6.5. Apparently the nonlinear analysis correlation is greatly superior to the linear analysis correlation. Clearly, the effect of multiple collisions and constraints of the joint restrainer tie bars are realistically represented in the nonlinear analytical model, see Fig. 6.6. Severe yielding of the tie bars developed maximum ductility factors μ_T, defined as the ratio of the maximum tie elongation to its yield elongation, i.e.,

$$\mu_T = \frac{u_T^E + u_T^P}{u_T^E} \tag{89}$$

where

u_T^E : elastic elongation of tie bar

u_T^P : plastic elongation of tie bar

equal to approximately 4 and 12 for expansion joints No. 1 and No. 2, respectively. Figure 6.7 shows the contact force between girders caused by collisions. The maximum contact force of approximately 4000 lbs was induced at the expansion joint No. 2. Predicted stresses of the columns did not reach to their yield strength; therefore, no plastic deformation was developed during the test.

C. HIGH INTENSITY SEISMIC EXCITATION (TEST H3)

1. Linear Analytical Correlation - Since it was apparent from the correlation of Test HV2 that the linear analysis could not achieve good results for high intensity excitations, the linear analysis correlation was performed only to provide comparative response data with the nonlinear analysis correlation.

The same linear analytical model used for Test HV2 was used for Test H3. It was subjected to the table motion as measured in the transverse direction. A time interval of 0.01025 second was adopted throughout this correlation. The comparative plots of the predicted and measured response are shown in Fig. 6.8. Like test HV2, the linearly predicted response is very much different from the measured response.

2. Nonlinear Analysis Correlation - Since the general behavior of responses in this excitation test is essentially the same as in Test HV2, the nonlinear analytical model formulated for Test HV2 was again used. The same damping factors, Coulomb friction coefficient, impact springs and tie bars were employed. The initial tie and joint gaps were chosen in the same manner described previously giving

$$\begin{aligned} &\Delta_T = 0.05 \text{ inch}, \quad \Delta_G = 0.04 \text{ inch} \quad \text{expansion joint No. 1} \\ &\Delta_T = 0.1 \text{ inch}, \quad \Delta_G = 0.05 \text{ inch} \quad \text{expansion joint No. 2} \end{aligned} \tag{90}$$

Comparative plots of the predicted and the measured responses are shown in Fig. 6.9. Like Test HV2, the nonlinear analysis correlation is greatly superior to the linear analysis correlation. Although permanent drifts take place in the measured response from approximately 2.1 seconds, it is beyond the scope of this analytical correlation to predict them as explained in Chapter IV. By comparing the predicted and measured responses at expansion joint No. 2, it is assessed that the critical failure of the shear key most likely was caused by a collision which took place at approximately 2 seconds. Figure 6.10 shows the predicted tie bar forces and tie yieldings of both expansion joints. The tie bar ductility factor μ_T defined in Eq. (89) reached approximately 10 and 13 at expansion joints No. 1 and No. 2, respectively. Figure 6.11 shows the contact force between girders caused by collisions. A maximum contact force of approximately 8000 lbs was induced at expansion joint No. 2. Like Test HV2, yielding of columns did not develop during the test.

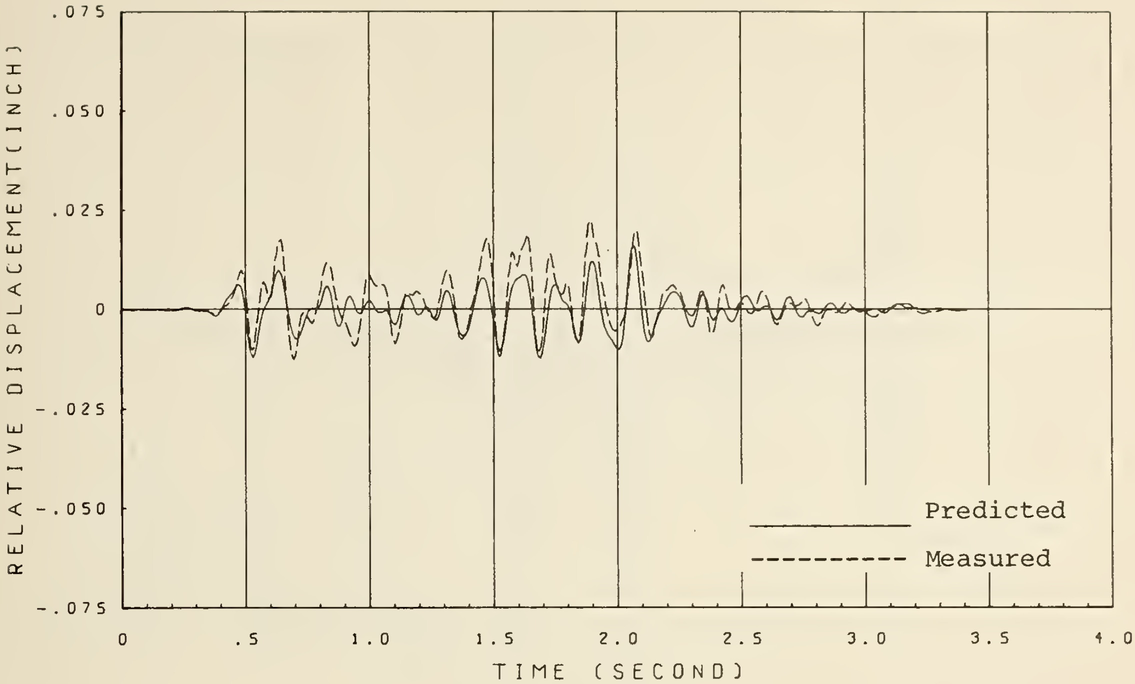

FIG. 6.1.1 LINEAR CORRELATION FOR TEST H1; SIDE GIRDER NO. 1; LONGITUDINAL (X) DIRECTION

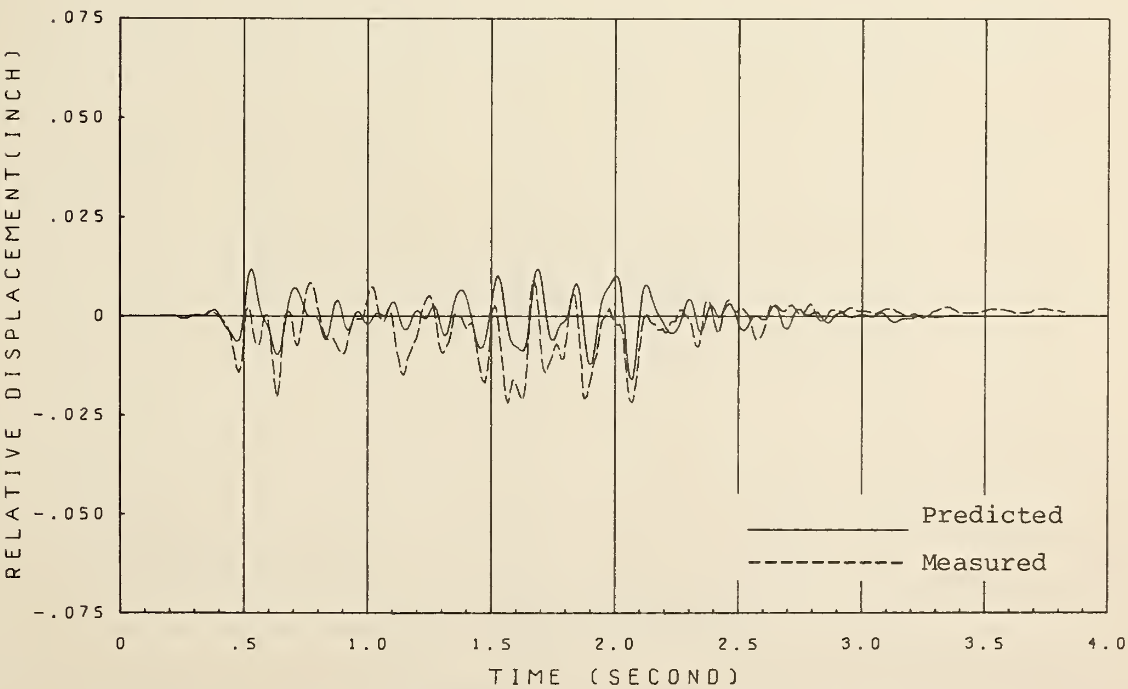

FIG. 6.1.2 LINEAR CORRELATION FOR TEST H1; SIDE GIRDER NO. 1; TRANSVERSE (Y) DIRECTION

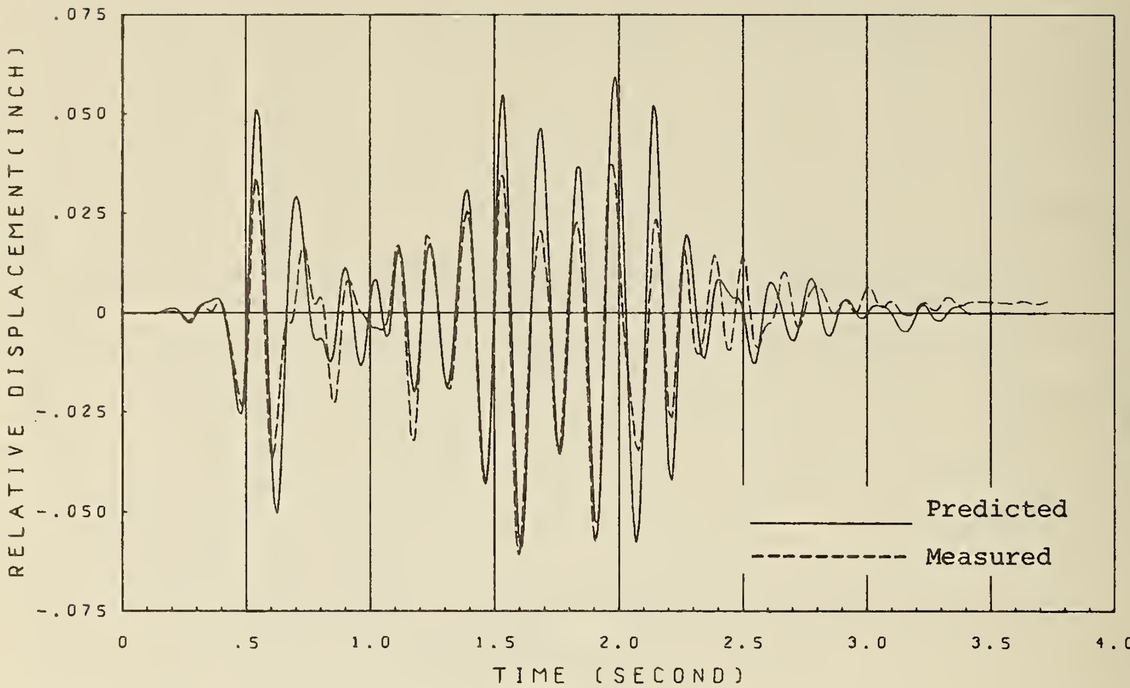

FIG. 6.1.3 LINEAR CORRELATION FOR TEST H1; CENTER GIRDER; TRANSVERSE (Y) DIRECTION

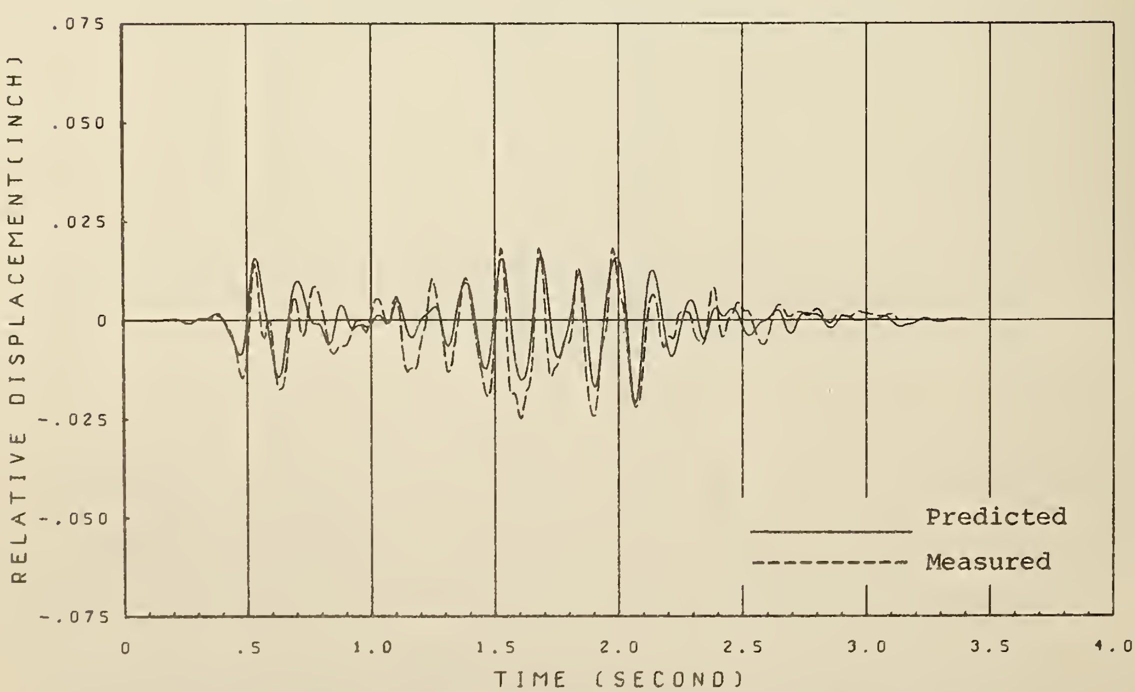

FIG. 6.1.4 LINEAR CORRELATION FOR TEST H1; SIDE GIRDER NO. 2; LONGITUDINAL (X) DIRECTION

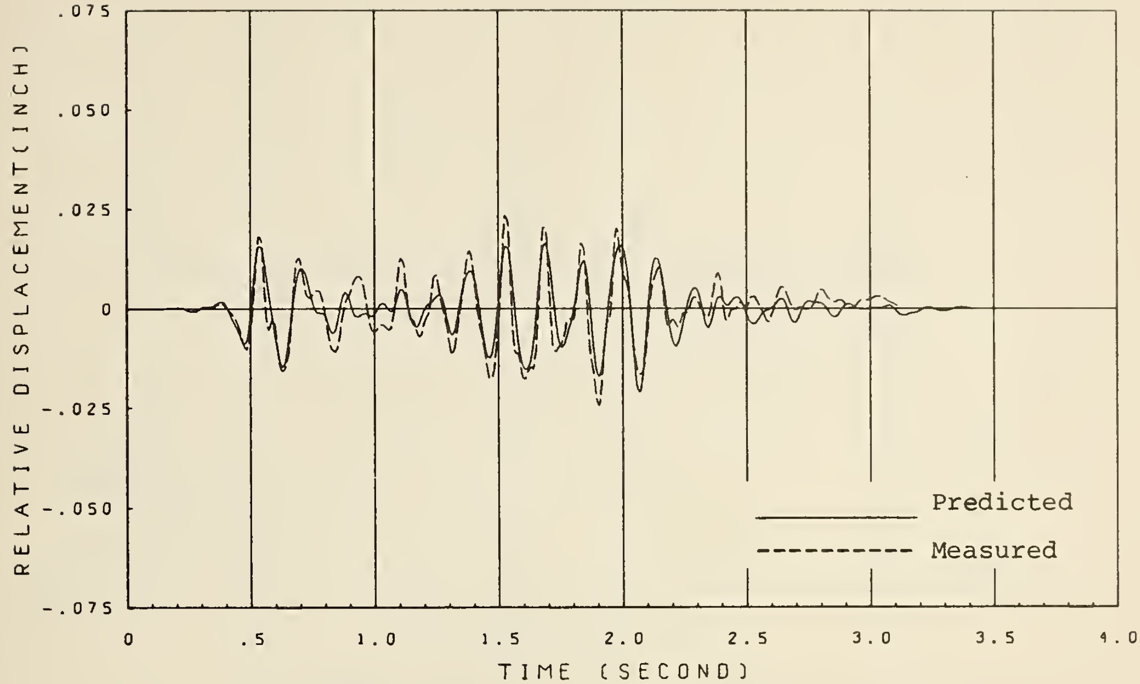

FIG. 6.1.5 LINEAR CORRELATION FOR TEST H1; SIDE GIRDER NO. 2; TRANSVERSE (Y) DIRECTION

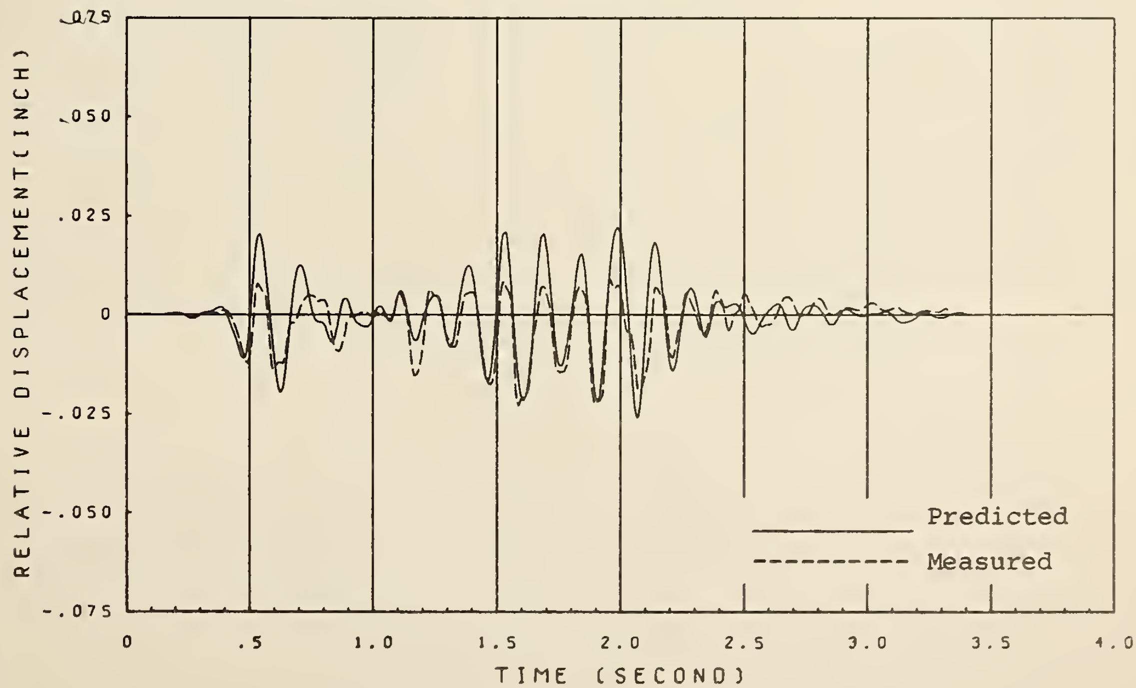

FIG. 6.1.6 LINEAR CORRELATION FOR TEST H1; EXPANSION JOINT NO. 1; INNER SIDE

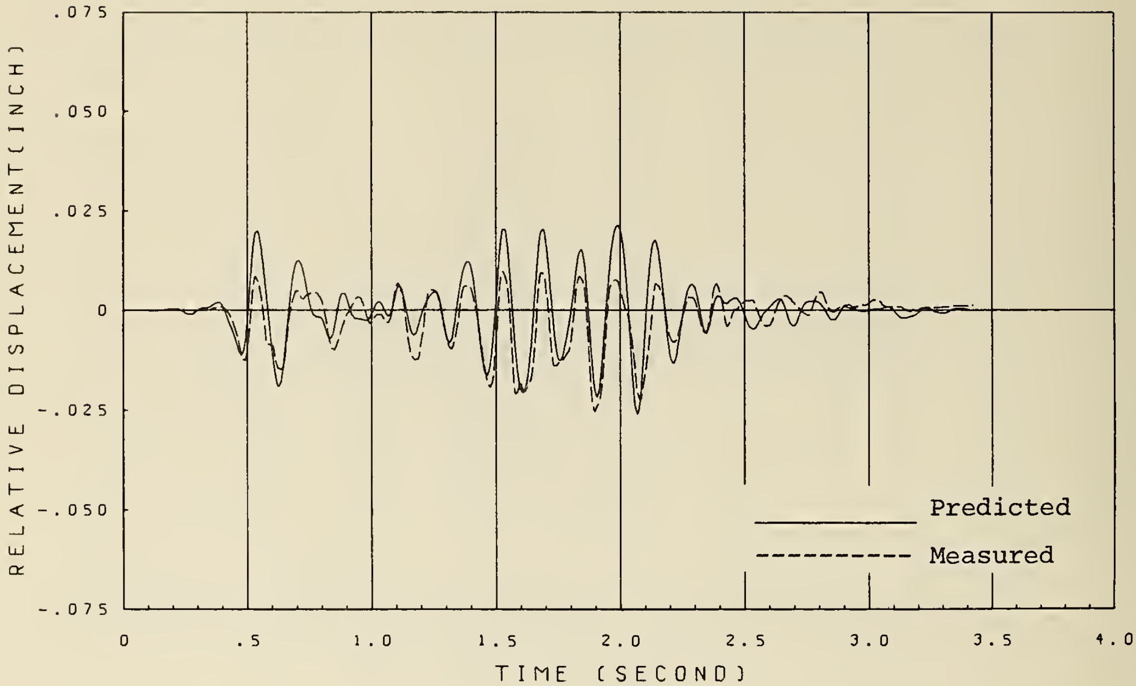

FIG. 6.1.7 LINEAR CORRELATION FOR TEST H1; EXPANSION JOINT NO. 1; OUTER SIDE

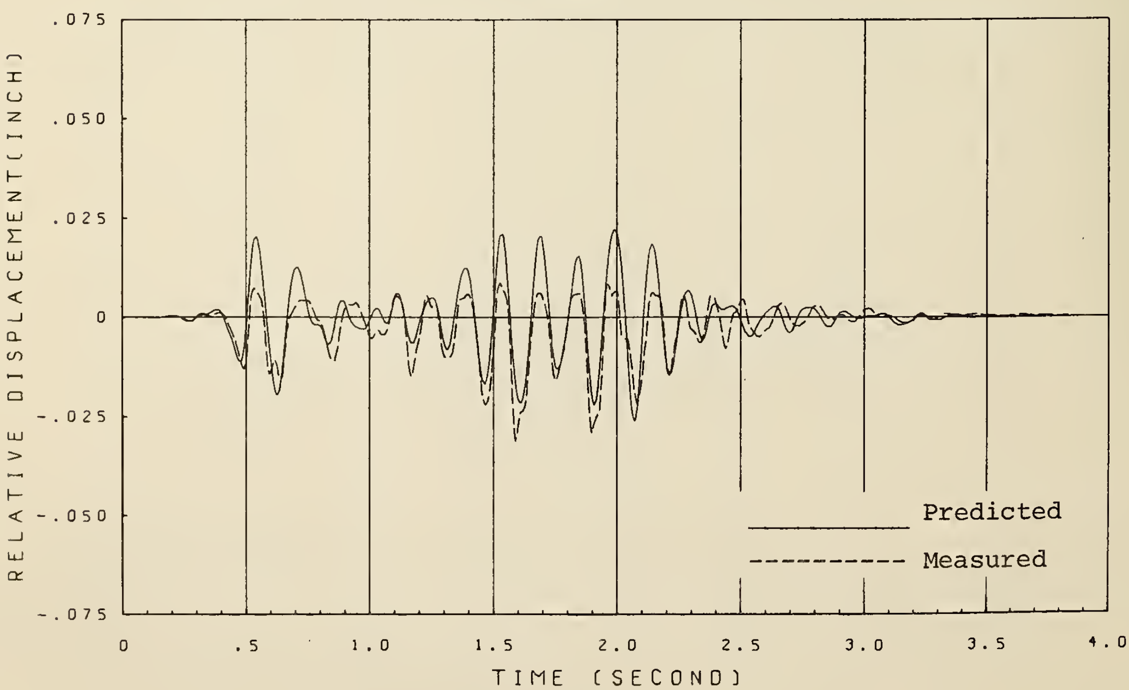

FIG. 6.1.8 LINEAR CORRELATION FOR TEST H1; EXPANSION JOINT NO. 2; INNER SIDE

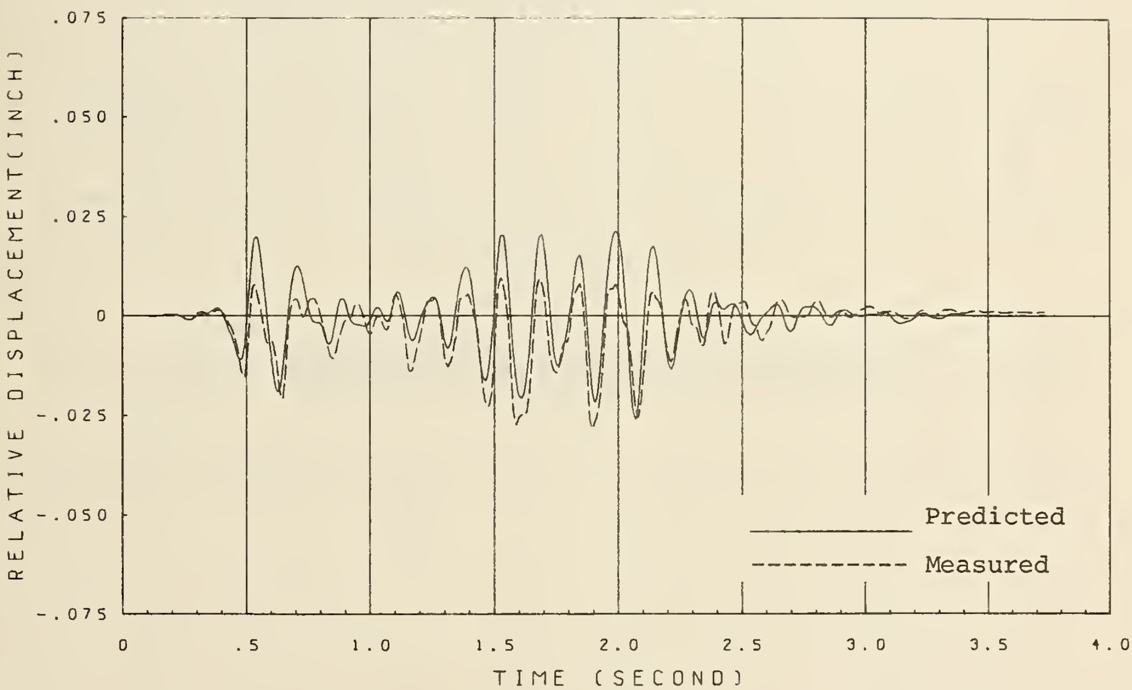

FIG. 6.1.9 LINEAR CORRELATION FOR TEST H1; EXPANSION JOINT NO. 2; OUTER SIDE

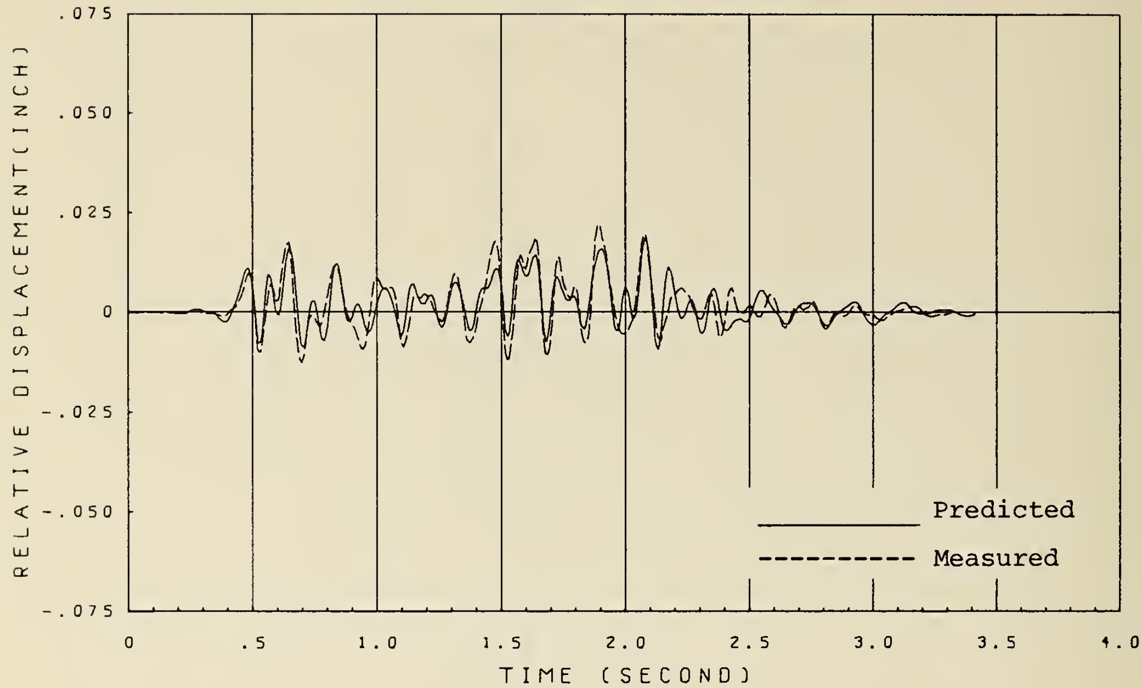

FIG. 6.2.1 NONLINEAR CORRELATION FOR TEST H1; SIDE GIRDER NO. 1; LONGITUDINAL (X) DIRECTION

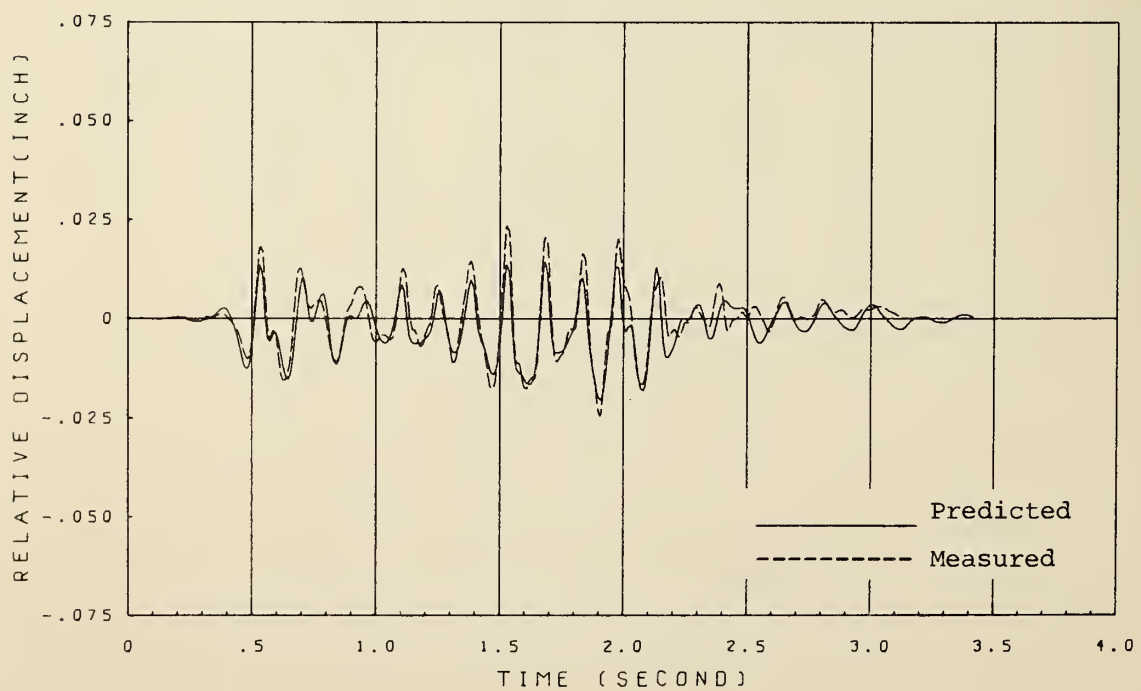

FIG. 6.2.2 NONLINEAR CORRELATION FOR TEST H1; SIDE GIRDER NO. 1; TRANSVERSE (Y) DIRECTION

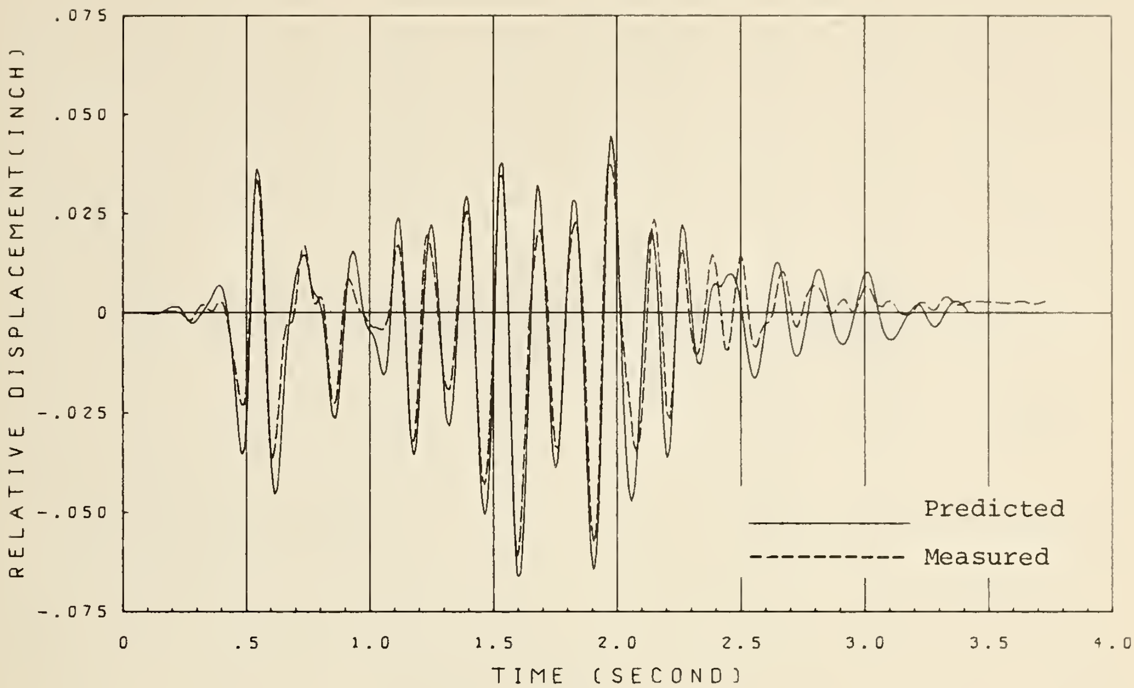

FIG. 6.2.3 NONLINEAR CORRELATION FOR TEST H1; CENTER GIRDER; TRANSVERSE (Y) DIRECTION

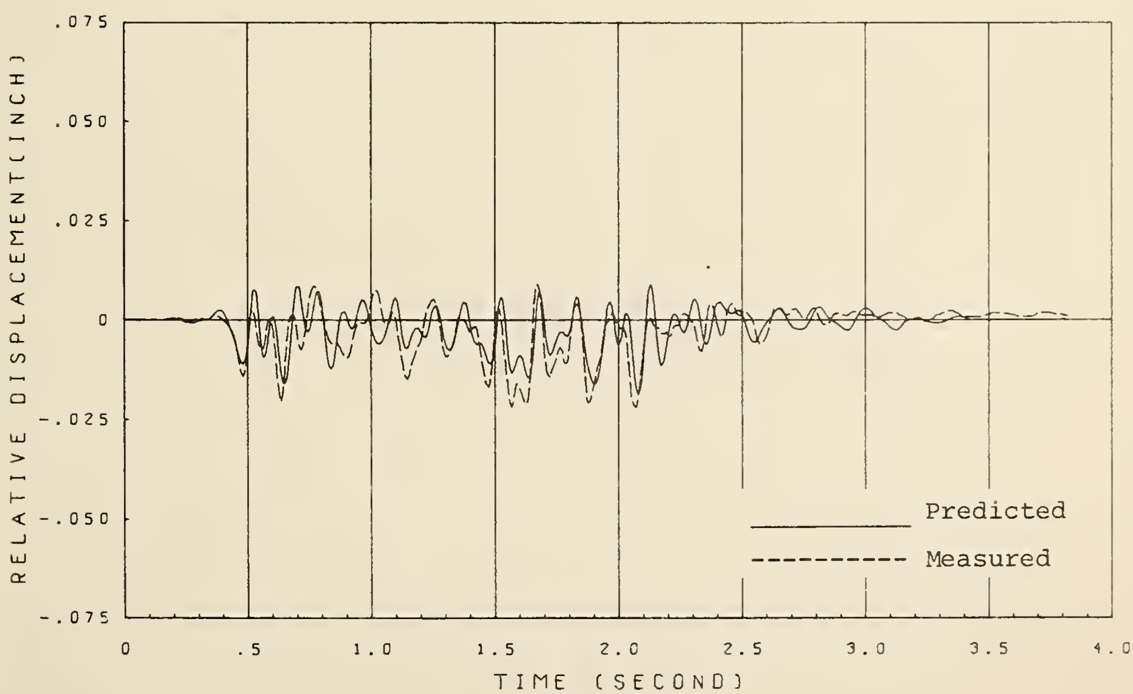

FIG. 6.2.4 NONLINEAR CORRELATION FOR TEST H1; SIDE GIRDER NO. 2; LONGITUDINAL (X) DIRECTION

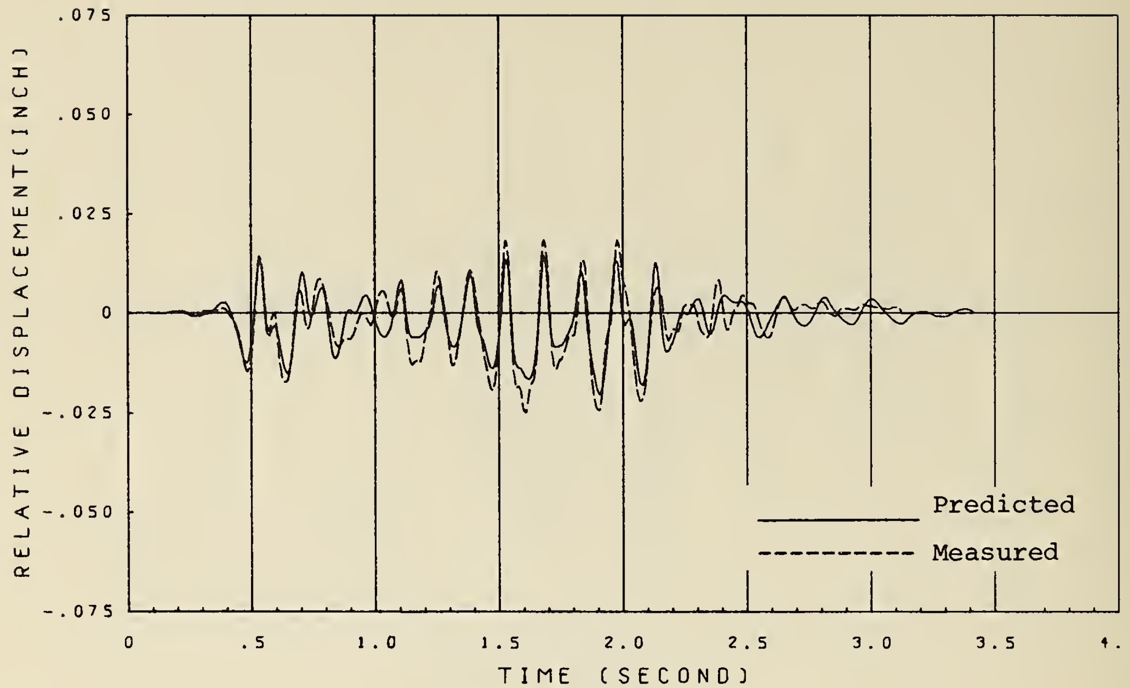

FIG. 6.2.5 NONLINEAR CORRELATION FOR TEST H1; SIDE GIRDER NO. 2; TRANSVERSE (Y) DIRECTION

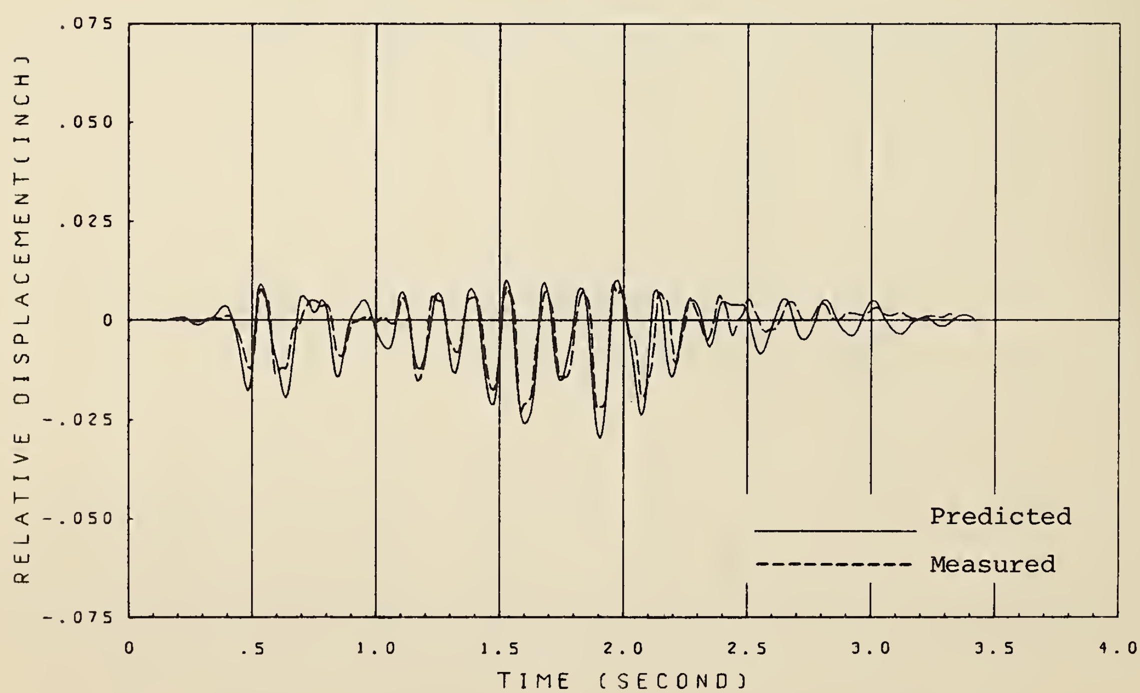

FIG. 6.2.6 NONLINEAR CORRELATION FOR TEST H1; EXPANSION JOINT NO. 1; INNER SIDE

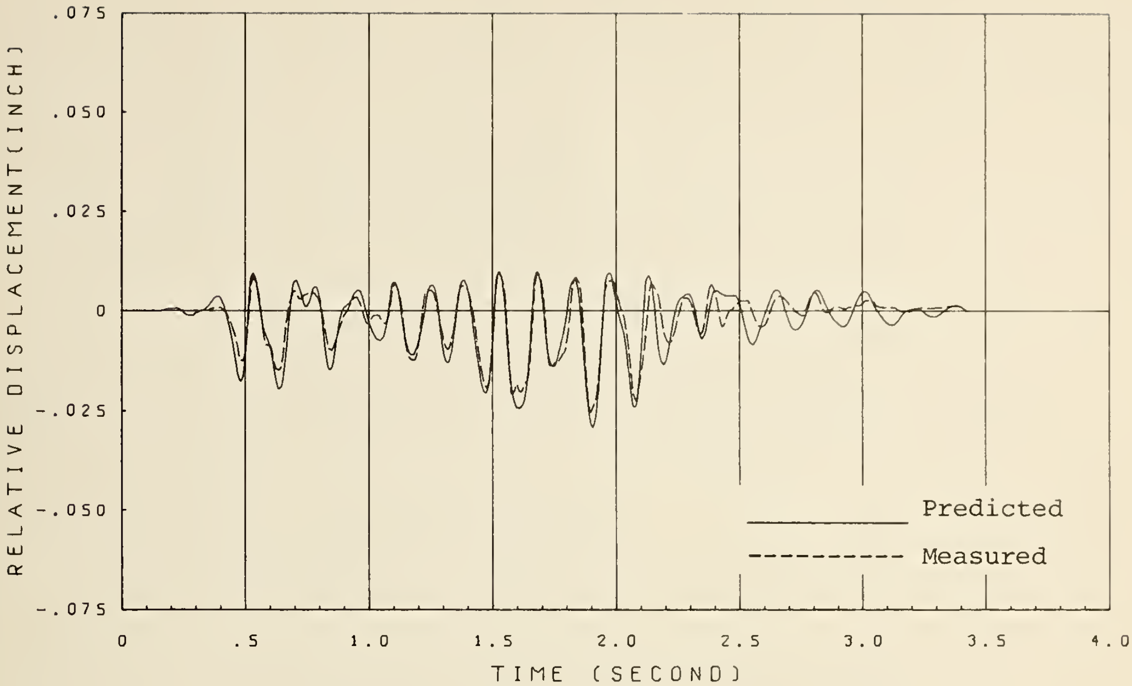

FIG. 6.2.7 NONLINEAR CORRELATION FOR TEST H1; EXPANSION JOINT NO. 1; OUTER SIDE

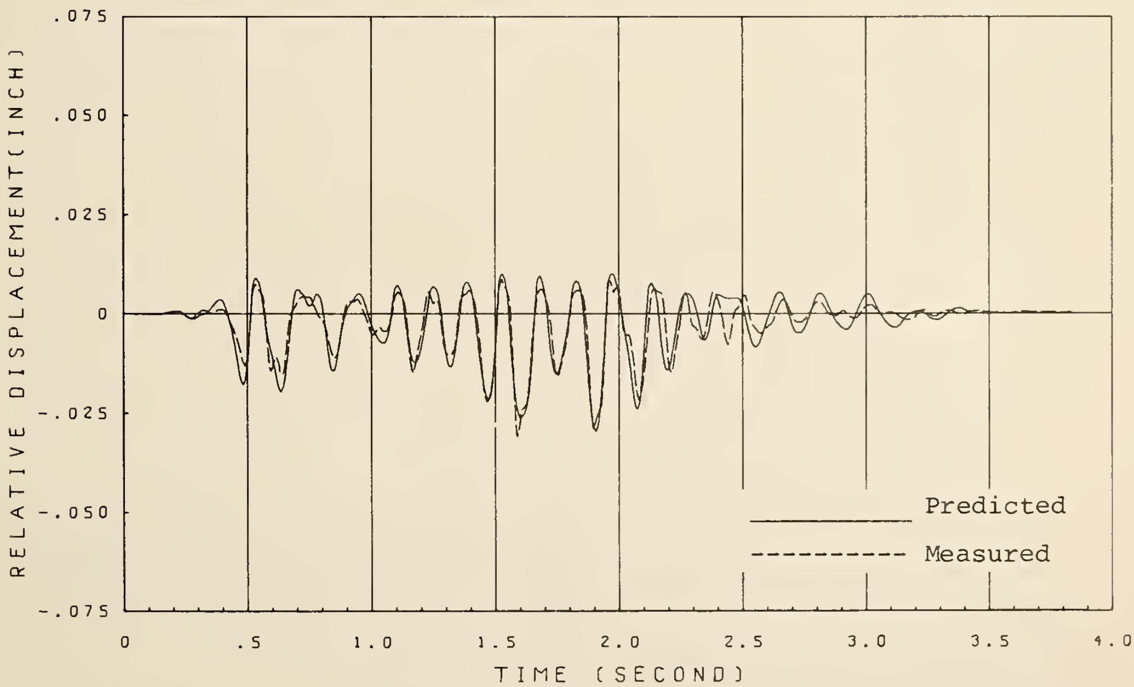

FIG. 6.2.8 NONLINEAR CORRELATION FOR TEST H1; EXPANSION JOINT NO. 2; INNER SIDE

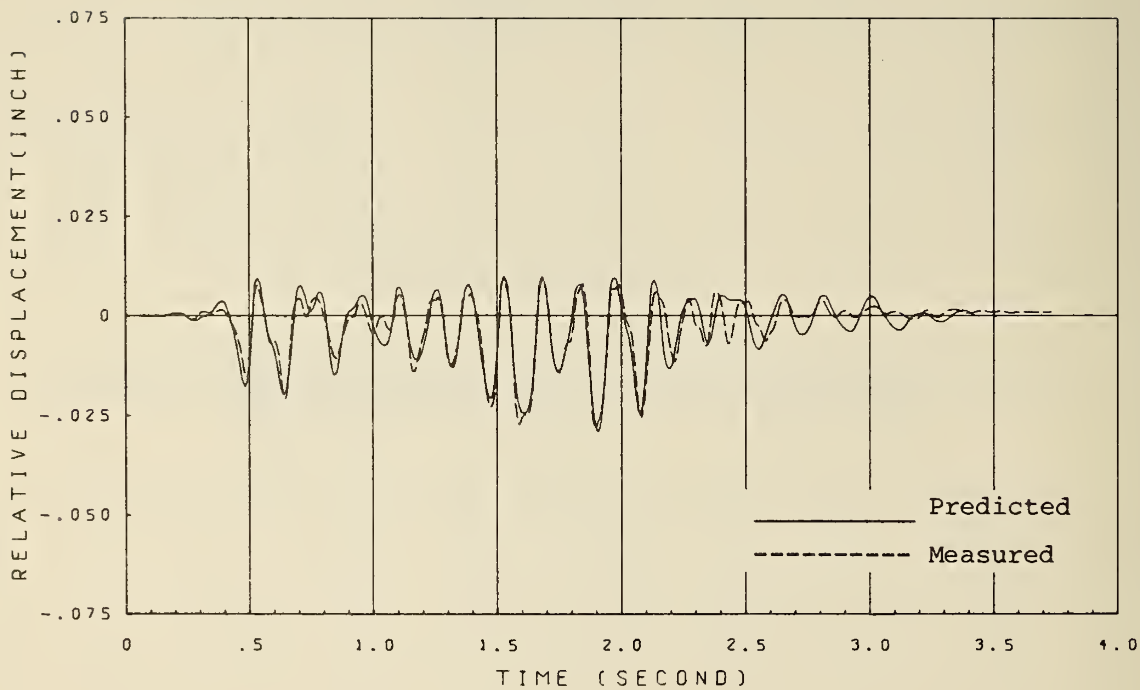

FIG. 6.2.9 NONLINEAR CORRELATION FOR TEST H1; EXPANSION JOINT NO. 2; OUTER SIDE

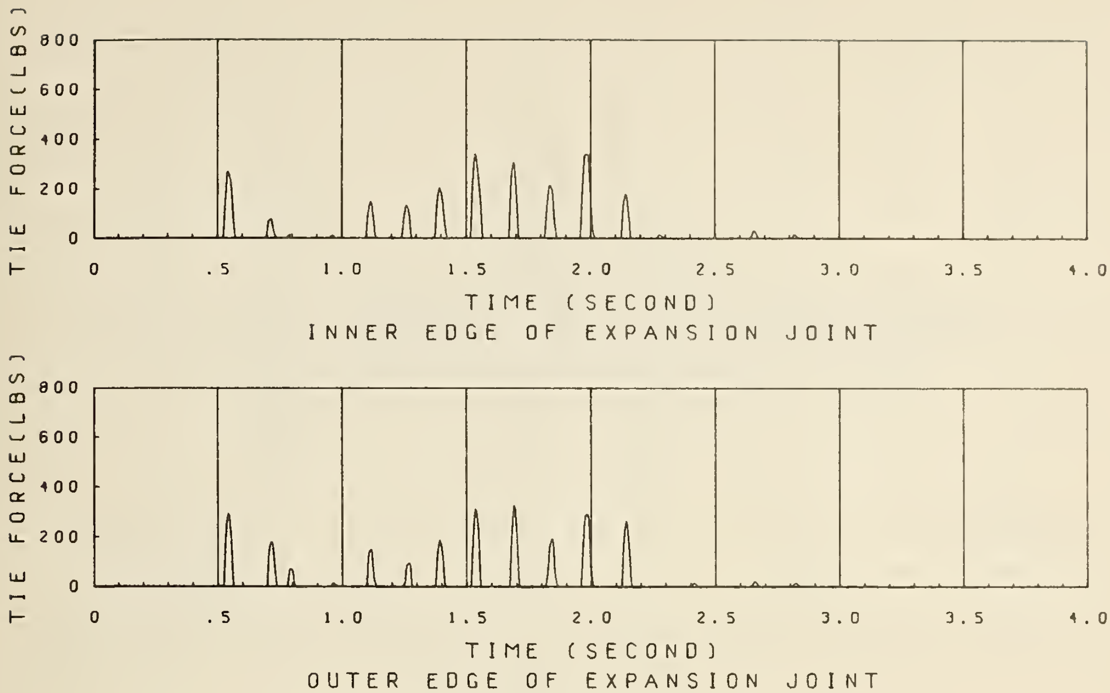

FIG. 6.3.1 PREDICTED TIE BAR FORCE FOR TEST H1; EXPANSION JOINT NO. 1

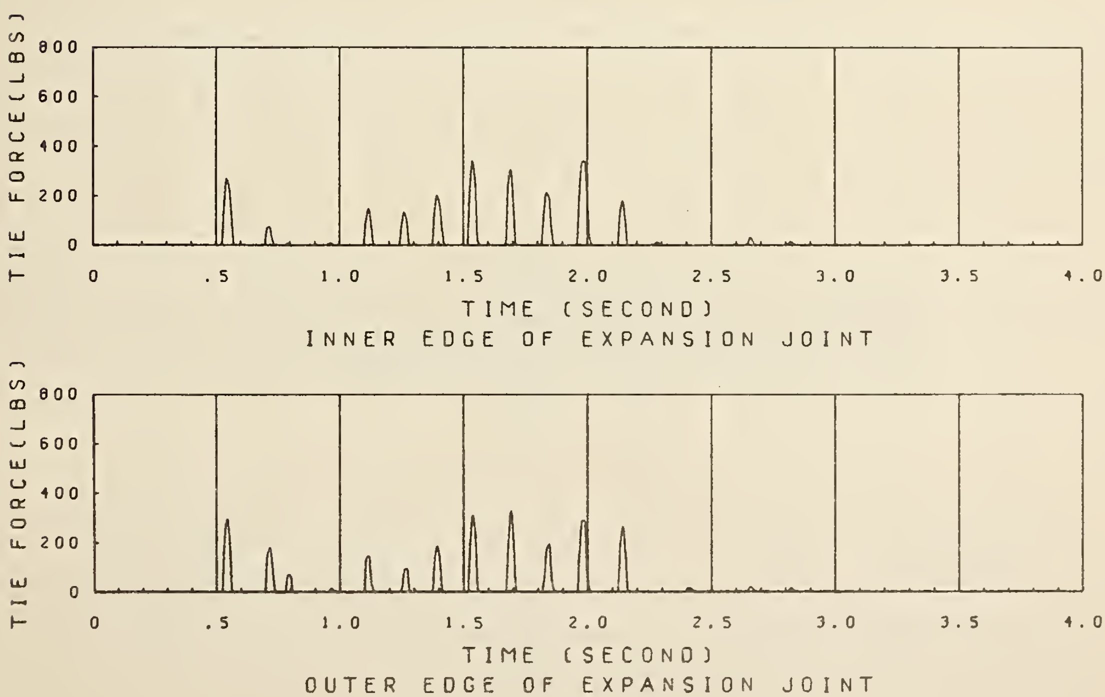

FIG. 6.3.2 PREDICTED TIE BAR FORCE FOR TEST H1; EXPANSION JOINT NO. 2

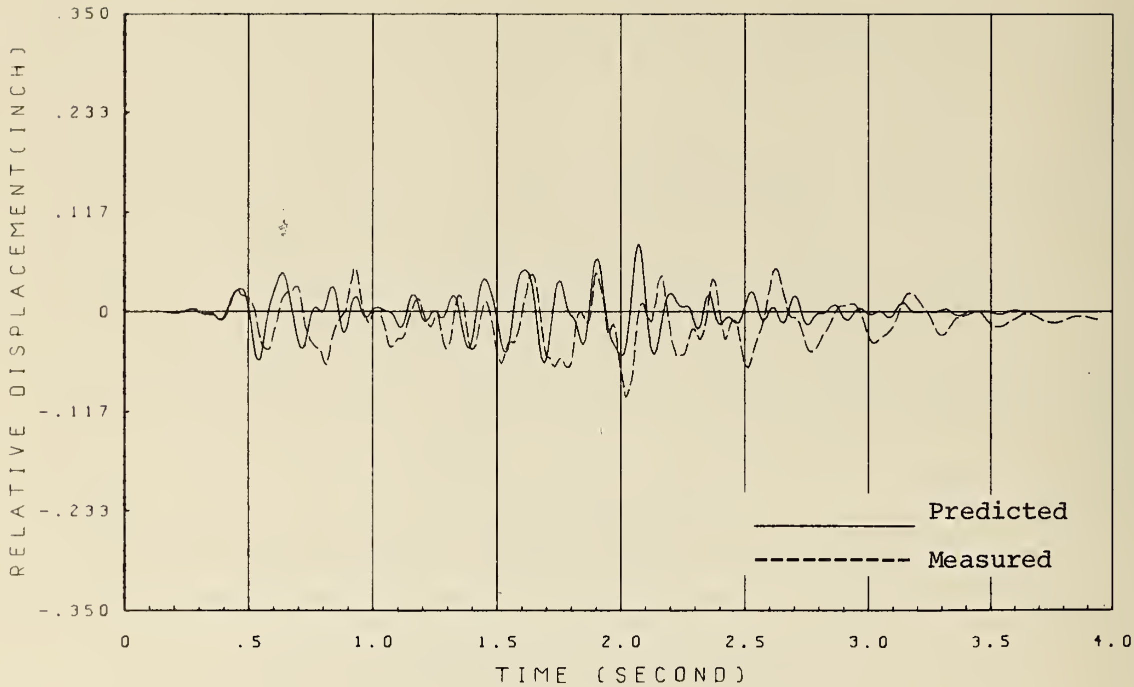

FIG. 6.4.1 LINEAR CORRELATION FOR TEST HV2; SIDE GIRDER NO. 1; LONGITUDINAL (X) DIRECTION

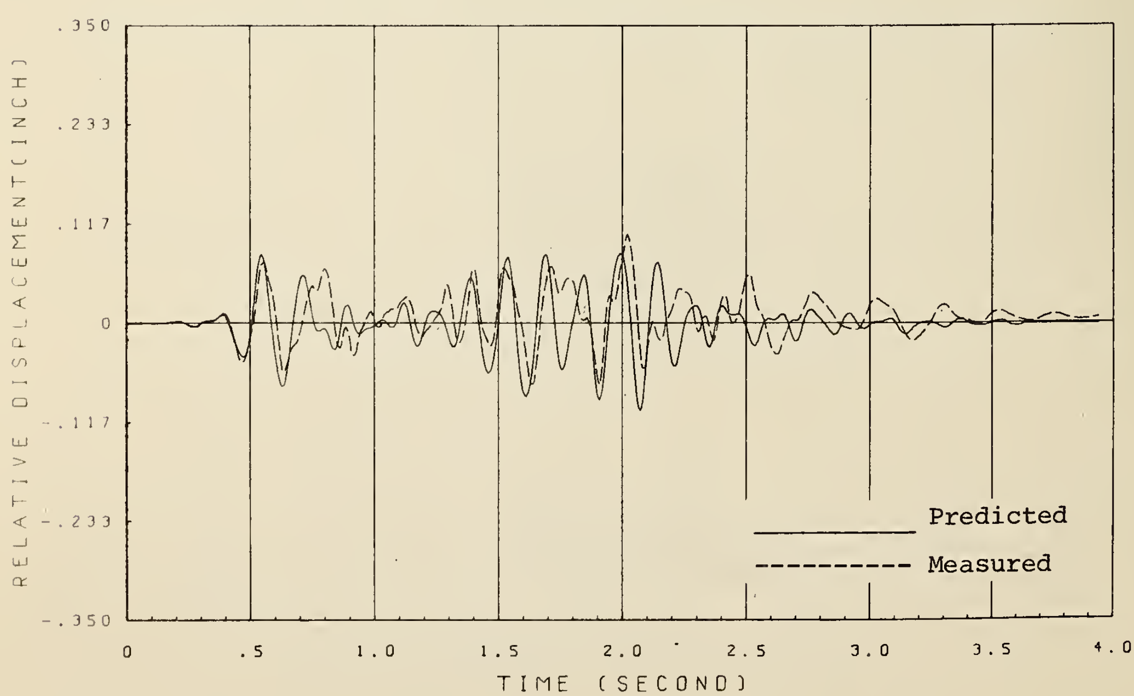

FIG. 6.4.2 LINEAR CORRELATION FOR TEST HV2; SIDE GIRDER NO. 1; TRANSVERSE (Y) DIRECTION

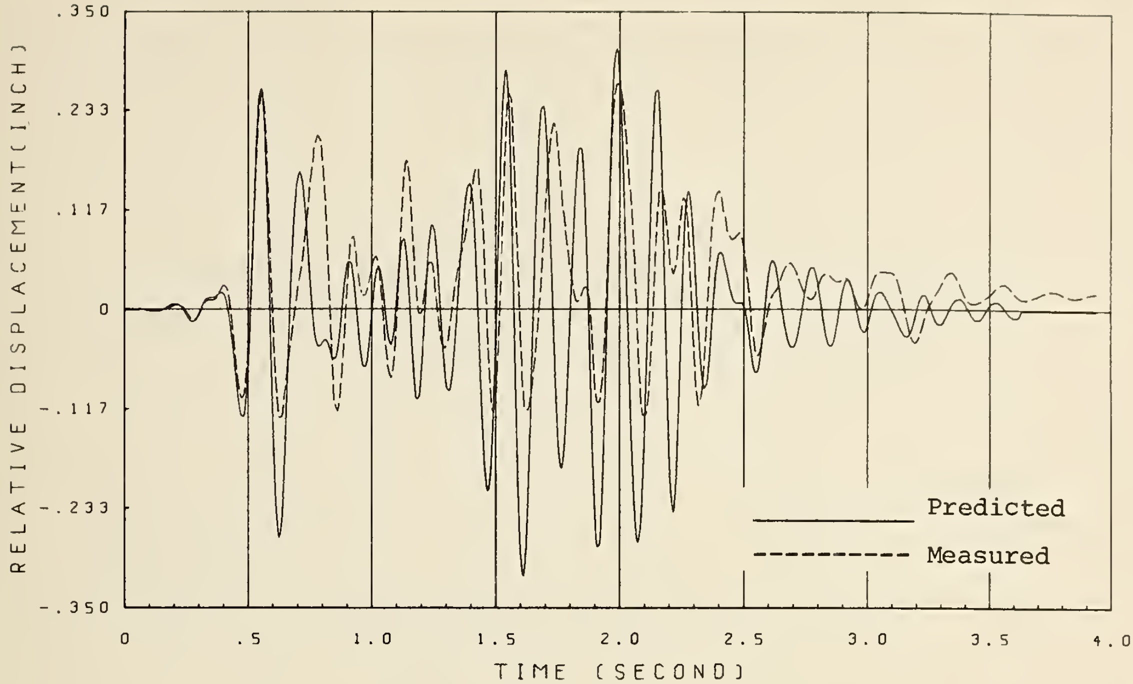

FIG. 6.4.3 LINEAR CORRELATION FOR TEST HV2; CENTER GIRDER; TRANSVERSE (Y) DIRECTION

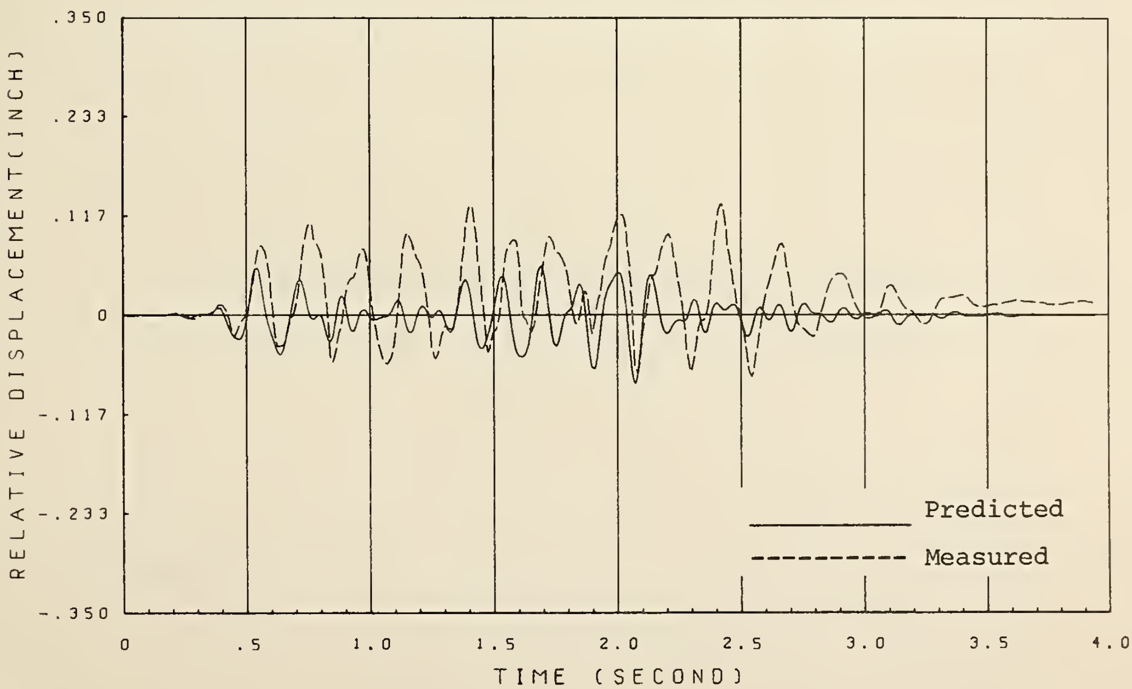

FIG. 6.4.4 LINEAR CORRELATION FOR TEST HV2; SIDE GIRDER NO. 2; LONGITUDINAL (X) DIRECTION

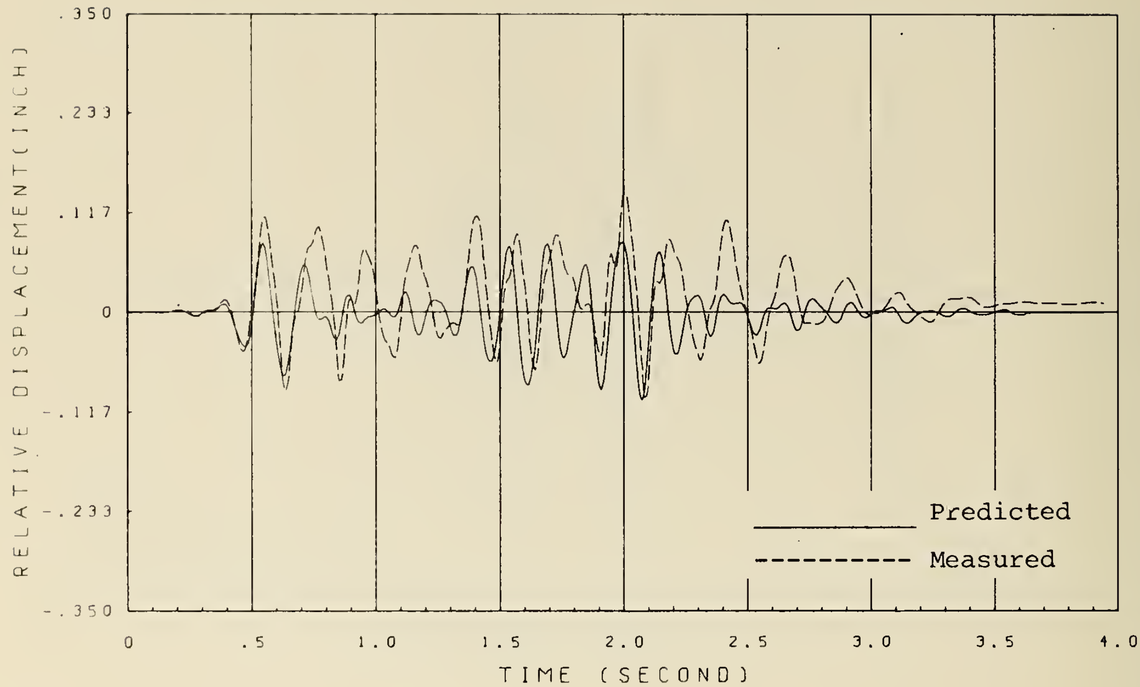

FIG. 6.4.5 LINEAR CORRELATION FOR TEST HV2; SIDE GIRDER NO. 2; TRANSVERSE (Y) DIRECTION

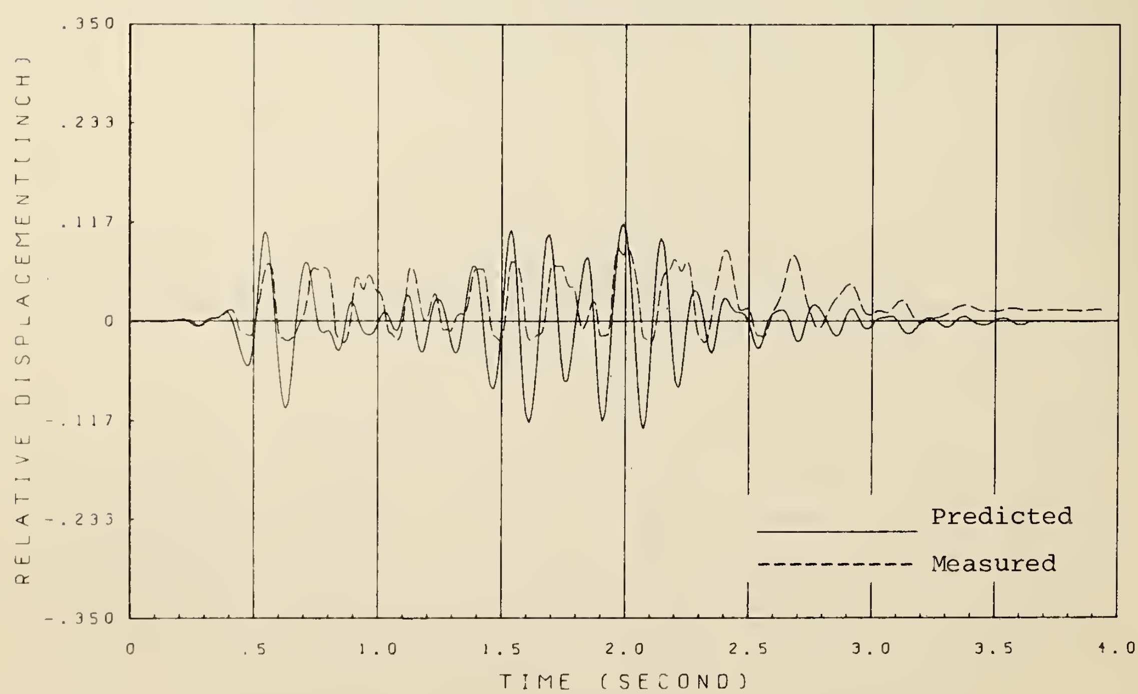

FIG. 6.4.6 LINEAR CORRELATION FOR TEST HV2; EXPANSION JOINT NO. 1; INNER SIDE

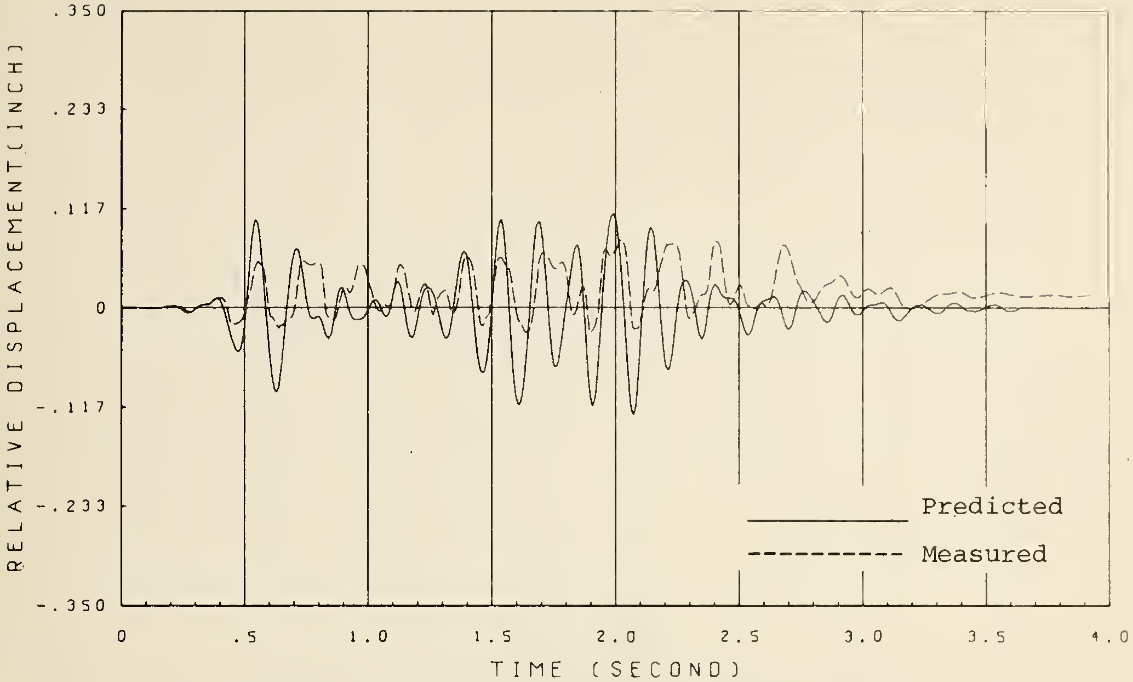

FIG. 6.4.7 LINEAR CORRELATION FOR TEST HV2; EXPANSION JOINT NO. 1; OUTER SIDE

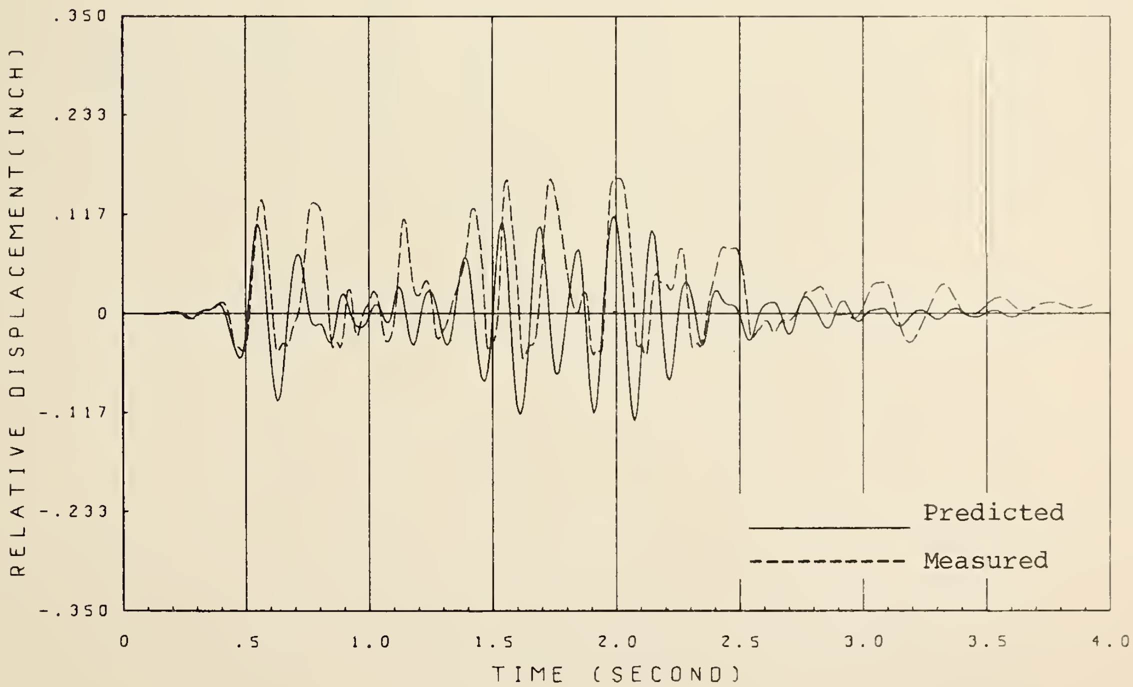

FIG. 6.4.8 LINEAR CORRELATION FOR TEST HV2; EXPANSION JOINT NO. 2; INNER SIDE

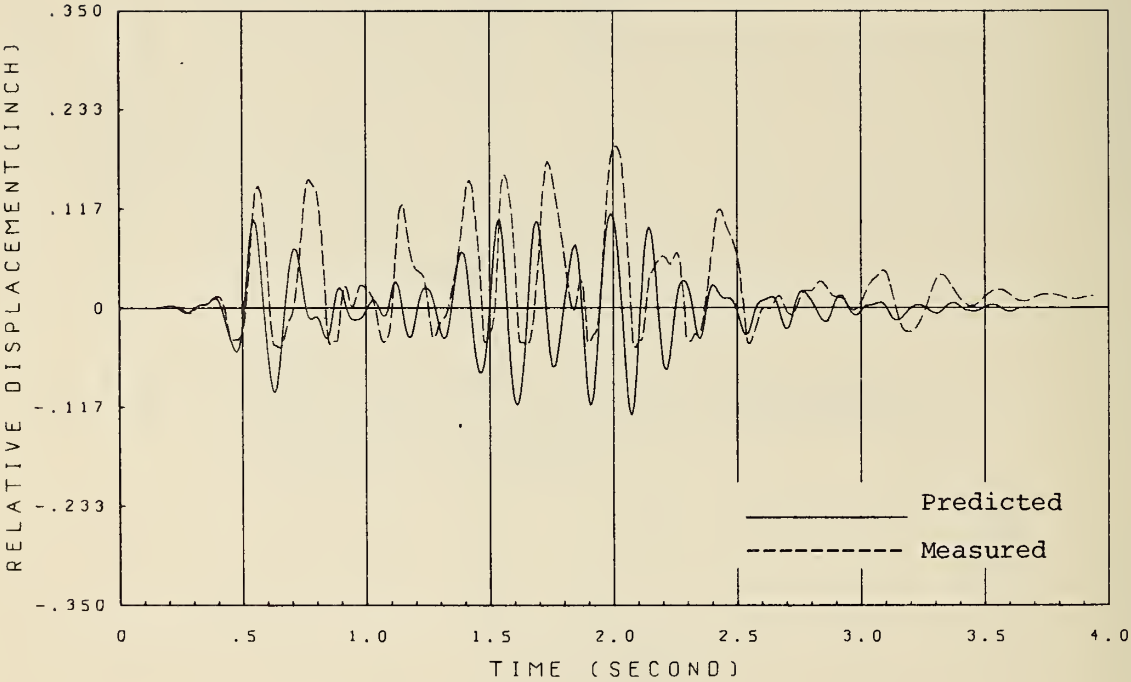

FIG. 6.4.9 LINEAR CORRELATION FOR TEST HV2; EXPANSION JOINT NO. 2; OUTER SIDE

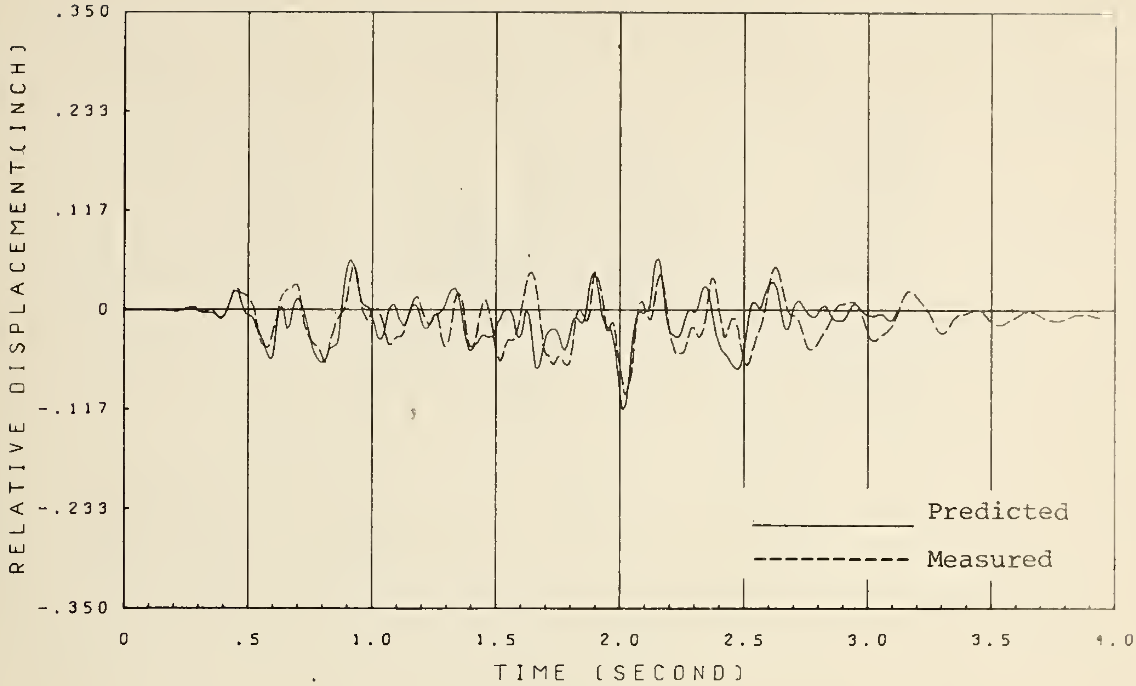

FIG. 6.5.1 NONLINEAR CORRELATION FOR TEST HV2; SIDE GIRDER NO. 1; LONGITUDINAL (X) DIRECTION

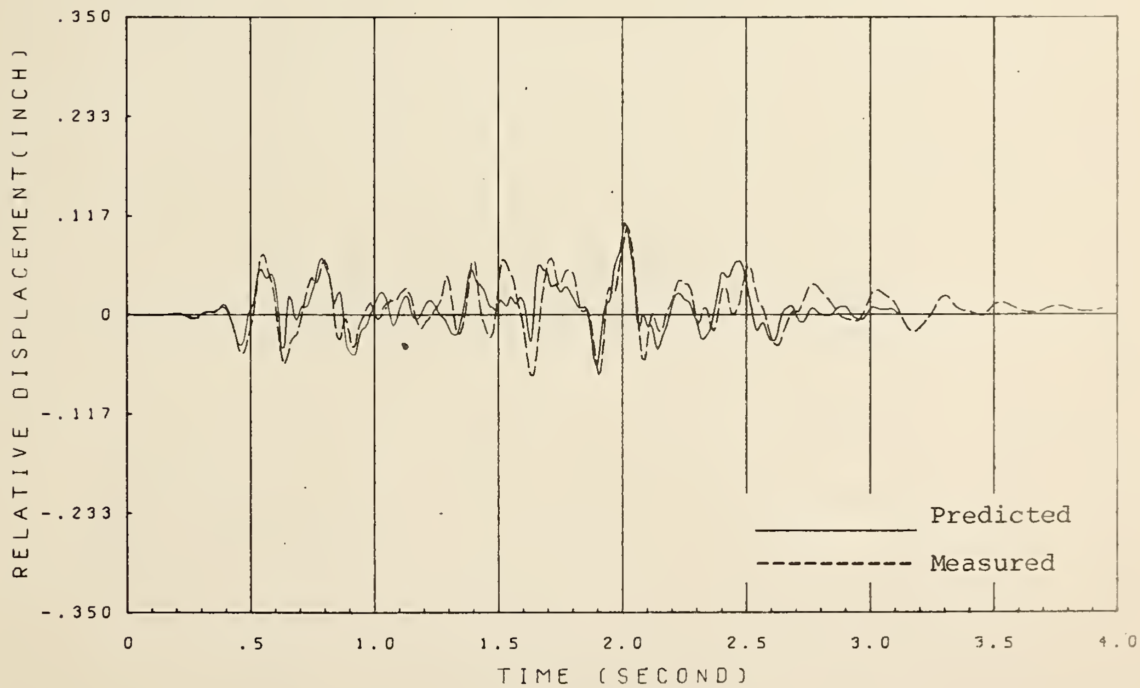

FIG. 6.5.2 NONLINEAR CORRELATION FOR TEST HV2; SIDE GIRDER NO. 1; TRANSVERSE (Y) DIRECTION

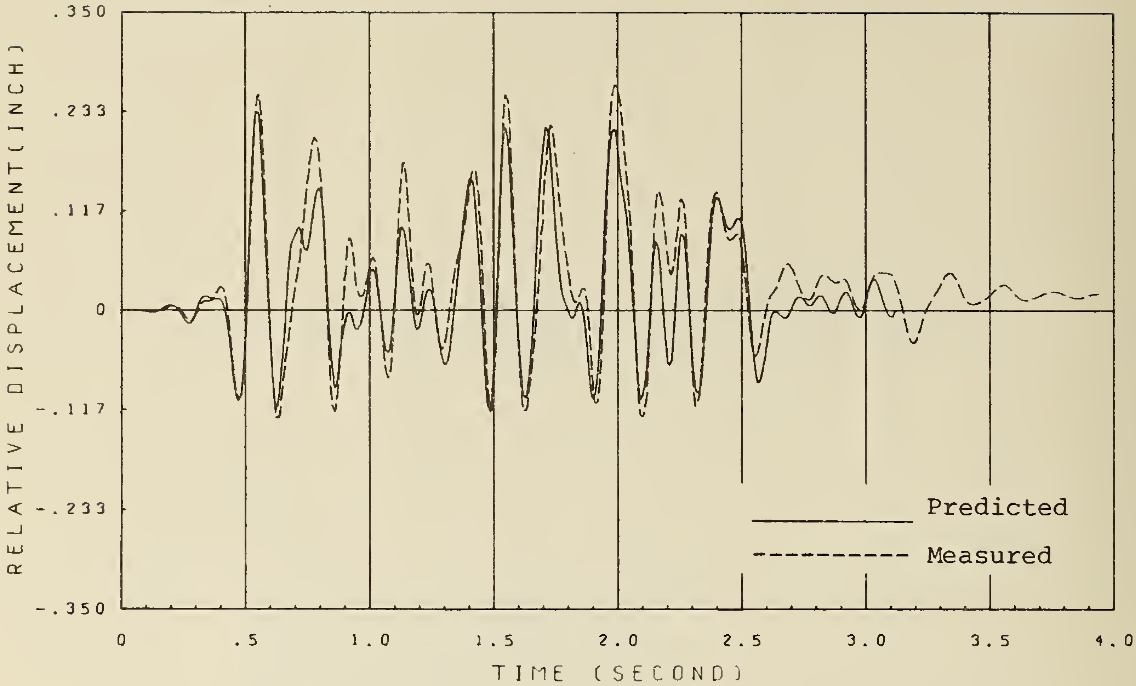

FIG. 6.5.3 NONLINEAR CORRELATION FOR TEST HV2; CENTER GIRDER; TRANSVERSE (Y) DIRECTION

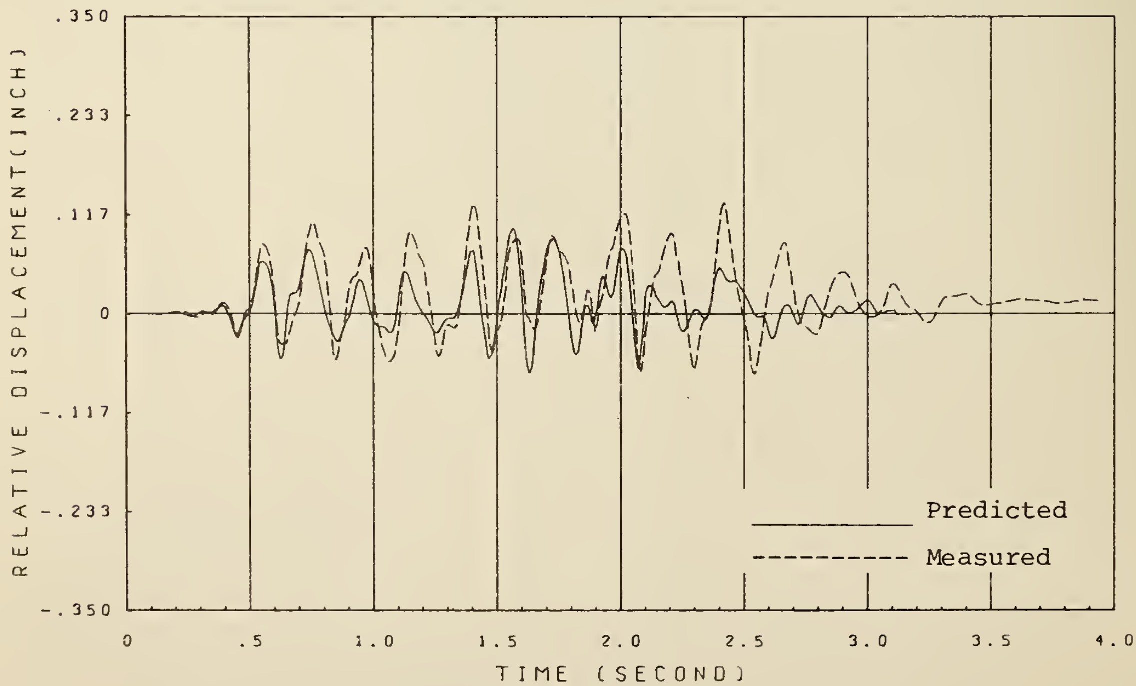

FIG. 6.5.4 NONLINEAR COORELATION FOR TEST HV2; SIDE GIRDER NO. 2; LONGITUDINAL (X) DIRECTION

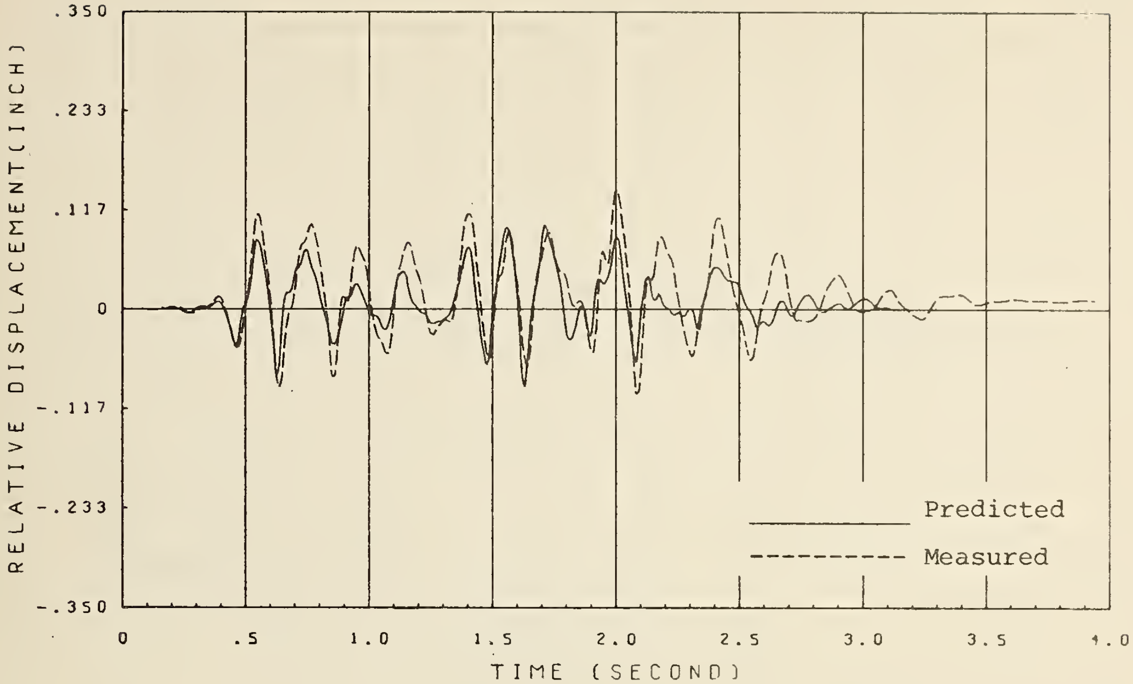

FIG. 6.5.5 NONLINEAR CORRELATION FOR TEST HV2; SIDE GIRDER NO. 2; TRANSVERSE (Y) DIRECTION

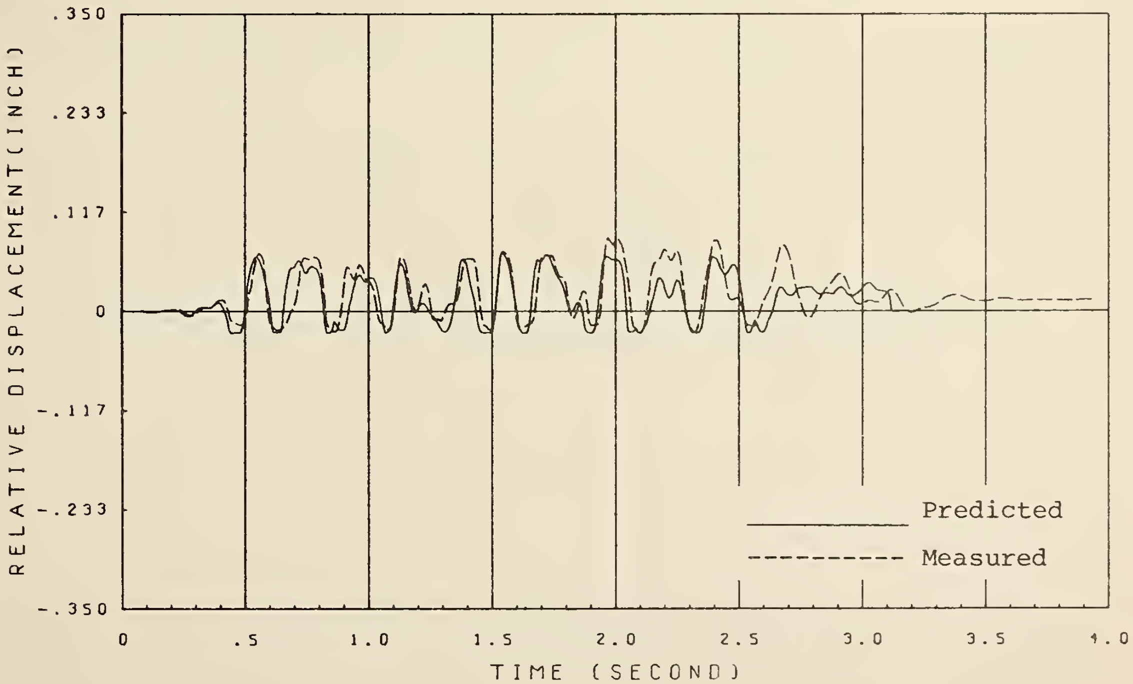

FIG. 6.5.6 NONLINEAR CORRELATION FOR TEST HV2; EXPANSION JOINT NO. 1; INNER SIDE

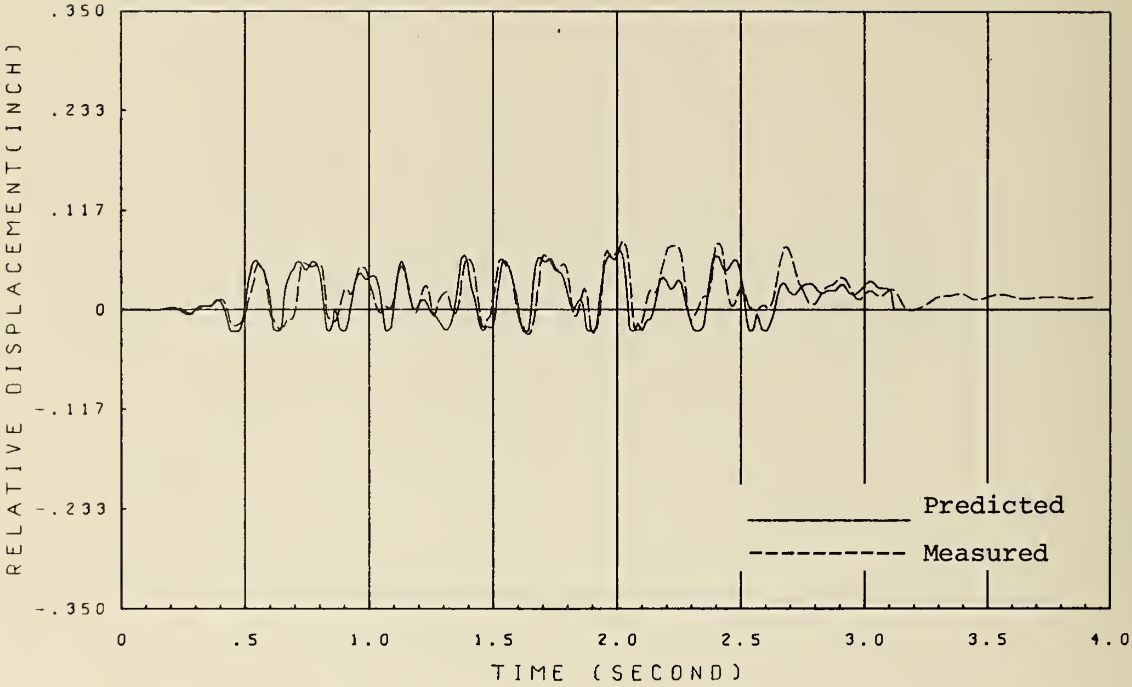

FIG. 6.5.7 NONLINEAR CORRELATION FOR TEST HV2; EXPANSION JOINT NO. 1; OUTER SIDE

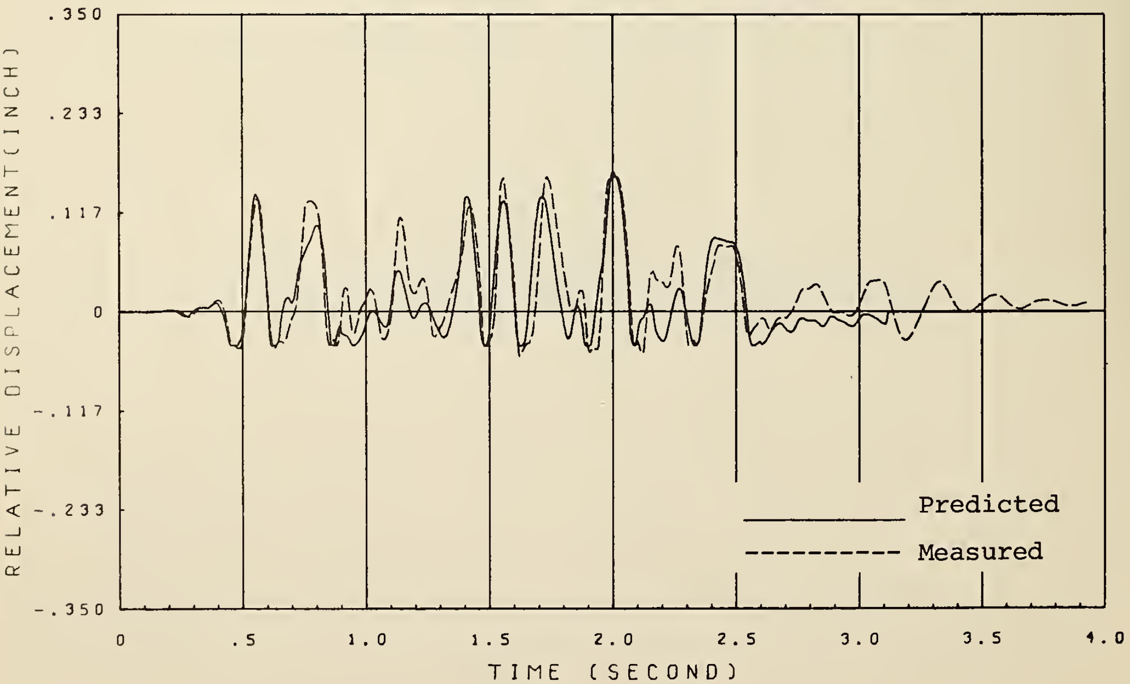

FIG. 6.5.8 NONLINEAR CORRELATION FOR TEST HV2; EXPANSION JOINT NO. 2; INNER SIDE

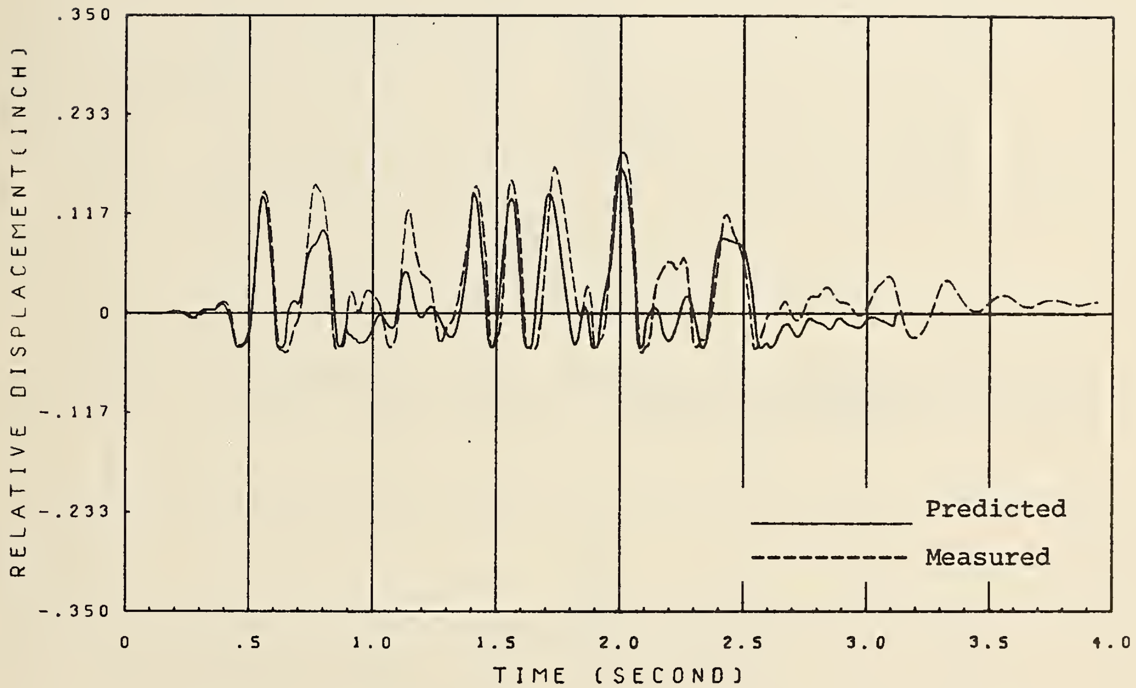

FIG. 6.5.9 NONLINEAR CORRELATION FOR TEST HV2; EXPANSION JOINT NO. 2; OUTER SIDE

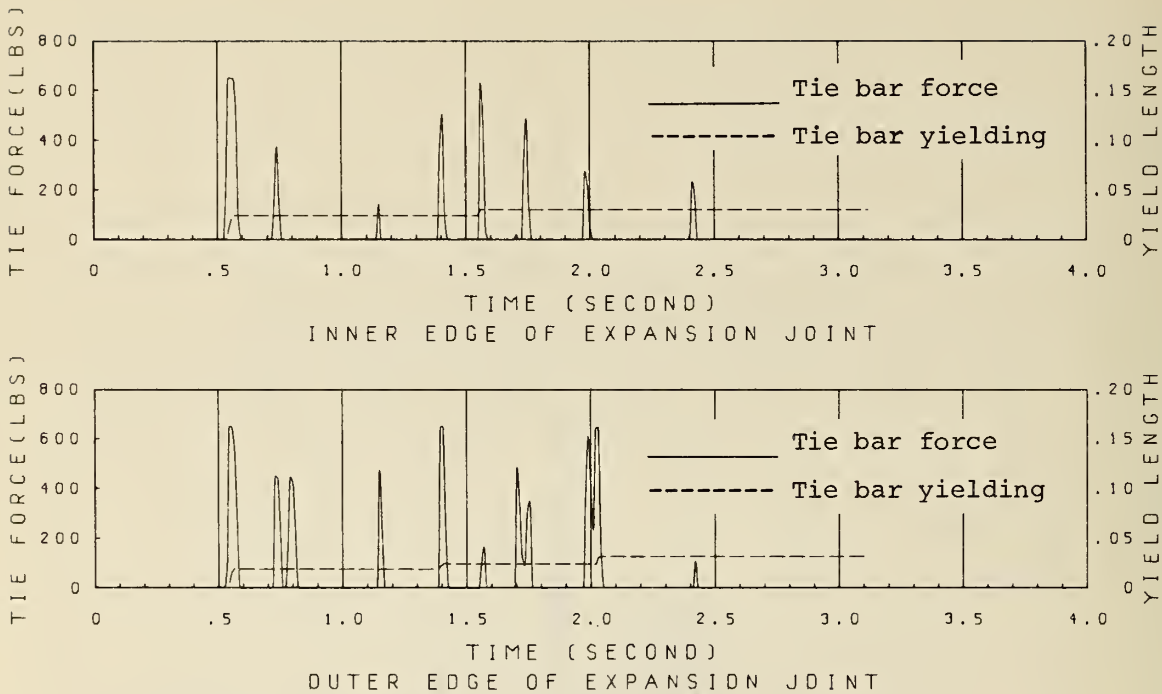

FIG. 6.6.1 PREDICTED TIE BAR FORCE AND YIELD LENGTH FOR TEST HV2; EXPANSION JOINT NO. 1

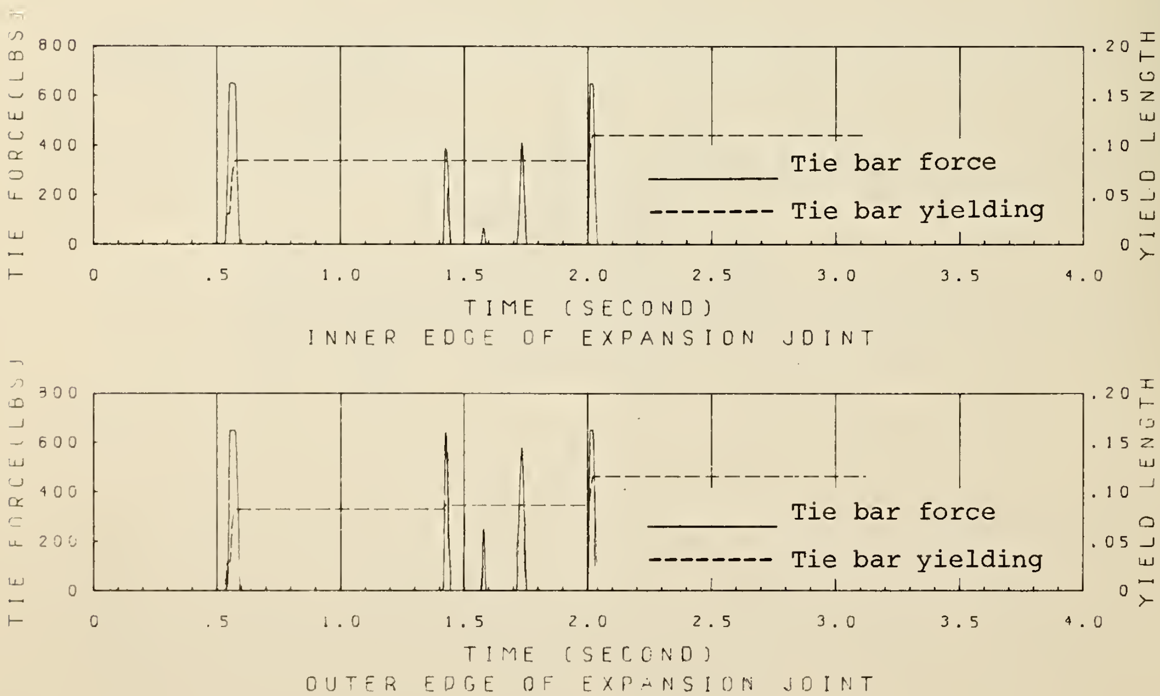

FIG. 6.6.2 PREDICTED TIE BAR FORCE AND YIELD LENGTH FOR TEST HV2; EXPANSION JOINT NO. 2

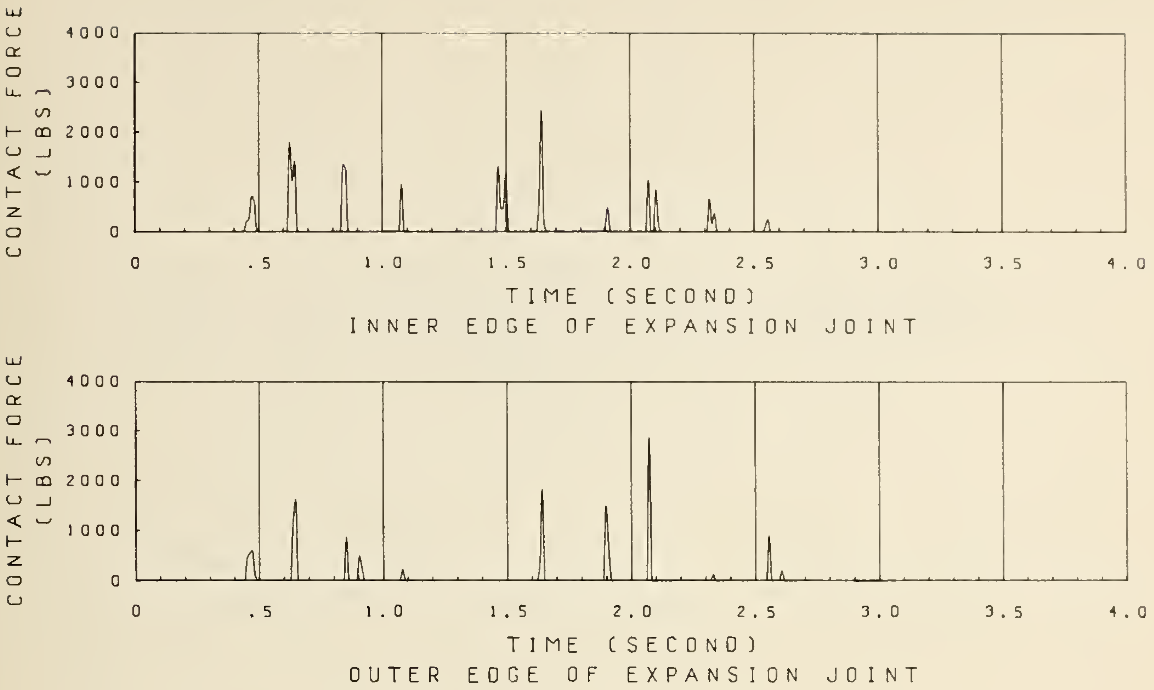

FIG. 6.7.1 PREDICTED CONTACT FORCE FOR TEST HV2; EXPANSION JOINT NO. 1

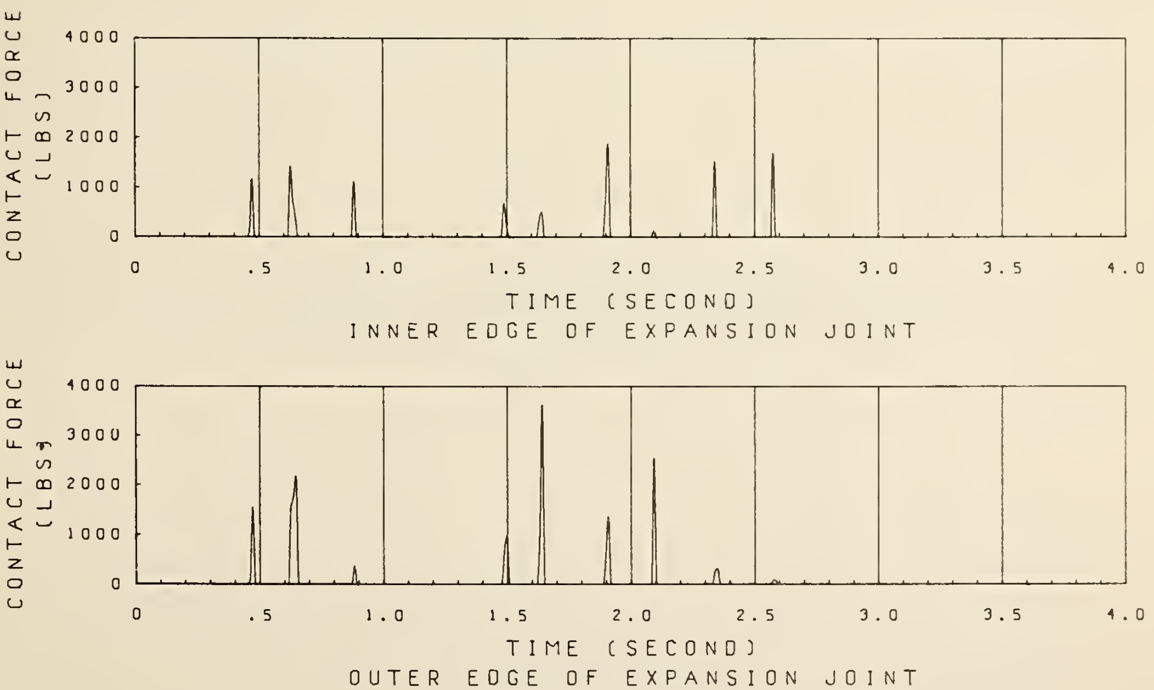

FIG. 6.7.2 PREDICTED CONTACT FORCE FOR TEST HV2; EXPANSION JOINT NO. 2

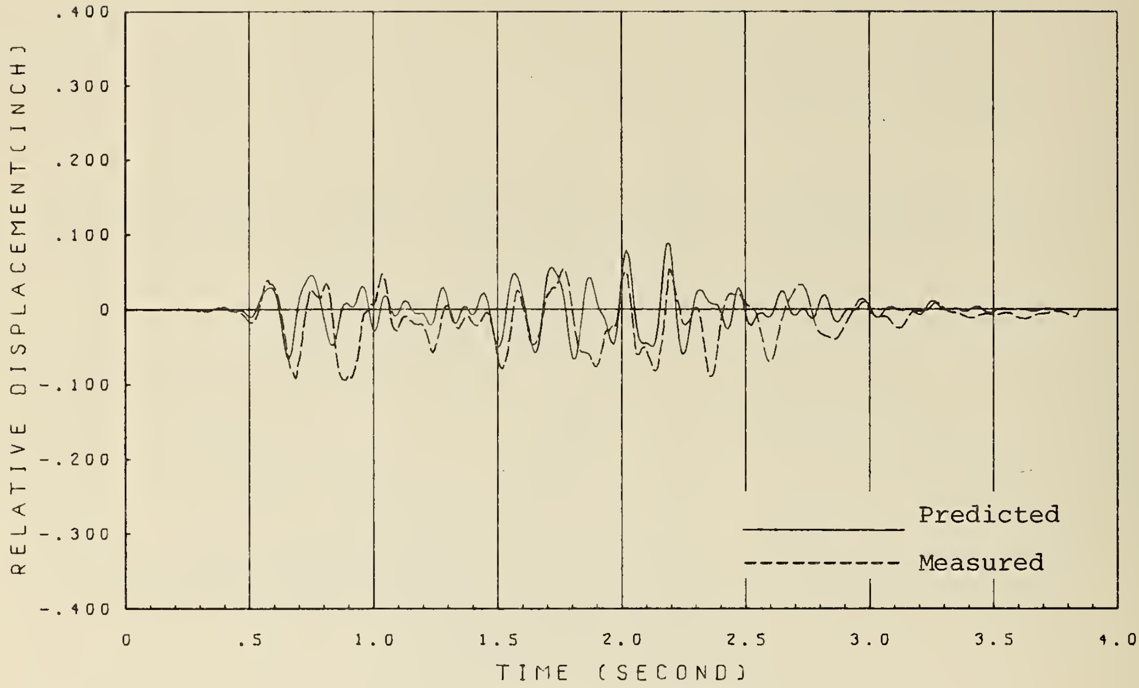

FIG. 6.8.1 LINEAR CORRELATION FOR TEST H3; SIDE GIRDER NO. 1; LONGITUDINAL (X) DIRECTION

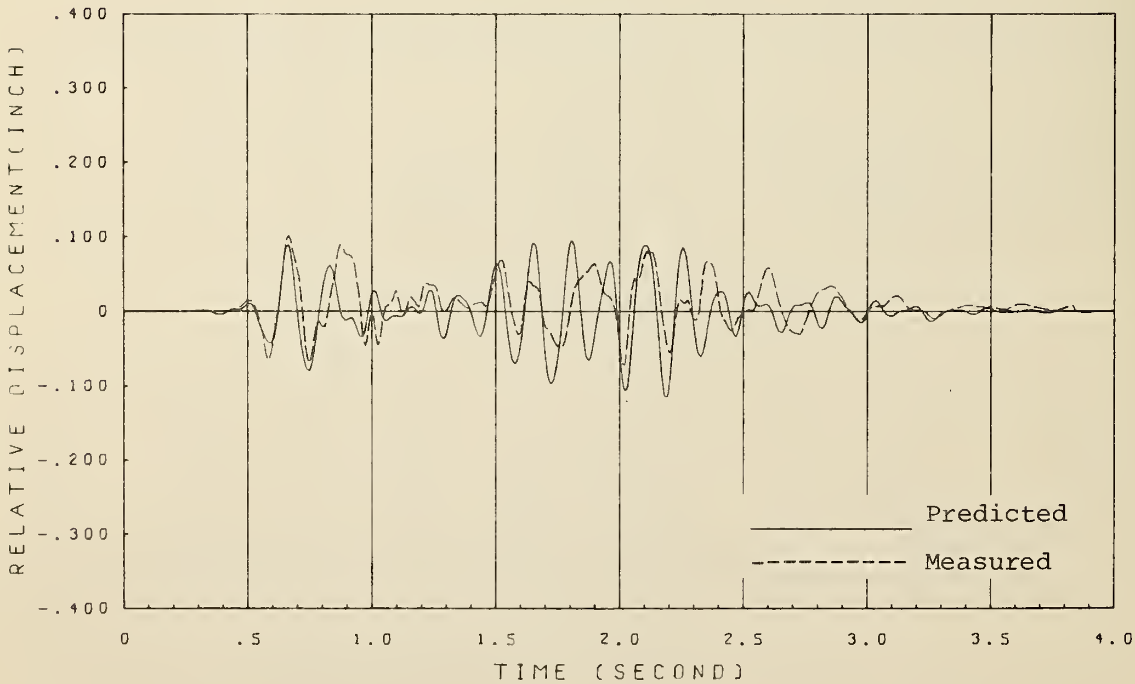

FIG. 6.8.2 LINEAR CORRELATION FOR TEST H3; SIDE GIRDER NO. 1; TRANSVERSE (Y) DIRECTION

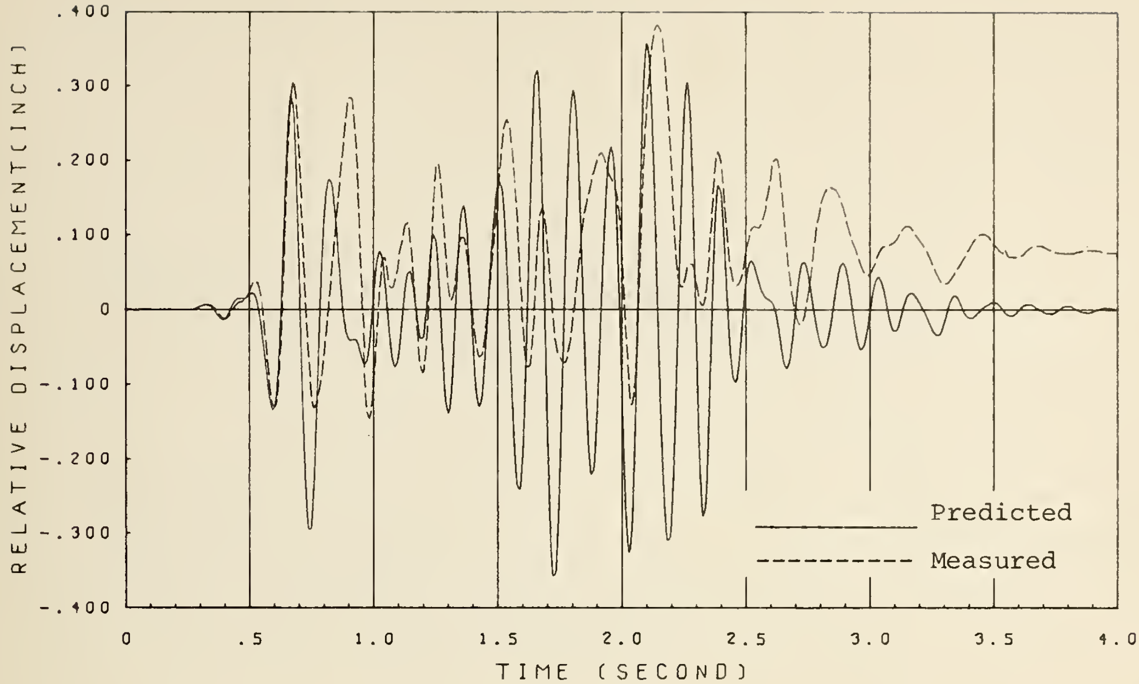

FIG. 6.8.3 LINEAR CORRELATION FOR TEST H3; CENTER GIRDER; TRANSVERSE (Y) DIRECTION

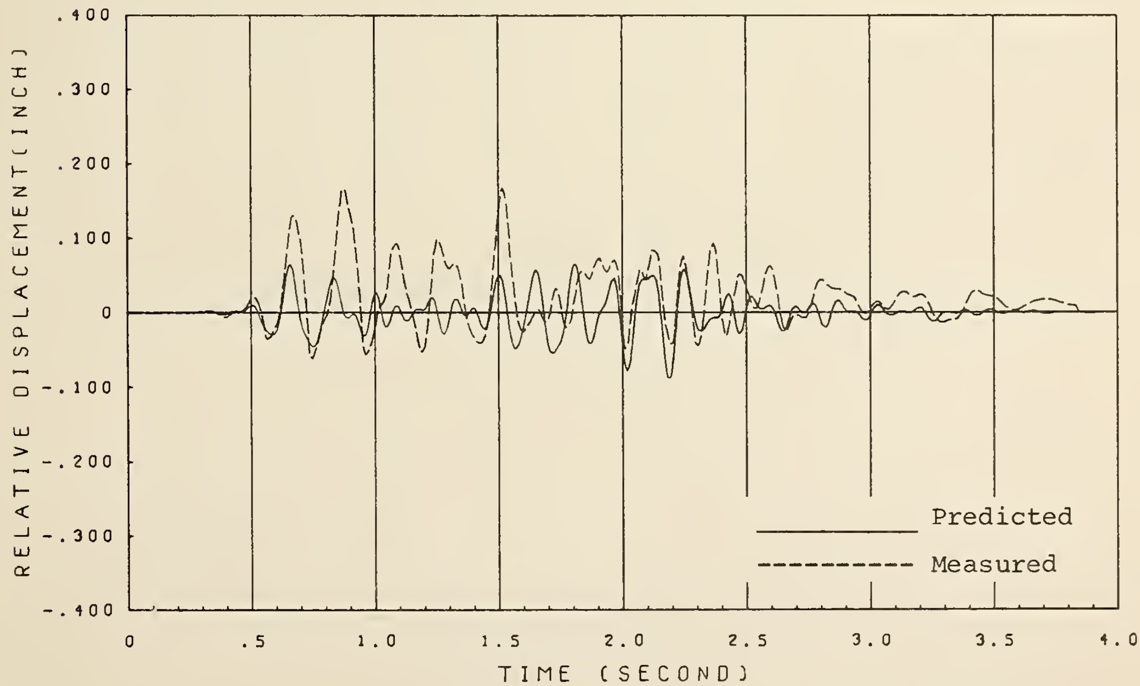

FIG. 6.8.4 LINEAR CORRELATION FOR TEST H3; SIDE GIRDER NO. 2; LONGITUDINAL (X) DIRECTION

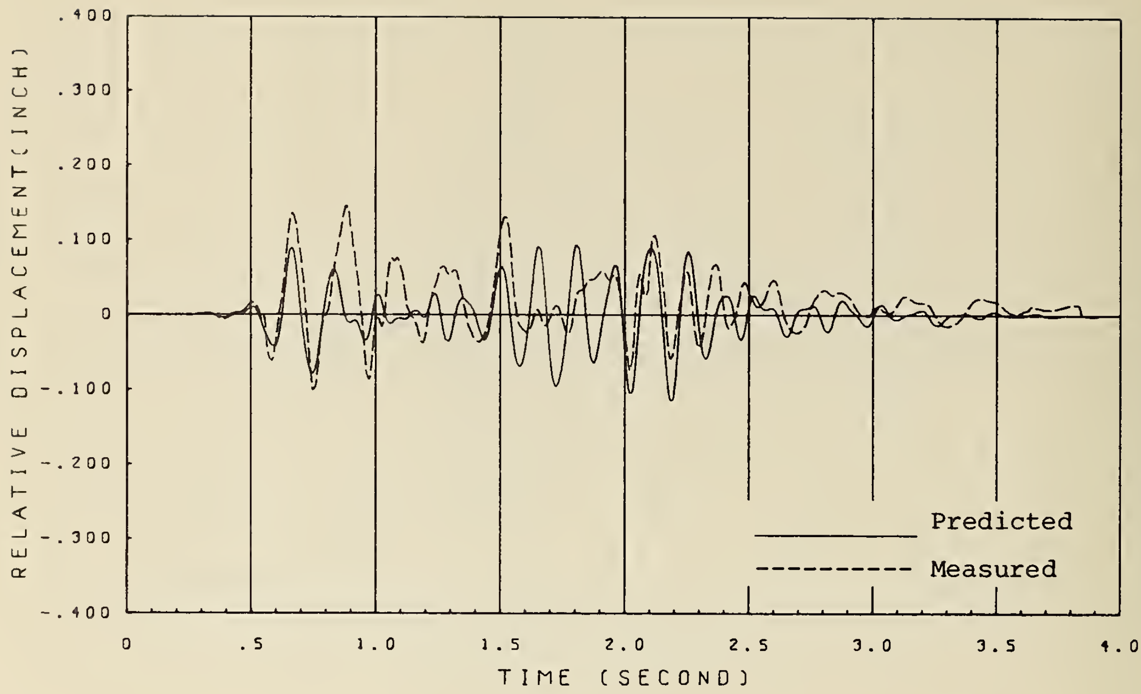

FIG. 6.8.5 LINEAR CORRELATION FOR TEST H3; SIDE GIRDER NO. 2; TRANSVERSE (Y) DIRECTION

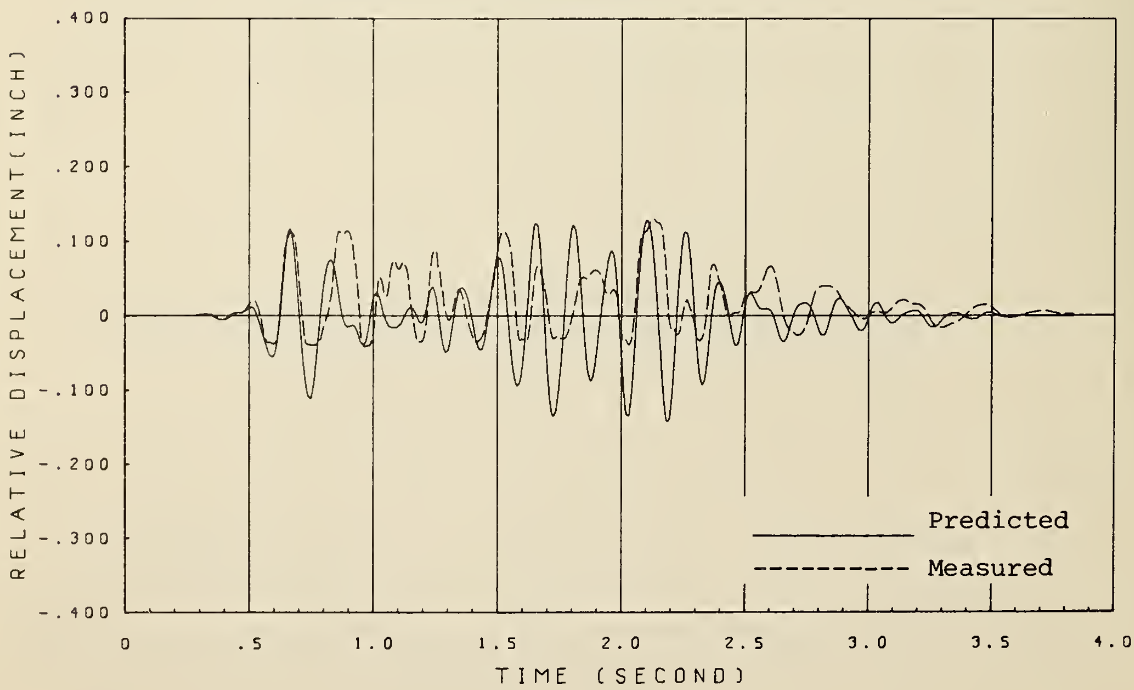

FIG. 6.8.6 LINEAR CORRELATION FOR TEST H3; EXPANSION JOINT NO. 1; INNER SIDE

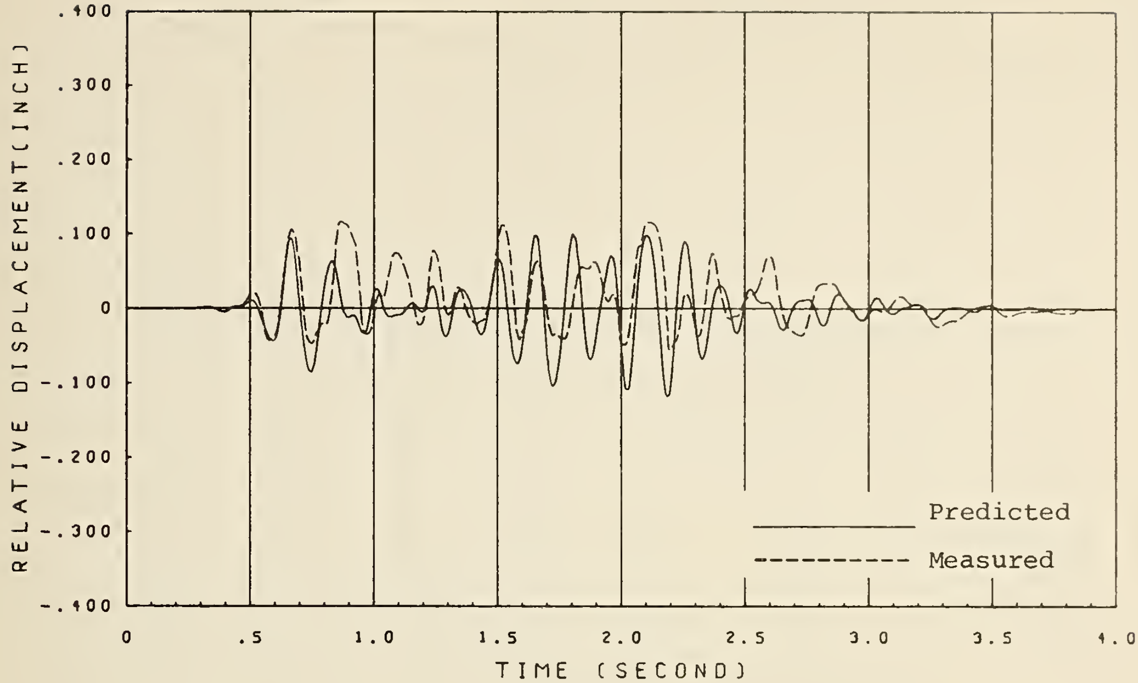

FIG. 6.8.7 LINEAR CORRELATION FOR TEST H3; EXPANSION JOINT NO. 1; OUTER SIDE

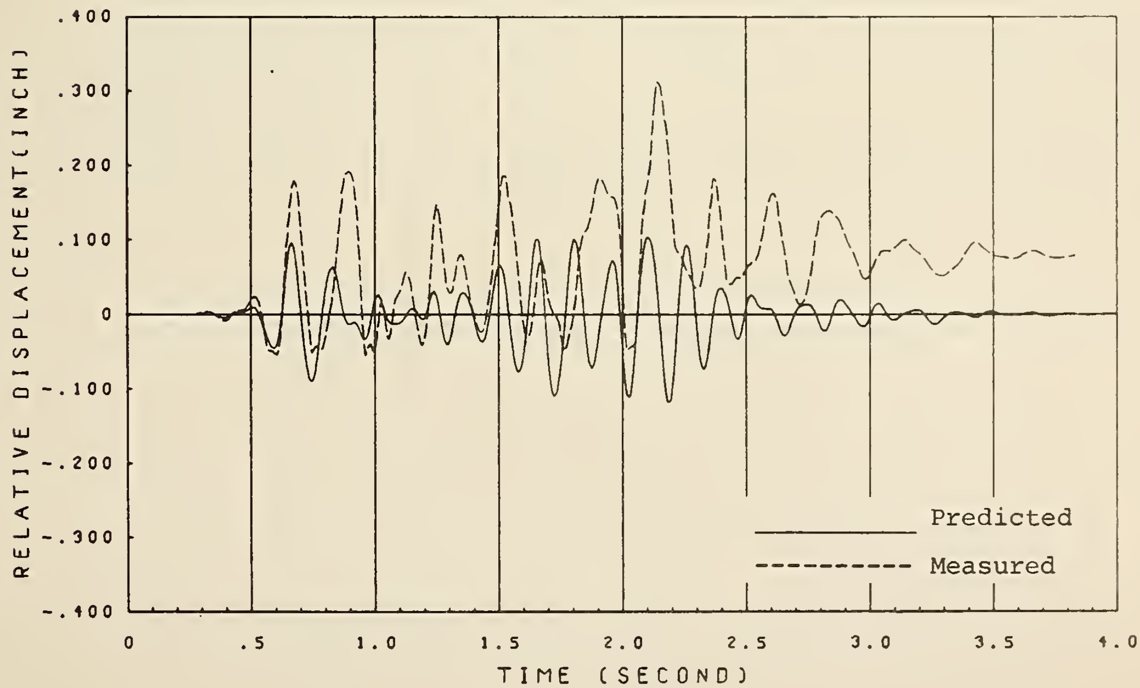

FIG. 6.8.8 LINEAR CORRELATION FOR TEST H3; EXPANSION JOINT NO. 2; INNER SIDE

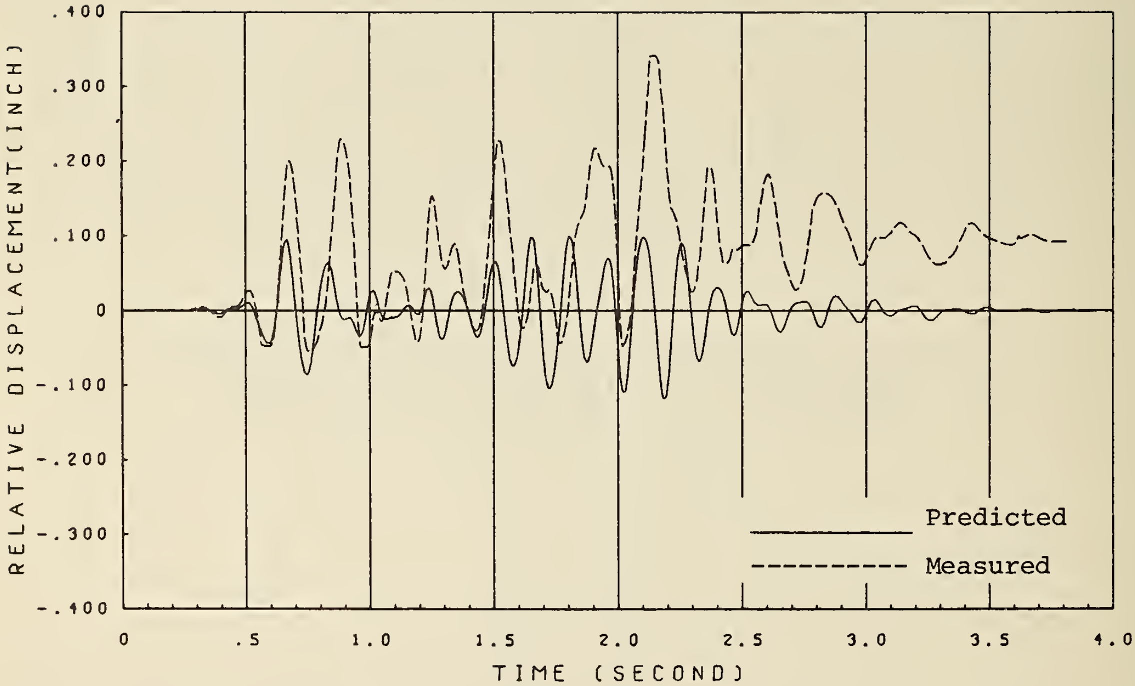

FIG. 6.8.9 LINEAR CORRELATION FOR TEST H3; EXPANSION JOINT NO. 2; OUTER SIDE

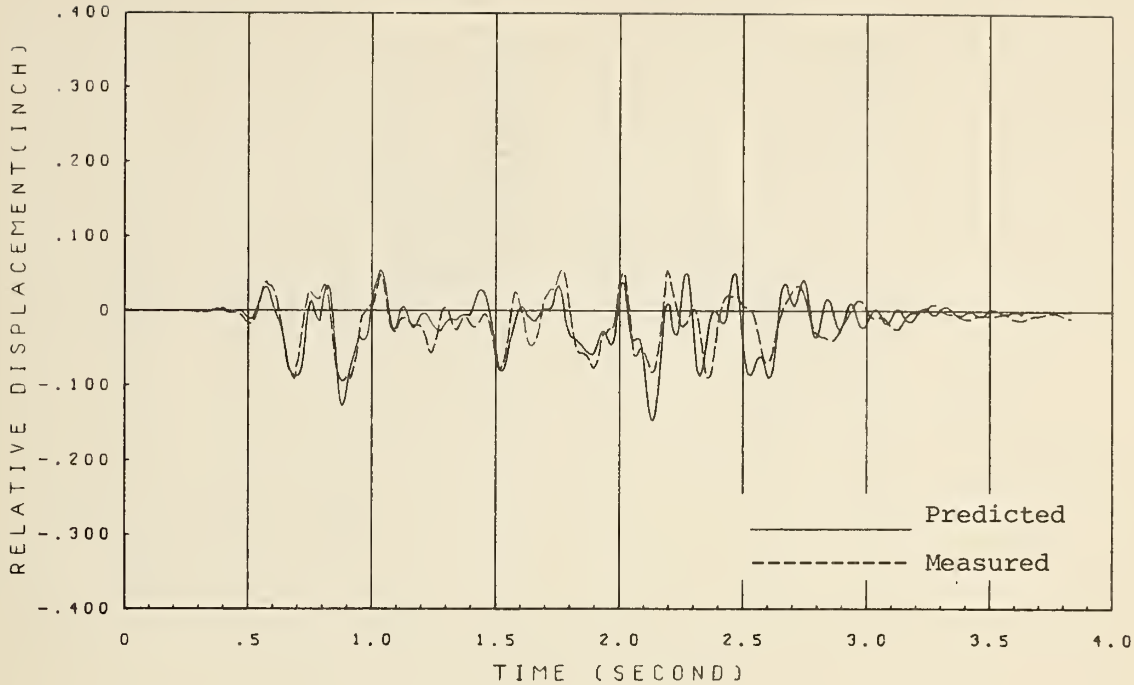

FIG. 6.9.1 NONLINEAR CORRELATION FOR TEST H3; SIDE GIRDER NO. 1; LONGITUDINAL (X) DIRECTION

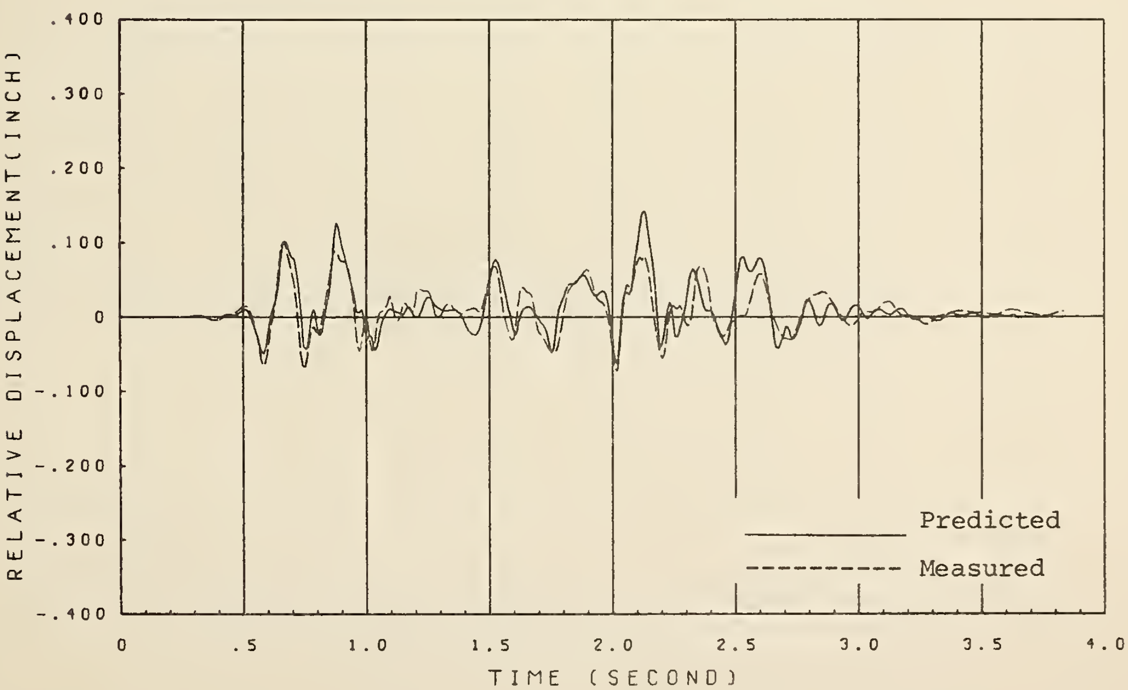

FIG. 6.9.2 NONLINEAR CORRELATION FOR TEST H3; SIDE GIRDER NO. 1; TRANSVERSE (Y) DIRECTION

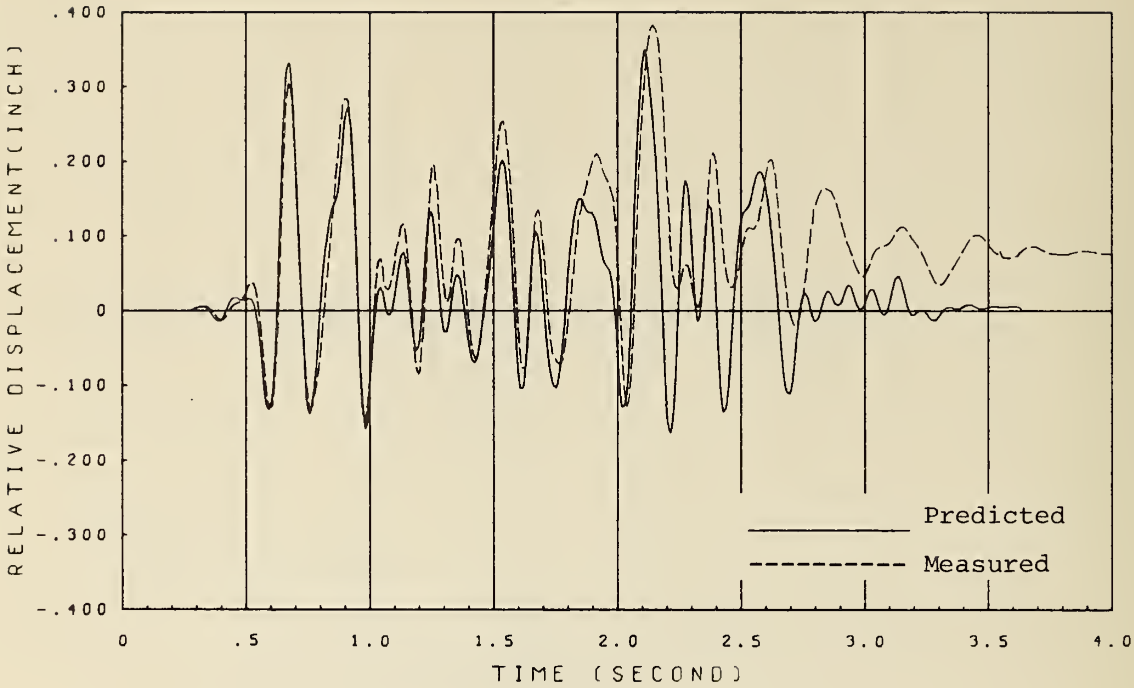

FIG. 6.9.3 NONLINEAR CORRELATION FOR TEST H3; CENTER GIRDER; TRANSVERSE (Y) DIRECTION

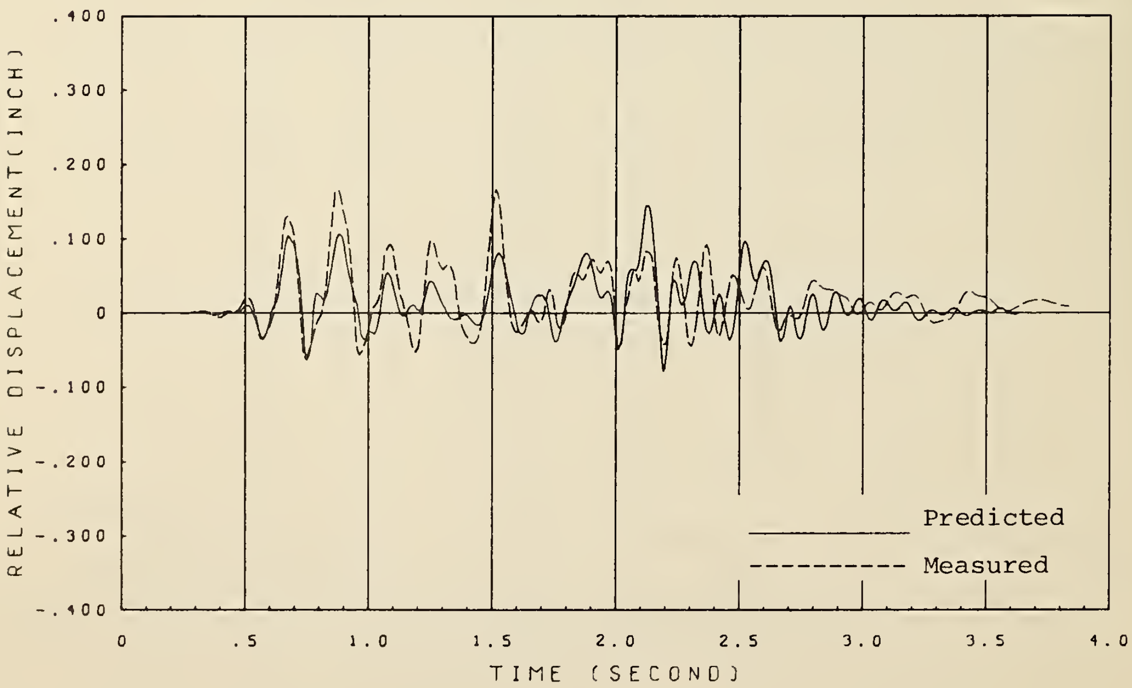

FIG. 6.9.4 NONLINEAR CORRELATION FOR TEST H3; SIDE GIRDER NO. 2; LONGITUDINAL (X) DIRECTION

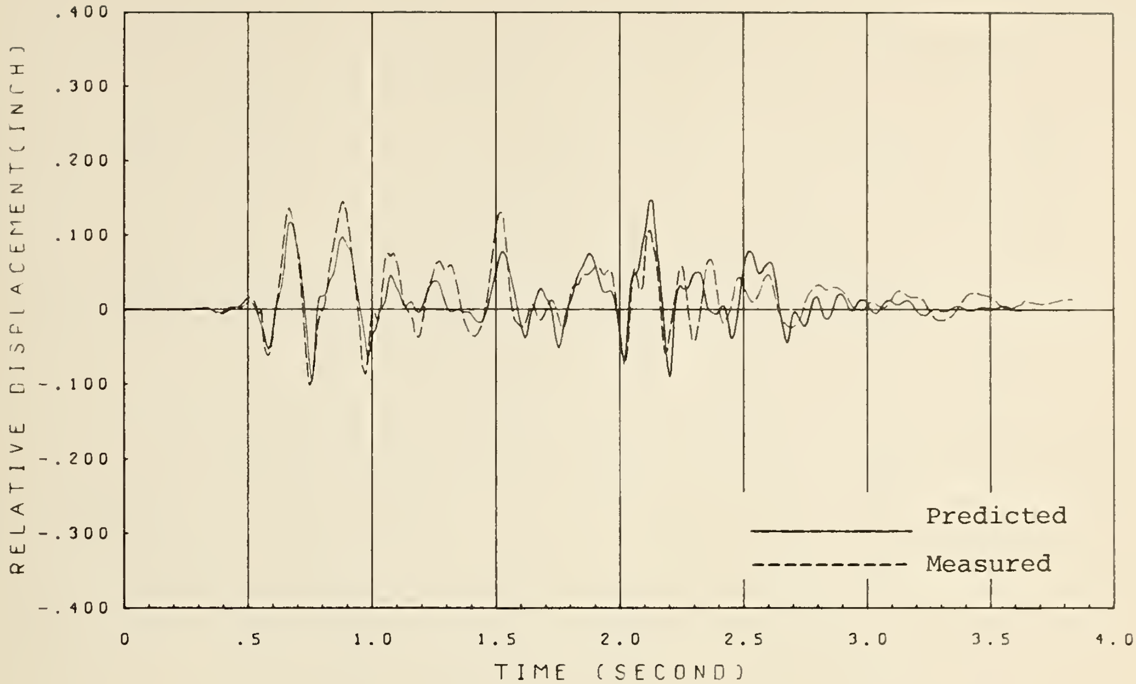

FIG. 6.9.5 NONLINEAR CORRELATION FOR TEST H3; SIDE GIRDER NO. 2; TRANSVERSE (Y) DIRECTION

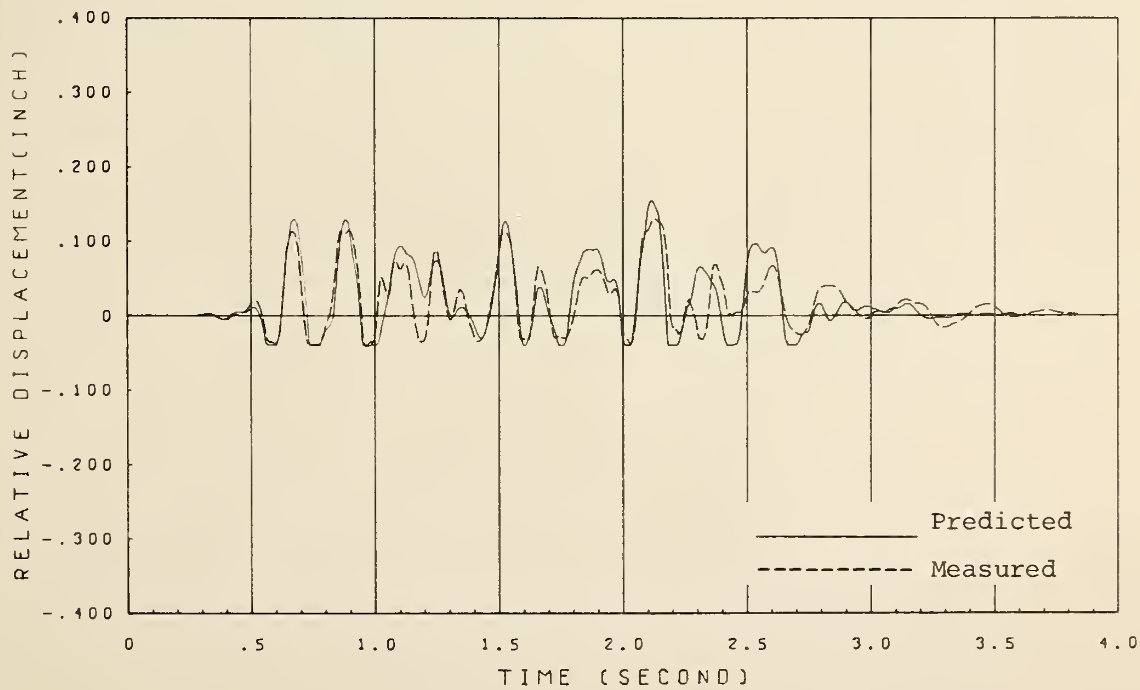

FIG. 6.9.6 NONLINEAR CORRELATION FOR TEST H3; EXPANSION JOINT NO. 1; INNER SIDE

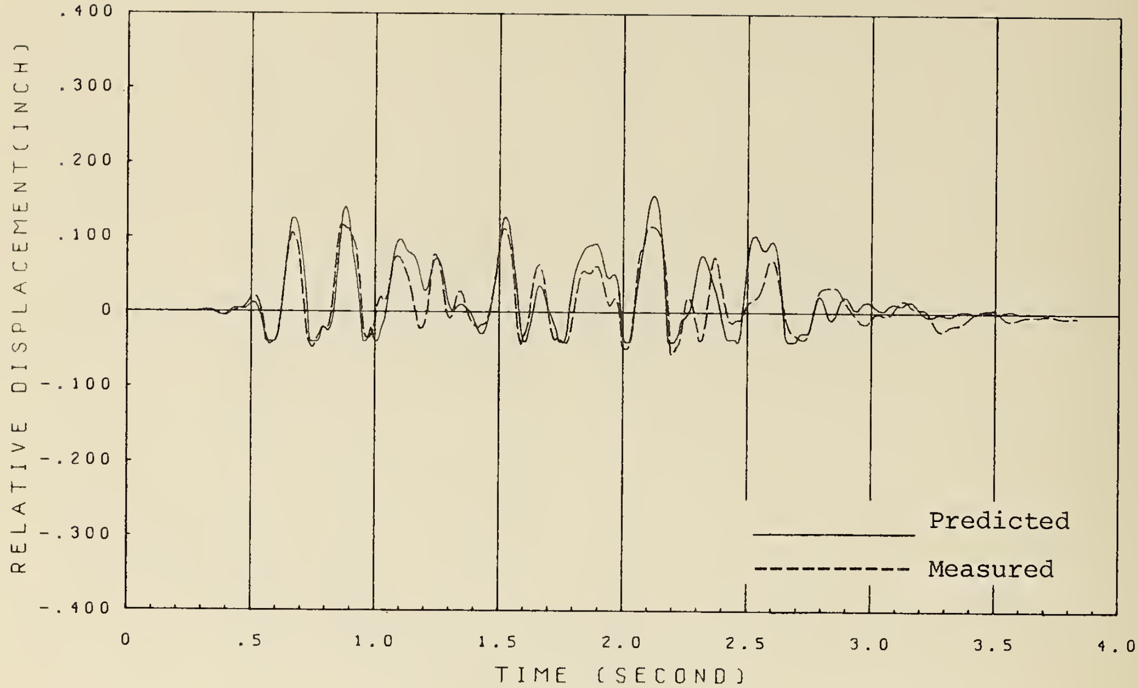

FIG. 6.9.7 NONLINEAR CORRELATION FOR TEST H3; EXPANSION JOINT NO. 1; OUTER SIDE

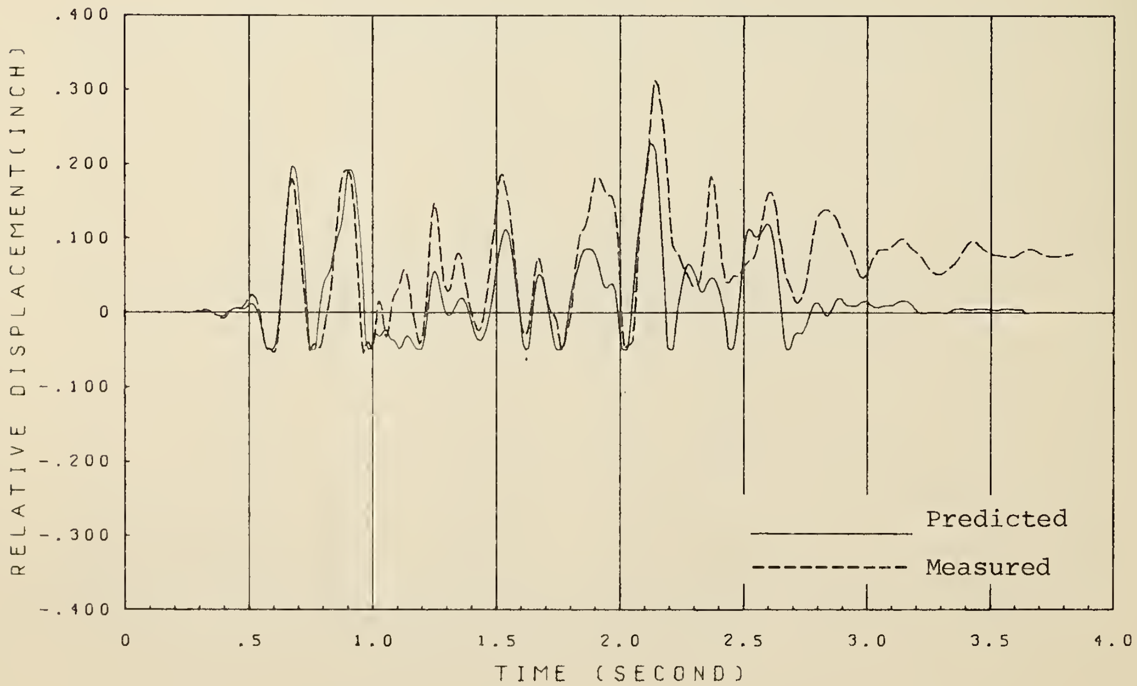

FIG. 6.9.8 NONLINEAR CORRELATION FOR TEST H3; EXPANSION JOINT NO. 2; INNER SIDE

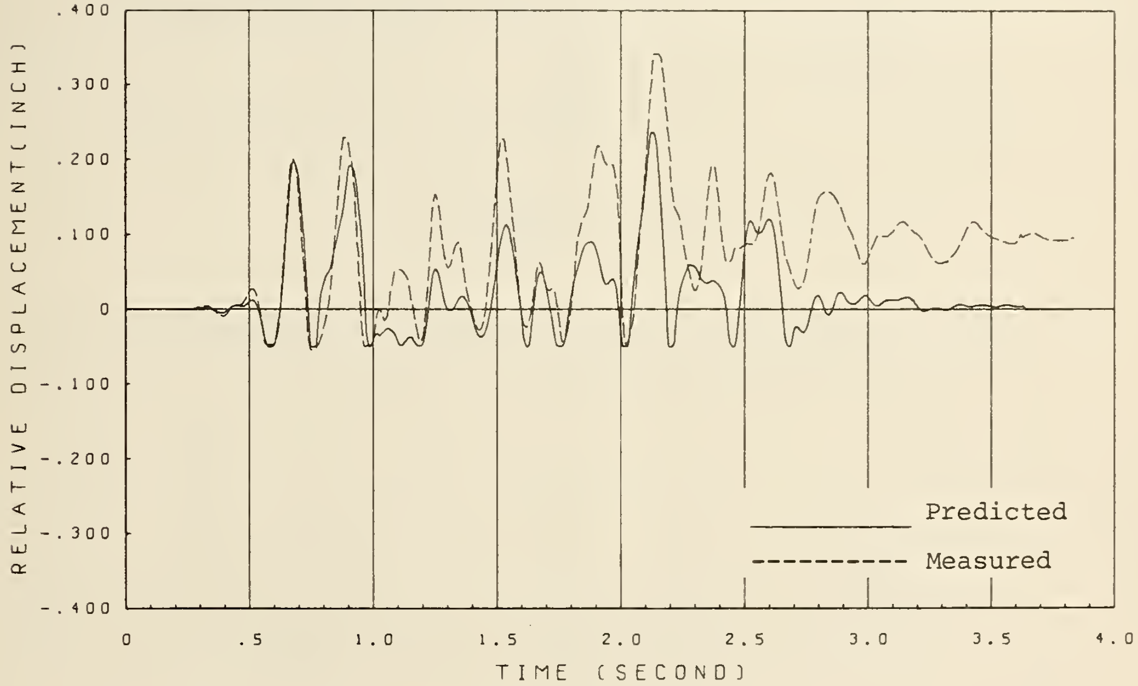

FIG. 6.9.9 NONLINEAR CORRELATION FOR TEST H3; EXPANSION JOINT NO. 2; OUTER SIDE

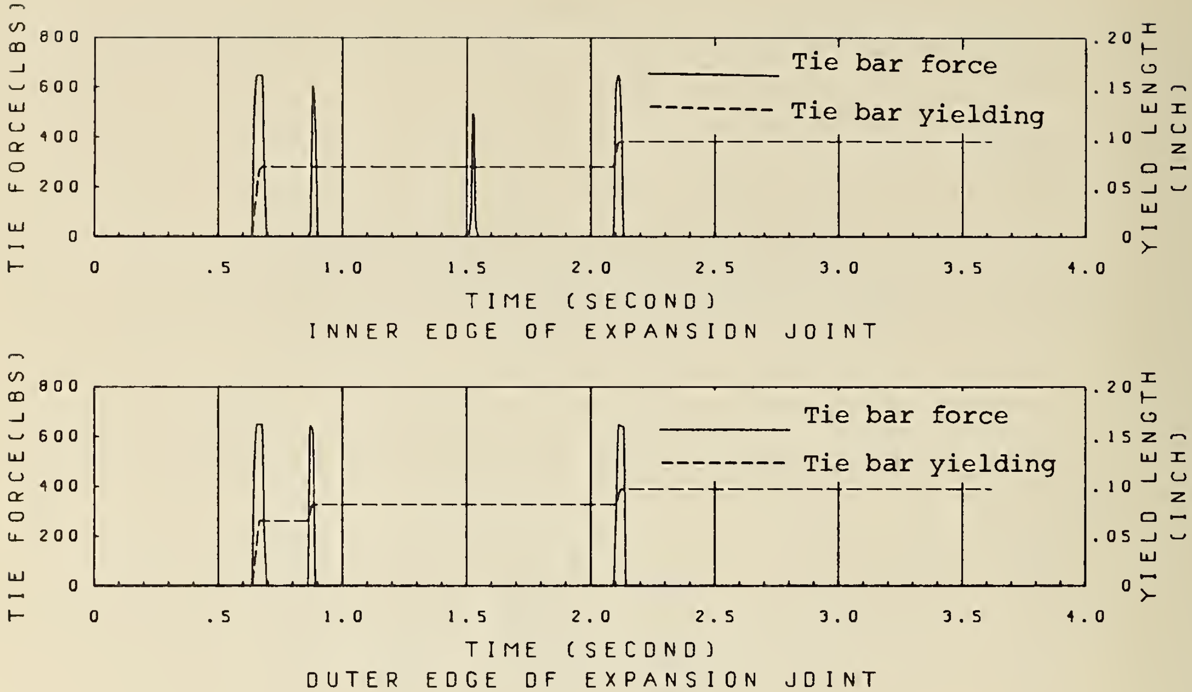

FIG. 6.10.1 PREDICTED TIE BAR FORCE AND YIELD LENGTH FOR TEST H3; EXPANSION JOINT NO. 1

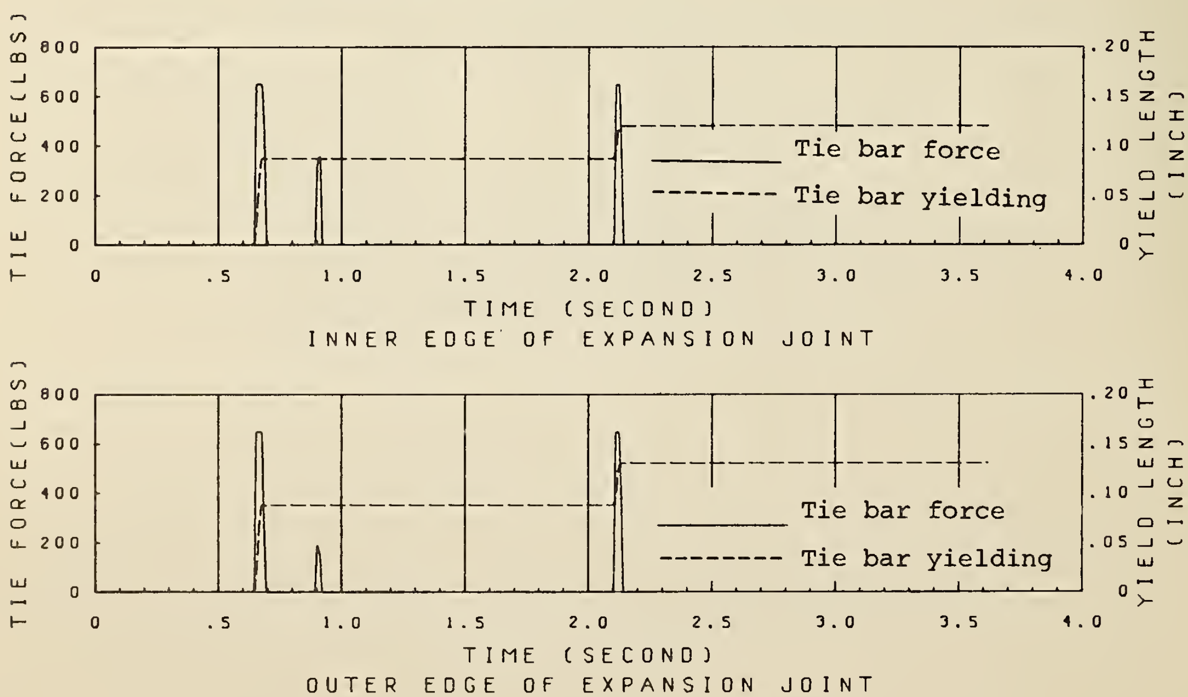

FIG. 6.10.2 PREDICTED TIE BAR FORCE AND YIELD LENGTH FOR TEST H3; EXPANSION JOINT NO. 2

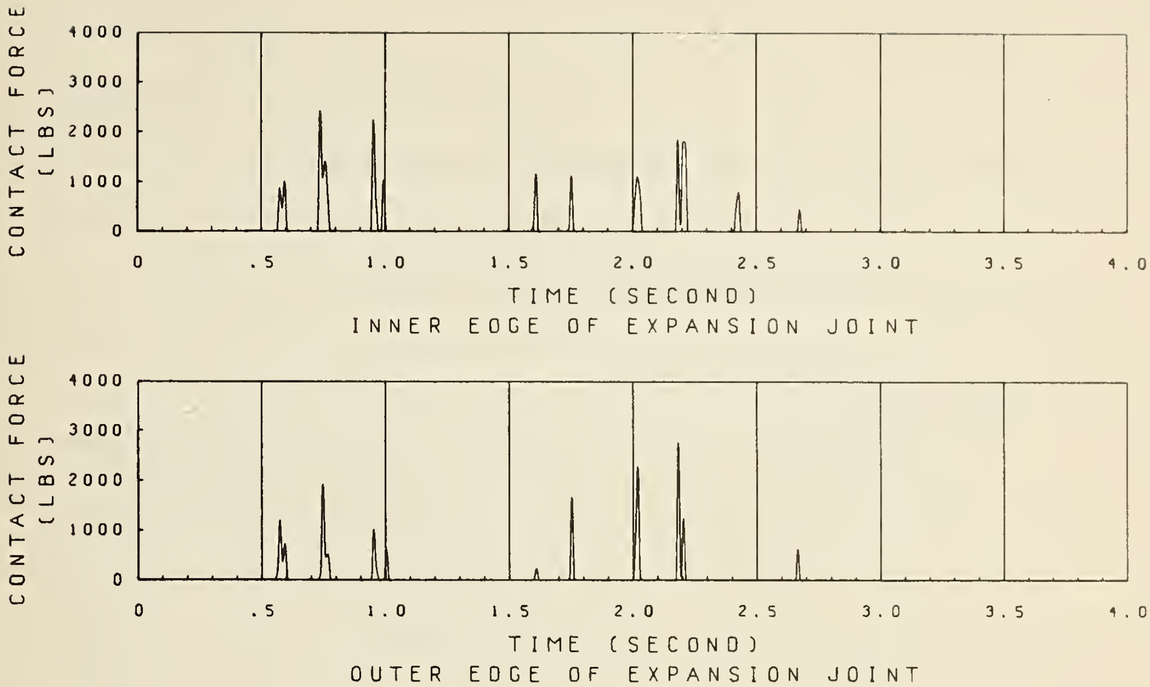

FIG. 6.11.1 PREDICTED CONTACT FORCE FOR TEST H3; EXPANSION JOINT NO. 1

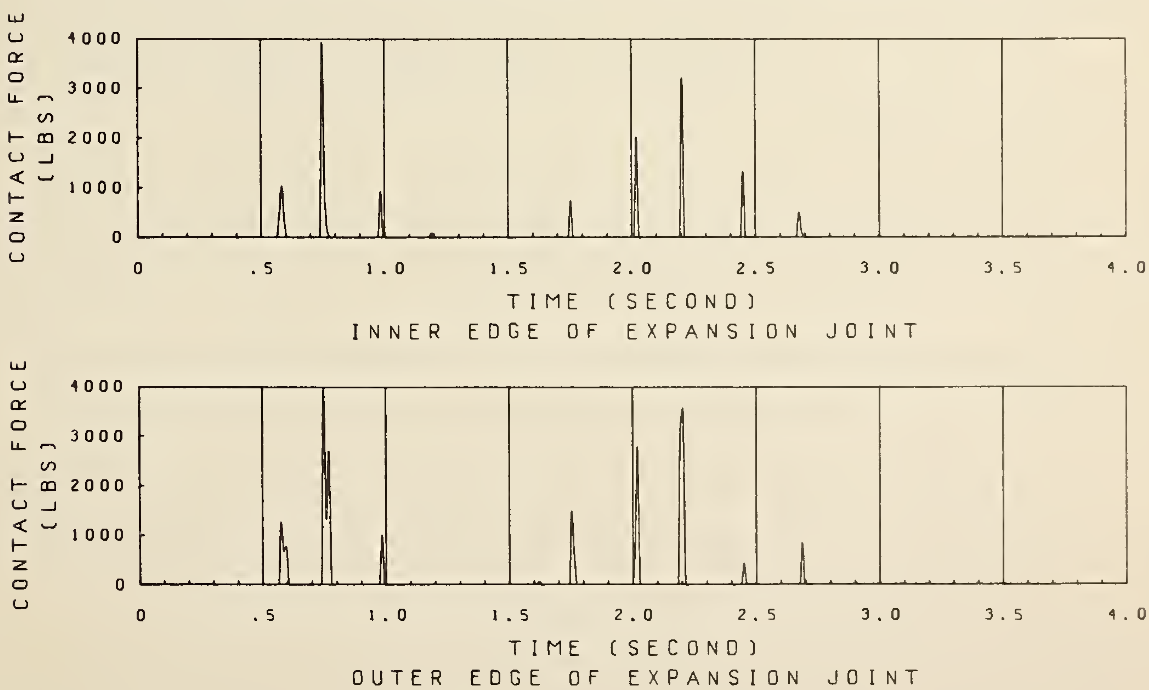

FIG. 6.11.2 PREDICTED CONTACT FORCE FOR TEST H3; EXPANSION JOINT NO. 2

VII. DISCUSSION OF CORRELATION RESULTS

The purpose of this chapter is to comment on the correlation results presented in the previous chapter. Since Test HV2 shows the most typical response of the bridge model under high intensity excitation including the tie bar yieldings,collisions, slippages and vertical excitation, these comments will concentrate on this test.

A. JOINT RESTRAINER TIE BARS

The experimental model consisted of three independent subassemblages having essentially different dynamic characteristics which were joined together by restrainer tie bars. The characteristics of these bars are extremely important in controlling the dynamic behavior of the bridge model both in the amplitude and in frequency content. Figure 7.1 shows an example of two different calculated responses which are compared with the corresponding predicted response adopted for the correlation of Test HV2. These three responses were calculated using the same nonlinear analytical model and damping factors but with different tie bar characteristics. In one case, the magnitude of the initial tie gap at expansion joint No. 2 was arbitrarily taken twice that value adopted for the correlation. In another case, it was assumed that no tie bars were provided at the expansion joints. It is apparent from this comparison that the joint restrainer tie bars can be extremely effective in reducing the seismic response of the bridge model, if properly designed. Further, it is apparent that small initial tie gaps are desirable for this purpose.

B. COLLISIONS

Although the general effects of collisions on the dynamic behavior of the bridge model is apparent from a comparison of responses between the linear analysis correlation and the nonlinear analysis correlation for the Test HV2 or Test H3, the differences observed in this comparison include the effects of other factors, e.g. tie bars, slippages, etc. Therefore in an attempt to isolate the effects of collisions, one response was calculated using the same nonlinear analytical model adopted finally for the correlation of the Test HV2 but eliminating the impact springs at both expansion joints. The comparative plot between this response and the response calculated for the correlation of Test HV2 is shown in Fig. 7.2. It is seen from this comparison that collisions are a major factor affecting the general behavior of the bridge model subjected to high intensity seismic excitations. It should be noted that even if the response amplitude in the negative direction is suppressed by a collision, the rebound from that collision can appreciably increase the positive response amplitude which follows immediately.

C. COULOMB FRICTION FORCE

Although a Coulomb friction coefficient of 0.4 was assumed throughout this study based on considerations of the surface condition of the contact plane, its actual value could be expected to vary from 0.3 to 0.6. Therefore, it is of interest to examine the sensitivity of this parameter on the dynamic behavior of the bridge model. Therefore, two responses were calculated using the nonlinear analytical model formulated for Test HV2 but with different Coulomb friction coefficients, i.e. 0.3 and 0.6. The comparative plot of these two responses is shown in Fig. 7.3 which could be compared with the response finally adopted in the correlation of Test HV2 using a friction coefficient of 0.4. It is apparent from this comparison that the Coulomb friction coefficient has low sensitivity in controlling seismic response. For example, if a Coulomb friction coefficient of 0.6 is used which could be considered a maximum, the maximum friction force acting on one expansion joint would be only 220 lbs corresponding to a vertical contact force of 380 lbs. In comparison, the maximum tie bar force acting on one expansion joint is approximately 1300 lbs which is roughly 6 times as large. Furthermore, the predicted maximum contact force caused by collisions reached approximately 4000 lbs which is roughly 18 times as large. It is clear from this comparison that the overall response was critically controlled by the tie bars for outward motion and by collisions for inward motion with the effects of friction being relatively small.

D. VERTICAL EXCITATION

Vertical excitation has an important effect on the vertical response of the bridge model. It also has some effect on horizontal response due to coupling between the horizontal and vertical vibration modes which is associated with deck curvature. Further, the vertical excitation causes vertical oscilatory motion in the superstructure resulting in changes of the vertical contact force at the expansion joints. This, in turn, affects the friction forces acting at expansion joints which affect horizontal response.

To check the influence of vertical excitation, one response was calculated using the nonlinear analytical model adopted for the correlation of Test HV2 but with the vertical excitation removed from the input. The comparative plot of responses with and without vertical excitation is shown in Fig. 7.4. It is apparent from this comparison that vertical excitation is less significant than horizontal excitation in the transverse direction. This observation is consistent with the relatively low sensitivity of Coulomb friction and relatively small effect caused by coupling of vertical and horizontal modes.

E. IMPACT SPRING STIFFNESS

In the analytical correlations presented in Chapter VI, the impact spring stiffness k_I of 10^7 lbs/inch was adopted. This value was selected so that k_I would be similar in magnitude to the longitudinal stiffness of neighboring curved beam elements representing the superstructure; see Appendix A. Since impact is important to response, the sensitivity of stiffness k_I was examined using the nonlinear analytical model adopted for the correlation of Test HV2 but using two different impact spring stiffnesses k_I, namely 10^6 and 10^9 lbs/inch which are, respectively, one tenth and a hundred times that of the impact spring stiffness adopted for the correlation study. It is apparent from the resulting responses shown in Fig. 7.5 that k_I is an insensitive parameter provided it is set sufficiently large. Therefore, the stiffness of 10^7 lbs/inch set in the correlation study is shown to be a proper value for the analysis purpose.

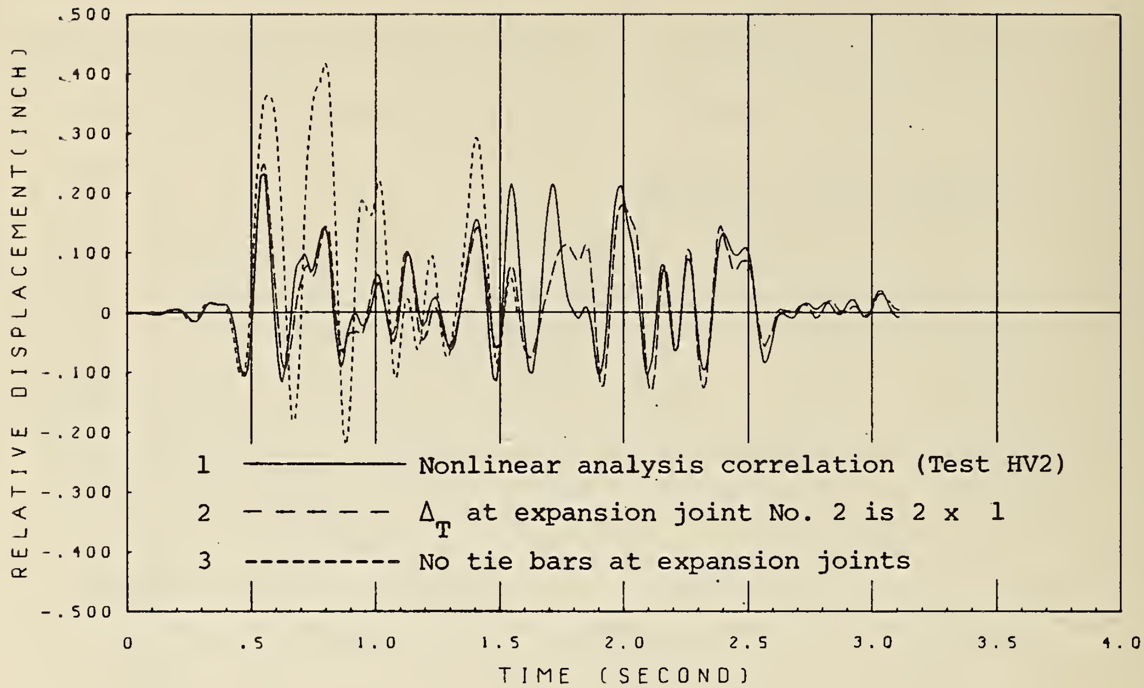

FIG. 7.1.1 EFFECT OF LONGITUDINAL RESTRAINER TIE BARS ON RESPONSE OF CENTER GIRDER; TEST HV2

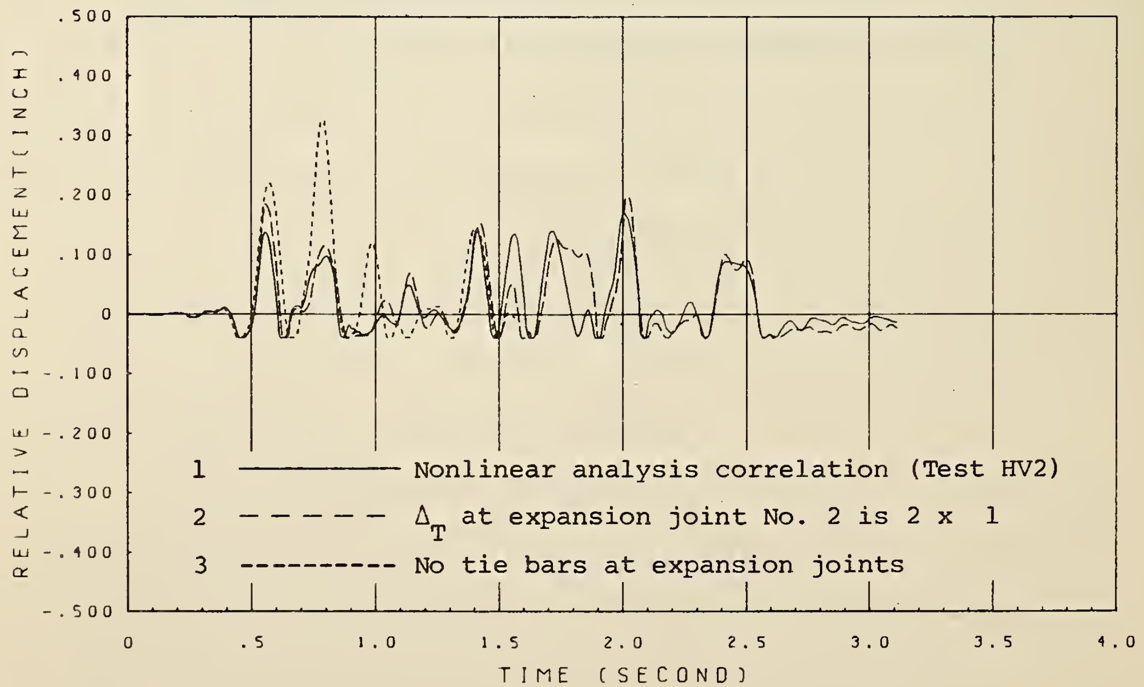

FIG. 7.1.2 EFFECT OF LONGITUDINAL RESTRAINER TIE BARS ON RELATIVE RESPONSE OF EXPANSION JOINT NO. 2 (OUTER SIDE); TEST HV2

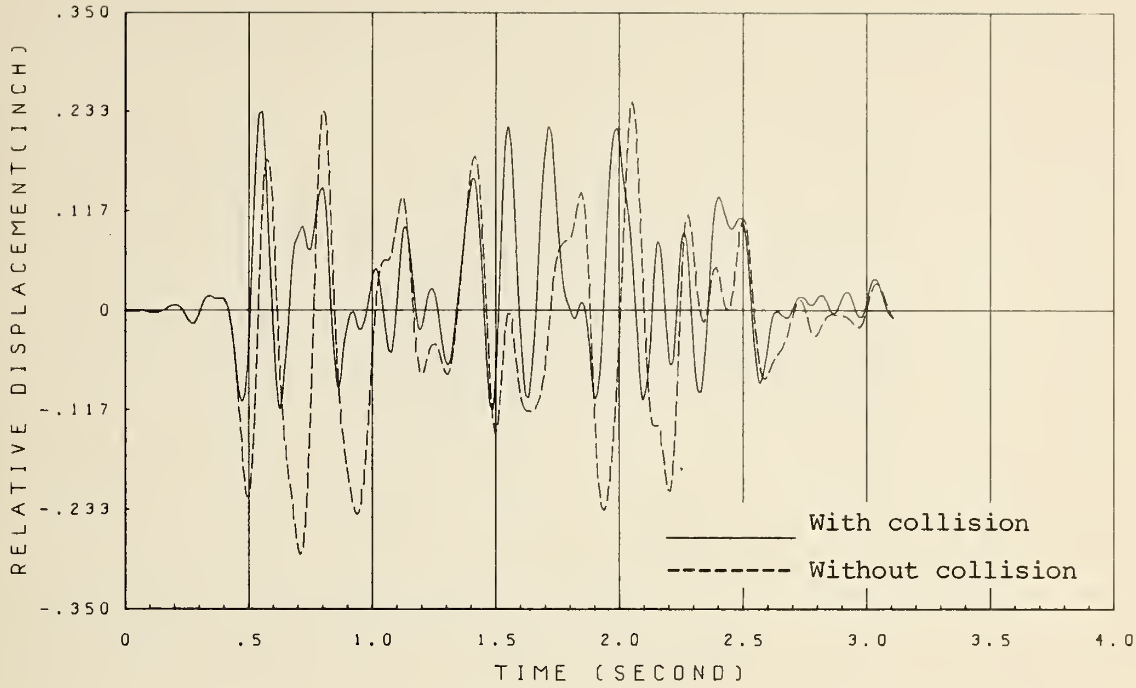

FIG. 7.2.1 EFFECT OF COLLISIONS ON RESPONSE OF CENTER GIRDER; TEST HV2

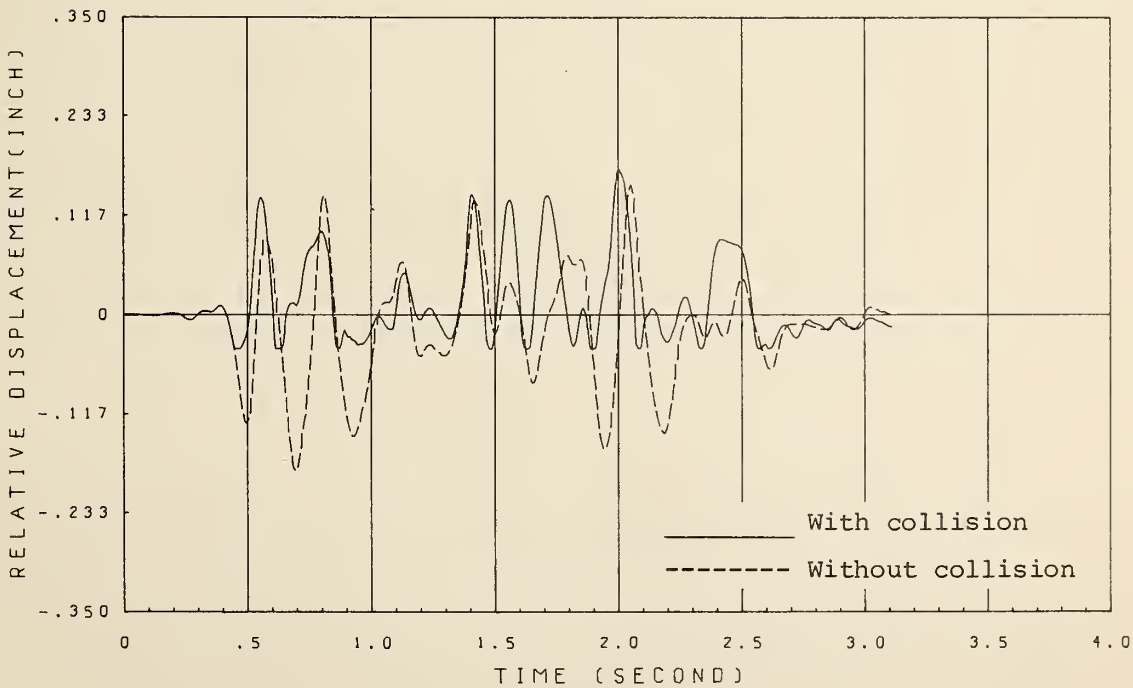

FIG. 7.2.2 EFFECT OF COLLISIONS ON RELATIVE RESPONSE OF EXPANSION JOINT NO. 2 (OUTER SIDE); TEST HV2

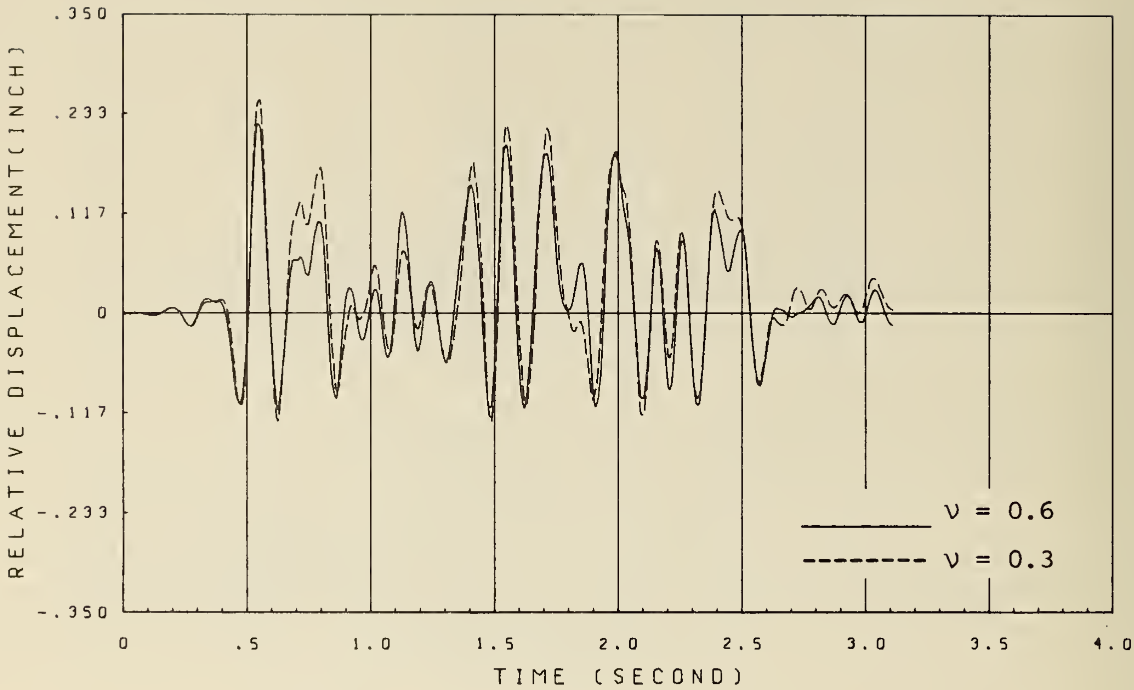

FIG. 7.3.1 EFFECT OF COULOMB FRICTION ON RESPONSE OF CENTER GIRDER; TEST HV2

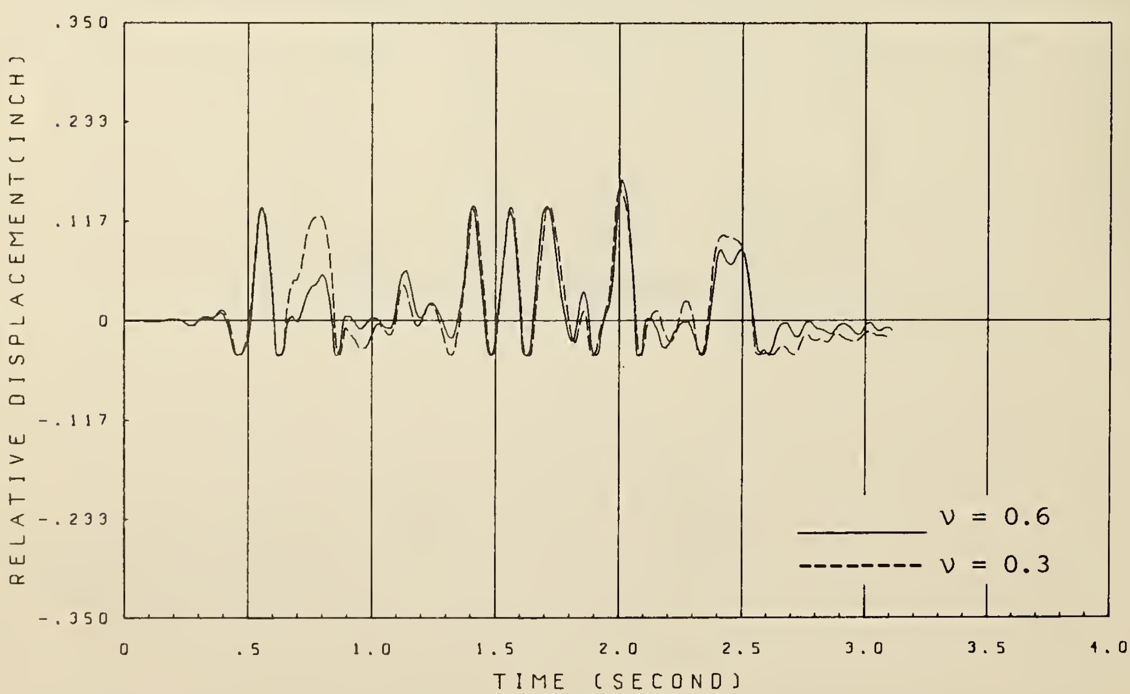

FIG. 7.3.2 EFFECT OF COULOMB FRICTION ON RELATIVE RESPONSE OF EXPANSION JOINT NO. 2 (OUTER SIDE); TEST HV2

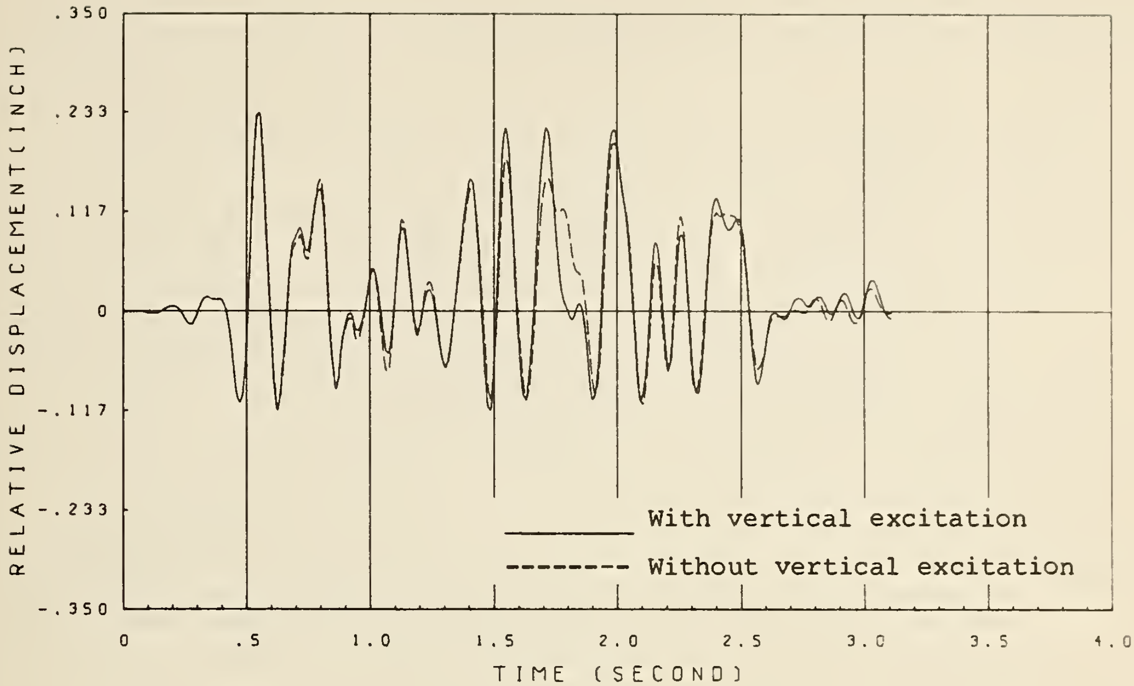

FIG. 7.4.1 EFFECT OF VERTICAL EXCITATION ON RESPONSE OF CENTER GIRDER; TEST HV2

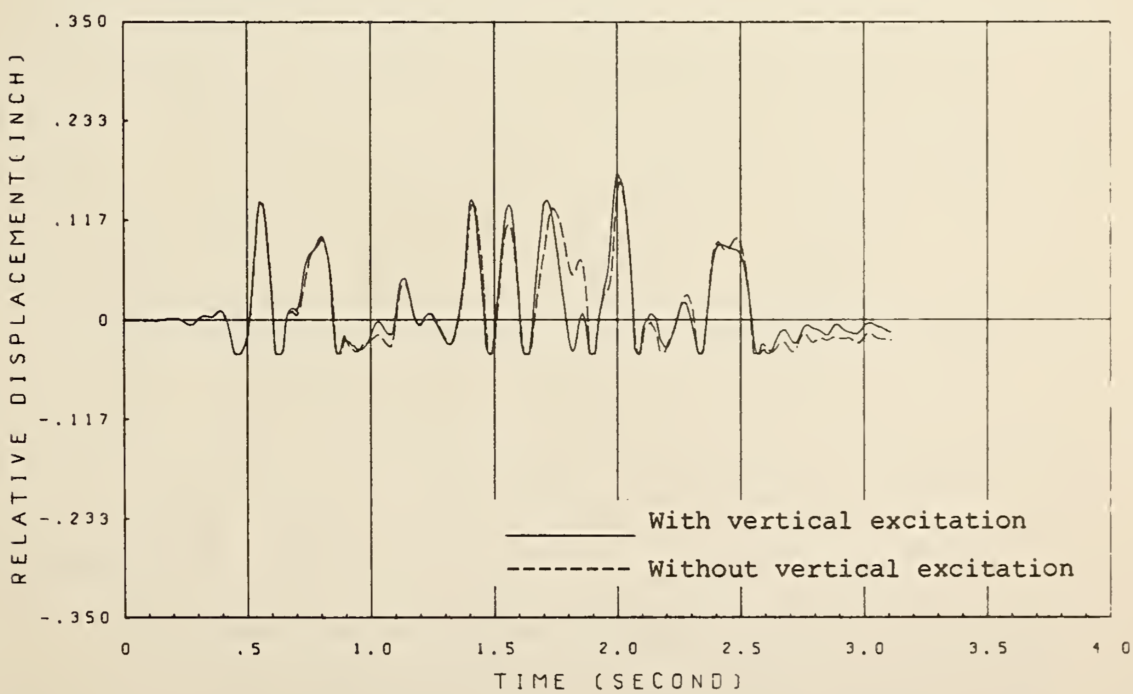

FIG. 7.4.2 EFFECT OF VERTICAL EXCITATION ON RELATIVE RESPONSE OF EXPANSION JOINT NO. 2 (OUTER SIDE); TEST HV2

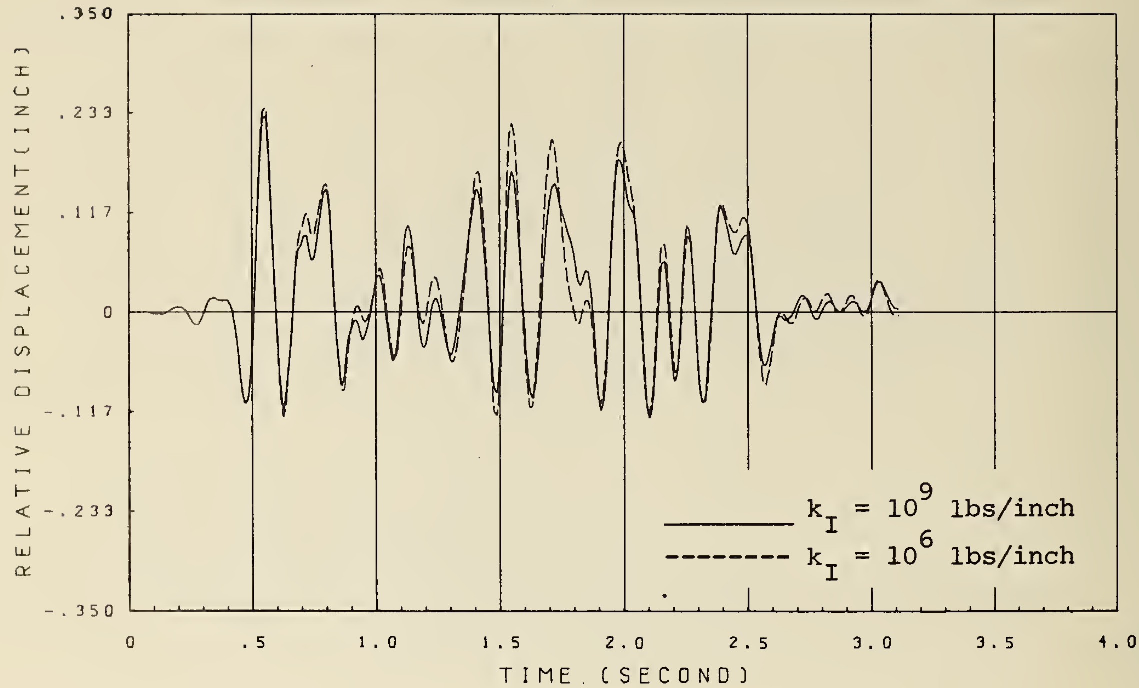

FIG. 7.5.1 EFFECT OF IMPACT SPRING STIFFNESS ON RESPONSE OF CENTER GIRDER; TEST HV2

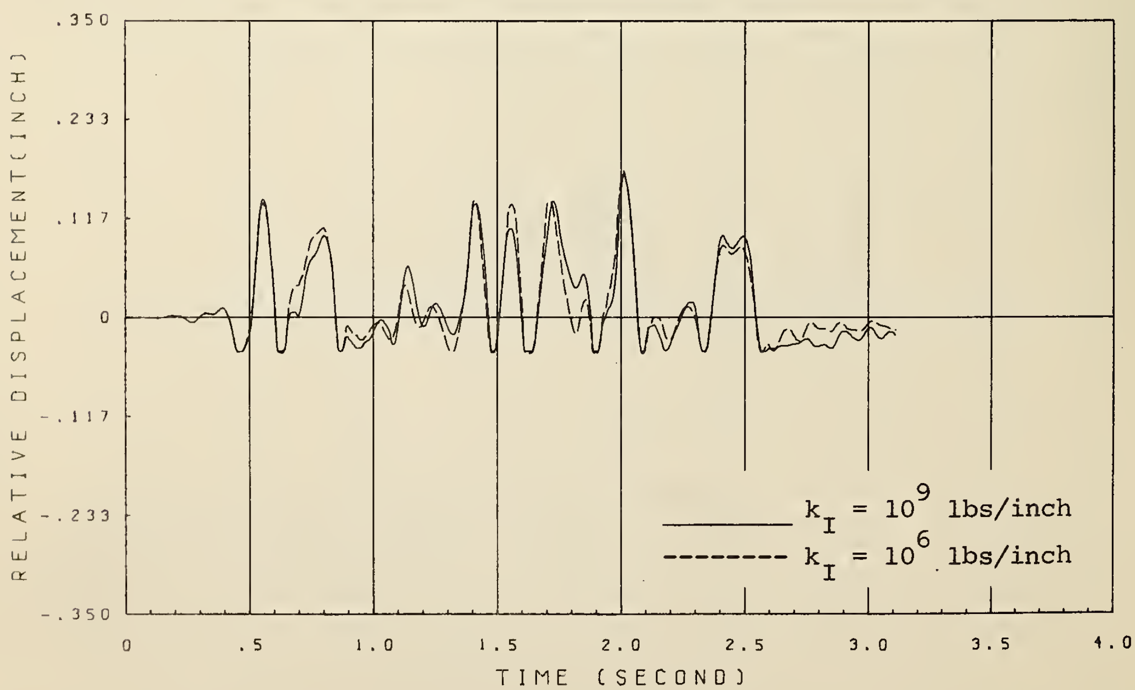

FIG. 7.5.2 EFFECT OF IMPACT SPRING STIFFNESS ON RELATIVE RESPONSE OF EXPANSION JOINT NO. 2 (OUTER SIDE); TEST HV2

VIII CONCLUSIONS

Based on the correlation results presented, the following conclusions may be deduced:

(1) The mathematical model and analytical procedure developed in Phase 2, which were modified and improved in Phase 5, predicts realistically the nonlinear response of the bridge model under low and high intensity seismic excitations as conducted in Phase 4.

(2) The displacement seismic response of the bridge model under low intensity excitation which does not result in significant yielding of the longitudinal joint restrainer tie bars and does not produce collision of the girders can be predicted with fairly good accuracy using the linear analytical model provided the low frequency characteristics of analytical model agree well with those of the physical model and provided a proper damping factor is used in the analysis.

(3) The linear analytical model cannot satisfactorly predict the seismic response of the bridge model under high intensity seismic excitations causing appreciable yielding of tie bars and multiple collisions of the girders, even if the low frequency characteristics and the damping factor of the analytical model are adjusted.

(4) The displacement seismic response of the bridge model produced by high intensity excitations resulting in severe yielding of tie bar and collisions of the girders can be predicted realistically using the nonlinear analytical model which accounts for the effects of collisions, slippages and tie bars.

(5) The expansion joints have a controlling effect on the dynamic behavior of the bridge model; thus, their characteristics must be properly represented in a realistic mathematic model of the bridge structure.

(6) Under high intensity seismic excitations, the dynamic response of the bridge model is primarily controlled by joint restrainer tie bars for motions in the outward direction and by multiple collisions for motions in the inward direction with the effects of Coulomb friction being relatively small.

(7) Vertical excitation has an important effect on the vertical response of the bridge model. However, the effect of vertical excitation on horizontal transverse response is relatively small due to the insensitivity of coupling of vertical and horizontal modes and of Coulomb friction on horizontal response.

(8) The longitudinal restrainer tie bars are very effective in reducing transverse response of the bridge model provided they are properly designed. Smaller tie gaps are also effective in reducing transverse response.

(9) The multiple collisions which take place between girders have a major influence on both the amplitude and the frequency characteristics of response and they cause large contact forces to be developed at expansion joints. Even though a negative response amplitude is suppressed by collision, the rebound from that collision can result in an increased positive response amplitude immediately following the collision.

(10) The mathematical model, analytical procedures, and computer program NEABS can be used to predict realistic dynamic response of prototype bridge structures subjected to high intensity rigid base seismic excitation.

BIBLIOGRAPHY

1. Iwasaki, T., Penzien, J. and Clough, R., "Literature Survey -- Seismic Effects on Highway Bridges," Report No. EERC 71-11, Earthquake Engineering Research Center, University of California, Berkeley, November 1972.

2. Tseng, W. S., and Penzien, J., "Analytical Investigations of the Seismic Response of Long Multiple Span Highway Bridges," Report No. EERC 73-12, Earthquake Engineering Research Center, University of California, Berkeley, June 1973.

3. Tseng, W. S., and Penzien, J., "Seismic Response of Highway Overcrossings," Proc. 5th World Conference on Earthquake Engineering, Rome, Italy, 1973.

4. Tseng, W. S., and Penzien, J., "Seismic Analysis of Long Multiple-Span Highway Bridges," International Journal of Earthquake Engineering and Structural Dynamics, Vol. 4, pp. 3-24, 1975.

5. Tseng, W. S., and Penzien, J., "Seismic Response of Long Multiple-Span Highway Bridges," International Journal of Earthquake Engineering and Structural Dynamics, Vol. 4, pp. 25-48, 1975.

6. Chen, M. C., and Penzien, J., "Analytical Investigations of Seismic Response of Short, Single, or Multiple-Span Highway Bridges," Report No. EERC 75-4, Earthquake Engineering Research Center, University of California, Berkeley, January 1975.

7. Goldsmith, W., "Impacts," Edward Arnold, London, 1960.

8. Clough, R. W., and Penzien, J., "Dynamics of Structure, McGraw Hill, 1975.

9. Ban, S., "Collisions of Building Structure during Earthquakes," Trans. of the Architectural Institute of Japan, Vol. 221, pp. 1-7, July, 1974, (In Japanese).

10. Takeyama, K., "Earthquake Response of A Building Collied with A Neighboring Building," Proc. of 5th World Conference on Earthquake Engineering, Rome, Italy, 1973.

11. Bathe, K. J., Wilson, E. L., and Peterson, F. E., "SAP IV -- A Structural Analysis Program for Static and Dynamic Response of Linear Systems, Report No. EERC 73-11, Earthquake Engineering Research Center, University of California, Berkeley, June 1973.

12. Newmark, N. M., "A Method of Computation for Structural Dynamics," Proc. ASCE, Vol. 85, No. EM3, pp. 67-94, July 1959.

13. Wilson, E. L., and Clough, R. W., "Dynamic Response by Step-by-Step Matrix Analysis," Proc. Symposium on the use of Computers in Civil Engineering, Lisbon, Portugal, 1962.

14. Clough, R. W., and Bathe, K. J., "Finite Element Analysis of Dynamic Response," 2nd U.S.-Japan Seminar on Matrix Methods of Structural Analysis and Design, pp. 153-179, August 1972.

15. Bathe, K. J., and Wilson, E. L., "Stability and Accuracy Analysis of Direct Integration Methods," International Journal of Earthquake Engineering and Structural Dynamics, Vol. 1, pp. 282-291, 1973.

16. Wilson, E. L., Farhoomand, I., and Bathe, K. J., "Nonlinear Dynamic Analysis of Complex Structures," International Journal of Earthquake Engineering and Structural Dynamics, Vol. 1, pp. 241-252, 1973.

17. Nickell, R. E., "Direct Integration Methods in Structural Dynamics," Proc. ASCE, Vol. 99, No. EM2, pp. 303-317, April 1973.

18. Kanaan, A. E., and Powell, G. H., "General Purpose Computer Program for Dynamics Analysis of Inelastic Plane Structures," Report No. EERC 73-6, Earthquake Engineering Research Center, University of California, Berkeley, 1973.

19. Hughes, T. J., Taylor, R. L., and Sackman, J. L., "Finite Element Formulation and Solution of Contact - Impact Problems in Continuous Mechanics," Report No. UC SESM 74-8, Structural Engineering Laboratory, University of California, Berkeley, 1974.

20. Mondkar, D. P., and Powell, G. H., "Static and Dynamic Analysis of Nonlinear Structures," Report No. EERC 75-10, University of California, Berkeley, March 1975.

21. Bathe, K. J., Wilson, E. L., and Iding, R. H., "NONSAP -- A Structural Analysis Program for Static and Dynamic Response of Nonlinear System," Report No. UC SESM 74-3, Structural Engineering Laboratory, University of California, Berkeley, 1974.

22. Bathe, K. J., Ozdemir, H., and Wilson, E. L., "Static and Dynamic Geometric and Material Nonlinear Analysis," Report No. UC SESM 74-4, Structural Engineering Laboratory, University of California, Berkeley, 1974.

23. Williams, D., and Godden, W. G., "Seismic Response of A Curved Highway Bridge Model," 54th Annual Meeting, Transportation Research Board, National Research Council, Washington, D. C., January, 1975.

24. Williams, D., and Godden, W. G., "Seismic Behavior of High Curved Overcrossings," Proc. of U. S. National Conference on Earthquake Engineering, Ann Arbor, 1975.

25. Howe, S., and Williams, D., "Private Memorandom on Test Procedures and Test Results of Model Bridge Structure," 1975.

26. Williams, D., and Godden, W. G., "16 m/m Film for Experimental Test of Model Bridge Structure, 1975.

27. Rea, D., and Penzien, J., "Dynamic Response of A 20 ft x 20 ft Shaking Table," Proc. of 5th World Conference on Earthquake Engineering, Rome, Italy, 1973.

28. Chopra, A. K., Bertero, V. V., and Mahin, S., "Response of the Olive View Medical Center Main Building during the San Fernando Earthquake," Proc. 5th World Conference on Earthquake Engineering, Rome, Italy, 1973.

29. Tang, D., and Clough, R. W., "Shaking Table Tests of A Steel Frame - A Progress Report," Report No. EERC 74-8, Earthquake Engineering Research Center, University of California, Berkeley, July 1975.

30. Tang, D., "Earthquake Simulatory Study of A Steel Frame Structure, Volume II - Analytical Results," Report No. EERC 75-36, Earthquake Engineering Research Center, University of California, Berkeley, October 1975.

31. Hidalgo, P., and Clough, R. W., "Earthquake Simulatory Study of A Reinforced Concrete Frame," Report No. EERC 74-13, Earthquake Engineering Research Center, University of California, Berkeley, December 1974.

32. Iemura, H., and Jennings, P. C., "Hysteretic Response of a Nine-Story Reinforced Concrete Building During the San Fernando Earthquake," Report No. EERL 73-7, Earthquake Engineering Research Laboratory, California Institute of Technology, Pasadena, October 1973.

33. Bouwkamp, J. G., and Rea, D., "Dynamic Testing and the Formulations of Mathematical Models," Earthquake Engineering, Wiegel, R. L., Coordinating Editor, Prentice Hall, 1970.

APPENDIX A

LONGITUDINAL COLLINEAR COLLISION OF TWO RODS

To check the mathematical model and analytical procedures used in representing joint impact as presented in Chapters II and III, respectively, consider the collinear collision of two uniform bars initially travelling in opposite directions with the same initial velocity V_o as shown in Fig. A.1. The approximate solution of the post-impact behavior obtained by these procedures can be compared with the exact solution obtained by classical wave propagation theory [7].

Assume both bars have the same properties as given by

$$\begin{aligned} &E \text{ (modulus of elasticity)} = 100 \\ &A \text{ (cross-sectional area)} = 1 \\ &\rho \text{ (mass density)} = 0.1 \\ &L \text{ (rod length)} = 10 \\ &V_o \text{ (initial rod velocity)} = \pm\, 0.1 \end{aligned} \qquad \text{(A-1)}$$

in which any convenient units may be used. For this example problem, the impact contact duration T_I is 0.2 units of time as given by the exact solution. This duration corresponds to the time required for a wave to propagate twice the length of the rod, i.e.

$$T_I = \frac{2L}{c_o} \qquad \text{(A-2)}$$

where c_o is the longitudinal wave velocity given by

$$c_o = \sqrt{E/\rho} \qquad \text{(A-3)}$$

In both the exact and approximate solutions, it is convienient to monitor the separation and rate of change of separation between the two bars as given by

$$u = u^R - u^L$$
$$\dot{u} = \dot{u}^R - \dot{u}^L \tag{A-4}$$

where u^R and $\dot{u}^R$ represent the displacement and velocity, respectively, of the contact surface of the right bar and u^L and $\dot{u}^L$ represent the displacement and velocity, respectively, of the contact surface of the left bar. A positive value of u represents a separation of the contact surfaces while a negative value of u represents an overlap of the contact surfaces. A negative value of u is, of course, not possible in reality as given by the exact solution.

Using the modelling procedures of Chapter II, the two bars can be represented by an impact spring and finite elements as shown in Fig. A-2. In this case, a zero value of u represents that position of the bars when initial contact is made on both sides with the impact spring; thus, a negative value of u is possible which corresponds to the shortening of the impact spring.

In modelling the two bar system in Fig. A-2, the impact spring stiffness K^I, the numerical time interval of integration Δt, and the number of finite elements n representing each rod are all factors influencing the predicted dynamic response following impact. The constant acceleration integration procedure with equilibrium iteration has been used in this example parameter study. The tolerances controlling the equilibrium iteration, as defined in Eqs. (51) and (63), were specified as

$$\Delta_{ps} = 0.001$$
$$\Delta^I_{ps} = 0.001 \tag{A-5}$$

Responses u and $\dot{u}$ as predicted by exact wave propagation theory are shown in Fig. A.3. Before collision, the relative separation velocity $\dot{u}$ equals -0.2 which instantaneously changes to zero upon collision. This velocity stays at a value of zero during the contact duration equal to 0.2 and then instantaneously changes to a value of +0.2. It should be noted that the instantaneous change in velocity represents a Dirac delta change in the acceleration, i.e. a pure acceleration pulse of duration and amplitude which tend to zero and infinity, respectively.

Turning now to the approximate solution, consider first the effect of the magnitude of the impact spring stiffness K^I upon response. Using a time interval of integration Δt equal to 0.01 T_I, a value of 10 for n, and five different values for K^I (10, 10^2, 10^3, 10^4 and 10^5), responses u and $\dot{u}$ as shown in Fig. A.4 were obtained. Comparing the relative displacement results in this figure with the corresponding results for the exact solution given in Fig. A.3 shows that the exact and approximate values of u are in good agreement for K^I equal to 10^2 and 10^3 but they are significantly in error for the larger values of K^I. Comparing the relative velocity results in these same figures shows considerable differences for all 5 values of K^I and it shows considerable vibrations taking place following unit time zero. These vibrations in velocity $\dot{u}$ increase in amplitude with increasing values of K^I. It is interesting to note that when the larger values of K^I are used, contact and separation of the bar ends are repeated many times during period T_I. To judge the best value of K^I it is convenient to introduce the dimensionless parameter

$$\gamma = \frac{K^I L}{n\ EA} \qquad \text{(A-6)}$$

which represents the ratio of the impact spring stiffness to an individual rod element stiffness. Comparing responses u and $\dot{u}$ in Figs. A.3 and A.4, it appears that a value of unity for γ yields the best overall correlation of the approximate results with exact results. This suggests that the numerical value of K^I should be approximately equal to the stiffness of its neighboring elements.

Let us now consider the effect of the magnitude of Δt upon response. Using K^I equal to 100 ($\gamma = 1$), n equal to 10, and Δt equal to 0.5 T_I, 0.05 T_I, and 0.01 T_I, responses u and $\dot{u}$ were obtained as shown in Fig. A.5. The displacement response u agrees well with the exact response shown in Fig. A.3 for Δt equal to 0.05 T_I and 0.01 T_I but shows considerable error for Δt equal to 0.5 T_I. These and similar results for other values of Δt indicate that the approximate response u will agree reasonable well with the exact response provided Δt is assigned a value less than 0.2 T_I. The velocity response $\dot{u}$ in Fig. A.5 shows an erroneous oscillation for Δt equal to 0.05 T_I and 0.01 T_I. However, if a smooth curve is drawn through these oscillations, it would agree reasonable well with the exact relation shown in Fig. A.3. The velocity response in Fig. A.5 for Δt equal to 0.5 T_I is greatly in error which again shows that Δt must be taken much smaller than 0.5 T_I.

Further, let us consider the effect of the value of n on dynamic response. Using K^I equal to 100, Δt equal to 0.01 T_I, and n equal to 2, 10, and 40, responses u and $\dot{u}$ were obtained as shown in Fig. A.6. The approximate displacement response for all three values of n agrees very closely with the exact response; however, the approximate velocity response agrees closely with the exact response only for the case of n equal to 40. Considerable disagreement in the velocity response is noted for n equal to 10 and an even larger disagreement is noted for n equal to 2.

Finally, let us consider the variations of particle velocity and longitudinal stress with position along both bars for the case of n equal to 10, K^I equal to 100 ($\gamma = 1$), and Δt equal to 0.05 T_I. The resulting variations along both bars for instantaneous times t equal to 0, 0.25 T_I, 0.50 T_I, 0.75 T_I, 1.00 T_I, and 1.25 T_I are shown in Fig. A.7. The ordinates representing particle velocity and stress have been normalized by dividing by the initial bar velocity (0.1) and the exact intensity of the stress wave ($\bar{V}_o \rho E = 0.2 \rho E$), respectively. Comparing these variations with the exact solution shows that reasonably accurate results can be obtained by the approximate method employing an impact spring.

Based on the above discussion, the effects of parameters K^I, Δt, and n on the dynamic response of two colliding rods can be summarized as shown in Table A.1.

TABLE A-1 EFFECTS OF VARIOUS PARAMETERS ON PREDICTED RESPONSE OF COLLIDING RODS

EFFECTS / PARAMETERS	Overlap Between Contact Planes	Velocity Change After Collision	Numerical Oscillation of u and $\dot{u}$	Numerical Duration of Collision T_I'	Stress During Collision
Increase of K^I	decreased	less significant	increased but approaches to a certain level	$T_I' \simeq T_I$ for $\gamma \geq 1$ $T_I' > T_I$ for $\gamma \ll 1$	less significant for $\gamma \geq 1$ becomes small for $\gamma \ll 1$
Increase of n	less significant	less significant	decreased	less significant	less significant
Decrease of Δt	less significant	less significant	less significant	$T_I' \simeq T_I$ for $\Delta t \leq \left(\frac{1}{4} \sim \frac{1}{6}\right) T_I$ $T_I' > T_I$ for $\Delta t > \left(\frac{1}{4} \sim \frac{1}{6}\right) T_I$	less significant as long as Δt is small enough to provide realistic solution

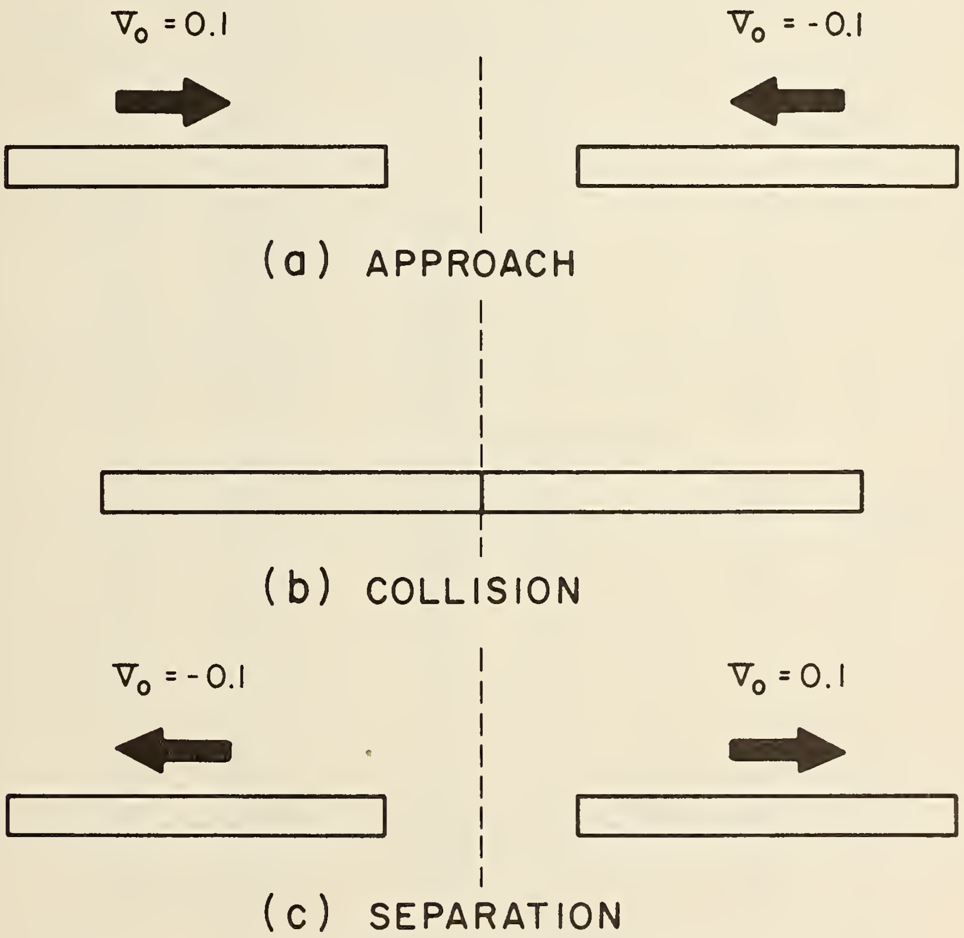

FIG. A.1 LONGITUDINAL COLLINEAR COLLISION OF TWO RODS

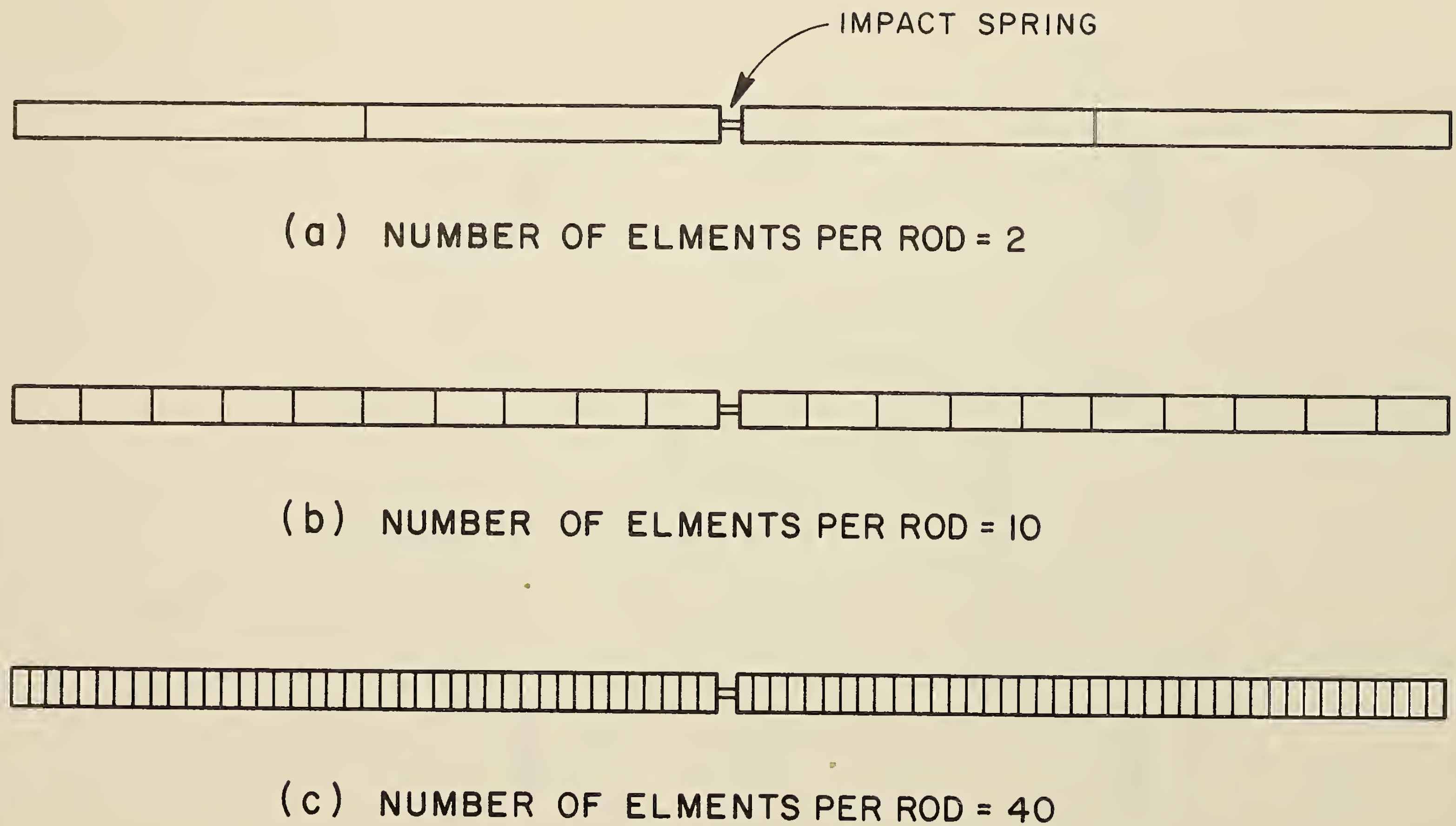

FIG. A.2 ANALYTICAL MODEL FOR COLLISION OF RODS

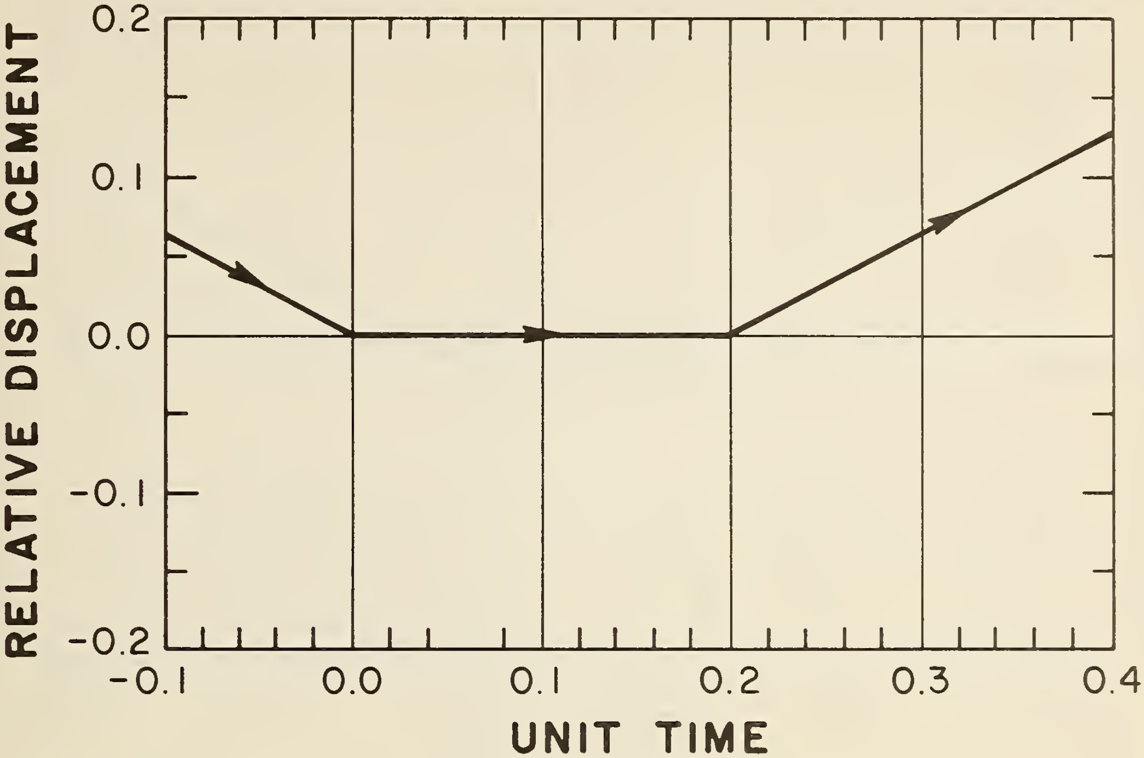

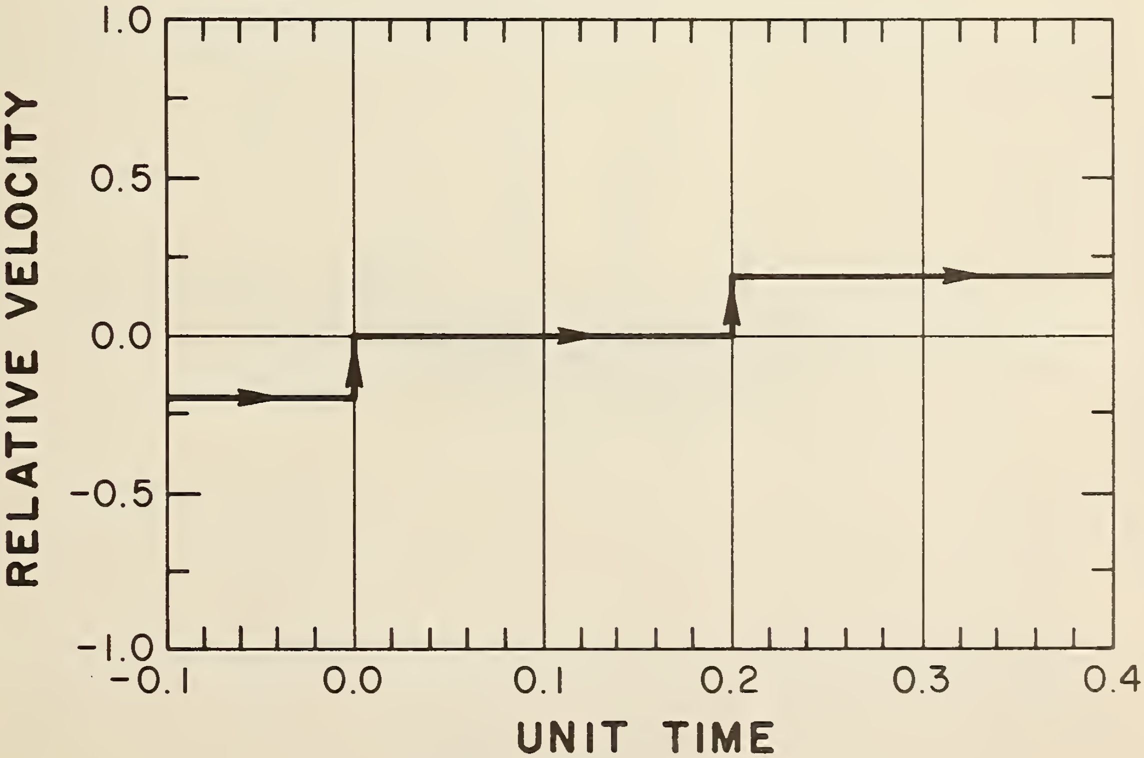

FIG. A.3 EXACT SOLUTION OF RELATIVE DISPLACEMENT AND RELATIVE VELOCITY

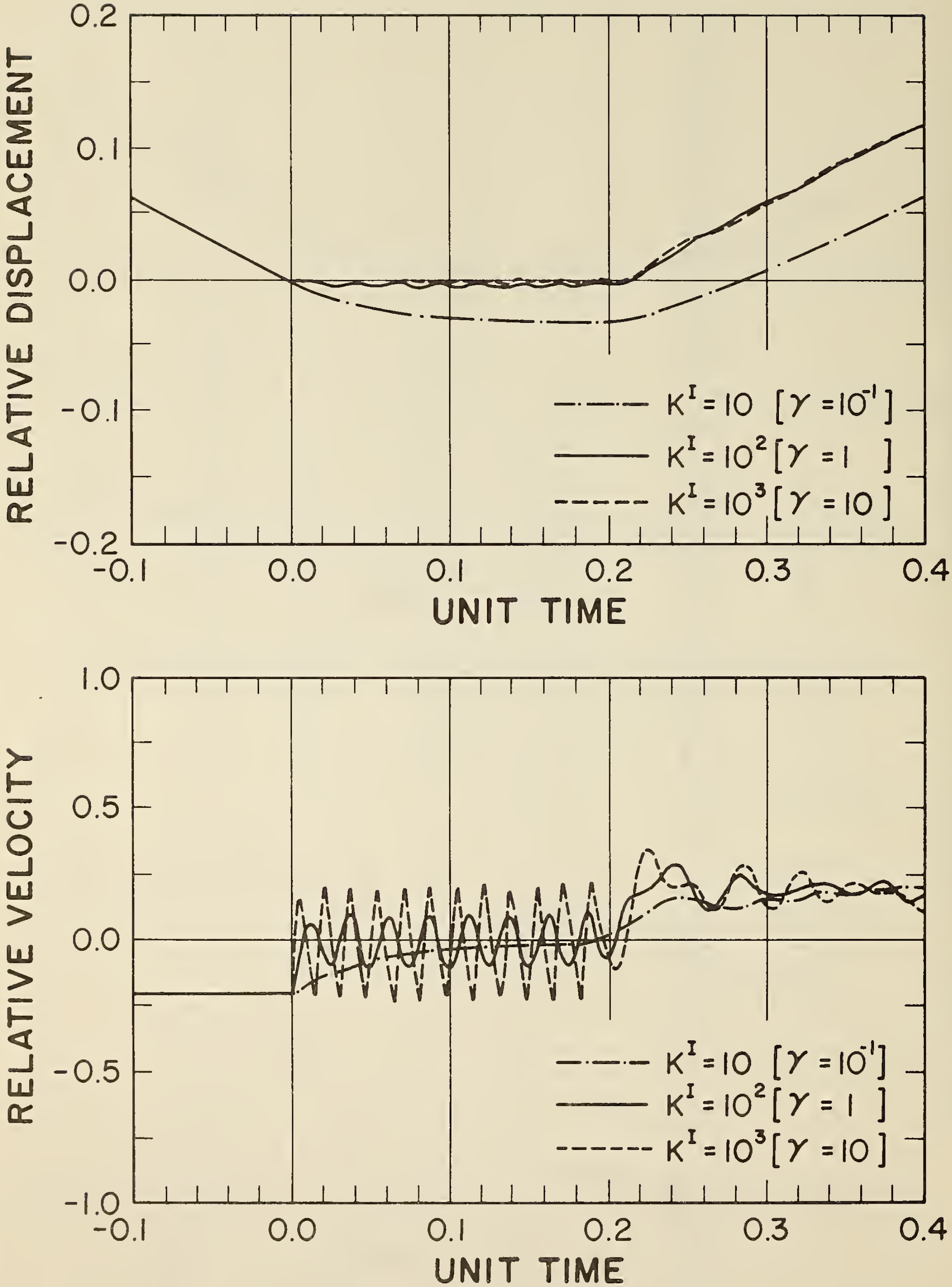

FIG. A.4.1 EFFECT OF IMPACT SPRING STIFFNESS ON RELATIVE RESPONSE OF RODS (K^I = 10, 10^2 and 10^3)

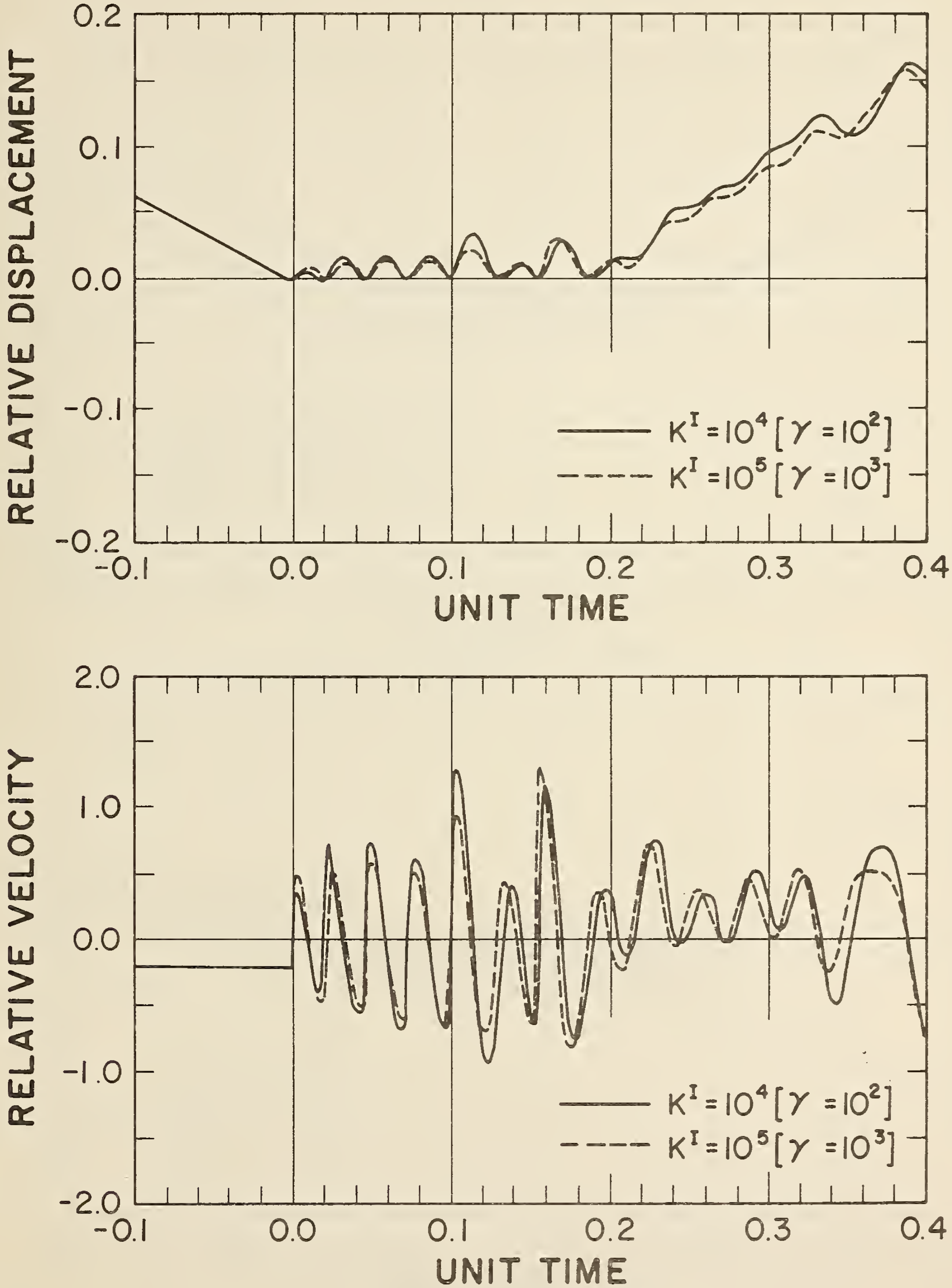

FIG. A.4.2 EFFECT OF IMPACT SPRING STIFFNESS ON RELATIVE RESPONSE OF RODS (K^I = 10^4 and 10^5)

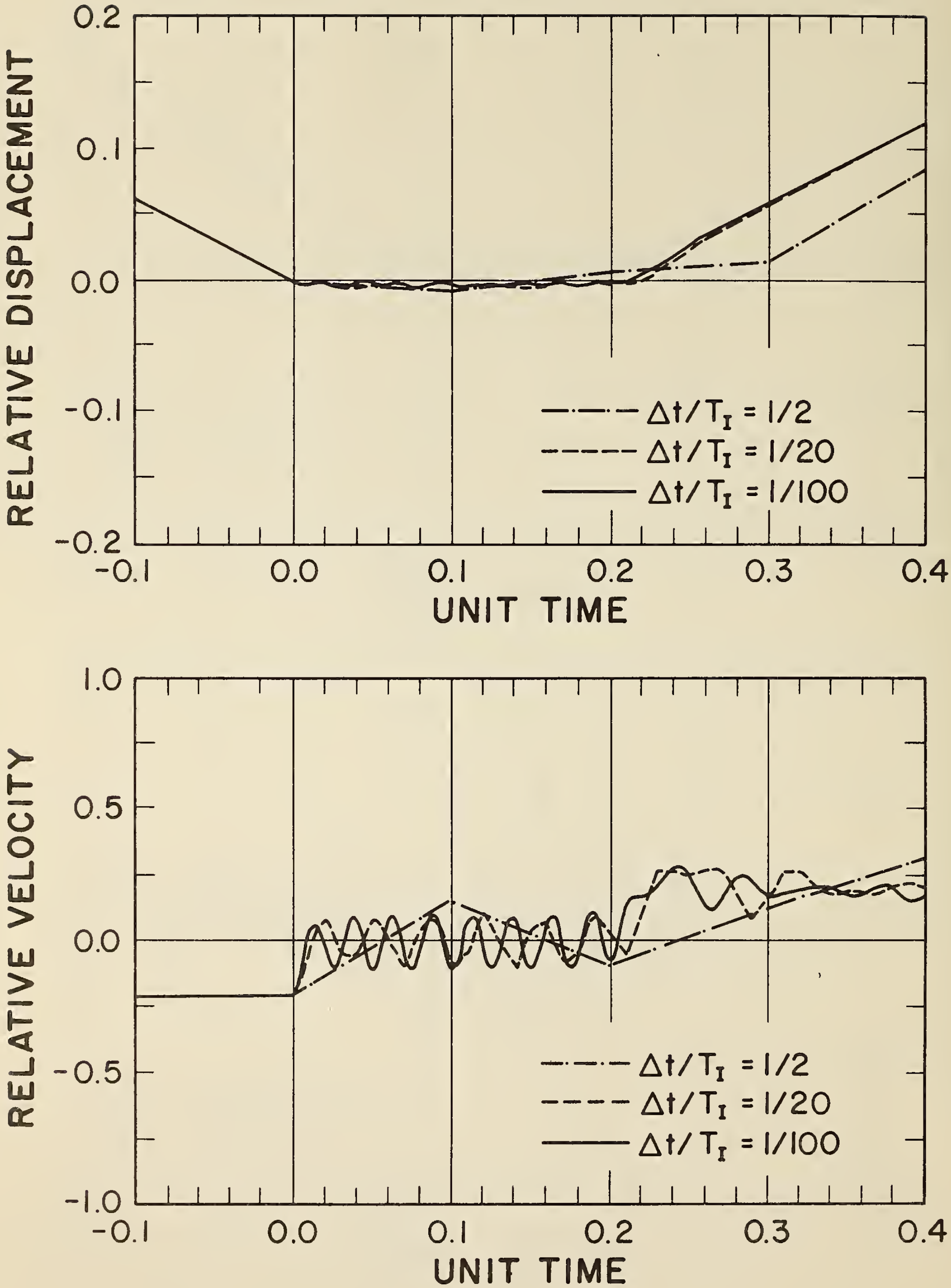

FIG. A.5 EFFECT OF TIME INTERVAL ON RELATIVE RESPONSE OF RODS

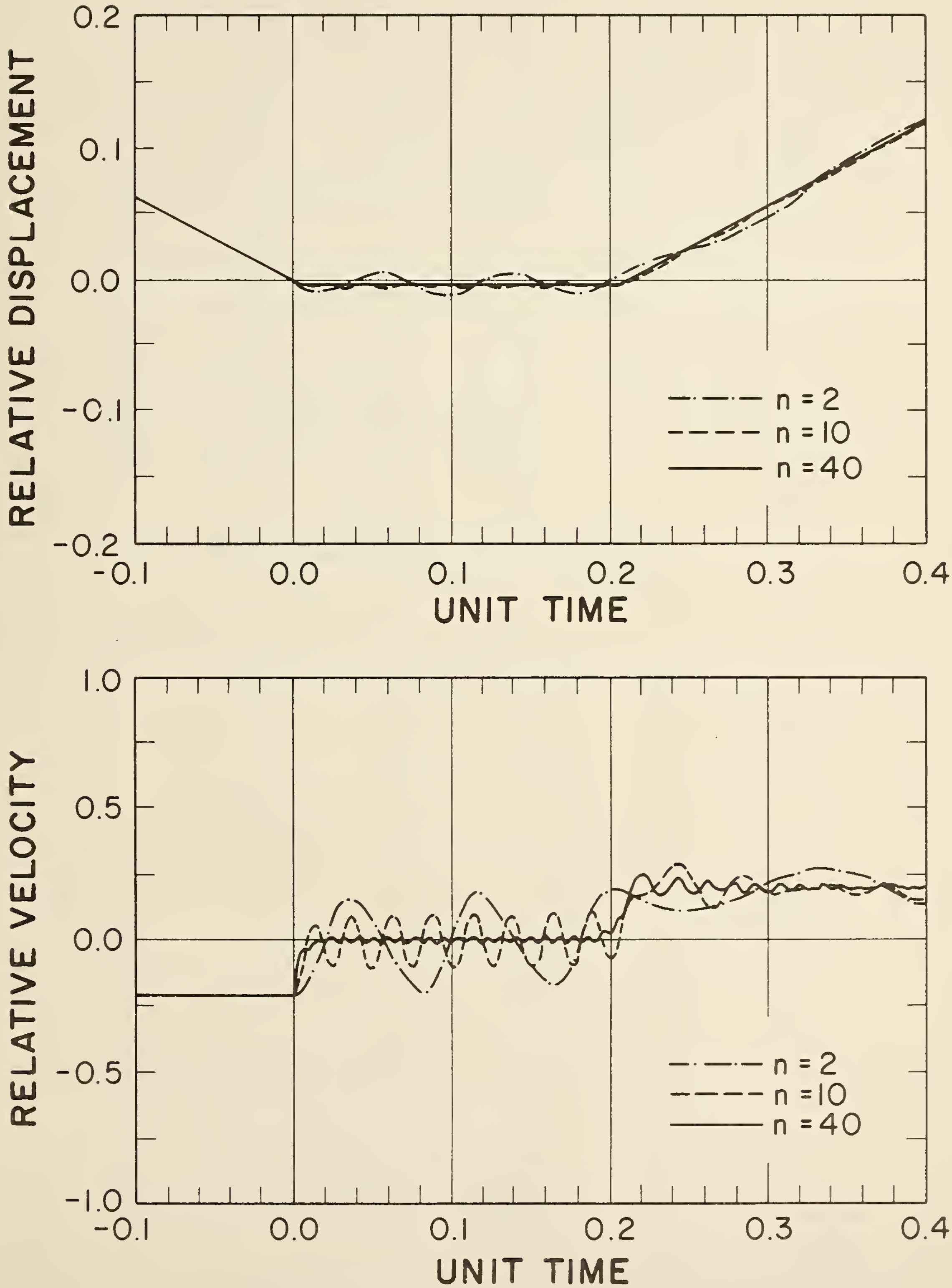

FIG. A.6 EFFECT OF ELEMENT NUMBER ON RELATIVE RESPONSE OF RODS

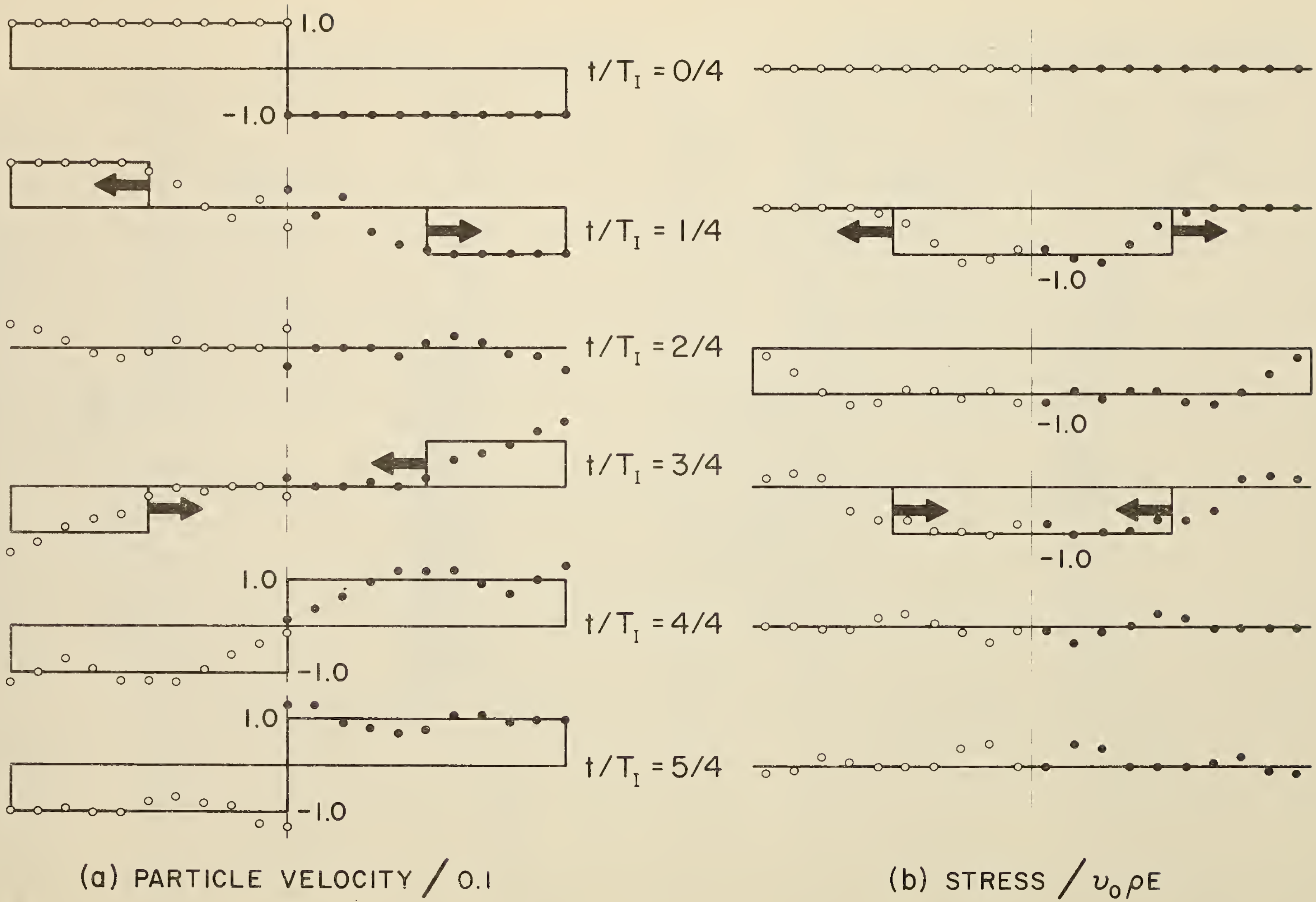

FIG. A.7 PREDICTED PARTICLE VELOCITY AND STRESS OF RODS

APPENDIX B

FREE VIBRATION OF A SINGLE SPRING-MASS SYSTEM WITH COULOMB FRICTION

Consider the rigid mass m shown in Fig. B.1 which is attached to a linear elastic spring of stiffness k and is supported on a surface which can develop Coulomb friction having a maximum absolute value of νmg (ν = Coulomb friction coefficient). If the mass is displaced to the right, elongating the spring by an amount x_o, where $x_o >> \Delta$ and where

$$\Delta = \frac{F}{k} = \frac{\nu mg}{k} \qquad \text{(B-1)}$$

, and it is then released from rest, the free vibration equation of motion becomes

$$m\,\ddot{x} + k\,x = -F\,\text{sign}(\dot{x}) \qquad \text{(B-2)}$$

Introducing two new variables, namely

$$\begin{aligned} x_1 &\equiv x + \Delta \\ x_2 &\equiv x - \Delta \end{aligned} \qquad \text{(B-3)}$$

, Eq. (B-2) can be written in the double form

$$\begin{aligned} m\,\ddot{x}_1 + k\,x_1 &= o \qquad \dot{x} > o \\ m\,\ddot{x}_2 + k\,x_2 &= o \qquad \dot{x} < o \end{aligned} \qquad \text{(B-4)}$$

, having solutions

$$\begin{aligned} x_1 &= A\ \cos\,(\omega_n t - \gamma) \qquad \dot{x} > o \\ x_2 &= A'\cos\,(\omega_n t - \gamma') \qquad \dot{x} < o \end{aligned} \qquad \text{(B-5)}$$

where $\omega_n = \sqrt{k/m}$ and A, A', γ, and γ' are arbitrary constants. The solution of Eq. (B-2) can now be written as

$$x = -\Delta + A \cos(\omega_n t - \gamma) \qquad \dot{x} > 0$$

$$x = \Delta + A' \cos(\omega_n t - \gamma') \qquad \dot{x} < 0 \qquad \text{(B-6)}$$

As an example, let x_o equal 12Δ. The resulting motion of the mass as represented by Eq. (B.6) is that motion shown in Fig. B.2. It is well known that the frequency of free vibration of the system with Coulomb friction is the same as the free vibration frequency with no damping. Further, it is well known that the amplitude of oscillation diminishes by an amount 4Δ with each full cycle. The block finally comes to rest in the first extreme position which is less than Δ. For this example, the final rest is reached at time $t = 6\pi/\omega_n$.

The above example problem has also been solved using the mathematical model and analytical procedures defined in Chapter II and III, respectively. The numerical data used in this approximate solution were the following:

$$m = 80/386.4 \text{ lbs sec}^2/\text{inch}$$

$$k = 400 \text{ lbs/inch}$$

$$\nu = 0.5$$

$$f_n = \frac{1}{2\pi}\sqrt{\frac{(400)(386)}{80}} = 6.98 \text{ c/s} \qquad \text{(B-7)}$$

$$\omega_n = 2\pi\ (6.98) = 43.8 \text{ c/s}$$

$$\Delta = \frac{F}{k} = \frac{(0.5)(80)}{400} = 0.1 \text{ inch}$$

$$x_o = 12\ \Delta = 1.2 \text{ inch}$$

In the numerical calculation, it is convenient to introduce the elastic deformation

$$u^e \equiv \frac{F}{k^e} \qquad \text{(B-8)}$$

where $F = \nu mg$ and k^e is the elastic stiffness of the Coulomb friction elastoplastic model defined in Fig. 2.4. The constant acceleration integration procedure with equilibrium interation is used for the analysis. The tolerances controlling the equilibrium iteration were specified as

$$\delta R_t \leq 0.1 \quad ; \quad \delta R_t^{(i)} \leq 0.01 \qquad \text{(B-9)}$$

where δR_t and $\delta R_t^{(i)}$ represent the residual forces at time t and during the ith iteration, respectively.

First, let us examine the effect of the value of u^e on response. Using a time interval Δt equal to $0.05(2\pi/\omega_n)$ throughout the calculations, the displacement response shown in Fig. B.3 is obtained. Clearly, the approximate solution approaches the exact solution with decreasing values of the ratio u^e/Δ. Quite good agreement is shown when this ratio is assigned the value 0.1, particularly for the higher amplitude oscillations.

Now let us examine the effect of the value of Δt on response. For this examination, let u^e equal $0.1\ \Delta$ and compare the resulting responses for Δt equal to $0.05(2\pi/\omega_n)$, $0.10(2\pi/\omega_n)$, and $0.166(2\pi/\omega_n)$ as shown in Fig. B.4. It is quite apparent from these results that the approximate solution is improved by decreasing the time interval Δt.

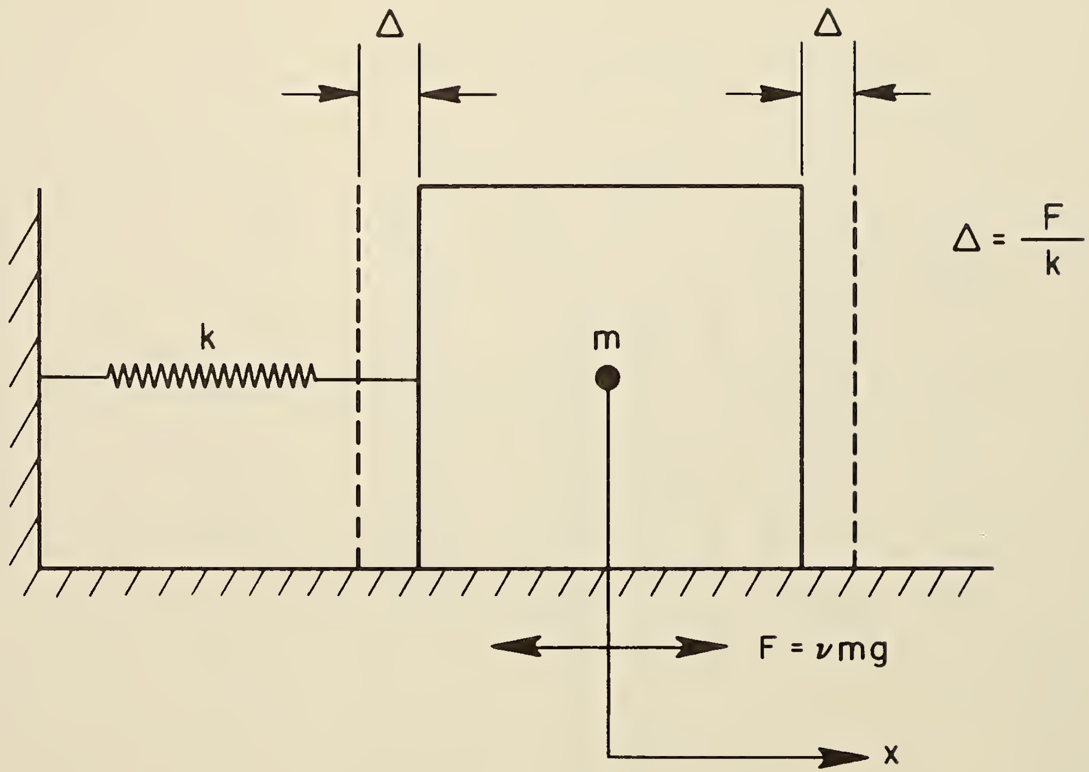

FIG. B.1 FREE VIBRATION OF A BLOCK WITH COULOMB FRICTION

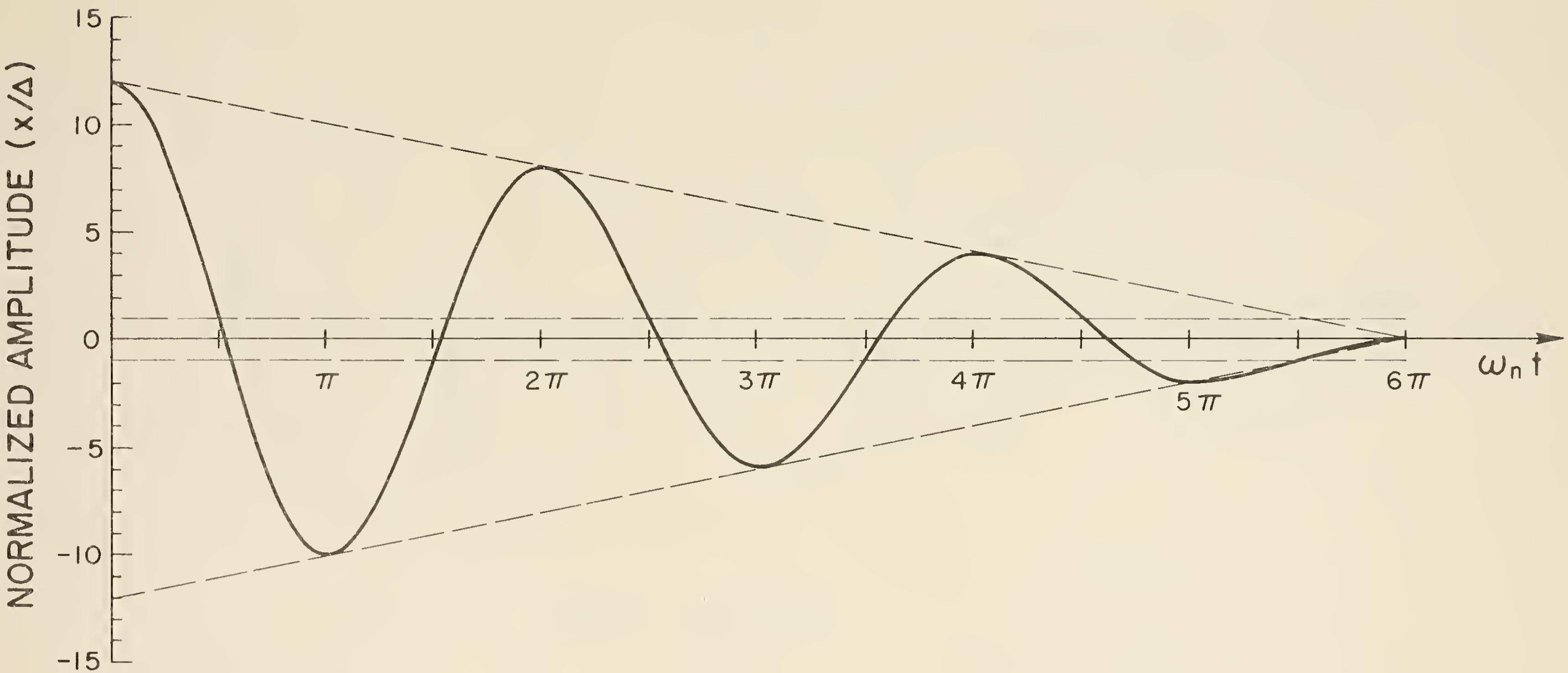

FIG. B.2 FREE VIBRATION RESPONSE OF A BLOCK WITH COULOMB FRICTION

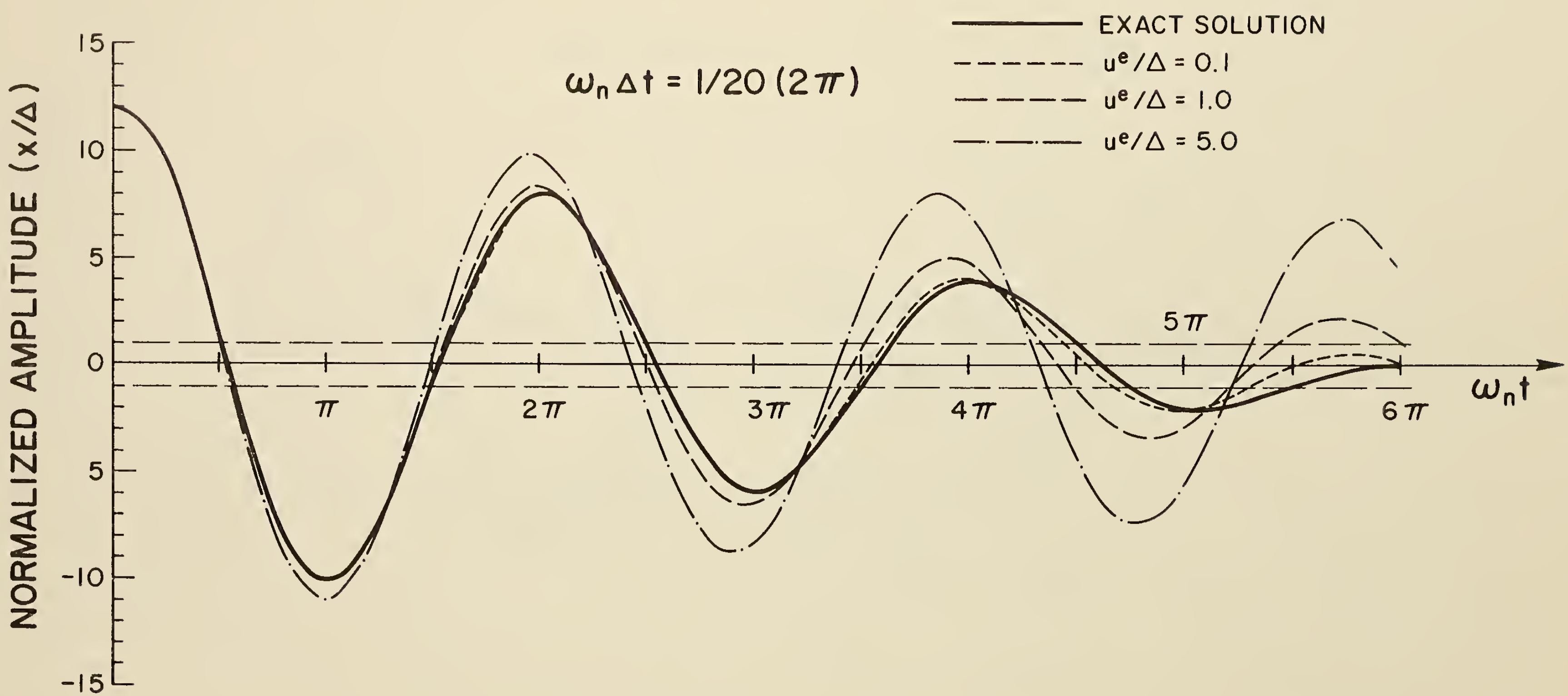

FIG. B.3 EFFECT OF MAGNITUDE OF u^e ON FREE VIBRATION RESPONSE OF A BLOCK

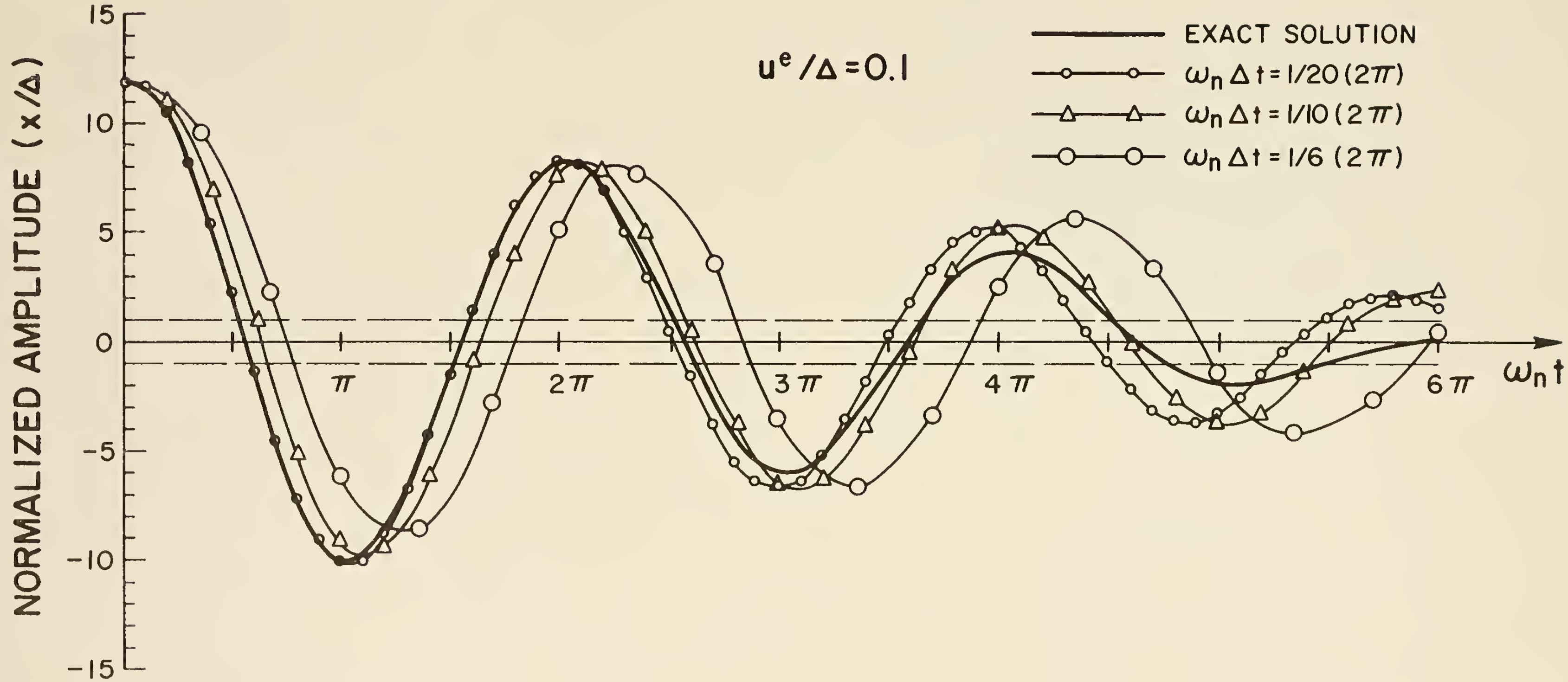

FIG. B.4 EFFECT OF TIME INTERVAL ON FREE VIBRATION RESPONSE OF A BLOCK

APPENDIX C

COMPUTER LISTING OF NEABS

```
                                    1.
*DECK NEABS
      PROGRAM NEABS (INPUT,OUTPUT,TAPE5=INPUT,TAPE6=OUTPUT,TAPE1,TAPE2,
     .               TAPE3=2100,TAPE4,TAPE7,TAPE8,TAPE9,TAPE10,TAPE12,
     .               TAPE30,PUNCH)
C
C
C     PROGRAM FOR NONLINEAR EARTHQUAKE ANALYSIS OF BRIDGE STRUCTURES
C     MODIFIED ON APRIL 2 1976
C
C
      COMMON/EPAR/ NPAR(14),NUMNP,NELTYP,NUMEL,NUMNEL,NEQ,MBAND,MTOT,
     .             NNN(7)
      COMMON/EMTX/ QQQQ(2043)
      COMMON/MISC/ NFN,NGM,NT,NOT,JJJ(10)
      COMMON/JUNK/ HED(12),I,II,TT,JLK(190)
      COMMON/ITSO/ IIII(40)
      COMMON/TEMP/ T(10)
C
C     PROGRAM CAPACITY CONTROLLED BY THE FOLLOWING TWO STATEMENTS...
C
      COMMON A(18500)
      MTOT=18500
C
C     PROGRAM CONTROL DATA
C
    5 CALL SECOND (T(1))
      READ (5,100) HED,NUMNP,NELTYP,NUMEL,NFN,NGM,NT,NOT
      IF (NUMNP.EQ.0) STOP
      WRITE(6,200) HED,NUMNP,NELTYP,NUMEL,NFN,NGM,NT,NOT
C
C     SETUP STRUCTURAL SYSTEM INPUTS
C
      CALL SETUP
      CALL SECOND (T(2))
C
C     STATIC ANALYSIS
C
      CALL STATIC
      CALL SECOND (T(3))
C
C     SETUP DYNAMIC LOAD INPUTS
C
      CALL LOADS
      CALL SECOND (T(4))
C
C     STEP-BY-STEP DYNAMIC ANALYSIS
C
      CALL INTGR
      CALL SECOND (T(5))
C
C     OUTPUT RESULTS OF STEP-BY-STEP DYNAMIC ANALYSIS
C
      CALL OUTPUT
      CALL SECOND (T(6))
C
                                    2.
C     OUTPUT CP EXECUTION TIMES
C
      TT=0.
      DO 90 I=1,5
      II=I+1
      T(I)=T(II)-T(I)
   90 TT=TT+T(I)
      T(6)=TT
      WRITE(6,205) (T(I),I=1,6)
C
      STOP
C
  100 FORMAT (12A6/7I5)
  200 FORMAT (1H1,12A6 ///
     .          30H  NUMBER OF NODAL POINTS      =  I5//
     .          30H  NUMBER OF ELEMENT TYPES     =  I5//
     .          30H  NUMBER OF TOTAL ELEMENTS    =  I5//
     .          30H  NUMBER OF TIME FUNCTIONS    =  I5//
     .          30H  GROUND MOTION INPUT CODE    =  I5//
     .          30H  NUMBER OF TIME STEPS (DT)   =  I5//
     .          30H  DT MULTIPLIER FOR OUTPUT    =  I5)
  205 FORMAT (21H1OVERALL TIME LOG....  ///
     .          33H  STRUCTURAL SYSTEM SETUP  ...... ,F8.2//
     .          33H  STATIC ANALYSIS  ............. ,F8.2//
     .          33H  SET UP DYNAMIC LOAD INPUTS ... ,F8.2//
     .          33H  STEP-BY-STEP DYNAMIC ANALYSIS . ,F8.2//
     .          33H  OUTPUT DYNAMIC RESPONSES ...... ,F8.2///
     .          33H  TOTAL SOLUTION TIME  .......... ,F8.2  )
C
      END
```

```
*DECK ERROR
      SUBROUTINE ERROR (MODE,N,PH)
C
C     PRINT APPROPRIATE ERROR MESSAGE...
C
      GO TO (1,2,3,4,5,6,7,8,9)  MODE
C
C     ERROR MODE 1
C
    1 WRITE(6,2001) N,PH
      GO TO 100
C
C     ERROR MODE 2
C
    2 WRITE(6,2002) N,PH
      GO TO 100
C
C     ERROR MODE 3
C
    3 WRITE(6,2003) N,PH
      GO TO 100
C
C     ERROR MODE 4
C
    4 WRITE(6,2004) N,PH
      GO TO 100
C
C     ERROR MODE 5
C
    5 WRITE(6,2005) N,PH
      GO TO 100
C
C     ERROR MODE 6
C
    6 WRITE(6,2006) N,PH
      GO TO 100
C
C     ERROR MODE 7
C
    7 WRITE(6,2007) N,PH
      GO TO 100
C
C     ERROR MODE 8
C
    8 WRITE(6,2008) N,PH
      GO TO 100
C
C     ERROR MODE 9
C
    9 WRITE(6,2009) N,PH
  100 STOP
C
 2001 FORMAT (1H1,44H*****DIMENSION IN BLANK COMMON A EXCEEDED BY,I6,
     .  20H    AT SUBROUTINE   ,A7/27H .....EXECUTION TERMINATED.)
 2002 FORMAT (1H1,42H*****WRONG INPUT FOR TOTAL NO. OF ELEMENTS ,I6,
     .  20H    AT SUBROUTINE   ,A7/27H .....EXECUTION TERMINATED.)
 2003 FORMAT (1H1,48H*****ELEMENT NONLINEAR PARAMETER NO. INPUT WRONG,
     .  10H   FOR NO. ,I6,17H    ELEMENT OF    ,A7/
     .  27H .....EXECUTION TERMINATED.)
 2004 FORMAT (1H1,50H*****ELEMENT DATA INPUT IN WRONG ORDER DETECTED AT,
     .  3HNO.,I6,17H    ELEMENT OF   ,A7/27H .....EXECUTION TERMINATED.)
 2005 FORMAT (1H1,16H*****ELEMENT NO. ,I6,9H    OF   ,A7,12HHAS 0 LENGTH
     .  27H .....EXECUTION TERMINATED.)
 2006 FORMAT (1H1,16H*****ELEMENT NO. ,I6,9H    OF   ,A7,17HHAS WRONG K
     .NODE. /27H .....EXECUTION TERMINATED.)
 2007 FORMAT (1H1,37H*****DATA INPUT NOT IN ORDER FOR NODE,I6,
     .  15H    DETECTED AT ,A7/27H .....EXECUTION TERMINATED.)
 2008 FORMAT (1H1,41H*****MULTIPLE GROUND MOTION INPUT AT NODE,I6/
     .  50H      NOT COMPATIBLE WITH THAT OF JOINT INPUT CODE ,
     .  13H DETECTED AT,A7/27H .....EXECUTION TERMINATED.)
 2009 FORMAT (1H1,25H*****NONLINEAR ELEMENT NO ,I6,16H    IS SINGULAR.
     .  15H    DETECTED AT ,A7/27H .....EXECUTION TERMINATED. )
      END
```

```
*DECK SETUP
      SUBROUTINE SETUP
C
      COMMON/EPAR/ NPAR(14),NUMNP,NELTYP,NUMFL,NUMNEL,NEQ,MBAND,MTOT,
     1             N1,N2,N3,N4,N5,N6,N7
      COMMON/EMTX/ GGGQ(2043)
      COMMON/MISC/ MFN,NGM,NT,NCT,JJJ(10)
      COMMON/JUNK/ JUK(205)
      COMMON A(1)
C
C     INPUT JOINT DATA----JOINT ID CODE ARRAY STORED ON TAPE 8
C
      N1=1
      N2=N1+NUMNP*6
      N3=N2+NUMNP
      N4=N3+NUMNP
      N5=N4+NUMNP
      IF (N5.GT.MTOT) CALL ERROR (1,N5-MTOT,7HINPUTM  )
      CALL INPUTM (A(N1),A(N2),A(N3),A(N4),NUMNP,NEQ)
C
C     INPUT ELEMENT DATA AND FORM ELEMENT STIFFNESSES---
C     STIFFNESS ON TAPE 2, STRESS ON TAPE 1, NONLINEAR DATA ON TAPE 3.
C
      N6=N5+NUMEL
      IF (N6.GT.MTOT) CALL ERROR (1,N6-MTOT,7HELSTF   )
      CALL ELSTF (A(N5),NUMEL)
      WRITE(6,2000) NEQ,MBAND
C
C     INPUT NODAL LOADS AND MASSES-----ON TAPE 9
C
      N3=N2+NUMNP
      N4=N3+NUMNP*6
      N5=N4+NEQ
      IF(N5.GT.MTOT) CALL ERROR (1,N5-MTOT,7HINLM    )
      CALL INLM (A(N1),A(N2),A(N3),A(N4),NUMNP,NEQ)
C
C     ASSEMBLE TOTAL STIFFNESS,LOAD---ON TAPE 4,  MASS---ON TAPE 9
C
      N2=N1+NEQ
      N3=N2+NEQ*MBAND
      N4=N3+NEQ
      IF(N4.GT.MTOT) CALL ERROR (1,N4-MTOT,7HACCSTF   )
      CALL ACCSTF (A(N1),A(N2),A(N3),NEQ,MBAND,NUMEL)
      RETURN
C
 2000 FORMAT (/////28H SYSTEM SETUP INFORMATION...  ///
     .         30H TOTAL NUMBER OF EQUATIONS    =  I5//
     .         30H BAND WIDTH                   =  I5)
      END
```

```
*DECK INPUTM
      SUBROUTINE INPUTM (ID,X,Y,Z,NUMNP,NEQ)
C
      DIMENSION ID(NUMNP,6),X(1),Y(1),Z(1),NID(6)
C
C     NODAL POINT INPUT AND GENERATION
C
      REWIND 8
      ND=6
      WRITE(6,200)
      WRITE(6,204)
      KO=1
      DO 10 I=1,6
   10 NID(I)=0
   11 READ (5,100) N,(ID(N,I),I=1,6),X(N),Y(N),Z(N),KN
      WRITE(6,203) N,(ID(N,I),I=1,6),X(N),Y(N),Z(N),KN
      DO 30 I=1,6
      IF (ID(N,I)) 21,22,23
   21 NID(I)=-1
      ID(N,I)=1
      GO TO 30
   22 IF (NID(I).EQ.-1) ID(N,I)=1
      GO TO 30
   23 NID(I)=0
   30 CONTINUE
C
C     CHECK IF GENERATION NEEDED THEN GENERATE NEW NODES
C
      IF (KO.EQ.1) GO TO 32
      IF (KN) 33,33,34
   32 KO=0
   33 CONTINUE
      NUMINT=1
      GO TO 45
   34 NUMINT=(N-NI)/KN
      DX=(X(N)-X(NI))/NUMINT
      DY=(Y(N)-Y(NI))/NUMINT
      DZ=(Z(N)-Z(NI))/NUMINT
      DO 41 J=1,NUMINT
      NN=NI+J*KN
      X(NN)=X(NN-KN)+DX
      Y(NN)=Y(NN-KN)+DY
      Z(NN)=Z(NN-KN)+DZ
C
C     SET DOF CODES SAME AS FIRST JOINT IN THE SERIES
C
      DO 40 JJ=1,6
      IF (ID(NI,JJ)-1) 37,36,35
   35 ID(NN,JJ)=ID(NI,JJ)+J*KN
      GO TO 40
   36 ID(NN,JJ)=ID(NI,JJ)
      GO TO 40
   37 ID(NN,JJ)=0
   40 CONTINUE
   41 CONTINUE
   45 NI=N
```

```
C
C     CHECK FOR LAST NODAL POINT
C
      IF (NUMNP-NI) 48,48,11
   48 CONTINUE
      WRITE(6,202)
      WRITE(6,204)
      DO 50 N=1,NUMNP
   50 WRITE(6,203) N,(ID(N,I),I=1,6),X(N),Y(N),Z(N)
C
C     COUNT AND NUMBER UNKNOWNS ---SET SLAVE NODE NEGATIVE OF MASTER
C
      NEQ=0
      DO 60 I=1,NUMNP
      DO 60 J=1,ND
      IF (ID(I,J).LT.0) GO TO 60
      IF (ID(I,J)-1) 57,58,59
   57 NEQ=NEQ+1
      ID(I,J)=NEQ
      GO TO 60
   58 ID(I,J)=0
      GO TO 60
   59 ID(I,J)=-ID(I,J)
   60 CONTINUE
C
C     PRINT INTERNAL EQUATION NUMBER
C
   90 WRITE(6,205)
      WRITE(6,206)
      WRITE(6,207) (N,(ID(N,I),I=1,6),N=1,NUMNP)
      WRITE (8) ID
      RETURN
C
  100 FORMAT (7I5,3F10.0,I5)
  200 FORMAT (31H1NODAL POINT DATA AS INPUT.....  //)
  202 FORMAT (31H1COMPLETE NODAL POINT DATA.....  //)
  203 FORMAT (I5,6I5,3F13.3,I5)
  204 FORMAT (5HONODE 6X 24HBOUNDARY CONDITION CODES 13X
     . 23HNODAL POINT COORDINATES /
     . 7H NUMBER 2X 1HX 4X 1HY 4X 1HZ 3X 2HXX 3X 2HYY 3X 2HZZ 12X 1HX
     . 12X 1HY 12X 1HZ  /)
  205 FORMAT (48H1EQUATION NUMBER OF NODAL DEGREES OF FREEDOM....  //)
  206 FORMAT (5HONODE 10X 15HEQUATION NUMBER 12X
     .        5H NODE 10X 15HEQUATION NUMBER  /
     . 7H NUMBER 2X 1HX 4X 1HY 4X 1HZ 3X 2HXX 3X 2HYY 3X 2HZZ  6X
     . 7H NUMBER 2X 1HX 4X 1HY 4X 1HZ 3X 2HXX 3X 2HYY 3X 2HZZ  /)
  207 FORMAT (7I5,6X,7I5)
      END
```

```
*DECK ELSTF
      SUBROUTINE ELSTF (IND,NEL)
C
      DIMENSION IND(NEL)
      COMMON/EPAR/ NPAR(14),NUMNP,NELTYP,NUMEL,NUMNEL,NEQ,MEANO,MTOT,
     .             NWA(7)
C
C     FORM ELEMENT STIFFNESSES AND STRESS ARRAY FOR EACH ELEMENT TYPE
C
      REWIND 1
      REWIND 2
      REWIND 3
      NUME=NUMEL
      NUMEL=0
      NUMNEL=0
      MBAND=0
      DO 200 M=1,NELTYP
      READ (5,1001) NPAR
      MTYPE=NPAR(1)
C
      GO TO ( 1,2,3,4,5 ) MTYPE
C
C     THREE DIMENSIONAL TRUSS ELEMENTS
C
    1 GO TO 100
C
C     THREE DIMENSIONAL STRAIGHT BEAM ELEMENTS
C
    2 CALL SBEAM
      GO TO 100
C
C     THREE DIMENSIONAL CURVED  BEAM ELEMENTS
C
    3 CALL CBEAM
      GO TO 100
C
C     THREE DIMENSIONAL BOUNDARY SPRING ELEMENTS
C
    4 CALL BOUND
      GO TO 100
C
C     EXPANSION JOINT FICTITIOUS ELEMENTS
C
    5 CALL EXPJT
C
  100 NUMEL=NUMEL+NPAR(2)
  200 CONTINUE
C
C     COUNT NUMBER OF NONLINEAR ELEMENTS
C
      IF (NUME.NE.NUMEL) CALL ERROR (2,NUMEL,7HELSTF   )
      DO 300 I=1,NUMEL
      IF (IND(I).GT.0) NUMNEL=NUMNEL+1
  300 CONTINUE
      WRITE(6,2000) NUMNEL
      WRITE(6,2001)
```

```
      WRITE(6,2002) (I,INC(I),I=1,NUMEL)
      WRITE (8) INC
      RETURN
C
 1001 FORMAT (14I5)
 2000 FORMAT (1H1,38HTOTAL NUMBER OF NONLINEAR ELEMENTS    =  ,I5  ///)
 2001 FORMAT (1H ,35HELEMENT TYPE OF L/NL INDICATOR.....   //
     .           1H ,5(14H  ELEMENT INC )/1H ,5(14H  NUMBER  TYPE)/)
 2002 FORMAT (1H ,5(I7,I6,1X))
      END




*DECK WRITET
      SUBROUTINE WRITET (MBAND,NDIF)
C
      COMMON/EPAR/ NPAR(14),NUMNP,NELTYP,NUMEL,NUMNEL,NEQ,NBAND,MTOT,
     .             NNN(7)
      COMMON/EMTX/ LM(24),ND,NS,S(24,24),P(24,4),XM(24),ST(12,24),
     .             TT(12,4)
C
C     CALCULATE BAND WIDTH AND WRITE ELEMENT INFORMATION ON TAPES
C
      MIN=100000
      MAX=0
      DO 450 L=1,ND
      IF (LM(L).EQ. 0 ) GO TO 450
      IF (LM(L).GT.NEQ) GO TO 450
      IF (LM(L).GT.MAX) MAX=LM(L)
      IF (LM(L).LT.MIN) MIN=LM(L)
  450 CONTINUE
      NDIF=MAX-MIN+1
      IF (NDIF.GT.MBAND) MBAND=NDIF
C
      WRITE (1) NS,ND,LM,ST,TT
      WRITE (2) LM,ND,NS,S,P,XM
C
      RETURN
      END
```

```
*DECK SLAVE
      SUBROUTINE SLAVE (X,Y,Z,ID,NUMNP,NI,NJ)
C
      DIMENSION X(1),Y(1),Z(1),ID(NUMNP,1)
      COMMON/EMTX/ LM(24),ND,NS,S(24,24),P(24,4),XM(24),SA(12,24),
     .             TT(12,4),ENPAR(24),SS(12,12),F(48),LMS(12),EC(12),
     .             T(3,3)
C
C     PERFORMS SLAVE...MASTER DISPLACEMENT TRANSFORMATION
C
      DO 10 I=1,12
      LMS(I)=0
   10 EC(I)=0.
      KK=0
      DO 100 NF=1,12,6
      NOD=NI
      IF (NF.EQ.7) NOD=NJ
      DO 80 K=1,3
      I=K+NF-1
      IF (LM(I).GE.0) GO TO 80
      LMS(I)=1
      M=-LM(I)
      LM(I)=ID(M,K)
      IF (K-2) 35,40,45
   35 D1=-(Y(NOD)-Y(M))
      D2=   Z(NOD)-Z(M)
      LM(ND+1)=ID(M,6)
      LM(ND+2)=ID(M,5)
      GO TO 50
   40 D1=-(Z(NOD)-Z(M))
      D2=   X(NOD)-X(M)
      LM(ND+1)=ID(M,4)
      LM(ND+2)=ID(M,6)
      GO TO 50
   45 D1=-(X(NOD)-X(M))
      D2=   Y(NOD)-Y(M)
      LM(ND+1)=ID(M,5)
      LM(ND+2)=ID(M,4)
   50 KK=KK+1
      EC(KK)=D1
      KK=KK+1
      EC(KK)=D2
C
C     TRANSFORMATION...ARRAYS INCREASE IN SIZE
C
      DO 60 II=1,ND
      S(ND+1,II)=S(I,II)*D1
      S(ND+2,II)=S(I,II)*D2
      XM(ND+1)=XM(I)*D1*D1
      XM(ND+2)=XM(I)*D2*D2
      S(II,ND+1)=S(II,I)*D1
      S(II,ND+2)=S(II,I)*D2
      DO 55 J=1,4
      P(ND+1,J)=P(I,J)*D1
      P(ND+2,J)=P(I,J)*D2
   55 CONTINUE
```

```
   60 CONTINUE
      DO 70 II=1,NS
      SA(II,ND+1)=SA(II,I)*D1
   70 SA(II,ND+2)=SA(II,I)*D2
C
      S(ND+1,ND+1)=S(I,I)*D1**2
      S(ND+2,ND+2)=S(I,I)*D2**2
      S(ND+1,ND+2)=S(I,I)*D1*D2
      S(ND+2,ND+1)=S(ND+1,ND+2)
      ND=ND+2
   80 CONTINUE
C
C     SET ROTATIONS
C
      DO 90 J=1,3
      K=NF+J+2
      IF(LM(K).GE.0)  GO TO 90
      M=-LM(K)
      LM(K)=ID(M,J+3)
   90 CONTINUE
C
  100 CONTINUE
C
      RETURN
      END
```

```
*DECK INLM
      SUBROUTINE INLM (ID,IN,TL,XL,NUMNP,NEQ)
C
      DIMENSION ID(NUMNP,1),IN(1),TL(NUMNP,1),XL(NEQ)
      COMMON/JUNK/ NT,KSHF,NE,N,R(6),NN,II,JJ,JLK(192)
C
      KSHF=0
      REWIND 9
    1 DO 5 I=1,NUMNP
      IN(I)=0
      DO 5 J=1,6
    5 TL(I,J)=0.0
      DO 10 I=1,NEQ
   10 XL(I)=0.
C
C     INPUT NODAL MASSES AND/OR LOADS
C
      NE=0
  100 READ(5,1001) N,R
      NE=NE+1
      IF (N.EQ.0) GO TO 300
      IF (NE.GT.1) GO TO 120
      IF (KSHF.EQ.0) WRITE (6,2003)
      IF (KSHF.EQ.1) WRITE (6,2002)
  120 WRITE (6,2001) N,R
      DO 150 J=1,6
  150 TL(N,J)=R(J)
      IN(N)=1
      GO TO 100
C
C     ASSEMBLE LOADS AND MASSES IN CORE
C
  300 DO 500 NN=1,NUMNP
      IF (IN(NN)) 500,500,310
  310 DO 400 J=1,6
      II=ID(NN,J)
      IF (II) 400,400,350
  350 XL(II)=TL(NN,J)
  400 CONTINUE
  500 CONTINUE
C
      WRITE (9) XL
      IF (KSHF) 600,600,700
  600 KSHF=1
      GO TO 1
  700 RETURN
C
 1001 FORMAT (I5,5X,6F10.0)
 2001 FORMAT (I5,5X,6F12.3)
 2002 FORMAT (23H1NODAL POINT LOADS.....   / 1CH NODE        27X
     .  14HAPPLIED LOADS                   / 10H  NO.        8X 2HRX 10X
     .   2HRY 10X 2HRZ 10X 2HMX 10X 2HMY 10X 2HMZ )
 2003 FORMAT (23H1NODAL POINT MASSES....  // 1CH NODE        27X
     .  19HCONCENTRATED MASSES             / 1CH  NO.        8X 2HMX 10X
     .   2HMY 10X 2HMZ 10X 3HI/X 9X 3HI/Y 9X 3HI/Z )
      END
```

```
*DECK ADDSTF
      SUBROUTINE ADDSTF (B,A,TM,NEQ,MBAND,NUMEL)
C
      DIMENSION B(NEQ),A(NEQ,MBAND),TM(NEQ),STIF(722)
      COMMON/EMTX/ LM(24),ND,NS,S(24,24),P(24,4),XM(24),ST(12,24),
     .             TT(12,4)
      COMMON/JUNK/ STR(4),LMN,II,JJ,N,I,J,JUK(195)
      EQUIVALENCE (STIF,LM)
C
C     FORM GLOBAL EQUILIBRIUM EQUATION IN CORE
C
      L=1
      NWA=NEQ*MBAND
      REWIND 2
      REWIND 4
      REWIND 9
      DO 40 I=1,4
   40 STR(I)=0.
      WRITE (6,2000)
      READ (5,1001) STR
      WRITE (6,2001) L,(STR(I),I=1,4)
C
      DO 100 I=1,NWA
  100 A(I)=0.
C
      READ (9) TM
      READ (9) B
      REWIND 9
      DO 500 N=1,NUMEL
      READ (2) STIF
      DO 400 I=1,ND
      II=LM(I)
      IF (II.LE.0.OR.II.GT.NEQ) GO TO 400
      LMN=1-II
      TM(II)=TM(II)+XM(I)
      DO 240 J=1,4
  240 B(II)=B(II)+P(I,J)*STR(J)
      DO 300 J=1,ND
      JJ=LM(J)
      IF (JJ.LE.0.OR.JJ.GT.NEQ) GO TO 300
      JJ=JJ+LMN
      IF (JJ) 300,300,250
  250 A(II,JJ)=A(II,JJ)+S(I,J)
  300 CONTINUE
  400 CONTINUE
  500 CONTINUE
C
      WRITE (4) (A(I),I=1,NWA)
      WRITE (9) (TM(I),I=1,NEQ)
      RETURN
C
 1001 FORMAT (4F10.0)
 2000 FORMAT (////49H ELEMENT LOAD MULTIPLIER FOR STATIC ANALYSIS.....//
     .  10H STRUCTURE  6X 24H ELEMENT LOAD MULTIPLIER /
     .  10H LOAD CASE 7X 1HA 9X 1HB 9X 1HC 9X 1HD //)
 2001 FORMAT (I6,5X,4F10.3)
      END
```

```
*DECK STATIC
      SUBROUTINE STATIC
      COMMON/EPAR/ NPAR(14),NUMNP,NELTYP,NUMEL,NUMNEL,NEQ,MBAND,MTOT,
     .             N1,N2,N3,N4,N5,N6,N7
      COMMON/EMTX/ QQQQ(2043)
      COMMON/MISC/ NFN,NGM,NT,NOT,JJJ(10)
      COMMON/JUNK/ JUK(205)
      COMMON A(1)
C
C     COMPUTE STATIC RESPONSE--- SOLVE FOR DISPLACEMENT UNKNOWNS
C
      N2=N1+NEQ
      N3=N2+NEQ*MBAND
      N4=N3+NEQ
      IF (N4.GT.MTOT) CALL ERROR (1,N4-MTOT,7HCOSOL    )
      CALL COSOL (A(N1),A(N2),A(N3),NEQ,MBAND)
C
C     OUTPUT DISPLACEMENTS
C
      N3=N2+NUMNP*6
      N4=N3+NUMNP*6
      N5=N4+NUMNP
      IF (N5.GT.MTOT) CALL ERROR (1,N5-MTOT,7HPRINTD      )
      CALL PRINTD (A(N1),A(N2),A(N3),A(N4),NEQ,NUMNP)
C
C     OUTPUT STATIC STRESSES OF EACH ELEMENT
C
      N3=N2+NUMEL
      IF (N3.GT.MTOT) CALL ERROR (1,N3-MTOT,7HSTRESS    )
      CALL STRESS (A(N1),A(N2),NEQ,NUMEL)
C
      RETURN
      END
```

```
*DECK COSCL
      SUBROUTINE COSOL (B,A,NBMAX,NEQ,MBAND)
C
      DIMENSION B(1),A(1),NBMAX(1)
C
C      TRIANGULARIZE BANDED MATRIX BY GAUSSIAN ELEMENATION
C
      IF (NEQ.EQ.1) RETURN
      NWA=NEQ*MBAND
      NE=NEQ-1
      DO 300 N=1,NE
      NBMAX(N)=0
      DO 100 I=N,NWA,NEQ
      IF (A(I).NE.0.) NBMAX(N)=I
  100 CONTINUE
C
      IF (A(N).EQ.0.) GO TO 300
      IL=N+NEQ
      IH=NBMAX(N)
      L=N
      DO 200 I=IL,IH,NEQ
      L=L+1
      IF (A(I).EQ.0.) GO TO 200
      C=A(I)/A(N)
      J=L-I
      DO 150 K=I,IH,NEQ
      IF (A(K).EQ.0.) GO TO 150
      A(K+J)=A(K+J)-C*A(K)
  150 CONTINUE
      A(I)=C
  200 CONTINUE
  300 CONTINUE
C
C     REDUCTION OF LOAD VECTOR
C
      IL=NEQ
      DO 400 N=1,NEQ
      C=B(N)
      IF(A(N).NE.0.) B(N)=B(N)/A(N)
      IF (N.EQ.NEQ) GO TO 450
      IL=IL+1
      IH=NBMAX(N)
      K=N+1
      DO 350 I=IL,IH,NEQ
      IF (A(I).EQ.0.) GO TO 350
      B(K)=B(K)-A(I)*C
  350 K=K+1
  400 CONTINUE
C
C     BACK-SUBSTITUTION
C
  450 IL=NEQ*2
  500 IL=IL-1
      N=N-1
      IF (N.EQ.0) RETURN
      IH=NBMAX(N)
      K=N+1
      DO 600 I=IL,IH,NEQ
      IF (A(I).EQ.0.) GO TO 600
      B(N)=B(N)-A(I)*B(K)
  600 K=K+1
      GO TO 500
      END
```

```
*DECK PRINTD
      SUBROUTINE PRINTD (X,ID,D,IN,NEQ,NUMNP)
C
      DIMENSION X(1),ID(NUMNP,6),D(NUMNP,6),IN(1)
C
C     PRINT NODAL DISPLACEMENTS OF STATIC ANALYSIS
C
      REWIND 8
      READ (8) ID
      NWD=NUMNP*6
      DO 10 I=1,NUMNP
   10 IN(I)=0
      DO 20 I=1,NWD
   20 D(I)=0.
C
      DO 200 I=1,NUMNP
      II=0
      JJ=0
      DO 100 J=1,6
      K=ID(I,J)
      IF (K) 60,50,70
   50 II=II+1
      GO TO 100
   60 JJ=JJ-1
      GO TO 100
   70 D(I,J)=X(K)
  100 CONTINUE
      IF (II.EQ.6) IN(I)= 1
      IF (JJ.LT.0) IN(I)=-1
  200 CONTINUE
      WRITE(6,2003)
      S1=5H
      S2=5HFIXED
      S3=5HSLAVE
      DO 300 I=1,NUMNP
      IF (IN(I)) 230,210,220
  210 S=S1
      GO TO 250
  220 S=S2
      GO TO 250
  230 S=S3
C
  250 WRITE (6,2004) I,S,(D(I,J),J=1,6)
  300 CONTINUE
      RETURN
C
 2003 FORMAT (35H1PRINT OF STATIC DISPLACEMENTS.....///
     .  5X,5H NODE,5X,5HNODE,11X,1HX,11X,1HY,11X,1HZ,10X,2HXX,
     .  10X,2HYY,10X,2HZZ/5X,5H  NO.,5X,5H TYPE //)
 2004 FORMAT (I9,6X,A5,1P6E12.3)
      END
```

```
*DECK STRESS
      SUBROUTINE STRESS (D,IND,NEQ,NUMEL)
C
      DIMENSION D(NEQ),IND(NUMEL)
      COMMON/EMTX/ ND,NS,LM(24),S(24,24),P(24,4),XM(24),SA(12,24),
     .             TT(12,4)
      COMMON/EPAR/ NPAR(14),NUMNP,NELTYP,MUMEL,NUMNEL,MEQ,MBAND,MTOT,
     .             NNN(7)
      COMMON/JUNK/ STR(4),MM,L,K,NTAG,NDYN,SIG(12),JUK(184)
C
C     COMPUTE AND PRINT STATIC STRESS OF EACH ELEMENT
C
      REWIND 1
      READ (8) IND
      L=1
      NTYPE=0
C
      DO 1000 MN=1,NUMEL
      MTYPE= IND(MN)
      IF (MTYPE.LT.0) MTYPE=-MTYPE
      IF (NTYPE.EQ.MTYPE) GO TO 250
      WRITE(6,2000)
      NPAR(1)=0
      NTAG=0
      NTYPE=MTYPE
      MM=1
  250 READ (1) NS,ND,LM,SA,TT
C
C     COMPUTE STRESS FROM DISPLACEMENT AND ADD LOCAL STRESS
C
      DO 300 N=1,NS
      SIG(N)=0.
      DO 280 I=1,4
  280 SIG(N)=SIG(N)+TT(N,I)*STR(I)
      DO 300 J=1,ND
      JJ=LM(J)
      IF (JJ.LE.0.OR.JJ.GT.NEQ) GO TO 300
  290 SIG(N)=SIG(N)+SA(N,J)*D(JJ)
  300 CONTINUE
C
C     PRINT STRESSES FOR EACH ELEMENT
C
      GO TO (301,302,303,304,305) MTYPE
C
  301 IF (NTAG.EQ.0) WRITE(6,2001)
      WRITE(6,3001) MM,L,SIG(1),SIG(2)
      GO TO 500
C
  302 IF (NTAG.EQ.0) WRITE(6,2002)
      WRITE(6,3002) MM,L,(SIG(I),I=1,12)
      GO TO 500
C
  303 IF (NTAG.EQ.0) WRITE(6,2003)
      WRITE(6,3003) MM,L,(SIG(I),I=1,12)
      GO TO 500
C
```

```
  304 IF (NTAG.EQ.0) WRITE(6,2004)
      WRITE(6,3004) MM,L,(SIG(I),I=1,6)
      GO TO 500
C
  305 IF (NTAG.EQ.0) WRITE(6,2005)
      WRITE(6,3005) MM,L,(SIG(I),I=1,12)
C
  500 MM=MM+1
      NTAG=1
      WRITE (8) NS,SIG
 1000 CONTINUE
      RETURN
C
 2000 FORMAT (27H1 STATIC STRESS OUTPUT.....  )
 2001 FORMAT (//26H0 ....TRUSS MEMBER FORCES  //
     .        46H0 MEMBER     LOAD          STRESS           FORCE  )
 2002 FORMAT (/38H0 ....STRAIGHT BEAM FORCES AND MOMENTS//
     . 10H0BEAM LOAD 5X 5HAXIAL  2(7X,5HSHEAR),5X 7HTORSION
     .  2(5X,7HBENDING)/ 10H  NO.  NO.  8X  2HR1  10X  2HR2  10X
     .  2HR3 10X 2HM1 10X 2HM2 10X 2HM3)
 2003 FORMAT (/36H0 ....CURVED BEAM FORCES AND MOMENTS//
     . 10H0BEAM LOAD 5X 5HAXIAL  2(7X,5HSHEAR),5X 7HTORSION
     .  2(5X,7HBENDING)/ 10H  NO.  NO.  8X  2HR1  10X  2HR2  10X
     .  2HR3 10X 2HM1 10X 2HM2 10X 2HM3)
 2004 FORMAT (/40H0 ....BOUNDARY SPRING FORCES AND MOMENTS  //
     .  10H0 BD. LOAD 5X 5HAXIAL 2(7X 5HSHEAR) 5X 7HTORSION
     .  2(5X 7HBENDING) /10H  NO   NO  8X 2HR1 10X 2HR2 10X 2HR3 10X
     .  2HM1 10X 2HM2 10X 2HM3 )
 2005 FORMAT (/40H0 ....EXPANSION JOINT FORCES AND MOMENTS  //
     .  10H0 JT. LOAD,5X,5HAXIAL,2(7X,5HSHEAR),7X,5HAXIAL,5X,7HBENDING,
     .  5X,7H  SHEAR/10H  NO.  NO. ,8X,2HR1,10X,2HR2,10X,2HR3,
     .  10X,2HR4,10X,2HR5,10X,2HR6)
 3001 FORMAT (2I8,F15.5,F15.3)
 3002 FORMAT (I5,I4,1PE11.3,5E12.3/8X,6E12.3/)
 3003 FORMAT (I5,I4,1PE11.3,5E12.3/8X,6E12.3/)
 3004 FORMAT (I5,I4,1PE11.3,5E12.3)
 3005 FORMAT (I5,I4,1PE11.3,5E12.3/8X,6E12.3/)
      END
```

```
*DECK LOADS
      SUBROUTINE LOADS
C
      COMMON/EPAR/ NPAR(14),NUMNP,NELTYP,NUMEL,NUMNEL,NEQ,MBAND,MTOT,
     .             N1,N2,N3,N4,N5,N6,N7
      COMMON/EMTX/ QQQQ(2043)
      COMMON/MISC/ NFN,NGM,NT,NOT,OT,ALFA,BETA,INTG,IGM(3),FGM(3)
      COMMON/JUNK/ JUK(205)
      COMMON/ITSO/ NSDIV,ITTYP,MAXIT,RTOLU,RTOLS,RTOLI,CONN(34)
      COMMON A(1)
C
C     READ AND PRINT LOAD INPUT CONTROLL OATA
C
      READ (5,1000) OT,ALFA,BETA,INTG
      WRITE(6,2000) OT,NT,NOT,NFN
      WRITE(6,2001) INTG,ALFA,BETA
C
C     READ AND PRINT SUBDIVISION CONTROL OATA
C
      READ (5,1100) NSDIV,RTOLS
      WRITE(6,2100) NSDIV,RTOLS
C
C      READ AND PRINT EQUILIBLIUM ITERATION CONTROL DATA
C
      READ (5,1200) MAXIT,ITTYP,RTOLI,RTOLU
      WRITE(6,2200) MAXIT,ITTYP,RTOLI,RTOLU
C
C     INPUT GROUND MOTION
C
      READ (5,1002) IGM,FGM
      WRITE(6,2002) IGM,FGM
      NG=0
      DO 5 I=1,3
      IF (IGM(I).LE.0) GO TO 5
      IF (FGM(I).EQ.0.) FGM(I)=1.0
      IF (IGM(I).LE.NG) GO TO 5
      NG=NG+1
      IF (NG.LE.NFN) GO TO 5
      WRITE(6,3000) I
      STOP
    5 CONTINUE
      DO 10 I=1,3
      IF (IGM(I).LE.NFN) GO TO 10
      WRITE(6,3000) I
      STOP
   10 CONTINUE
C
C     SETUP NODAL DYNAMIC LOAD COEFFICIENT MATRIX
C
      N1=1
      N2=N1+NEQ*NFN
      N3=N2+NUMNP*6
      N4=N3+NEQ
      N5=N4+NEQ
      CALL LOADR (A(N1),A(N2),A(N3),A(N4),NEQ,NFN,NUMNP)
C
```

```
C      INPUT HISTRIES OF LCAD FUNCTIONS
C
       N3=N2+NT*NFN
       MAX=IMTCT-N3)/2
       IF IMAX.GE.NT) GO TO 20
       N4=2*INT-MAX)
       CALL ERROR I1,N4,7HINTHIS  )
   20  N4=N3+MAX
       CALL INTHIS IAIN2),A(N3),AIN4),NFN,NT,OT,MAX)
C
C      FCRM CYNAMIC NOLAL LOAC VECTOR
C
       N4=N3+NEQ
       CALL LOADV IAIN1),AIN2),AIN3),NEQ,NFN,NT)
C
       RETURN
 1000 FORMAT I3F10.0,I5)
 1002 FCRMAT I3I5,3F10.0)
 1100 FORMAT II5,F10.0)
 1200 FORMAT I2I5,2F10.0)
 2000 FCRMAT I37H1DYNAMIC LCAC INPUT CONTROL CATA..... ///
    .   32H   TIMC INCREMENT CT  ISEC)      =  F8.3//
    .   32H   TOTAL NUMBER OF TIME STEPS    =  I5  //
    .   32H   CUTPUT INTERVAL               =  I5  //
    .   32H   NUMBER OF TIME FUNCTIONS      =  I5  //                  )
 2001 FCRMAT I////48H STEP-BY-STEP CYNAMIC ANALYSIS CONTRCL UATA.....///
    .   32H   INTEGRATION INCICATOR         =  I5  //
    .   32H   CAMPING FACTCR  ALPHA         =  1PE12.3//
    .   32H   UAMPING FACTCR  BETA          =  1PE12.3    )
 2002 FCRMAT (30H1GROUNC MCTICN INPUT KEY......  ///
    .   30X, 9HCIRECTION/24X,1HX,7X,1HY,7X,1HZ   //
    .   20H   FUNCTION NUMBER... ,I5,2I8 //
    .   20H   SCALE FACTCR.......3F8.3)
 2100 FCRMAT(49H1SUBDIVISICN CF TIME INCREMENT CCNTROL CATA ..... ///
    .   43H   NUMBER OF SUBCIVISICN                  = I5//
    .   43H   RELATIVE TCLERANCE CF SUBDIVISION       = F15.7 )
 2200 FCRMAT(41H1EQUILIBRIUM ITERATICN CCNTRCL CATA ..... ///
    .   43H   MAXIMUM NUMBER OF ITERATION             = I5//
    .   43H   TYPE OF ITERATION                       = I5//
    .   43H   RELATIVE TCLERANCE TO USE ITERATICN     = E15.7//
    .   43H   RELATIVE TCLERANCE FCR CCNVERGENCE      = E15.7 )
 3000 FCRMAT (65H1ERRCR.....INPUT DATA FCR GRCUNC MCTION  FUNCTICN NUMBE
    .R INCCRRECT/11X,20HEXECUTICN TERMINATED  )
C
       END
```



```
*DECK LOADR
       SUBRCUTINE LOADR IR,IC,MASS,XM,NEQ,NFN,NUMNP)
C
       CIMENSION RINEQ,1),ICINUMNP,6),MASSI1),XMINEQ)
       CCMMCN/MISC/ MMMI8),IGMI3),FGMI3)
       CCMMCN/JUNK/ I,J,K,L,N,II,P,JUKI198)
C
       REWIND  8
       REWIND  9
       REWIND 10
       READ (8) IC
       READ (9) XM
       DO 10 I=1,NEQ
       MASSII)=0
       DO 10 J=1,NFN
   10  R(I,J)=0.
       DO 15 I=1,3
       IF (IGMII).GT.0) GO TO 16
   15  CONTINUE
       GO TC 110
C
   16  L=1
       DO 50 N=1,NUMNP
       DO 40 I=1,6
       II=IC(N,I)
       IF (II.LE.0) GO TO 40
       IF (I .GT.3) GO TO 30
       MASS(L)=I
   30  L=L+1
   40  CONTINUE
   50  CCNTINUE
       DC 100 J=1,3
       IF (IGMIJ).LE.0) GO TC 100
       K=IGM(J)
       DO 80 I=1,NEQ
       L=MASS(I)
       IF (L.EQ.J) R(I,K)=-FCM(J)*XM(I)
   80  CCNTINUE
  100  CCNTINUE
       DO 105 I=1,2
       IF (IGM(I).EQ.0) GC TC 105
       K=I+1
       DC 104 J=K,3
       IF (IGM(J).EQ.0) GO TC 104
       IF(IGM(J).EQ.IGM(I)) IGMIJ)=0
  104  CONTINUE
  105  CONTINUE
C
  110  WRITE (10) (MASS(I),I=1,NEQ)
       L=0
  120  READ (5,1000) N,J,K,P
       IF (N.EQ.0) GO TU 200
       IF (L.GT.C) GO TO 150
       WRITE (6,2000)
       L=1
  150  WRITE (6,2001) N,J,K,P
```

24

```
      DO 160 I=1,3
      IF (K.NE.IGM(I)) GO TO 160
      WRITE (6,3000)
      STOP
  160 CONTINUE
      I=ID(N,J)
      IF (I.LE.0.OR.I.GT.NEQ) GO TO 120
      R(I,K)=P
      GO TO 120
  200 RETURN
C
 1000 FORMAT (3I5,F10.0)
 2000 FORMAT (30H1NODAL DYNAMIC LOAD INPUT...../// 
     . 5X,53H NODE      DISPLACEMENT     TIME HISTORY    FUNCTION      /
     . 5X,53HNUMBER       COMPONENT          NUMBER         SCALAR     //)
 2001 FORMAT (I9,I12,I16,F16.3)
 3000 FORMAT (84H1***ERROR***DYNAMIC LOAD INPUT TIME HISTORY DUPLICATES
     .A GROUND MOTION TIME HISTORY    /  12X,21HEXECUTION TERMINATED    I
      END
```

12

25.

```
*DECK INTHIS
      SUBROUTINE INTHIS (Z,T,F,NFN,NT,DT,MAX)
C
      DIMENSION Z(NT,1),T(1),F(1)
      COMMON/JUNK/ TITLE(12),I,J,K,L,DOF,DOT,IH,NOT,NN,SFTR,ZCOR,TINC,
     .                    TIME,SLOPE,JUK(179)
C
      NN=NT*NFN
      DO 5 I=1,NT
      DO 5 J=1,NFN
    5 Z(I,J)=0.
      DO 400 J=1,NFN
      READ (5,1000) TITLE,NDT,SFTR,TINC,ZCOR
      IF (NDT.LE.0) GO TO 400
      IF (SFTR.EQ.0.) SFTR=1.
      WRITE(6,2000) J,TITLE,NDT,SFTR,TINC,ZCOR
      IF (NOT.LE.MAX) GO TO 10
      WRITE (6,3000) J,NDT,MAX
      STOP
   10 IF (TINC) 100,100,20
   20 READ (5,1001) (F(I),I=1,NOT)
      IF (ZCOR.EQ.0.) GO TO 23
      DO 22 I=1,NOT
   22 F(I)=F(I)-ZCOR
   23 CONTINUE
      IF (SFTR.EQ.1.) GO TO 30
      DO 25 I=1,NOT
   25 F(I)=F(I)*SFTR
   30 IF (TINC-DT) 60,40,60
   40 NN=NDT
      IF (NN.GT.NT) NN=NT
      DO 50 I=1,NN
   50 Z(I,J)=F(I)
   60 K=0
      DO 70 I=1,NOT,8
      K=K+1
      IH=I+7
      IF (IH.GT.NDT) IH=NDT
   70 WRITE (6,2005) K,(F(L),L=I,IH)
      IF (TINC.EQ.DT) GO TO 400
      TIME=0.
      DO 80 I=1,NDT
      TIME=TIME+TINC
   80 T(I)=TIME
      GO TO 200
  100 READ (5,1002) (T(I),F(I),I=1,NDT)
      IF (ZCOR.EQ.0.) GO TO 110
      DO 105 I=1,NDT
  105 F(I)=F(I)-ZCOR
  110 CONTINUE
      IF (SFTR.EQ.1) GO TO 150
      DO 120 I=1,NOT
  120 F(I)=F(I)*SFTR
  150 WRITE (6,2001)
      WRITE (6,2002) (T(I),F(I),I=1,NDT)
C
```

```
200 K=1
    L=1
    TIME=T(1)
210 L=L+1
    IF (NDT-L) 300,220,220
220 DDT=T(L)-T(L-1)
    DDF=F(L)-F(L-1)
    IF (DDT) 225,210,230
225 WRITE (6,2003) T(L),F(L)
    GO TO 210
230 SLOPE=DDF/DDT
235 IF (T(L)-TIME) 210,240,240
240 Z(K,J)=F(L-1)+(TIME-T(L-1))*SLOPE
    TIME=TIME+DT
    K=K+1
    IF (NT-K) 300,235,235
300 WRITE (6,2004) NT,DT
310 K=0
    DO 350 I=1,NT,8
    K=K+1
    IH=I+7
    IF (IH.GT.NT) IH=NT
350 WRITE (6,2005) K,(Z(L,J),L=I,IH)
400 CONTINUE
    DO 450 I=1,NT
450 WRITE (10) (Z(I,J),J=1,NFN)
    RETURN
C
1000 FORMAT (12A6/I5,3F10.0)
1001 FORMAT (10F8.5)
1002 FORMAT (12F6.0,8X)
2000 FORMAT (17H1TIME HISTORY NO. ,I3,5H.....,12A6 ///
    . 5X,30H NUMBER OF DATA POINT          = ,I5  //
    . 5X,30H SCALING FACTOR                = ,F10.4//
    . 5X,30H TIME INCREMENT OF DATA (SEC)= ,F10.6//
    . 5X,30H ZERO CORRECTION               = ,F10.4//)
2001 FORMAT (/5X,5(20H    TIME      INPUT       )//)
2002 FORMAT (5X,5(F8.3,F10.6,2X))
2003 FORMAT (5X,20HOBAD DATA POINT       ,F8.3,F10.6)
2004 FORMAT (53H1GENERATED TIME HISTORY FOR RESPONSE CALCULATION.....//
   ./5X,30H NUMBER OF DATA GENERATED     =,I5   //
    . 5X,30H TIME INCREMENT OF DATA (SEC)=,F10.4//)
2005 FORMAT (I8,2X,8F13.3)
3000 FORMAT (38H1****ERROR.....INPUT TIME HISTORY NO. ,I3,5H  HAS,I6,
    .  13H  DATA POINTS  /15X,30HWHICH IS GREATER THAN THE MAX.  ,I6,
    .  24H  ALLOWED IN THIS PROGRAM  /15X,20HEXECUTION TERMINATED  )
    END
```

```
*DECK LOADV
      SUBROUTINE LOADV (R,Z,P,NEQ,NFN,NT)
C
      DIMENSION R(NEQ,1),Z(NT,1),P(1)
C
C     FORM DYNAMIC LOAD VECTOR AT EACH TIME STEP
C
      REWIND 12
      DO 200 N=1,NT
      DO 150 I=1,NEQ
      XX=0.
      DO 100 J=1,NFN
  100 XX=XX+R(I,J)*Z(N,J)
  150 P(I)=XX
      WRITE (12) (P(I),I=1,NEQ)
  200 CONTINUE
      RETURN
      END
```

```
*DECK INTGR
      SUBROUTINE INTGR
C
      COMMON/EPAR/ CONT(14),NUMNP,NELTYP,NUMEL,NUMNEL,NEQ,MBAND,MTOT,
     .             N1,N2,N3,N4,N5,N6,N7
      COMMON/EMTX/ QQQQ(2043)
      COMMON/MISC/ NFN,NGM,NT,NDT,JJJ(10)
      COMMON/ITSC/ MMM(40)
      COMMON/JUNK/ JUK(205)
      COMMON A(1)
C
C     STEP-BY-STEP INTEGRATION IN CORE
C
C     (FIT,REF),(NBMAX,PN),(CX,XG)----ON SAME CORE LOCATION
C
      NWA=NEQ*MBAND
      N1=1
      N2=N1+NWA
      N3=N2+NWA
      N4=N3+NEQ
      N5=N4+NEQ
      N6=N5+NEQ
      N7=N6+NEQ
      N8=N7+NEQ
      N9=N8+NEQ
      N10=N9+NEQ
      N11=N10+NEQ
      N12=N11+NEQ
      N13=N12+NEQ
      N14=N13+NEQ
```

```
      N15=N14+NEQ
      N16=N15+NEQ
      N17=N16+NEQ
      N18=N17+NUMNEL*12
      N19=N18+NUMNEL*12
      N20=N19+NUMNEL*12
      N21=N20+NUMNEL*12
      N22=N21+NUMNEL
      N23=N22+NUMNEL
      N24=N23+NFN
      N25=N24+NUMEL
      WRITE(6,9000) N25
 9000 FORMAT(1H ,5HN25 =,I10)
      IF  (N25.GT.MTOT) CALL ERROR (1,N25-MTOT,7HSTEPC    )
C
C     INITIALIZATION
C
      CALL START (A(N1),A(N2),A(N3),A(N4),A(N5),A(N7),A(N8),A(N10),
     .            A(N11),A(N14),A(N9),A(N15),A(N17),A(N19),A(N21),
     .            A(N22),A(N24),NEQ,MBAND,NUMEL,NUMNEL)
C
C     STEP BY STEP INTEGRATION
C
      CALL SBSITG (A(N1),A(N2),A(N3),A(N4),A(N5),A(N6),A(N6),A(N7),A(N8)
     .,           A(N9),A(N10),A(N11),A(N12),A(N13),A(N14),A(N9),A(N16),
     .            A(N13),A(N15),A(N17),A(N18),A(N19),A(N20),A(N21),
     .            A(N22),A(N23),NEQ,MBAND,NWA,NUMNEL,NFN)
C
      RETURN
C
      END

*DECK START
      SUBROUTINE START (A,B,X,X1,X2,MASS,XM,MBMAX,MHMAX,PL,PN,PP,STR,
     .                  UPL,NINC,NSS,INC,NEQ,MBAND,NUMEL,NUMNEL)
C
      DIMENSION A(NEQ,MBAND),B(NEQ,MBAND),X(NEQ),X1(NEQ),X2(NEQ),
     .          MASS(NEQ),XM(NEQ),MBMAX(NEQ),MHMAX(NEQ),PL(NEQ),PN(NEQ),
     .          PP(NEQ),STR(NUMNEL,12),UPL(NUMNEL,12),NINC(NUMNEL),
     .          NSS(NUMNEL),INO(NUMEL)
      COMMON/EPAR/ CCNT(14),NUMNP,NELTYP,MUMEL,MUMNEL,MEQ,NBAND,MTOT,
     .             NNN(7)
      COMMON/MISC/ MMM(4),DT,ALFA,BETA,INTG,IGM(3),FGM(3)
      COMMON/ITSC/ NSCIV,ITTYP,MAXIT,RTCLU,RTCLS,RTOL1,CONS(14),CCNI(14)
     .,            CCNB(6)
      COMMON/JUNK/ I,J,K,N,DELTA,ASCIV,NEQM,NEQ1,NS,SIG(12),NB,JUK(183)
      COMMON/COLB/ USP(10,2),USPF(10,2),KF(6),UPSLIP(2)

C
      REWIND 4
      REWIND 9
      REWIND 10
C
C     GENERATE COMPUTATIONAL CONSTANTS
C
      IF (NSDIV.EQ.0) GO TO 10
      ASCIV=FLOAT(NSCIV)
      DT=DT/ASDIV
   10 DELTA=0.5
      IF(INTG) 150,150,160
  150 SIGMA=0.25
      GO TO 200
  160 SIGMA=1./6.
C
  200 DO 255 N=1,2
      IF (N.EQ.2.AND.NSCIV.NE.0) CT=CT*ASDIV
      CCNT( 1)=1.0/(SIGMA*DT*DT)
      CCNT( 2)=1.0/(SIGMA*DT)
      CCNT( 3)=0.5/SIGMA
      CCNT( 4)=DELTA/(SIGMA*DT)
      CCNT( 5)=DELTA/SIGMA
      CONT( 6)=(0.5*DELTA/SIGMA-1.0)*CT
C
C     GENERALIZED CONSTANTS
C
      CONT( 7)=CCNT( 1)+ALFA*CONT( 4)
      CCNT( 8)=BETA*CCNT( 4)
      CCNT( 9)=CCNT( 2)+ALFA*CONT( 5)-ALFA
      CCNT(10)=CCNT( 3)+ALFA*CONT( 6)-1.0
      CCNT(11)=BETA*(CONT( 5)-1.0)
      CCNT(12)=BETA*CCNT( 6)
      IF(N.EQ.2) GO TO 255
      DO 250 I=1,12
  250 CCNS(I)=CCNT(I)
  255 CONTINUE
      DO 260 I=1,12
  260 CCNI(I)=CCNT(I)
      XX=1.0/(DELTA-SIGMA-0.5)
      CCNB( 1)=XX/DT**2
      CONB( 2)=XX/DT
      CCNB( 3)=XX*(SIGMA-DELTA)
      CCNB( 4)=XX*(DELTA-1.0)/DT
      CCNB( 5)=XX*(SIGMA-0.5)
      CCNB( 6)=XX*(0.5*DELTA-SIGMA)*CT
C
C     SET UP STIFFNESS AND MASS MATRIX
C
      READ  (4)  ((B(I,J),I=1,NEQ),J=1,MBAND)
      READ  (9)  (XM(I),I=1,NEQ)
      READ (10)  (MASS(I),I=1,NEQ)
      DO 500 I=1,NEQ
      DO 500 J=1,MBAND
  500 A(I,J)= B(I,J)
C
```

```
C     INITIALIZATION
C
      DO 540 I=1,NEQ
      X(I)=0.
      X1(I)=0.
      X2(I)=0.
      PU(I)=0.
      PN(I)=0.
  540 PP(I)=0.
      DO 550 I=1,20
  550 USP(I)=0.
C
C     INITIALIZE NONLINEAR ELEMENT STRESSES TO BE STATIC STRESSES
C
      READ (8) IND
      K=0
      DO 600 N=1,NUMEL
      READ (8) NS,SIG
      IF (IND(N).LE.0) GO TO 600
      K=K+1
      NINC(K)=0
      NSS(K)=NS
      DO 580 I=1,12
      STR(K,I)=SIG(I)
  580 UPL(K,I)=0.
  600 CONTINUE
C
C     FIND HEIGHT AND WIDTH OF LINEAR TOTAL STIFNESS MATRIX A
C
      NEQ1=NEQ-1
      NEQM=NEQ*MBAND
      DO 720 N=1,NEQ
      MBMAX(N)=0
      MHMAX(N)=0
      DO 700 I=N,NEQM,NEQ
      IF(A(I).NE.0.0) MBMAX(N)=I
  700 CONTINUE
      DO 710 I=1,MBAND
      IF(I.GT.N) GO TO 710
      J=NEQ1*(I-1)+N
      IF(A(J).NE.0.0) MHMAX(N)=J
  710 CONTINUE
  720 CONTINUE
C
      RETURN
      END
```

```
*DECK SBSITG
      SUBROUTINE SBSITG (A,B,X,X1,X2,DX,XG,MASS,XM,NBMAX,MBMAX,MHMAX,
     .                   PEXT,FIT,PU,PN,PM,REF,PP,STR,STRF,UPL,UPLF,NIND
     ..                  NSS,PR,NEQ,MBAND,NWA,NLMNEL,NFN)
C
      DIMENSION A(NWA),B(NWA),X(NEQ),X1(NEQ),X2(NEQ),DX(NEQ),MASS(NEQ),
     .          XM(NEQ),XC(NEQ),NBMAX(NEQ),MBMAX(NEQ),MHMAX(NEQ),
     .          PEXT(NEQ),FIT(NEQ),PL(NEQ),PN(NEQ),REF(NEQ),PP(NEQ),
     .          STR(NUMNEL,12),STRF(NUMNEL,12),UPL(NUMNEL,12),
     .          UPLF(NUMNEL,12),NINC(NUMNEL),NSS(NUMNEL),PR(NFN),PM(NEQ)
      COMMON/EPAR/ CONT(14),NNNN(14)
      COMMON/EMTX/ CCCC(2043)
      COMMON/MISC/ MFN,NGM,NT,NCT,DT,ALFA,BETA,INTG,IGM(3),FGM(3)
      COMMON/ITSC/ NSCIV,ITTYP,MAXIT,RTCLU,RTCLS,RTOLI,CCNS(14),CCNI(14)
     ..            CCNB(6)
      COMMON/JUNK/ I,J,K,MB,MH,N1,N2,XX1,XX2,XX,DD,JJ,JUK(193)
      COMMON/COLB/ USP(10,2),USPF(10,2),KF(6),LPSLIP(2)
C
C     STEP-BY-STEP INTEGRATION OF EQUATION OF MOTION
C
      REWIND  9
      REWIND 12
      ICCR=0
      NOT=1
      NCUT=NOT
      NEQ1=NCQ-1
      ASCIV=FLOAT(NSOIV)
      MSCIV=0
      NITRN=0
      MITRN=0
C
C     READ EXTERNAL FORCE
C
  100 READ(12) (PEXT(I),I=1,NEQ)
      WRITE(6,2000) NOT
      ISCIV=0
C
  110 IF (NSCIV.EQ.0.OR.ISCIV.EQ.0) GO TO 150
      WRITE(6,2100) ISOIV
      DO 120 I=1,NEQ
  120 PEXT(I)=PEXT(I)+PP(I)
  150 CONTINUE
C
C     FORM EFFECTIVE DYNAMIC STIFFNESS MATRIX AND LOAD VECTOR
C
      DO 190 I=1,NEQ
  190 PM(I)=CONT(11)*X1(I)+CONT(12)*X2(I)-X(I)
      DO 215 I=1,NEQ
      A(I)=A(I)+CONT(7)*XM(I)+CONT(8)*B(I)
      MB=MBMAX(I)
      MH=MHMAX(I)
      N1=I+NEQ
      IF (MB.LT.N1) GO TO 200
      DO 195 J=N1,MB,NEQ
      IF (B(J).EQ.0.) GO TO 195
      A(J)=A(J)+CONT(8)*B(J)
```

```
  195 CONTINUE
  200 XX=PEXT(I)-PU(I)-PN(I)+XM(I)*(CONT(9)*X1(I)+CONT(10)*X2(I))
      K=I
      IF (MB.LT.I) GO TO 210
      DO 205 J=I,MB,NEQ
      IF (B(J).EQ.0.) GO TO 205
      XX=XX+B(J)*PM(K)
  205 K=K+1
  210 IF (I.EQ.1) GO TO 215
      N2=N1-1
      IF (MH.LT.N2) GO TO 215
      K=I-1
      DO 212 J=N2,MH,NEQ1
      IF (B(J).EQ.0.) GO TO 212
      XX=XX+B(J)*PM(K)
  212 K=K-1
  215 FIT(I)=XX
C
C     SOLVE FOR DYNAMIC INCREMENT
C
      CALL TRIA (A,NBMAX,NEQ,MBAND)
      CALL BACK (A,NBMAX,FIT,NEQ)
C
C     COMPUTE NEW DISPLACEMENT, VELOCITY AND ACCELERATION
C
      DO 218 I=1,NEQ
      DD=FIT(I)
      XX1=X1(I)
      XX2=X2(I)
      X2(I)=X2(I)+CONT(1)*DD-CONT(2)*XX1-CONT(3)*XX2
      X1(I)=X1(I)+CONT(4)*DD-CONT(5)*XX1-CONT(6)*XX2
      X(I)=X(I)+DD
  218 DX(I)=DD
C
C     FORM NONLINEAR ELEMENT FORCE AND STIFFNESS MATRIX
C
      CALL NELSTF (A,B,X,X1,X2,DX,XM,MBMAX,MHMAX,PEXT,FIT,PU,PN,PM,REF,
     .             STR,STRF,UPL,LPLF,NINC,NSS,NEQ,MBAND,NUMNEL,1,ISDIV,
     .             ICOR,RTOL)
      WRITE(6,2200) RTOL
C
C     CHECK CORRECTNESS OF SOLUTION
C
      IF (NSDIV.EQ.0) GO TO 220
      IF (RTOL.GT.RTOLS) GO TO 230
  220 IF (MAXIT.EQ.0) GO TO 500
      IF (RTOL.GT.RTOLI) GO TO 400
      GO TO 500
C
C     INITIALIZATION FOR SUBDIVISION OF TIME STEP
C
  230 IF (ISDIV) 290,250,290
  250 ISDIV=1
      MSDIV=MSDIV+1
      ICOR=1
      DO 260 I=1,NEQ
```



```
      DD=DX(I)
      XX1=X1(I)
      XX2=X2(I)
      X2(I)=CCNB(1)*DD-CCNB(2)*XX1-CCNB(3)*XX2
      X1(I)=CCNB(4)*DD-CCNB(5)*XX1-CCNB(6)*XX2
      X(I)=X(I)-DD
  260 DX(I)=0.
      DO 270 I=1,12
  270 CONT(I)=CONS(I)
      DO 275 I=1,NUMNEL
      DO 275 J=1,12
      STR(I,J)=STRF(I,J)
  275 UPL(I,J)=UPLF(I,J)
      DO 276 I=1,20
  276 USP(I)=USPF(I)
      DO 280 I=1,NEQ
      XX=PP(I)
      PP(I)=(PEXT(I)-XX)/ASDIV
  280 PEXT(I)=XX
C
      CALL NELSTF (A,B,X,X1,X2,DX,XM,MBMAX,MHMAX,PEXT,FIT,PU,PN,PM,REF,
     .             STR,STRF,UPL,UPLF,NINC,NSS,NEQ,MBAND,NUMNEL,2,ISDIV,
     .             ICOR,RTOL)
      GO TO 110
  290 CONTINUE
C
C     EQUILIBRIUM ITERATION
C
      IF (MAXIT.EQ.0.OR.RTOL.LE.RTOLI) GO TO 500
  400 ICOR=1
      MITRN=MITRN+1
      CALL ITERN (A,B,XM,X,X1,X2,DX,FIT,REF,PL,PN,PM,PEXT,NBMAX,MBMAX,
     .            MHMAX,NINC,NSS,STR,STRF,UPL,LPLF,NEQ,MBAND,NUMNEL,
     .            ISDIV,ICOR,NOT,NITRN)
C
C     CHECK FOR LAST SUBDIVISION
C
  500 IF (NSDIV.EQ.0.OR.ISDIV.EQ.0) GO TO 600
      IF (ISDIV.EQ.NSDIV) GO TO 510
      ISDIV=ISDIV+1
      GO TO 110
  510 DO 520 I=1,12
  520 CONT(I)=CONI(I)
C
C     COMPUTE GROUND ACCELERATION
C
  600 READ(10) (PR(I),I=1,NFN)
      DO 610 I=1,NEQ
      XG(I)=0.
      J=MASS(I)
      IF (J.LE.0) GO TO 610
      JJ=IGM(J)
      IF (JJ.LE.0) GO TO 610
      XG(I)=FGM(J)*PR(JJ)
  610 CONTINUE
C
```

```
C     STORE DISPLACEMENT AND ABSOLUTE ACCELERATION ON TAPE 8
C
      DO 650 I=1,NEQ
  650 XG(I)=XG(I)+X2(I)
      IF (NDT.EQ.NOUT) WRITE(8) (X(I),I=1,NEQ),(XG(I),I=1,NEQ)
C
C     STORE NONLINEAR STRESS AND DEFORMATION ON TAPE 9
C
      IF (NDT.EQ.NOUT) WRITE(9) NSS,STR,UPL
C
C     STORE FORMER EXTERNAL FORCE
C
      IF (NSDIV) 705,715,705
  705 DO 710 I=1,NEQ
  710 PP(I)=PEXT(I)
  715 CONTINUE
C
C     CHECK FOR LAST TIME STEP
C
      IF (NDT.EQ.NOUT) NOUT=NOUT+NOT
      NDT=NDT+1
      IF (NDT-NT) 100,100,800
C
  800 IF (NSDIV.NE.0) WRITE(6,2300) MSDIV
      IF (MAXIT.NE.0) WRITE(6,2400) MITRN,NITRN
C
      RETURN
C
 2000 FORMAT(1H ,5HNDT =,I5)
 2100 FORMAT(1H ,10X,7HISDIV =,I5)
 2200 FORMAT(1H ,25X,38HRELATIVE NORM OF UNBALANCED FORCE..... ,F15.7)
 2300 FORMAT(1H1,53HNUMBER OF TIME STEP FOR WHICH SUBDIVISION WAS USED..
     .. ,I5//)
 2400 FORMAT(1H1,53HNUMBER OF TIME STEP FOR WHICH ITERATION WAS USED....
     .. ,I5/1H , 53HTOTAL NUMBER OF ITERATION...........................
     .. ,I5)
C
      END
```

```
*DECK TRIA
      SUBROUTINE TRIA (A,NBMAX,NEQ,MBAND)
C
      DIMENSION A(1),NBMAX(1)
C
C     TRIANGULARIZE BANDED MATRIX BY GAUSS ELIMINATION
C
      IF (NEQ.EQ.1) RETURN
      MM=NEQ*MBAND
      NE=NEQ-1
      DO 300 N=1,NE
C
C     DETERMINE VARIABLE BAND WIDTH
C
      NBMAX(N)=0
      DO 100 I=N,MM,NEQ
      IF (A(I).NE.0.0) NBMAX(N)=I
  100 CONTINUE
C
C     REDUCTION OF EQUATIONS WITHIN BAND
C
      IF (A(N).EQ.0.0) GO TO 300
      IL=N+NEQ
      IH=NBMAX(N)
      L=N
      DO 200 I=IL,IH,NEQ
      L=L+1
      IF (A(I).EQ.0.0) GO TO 200
      C=A(I)/A(N)
      J=L-I
      DO 150 K=I,IH,NEQ
      IF (A(K).EQ.0.) GO TO 150
      A(K+J)=A(K+J)-C*A(K)
  150 CONTINUE
      A(I)=C
  200 CONTINUE
  300 CONTINUE
      RETURN
      END
```

20.

```
*DECK BACK
      SUBROUTINE BACK (A,NBMAX,B,NEQ)
C
      DIMENSION A(1),NBMAX(1),B(1)
C
C     REDUCTION OF LOAD VECTOR AND BACKSUBSTITUTION
C
      IL=NEQ
      DO 400 N=1,NEQ
      C=B(N)
      IF (A(N).NE.0.0) B(N)=B(N)/A(N)
      IF (N.EQ.NEQ) GO TO 450
      IL=IL+1
      IH=NBMAX(N)
      K=N
      DO 350 I=IL,IH,NEQ
      K=K+1
      IF (A(I).EQ.0.) GO TO 350
      B(K)=B(K)-A(I)*C
  350 CONTINUE
  400 CONTINUE
C
  450 IL=2*NEQ
  500 IL=IL-1
      N=N-1
      IF (N.EQ.0) RETURN
      IH=NBMAX(N)
      K=N
      DO 600 I=IL,IH,NEQ
      K=K+1
      IF (A(I).EQ.0.) GO TO 600
      B(N)=B(N)-A(I)*B(K)
  600 CONTINUE
      GO TO 500
      END
```

39.

```
*DECK NELSTF
      SUBROUTINE NELSTF (A,B,X,X1,X2,OX,XM,MBMAX,MHMAX,PEXT,FIT,PU,PN,PM
     .,                  REF,STR,STRF,UPL,UPLF,NINO,NSS,NEQ,MBANC,NUMNEL
     .,                  ICONO,ISOIV,ICOR,RTOL)
C
      DIMENSION A(NEQ,MBANC),B(NEQ,MBANO),X(1),X1(1),X2(1),OX(1),XM(1),
     .          MBMAX(1),MHMAX(1),PEXT(1),FIT(1),PU(1),PN(1),PM(1),
     .          REF(1),STR(NUMNEL,12),STRF(NUMNEL,12),UPL(NUMNEL,12),
     .          UPLF(NUMNEL,12),NINC(1),NSS(1),STIF(1131)
      COMMON/EMTX/ MTYPE,LM(24),ND,NS,ASA(24,24),SA(12,24),S(12,12),
     .             ENPAR(24),TTT(72),ASSA(24,24),SSA(12,24),OF(24),
     .             F(12),UP(12)
      COMMON/NEM / EX(24),EX1(24),OEX(24),OFF(12),OP(12),FF(12),P(12),
     .             SS(12,12),U(12),EFI(12)
      COMMON/ITSC/ NSCIV,ITTYP,MAXIT,RTOLU,RTOLS,RTOL1,CONN(34)
      COMMON/MISC/ MPP(4),OT,ALFA,BETA,INTG,LLLI6)
      COMMON/JUNK/ I,II,J,JJ,LMN,JUK(200)
      COMMON/COLB/ USP(10,2),USPF(10,2),KF(6),LPSLIP(2)
      EQUIVALENCE  (STIF,MTYPE)
C
C     INITIALIZATION
C
      REWIND 3
      DO 10 I=1,NEQ
      PU(I)=0.
   10 PN(I)=0.
      IF (ICONO.EQ.2) GO TO 13
      DO 12 I=1,20
   12 USPF(I)=USP(I)
   13 CONTINUE
C
      IF (ITTYP.EQ.0.AND.ICONC.EQ.3.AND.ICOR.NE.0) GO TO 20
      DO 15 I=1,NEQ
      DO 15 J=1,MBANO
   15 A(I,J)=B(I,J)
   20 CONTINUE
      IF (NUMNEL.EQ.0) RETURN
C
C     COMPUTE NONLINEAR ELEMENT STIFFNESS MATRIX AND FORCE
C
      M=0
      DO 700 N=1,NUMNEL
C
      DO 50 I=1,24
      EX(I)=0.
      EX1(I)=0.
   50 OEX(I)=0.
C
      READ(3) STIF
C
      DO 100 I=1,ND
      II=LM(I)
      IF (II.LE.0.OR.II.GT.NEQ) GO TO 100
      EX(I)=X(II)
      EX1(I)=X1(II)
      OEX(I)=OX(II)
```

```
  100 CONTINUE
C
      DO 200 I=1,12
      F(I)=STR(N,I)
  200 UP(I)=UPL(N,I)
      IF (NSCIV.EQ.0.OR.ICONC.NE.1.OR.ISOIV.NE.0) GO TO 220
      DO 210 I=1,12
      STRF(N,I)=F(I)
  210 UPLF(N,I)=UP(I)
  220 CONTINUE
C
      INC=NINC(N)
      GO TO (310,320,330,340,350) MTYPE
C
C     NONLINEAR TRUSS ELEMENT.....SKIP
C
  310 GO TO 400
C
C     ELASTO-PLASTIC BEAM ELEMENT.....SKIP
C
  320 GO TO 400
C
C     NONLINEAR CURVED BEAM ELEMENT.....SKIP
C
  330 GO TO 400
C
C     BILINEAR BOUNDARY ELEMENT.....SKIP
C
  340 GO TO 400
C
C     NONLINEAR EXPANSION JOINT ELEMENT
C
  350 M=M+1
      CALL NEXPJT (M,INO)
C
  400 NINO(N)=INO
C
C     COMPUTE NONLINEAR RESTORING FORCE
C
      IF (INO) 410,440,410
  410 DO 435 I=1,NO
      II=LM(I)
      IF (II.LE.0.OR.II.GT.NEQ) GO TO 435
      PN(II)=PN(II)+EFI(I)
  435 CONTINUE
  440 CONTINUE
C
C     COMPUTE COULOMB FRICTIONAL FORCE
C
      IF (MTYPE.NE.5) GO TO 525
      DO 520 I=1,NO
      II=LM(I)
      IF (II.LE.0.OR.II.GT.NEQ) GO TO 520
      PU(II)=PU(II)+OF(I)
  520 CONTINUE
  525 CONTINUE
```



```
C
C     ASSEMBLE NEW TOTAL STIFFNESS MATRIX
C
      IF (ITTYP.EQ.0.AND.ICONC.EQ.3.AND.ICOR.NE.0) GO TO 555
      IF (INO.EQ.0.AND.MTYPE.NE.5) GO TO 555
      DO 550 I=1,NO
      II=LM(I)
      IF (II.LE.0.OR.II.GT.NEQ) GO TO 550
      LMN=1-II
      DO 540 J=1,NO
      JJ=LM(J)
      IF (JJ.LE.0.OR.JJ.GT.NEQ) GO TO 540
      JJ=JJ+LMN
      IF (JJ) 540,540,535
  535 A(II,JJ)=A(II,JJ)+ASSA(I,J)-ASA(I,J)
  540 CONTINUE
  550 CONTINUE
  555 CONTINUE
C
C     UPDATE NONLINEAR ELEMENT STRESS AND DEFORMATION
C
      IF (ICOND.EQ.2) GO TO 580
      IF (ITTYP.EQ.0.AND.ICONC.EQ.3.AND.ICOR.NE.0) GO TO 580
      NSS(N)=NS
      DO 570 I=1,12
      STR(N,I)=F(I)
  570 UPL(N,I)=UP(I)
  580 CONTINUE
C
  700 CONTINUE
C
C     COMPUTE RESIDUAL FORCE
C
      GO TO (710,720,710) ICONO
  710 CALL RESIDF(B,XM,X,X1,X2,PEXT,MBMAX,MHMAX,PM ,REF,PN,NEC,
     .            MBAND,RTOL,PU)
C
  720 RETURN
      END
```

19

42.

```
*OECK RESIDF
      SUBROUTINE RESIDF (B,XM,X,X1,X2,PEXT,MBMAX,MHMAX,PM,REF,PN,NEC,
     .                  MBAND,RTOL,PU)
C
      DIMENSION B(1),XM(1),X(1),X1(1),X2(1),PEXT(1),MBMAX(1),MHMAX(1),
     .          PM(1),PN(1),REF(1),PL(1)
      COMMON/MISC/ MMM(4),DT,ALFA,BETA,INTG,LLL(6)
      COMMON/JUNK/ FNM1,FNM2,OFNM,NEQ1,I,XX,MB,MH,K,J,N2,JUK(194)
      COMMON/COLB/ USP(10,2),USPF(10,2),KF(6),LPSLIP(2)
C
C     COMPUTE RESIDUAL FORCE
C
      FNM1=0.
      FNM2=0.
      OFNM=0.
      RTOL=0.0
      NEQ1=NEQ-1
      DO 10 I=1,NEQ
   10 PM(I)=X(I)+BETA*X1(I)
      DO 150 I=1,NEQ
      XX=-PN(I)-XM(I)*(X2(I)+ALFA*X1(I))-PU(I)
      MB=MBMAX(I)
      MH=MHMAX(I)
      K=I
      IF (MB.LT.I) GO TO 30
      DO 20 J=I,MB,NEQ
      IF (B(J).EQ.0.) GO TO 20
      XX=XX-B(J)*PM(K)
   20 K=K+1
   30 IF (I.EQ.1) GO TO 100
      N2=I+NEQ1
      IF (MH.LT.N2) GO TO 100
      K=I-1
      DO 50 J=N2,MH,NEQ1
      IF (B(J).EQ.0.) GO TO 50
      XX=XX-B(J)*PM(K)
   50 K=K-1
  100 REF(I)=PEXT(I)+XX
      FNM1=FNM1+PEXT(I)**2
      FNM2=FNM2+XX*XX
      OFNM=OFNM+REF(I)**2
  150 CONTINUE
C
      XX=SQRT(FNM1)+SQRT(FNM2)
      IF (XX.EQ.0.) GO TO 200
      RTOL=SQRT(OFNM)/XX
C
  200 RETURN
      END
```

43.

```
*OECK ITERN
      SUBROUTINE ITERN (A,B,XM,X,X1,X2,OX,FIT,REF,PU,PN,PM,PEXT,NBMAX,
     .                  MBMAX,MHMAX,NINC,NSS,STR,STRF,UPL,UPLF,NEC,MBAND
     ..                 NUMNEL,ISOIV,ICOR,NOT,NITRN)
C
      DIMENSION A(1),B(1),XM(1),X(1),X1(1),X2(1),OX(1),FIT(1),REF(1),
     .          PU(1),PN(1),PM(1),PEXT(1),NBMAX(1),MBMAX(1),MHMAX(1),
     .          NINO(1),NSS(1),STR(NUMNEL,12),STRF(NUMNEL,12),
     .          UPL(NUMNEL,12),UPLF(NUMNEL,12)
      COMMON/EPAR/ CONT(14),NNNN(14)
      COMMON/ITSO/ NSDIV,ITTYP,MAXIT,RTOLU,RTOLS,RTOLI,CCNN(34)
      COMMON/MISC/ MMM(14)
      COMMON/JUNK/ I,J,MB,MH,N1,DO,JUK(199)
      COMMON/COLB/ USP(10,2),USPF(10,2),KF(6),LPSLIP(2)
C
C     ITERATION OF EQUATION OF MOTION
C
      XNM1=0.
      DO 5 I=1,NEQ
    5 XNM1=XNM1+X(I)**2
      IF (XNM1.EQ.0.) GO TO 200
C
      ITRN=0
    6 ITRN=ITRN+1
      WRITE(6,1000) ITRN
C
C     FORM EFFECTIVE DYNAMIC STIFFNESS MATRIX AND LOAD VECTOR
C
      IF (ITTYP) 8,20,8
    8 DO 10 I=1,NEQ
   10 PM(I)=CONT(11)*X1(I)+CONT(12)*X2(I)-X(I)
      DO 15 I=1,NEQ
      A(I)=A(I)+CONT(7)*XM(I)+CONT(8)*B(I)
      MB=MBMAX(I)
      MH=MHMAX(I)
      N1=I+NEQ
      IF (MB.LT.N1) GO TO 15
      DO 12 J=N1,MB,NEQ
      IF (B(J).EQ.0.) GO TO 12
      A(J)=A(J)+CONT(8)*B(J)
   12 CONTINUE
   15 CONTINUE
C
C     TRIANGULARIZE EFFECTIVE DYNAMIC STIFFNESS MATRIX
C
      CALL TRIA (A,NBMAX,NEQ,MBAND)
   20 CONTINUE
C
C     SOLVE FOR CORRECTIVE DISPLACEMENT INCREMENT
C
      CALL BACK (A,NBMAX,REF,NEQ)
C
C     COMPUTE DISPLACEMENT, VELOCITY AND ACCELERATION
C
      OXNM=0.
      XNM2=0.
```

```
      DO 50 I=1,NEQ
      DD=REF(I)
      X(I)=X(I)+DD
      X1(I)=X1(I)+CONT(4)*DD
      X2(I)=X2(I)+CONT(1)*DD
      DX(I)=00
      XNM2=XNM2+X(I)**2
   50 DXNM=DXNM+DD*DD
C
C     CHECK CORRECTNESS OF NEW SOLUTION
C
      RTOL=SQRT(DXNM)/(SQRT(XNM1)+SQRT(XNM2))
      IF (RTOL.LT.RTOLU) ICOR=0
      WRITE(6,1200) RTOL
C
C     COMPUTE NEW STIFFNESS MATRIX AND RESIDUAL FORCE
C
      CALL NELSTF (A,B,X,X1,X2,DX,XM,MBMAX,MHMAX,PEXT,FIT,PU,PN,PM,REF,
     .             STR,STRF,UPL,UPLF,NINC,NSS,NEQ,MBAND,NUMNEL,3,ISDIV,
     .             ICOR,RTOL)
C
C     CHECK FOR NUMBER OF ITERATION
C
      IF (ICOR.EQ.0) GO TO 200
      IF (ITRN.LT.MAXIT) GO TO 6
      WRITE(6,1100) NDT,ITRN
      STOP
C
  200 NITRN=NITRN+ITRN
      RETURN
C
 1000 FORMAT(1H ,20X,21HNUMBER OF ITERATION =,I5)
 1100 FORMAT(1H1,51H*****EQUILIBRIUM ITERATION FAILED TO CONVERGE*****
     .       /5HNCT =,I5/3X,6HITRN =,I5/26H.....EXECUTION TERMINATED. )
 1200 FORMAT(1H ,25X,45HRELATIVE NORM OF CORRECTIVE DISPLACEMENT..... ,
     .       F15.7)
      END
```

```
*DECK OUTPUT
      SUBROUTINE OUTPUT
C
      COMMON/EPAR/ PAR(14),NUMNP,NELTYP,NUMEL,NUMNEL,NEQ,MBAND,MTOT,
     .             N1,N2,N3,N4,N5,N6,N7
      COMMON/EMTX/ QQQQ(2043)
      COMMON/MISC/ NFN,NGM,NT,NOT,DDT,LLL(9)
      COMMON/JUNK/ NDS,DT,KK1,KK2,ISP1,ISP2,NSD,NSS,NNS,MDIS,MSTR,
     .             NDISB,NSTRB,NBD,NBS,JUK(190)
      COMMON A(1)
C
C     INPUT SPECIFICATIONS FOR OUTPUT OF RESPONSE TIME HISTORIES
C
      DT=DDT
      N1=1
      N2=N1+NUMNEL*12
      N3=N2+NEQ
      N4=N3+NUMEL
      CALL INOUT (A(N1),A(N2),A(N3),A(N4),NUMNP,NEQ,NUMEL,NUMNEL)
C
C     PACK RESPONSE TIME HISTORIES IN BLOCKS
C
      DT=NOT*DT
      NDS=NT/NOT
      NDISB=(MTOT-N3-NEQ*2)/(MDIS*2)
      MDISB=(MTOT-N3-9*NDS)/(MDIS*2)
      IF (NDISB.GT.MDISB) NDISB=MDISB
      IF (NDISB.GT.NDS) NDISB=NDS
      NBD=(NDS-1)/NDISB+1
C
      NSTRB=(MTOT-N3-NUMNEL*25)/(MSTR*2)
      MSTRB=(MTOT-N3-9*NDS)/(MSTR*2)
      IF (NSTRB.GT.MSTRB) NSTRB=MSTRB
      IF (NSTRB.GT.NDS) NSTRB=NDS
      NBS=(NDS-1)/NSTRB+1
C
      N4=N3+NEQ
      N5=N4+NEQ
      N6=N5+MDIS*NDISB
C
      N7=N3+NUMNEL
      N8=N7+NUMNEL*12
      N9=N8+NUMNEL*12
      N10=N9+MSTR*NSTRB
      N11=N10+MSTR*NSTRB
      CALL REPACK (A(N1),A(N2),A(N3),A(N4),A(N5),A(N6),
     .             A(N3),A(N7),A(N8),A(N9),A(N10),NDS,NEQ,
     .             MDIS,NDISB,NUMNEL,MSTR,NSTRB,NBD,NBS )
C
      MT=0
      NFILE=0
      IF (KK1.EQ.4) NFILE=NFILE+NSD*2
      IF (KK2.EQ.4) NFILE=NFILE+NSS+NNS
      IF (NFILE.EQ.0) GO TO 100
      MT=30
      REWIND MT
```

```
      WRITE (MT) NFILE,NDS,DT
  100 N4=N3+NDS
      N5=N4+NCS*8
      N6=N5+MDIS*NDISB
      N7=N5+MSTR*NSTRB
      IF=0
C
C     CUTPUT SELECTED (ABSCLUTE) ACCELERATICN TIME HISTCRY
C
      REWIND 4
      CALL CUTHIS (A(N1),A(N2),A(N3),A(N4),A(N5),A(N6),NUMNEL,
     .           NCS,MDIS,NCISB,NSD,NBC,2,KK1,ISP1,4,12,7,MT,IF)
C
C     CUTPLT SELECTED (RELATIVE) DISPLACEMENT TIME HISTORY
C
      REWIND 4
      CALL CUTHIS (A(N1),A(N2),A(N3),A(N4),A(N5),A(N6),NUMNEL,
     .           NDS,MDIS,NCISB,NSC,NBC,1,KK1,ISP1,4,3 ,7,MT,IF)
C
C     CUTPLT SELECTED STRESS TIME HISTORIES CF LINEAR ELEMENTS
C
      REWIND 7
      CALL OUTHIS (A(N1),A(N2),A(N3),A(N4),A(N5),A(N6),NUMNEL,
     .           NCS,MCIS,NCISB,NSS,NBC,3,KK2,ISP2,4,3 ,7,MT,IF)
C
C     CUTPUT SELECTEC STRESS TIME HISTORIES OF NONLINEAR ELEMENTS
C
      REWINC 2
      CALL CUTHIS (A(N1),A(N2),A(N3),A(N4),A(N5),A(N7),NUMNEL,
     .           NDS,MSTR,NSTRB,NNS,NBS,4,KK2,ISP2,2,10,7,MT,IF)
C
      RETURN
      END
```

```
*DECK INOUT
      SUBRCUTINE INOUT (ISTR,IDIS,INC,ID,NUMNP,NEQ,NUMEL,NUMNEL)
C
      CIMENSICN ISTR(NUMNEL,12),IDIS(NEQ),INC(NLMEL),ID(NUMNP,6)
      CCMMCN/EMTX/ NS,NC,LM(24),SA(12,24),KLM(8,24),SSA(8,24),QCCC(1345)
      CCMMCN/JUNK/ NCS,CT,KK1,KK2,ISP1,ISP2,NSC,NSS,NNS,MDIS,MSTR,
     .             NCISB,NSTRB,NBC,NBS,KD(4,8),SD(8),NKS(4,8),SNC(8),
     .             IC(6),IS(12),NCOF,SIG(12)
C
C     INPUT SPECIFICATICNS FOR OUTPUT RESPONSE TIME HISTORY
C
      REWIND 1
      REWINC 2
      REWIND 4
      REWIND 7
      REWIND 8
C
      READ (8) ID
C
      DO 10 I=1,NEQ
   10 IDIS(I)=0
      DO 20 I=1,NUMNEL
      DO 20 J=1,12
   20 ISTR(I,J)=0
C
C     READ ANC PRINT CISPLACEMENT OUTPUT SPECIFICATIONS
C
      L=0
      K=0
      READ (5,1000) KK1,ISP1
  100 READ (5,1000) NP,IC
      IF (NP.GT.0) GO TO 110
      IF (L .EQ.0) GO TC 200
      WRITE (4) KD,SD,L
      K=K+1
      GO TC 200
C
  110 IF (K.EQ.0.AND.L.EQ.0)  WRITE(6,2000)
      WRITE(6,2001) NP,IC
      DO 150 I=1,6
      II=IC(I)
      IF (II.LE.0) GO TO 150
      JJ=ID(NP,II)
      IF (JJ.LE.NEQ) GO TC 120
  115 WRITE(6,4001) NP,II
      GO TC 150
  120 IF (JJ.LE.0) GO TC 115
      L=L+1
      KD(1,L)=6
      KD(2,L)=NP
      KD(3,L)=II
      KD(4,L)=JJ
      SD(  L)=0.
      IDIS(JJ)=1
      IF (L.LT.8) GO TO 150
      WRITE (4) KD,SD,L
```

```
      K=K+1
      L=0
  150 CONTINUE
      GO TO 100
C
C     READ AND PRINT STRESS OUTPUT SPECIFICATIONS
C
  200 NSD=K
      WRITE(6,4000) KK1,ISP1
C
      READ (8) IND
      L=0
      LL=0
      K=0
      KK=0
      READ (5,1000) KK2,ISP2
      NREAD=1
      NTYPE=0
      NUMNE=0
C
      DO 600 N=1,NUMEL
      MTYPE=INO(N)
      IF (MTYPE.GT.0) GO TO 205
      MTYPE=-MTYPE
      GO TO 210
  205 NUMNE=NUMNE+1
  210 IF (NTYPE.EQ.MTYPE) GO TO 220
      NTYPE=MTYPE
      NUME=0
  220 NUME=NUME+1
      READ (1) NS,NO,LM,SA
      READ (8) NOOF,SIG
      IF (NREAD.EQ.0) GO TO 300
  225 READ (5,1000) NELTYP,NEL,IS
      IF (NEL.GT.0) GO TO 250
      IF ( L .EQ.0) GO TO 230
      WRITE (4) KO,SO,L
      WRITE (7) KLM,SSA,ND
      K=K+1
  230 IF (LL .EQ.0) GO TO 700
      WRITE (2) NKS,SNO,LL
      KK=KK+1
      GO TO 700
C
  250 IF (N.EQ.1)  WRITE(6,3000)
      WRITE(6,3002) NELTYP,NEL,IS
C
  300 IF (NELTYP.EQ.NTYPE.AND.NEL.EQ.NUME) GO TO 350
      NREAD=0
      GO TO 600
  350 NREAD=1
      IF (INO(N)) 400,400,500
C
C     STRESSES FOR LINEAR ELEMENTS
C
  400 DO 450 I=1,NS
      II=IS(I)
      IF (II.EQ.0) GO TO 450
      L=L+1
      KO(1,L)=NTYPE
      KO(2,L)=NEL
      KO(3,L)=II
      KO(4,L)=0
      SO(  L)=SIG(II)
      DO 440 J=1,NO
      SSA(L,J)=SA(II,J)
      KLM(L,J)=0
      LMJ=LM(J)
      IF (LMJ.GT.NEQ) GO TO 440
      IF (LMJ.LE. 0 ) GO TO 440
      KLM(L,J)=LMJ
      IOIS(LMJ)=1
  440 CONTINUE
      IF (L.LT.8) GO TO 450
      WRITE (4) KO,SO,L
      WRITE (7) KLM,SSA,ND
      L=0
      K=K+1
  450 CONTINUE
      GO TO 600
C
C     STRESSES FOR NONLINEAR ELEMENTS
C
  500 DO 550 I=1,NS
      II=IS(I)
      IF (II.EQ.0) GO TO 550
      LL=LL+1
      NKS(1,LL)=NTYPE
      NKS(2,LL)=NEL
      NKS(3,LL)=II
      NKS(4,LL)=NUMNE
      SNO(  LL)=0.
      LL=LL+1
      NKS(1,LL)=NTYPE
      NKS(2,LL)=NEL
      NKS(3,LL)=II
      NKS(4,LL)=NUMNE
      SNO(  LL)=0.
      ISTR(NUMNE,II)= 1
      IF (LL.LT.8) GO TO 550
      WRITE (2) NKS,SNO,LL
      LL=0
      KK=KK+1
  550 CONTINUE
  600 CONTINUE
      GO TO 225
C
  700 NSS=K
      NNS=KK
      WRITE(6,4000) KK2,ISP2
      IF (N.GE.NUMEL) GO TO 750
      N=N+1
```

```
      OO 720 I=N,NUMEL
      READ (8)
  720 CONTINUE
C
  750 MOIS=0
      MSTR=0
      OO 800 I=1,NEQ
      IF (IDIS(I).EQ.0) GC TO 800
      MOIS=MOIS+1
      IOIS(I)=MOIS
  800 CONTINUE
C
      OO 900 I=1,NUMNEL
      DO 900 J=1,12
      IF (ISTR(I,J).EQ.0) GO TO 900
      MSTR=MSTR+1
      ISTR(I,J)=MSTR
  900 CONTINUE
C
      RETURN
C
 1000 FORMAT (14I5)
 2000 FORMAT (36HDISPLACEMENT  COMPCNENTS  FCR WHICH  /
     .         36H OUTPUT TIME HISTORY IS REQUIREO....  //
     .          5H NODE 4X 23HDISPLACEMENT CUMPCNENTS /)
 2001 FORMAT (I5,4X,6I4)
 3000 FORMAT (36HIELEMENT STRESS COMPONENTS FOR WHICH /
     .         36H OUTPUT TIME HISTORY IS REQUIREO....  //
     .         40H  ELEMENT       OESIREO STRESS COMPONENTS /
     .         10H TYPE  NC.   /)
 3002 FORMAT (2I4,5X,12I3)
 4000 FORMAT (/16H OUTPUT TYPE.... ,I2 /
     .          16H PLOT SPACING... ,I2 )
 4001 FCRMAT (I5,4X,I4,4X,21HFIXEO CCF...NO OUTPUT )
      END

*DECK REPACK
      SUBRCUTINE REPACK (ISTR,IOIS,X,X2,XH,X2H,NSS,STR,UPL,STH,UPH,
     .                   NOS,NEQ,MOIS,NOISB,NUMNEL,MSTR,NSTRB,NBO,NBS)
C
      DIMENSICN ISTR(NUMNEL,1),IOIS(1),X(NEQ),XH(MOIS,NCISB),
     .          NSS(NUMNEL),STR(NUMNEL,12),UPL(NUMNEL,12),
     .          STH(MSTR,NSTRB),UPH(MSTR,NSTRB),X2(NEQ),X2H(MOIS,NOISB)
C
C     PACK RESPCNSE TIME HISTORY IN CPTIMAL AVAILABLE STORAGE BLOCKS
C
      REWIND 3
      REWIND 9
      REWIND 10
      REWIND 12
      L=0
      K=0
      OO 200 N=1,NDS
      READ (8) X,X2
      L=L+1
      OO 100 I=1,NEQ
      II=IOIS(I)
      IF (II) 100,100,90
   90 XH (II,L)=X (I)
      X2H(II,L)=X2(I)
  100 CCNTINUE
      IF (L.LT.NOISB) GC TO 200
      WRITE (3)  L,XH
      WRITE (12) L,X2H
      K=K+1
      L=0
  200 CONTINUE
      IF (L) 220,220,210
  210 WRITE (3)  L,XH
      WRITE (12) L,X2H
      K=K+1
  220 IF (NBO.NE.K) NBO=K
C
      L=0
      K=0
      IF (NUMNEL.LE.0) GO TO 420
      DO 400 N=1,NDS
      READ (9) NSS,STR,UPL
      L=L+1
      OO 300 I=1,NUMNEL
      NS=NSS(I)
      OO 250 J=1,NS
      II=ISTR(I,J)
      IF (II) 250,250,240
  240 STH(II,L)=STR(I,J)
      UPH(II,L)=UPL(I,J)
  250 CONTINUE
  300 CONTINUE
      IF (L.LT.NSTRB) GO TO 400
      WRITE (10) L,STH,UPH
      L=0
      K=K+1
  400 CONTINUE
      IF (L) 420,420,410
  410 WRITE (10) L,STH,UPH
      K=K+1
  420 IF (NBS.NE.K) NBS=K
C
      RETURN
      END
```

```
*DECK OUTHIS
      SUBROUTINE OUTHIS (ISTR,IDIS,T,X,XH,UH,NEL,NOS,NOI,NOJ,
     .                   NOB,NHB,KKK,KKI,ISPI,IT,JT,KT,MT,IF)
C
      DIMENSION ISTR(NEL,1),IDIS(1),T(1),X(8,NCS),XH(NOI,NOJ),
     .          UH(NOI,NOJ)
      COMMON/EMTX/ KLM(8,24),SA(8,24),ND,SM(8)
      COMMON/JUNK/ NPT,CT,NDATA(13),L,K,KO(4,8),XO(8),TM(8),XM(8)
      DATA SM /1H1,1HA,1H2,1H8,1H3,1HC,1H4,1HC/
C
C     OUTPUT RESPONSE TIME HISTORIES ON SPECIFIED DISPLAY MEDIUM
C
C     TAPE IT   INPUT  TAPE    STORE KO(4,8),XC(8),L
C     TAPE JT   INPUT  TAPE    STORE XH(NCI,NCJ),UH(NOI,NCJ),K
C     TAPE KT   INPUT  TAPE    STORE KLM(8,24),SA(8,24),ND
C     TAPE MT   OUTPUT TAPE    STORE IF,KKK,L,KC,XM,X(8,NCS)
C
      IF (NOB.EQ.0) RETURN
C
      DO 900 M=1,NOB
      IF=IF+1
      REWIND JT
      READ (IT) KO,XO,L
      IF (KKK.EQ.3) READ (KT) KLM,SA,ND
      DO 100 I=1,8
      TM(I)=0.
      XM(I)=0.
  100 CONTINUE
C
C     PRINT APPROPRIAT TITLE
C
      GO TO (110,200,130,110) KKI
C
  110 GO TO (111,112,113,114) KKK
  111 WRITE(6,1001) M,IF
      WRITE(6,1002) (KC(2,I),KO(3,I),I=1,L)
      GO TO 200
  112 WRITE(6,2001) M,IF
      WRITE(6,1002) (KC(2,I),KO(3,I),I=1,L)
      GO TO 200
  113 WRITE(6,3001) M,IF
      WRITE(6,3002) (KC(1,I),KO(2,I),KO(3,I),I=1,L)
      GO TO 200
  114 WRITE(6,4001) M,IF
      WRITE(6,4002) (KO(1,I),KO(2,I),KO(3,I),I=1,L)
      GO TO 200
C
  130 IF (M.GT.1) GO TO 200
      GO TO (131,132,133,131) KKK
  131 WRITE(6,1003)
      WRITE(6,1010)
      GO TO 200
  132 WRITE(6,2003)
      WRITE(6,2010)
      GO TO 200
  133 WRITE(6,3003)
```



```
      WRITE(6,3010)
C
C     ARRANGE RESPONSE TIME HISTORIES IN OUTPUT FORM
C
  200 TT=0.
      N =0
      DO 600 NB=1,NHB
      GO TO (210,210,210,220) KKK
  210 READ (JT) K,XH
      GO TO 250
  220 READ (JT) K,XH,UH
  250 DO 500 J=1,K
      N=N+1
      TT=TT+DT
      MM=-1
      DO 400 I=1,L
C
      GO TO (310,310,330,340) KKK
C
  310 JJ=KO(4,I)
      II=IDIS(JJ)
      XX=XH(II,J)
      GO TO 350
C
  330 XX=XC(I)
      DO 335 KK=1,ND
      JJ=KLM(I,KK)
      IF (JJ) 335,335,334
  334 II=IDIS(JJ)
      XX=XX+SA(I,KK)*XH(II,J)
  335 CONTINUE
      GO TO 350
C
  340 JJ=KC(3,I)
      NN=KC(4,I)
      II=ISTR(NN,JJ)
      IF (MM) 341,341,342
  341 XX=XH(II,J)
      GO TO 345
  342 XX=UH(II,J)
  345 MM=-1*MM
C
  350 AX=ABS(XX)
      IF (AX-XM(I)) 370,370,360
  360 XM(I)=AX
      TM(I)=TT
  370 X (I,N)=XX
      T ( N )=TT
  400 CONTINUE
C
  500 CONTINUE
  600 CONTINUE
C
      GO TO (610,620,630,640) KKI
C
C     PRINT RESPONSE TIME HISTORY
```

```
C
  610 DO 611 N=1,NOS
  611 WRITE(6,1004) T(N),(X(I,N),I=1,L)
      WRITE(6,1005) (XM(I),I=1,L)
      WRITE(6,1006) (TM(I),I=1,L)
      GO TO 900
C
C     PLOT RESPONSE TIME HISTORY
C
  620 GO TO (621,623,625,627) KKK
C
  621 ISO=1
      WRITE(6,1008) M
      WRITE(6,1010)
      GO TO 624
  623 ISO=1
      WRITE(6,2008) M
      WRITE(6,2010)
  624 WRITE(6,2011) (KO(2,I),KO(3,I),XM(I),TM(I),I,I=1,L)
      GO TO 629
  625 ISO=1
      WRITE(6,3008) M
      WRITE(6,3010)
      WRITE(6,3011) (KO(1,I),KO(2,I),KO(3,I),XM(I),TM(I),I,I=1,L)
      GO TO 629
  627 ISO=2
      WRITE(6,4009) M
      WRITE(6,3010)
      DO 628 I=1,L,2
      II=I+1
      WRITE(6,4011) KO(1,I),KO(2,I),KO(3,I),XM(I),TM(I),SM(I)
  628 WRITE(6,4012) XM(II),TM(II),SM(II)
C
  629 CALL PLOT (X,XM,L,DT,NOS,ISP1,ISO)
      GO TO 900
C
C     PRINT MAXIMUM RESPONSE ONLY
C
  630 GO TO (631,631,635,637) KKK
  631 WRITE(6,1007) (KO(1,I),KO(2,I),XM(I),TM(I),I=1,L)
      GO TO 900
  635 WRITE(6,3007) (KO(1,I),KO(2,I),KO(3,I),XM(I),TM(I),I=1,L)
      GO TO 900
  637 DO 638 I=1,L,2
      II=I+1
      WRITE(6,4007) KO(1,I),KO(2,I),KO(3,I),XM(I),TM(I)
  638 WRITE(6,4008) XM(II),TM(II)
      GO TO 900
C
C     STORE RESPONSE TIME HISTORIES ON OUTPUT TAPE MT
C
  640 IF (KK1.EQ.4) WRITE (MT) IF,KKK,L,KO,XM,X
      GO TO 610
C
  900 CONTINUE
      RETURN
```

```
C
 1001 FORMAT (50H1TIME HISTORY FOR SELECTED DISPLACEMENT COMPONENTS ,
     .  5H..... ,I3,37X,8HFILE NO.,I3 //
     .                   20X,40HNODE NUMBERS AND DISPLACEMENT COMPONENTS  )
 1002 FORMAT (8H    TIME,2X,8(I8,1H-,I2,X))
 1003 FORMAT (59H1MAXIMUM DISPLACEMENT VALUES FROM DYNAMIC RESPONSE ANAL
     .YSIS // )
 1004 FORMAT (0PF8.3,2X,1P8E12.3)
 1005 FORMAT (/24H MAXIMUM ABSOLUTE VALUES  /10H MAXIMUM    ,1P8E12.3)
 1006 FORMAT (10H TIME        ,1P8E12.3)
 1007 FORMAT (I6,I13,1PE18.3,E12.3,5X,2HNA )
 1008 FORMAT (59H1NORMALIZED PLOT OF DISPLACEMENT RESPONSE TIME HISTORIE
     .S... ,I3 /)
 1010 FORMAT (57H   NODE     DISPLACEMENT    MAXIMUM       TIME AT    PLO
     .T       /58H  NUMBER    COMPONENT       VALUES        MAXIMUM    SYM
     .BOL  )
 2001 FORMAT (50H1TIME HISTORY FOR SELECTED ACCELERATION COMPONENTS ,
     .  5H..... ,I3,37X,8HFILE NO.,I3 //
     .                   20X,40HNODE NUMBERS AND ACCELERATION COMPONENTS  )
 2003 FORMAT (59H1MAXIMUM ACCELERATION VALUES FROM DYNAMIC RESPONSE ANAL
     .YSIS // )
 2008 FORMAT (59H1NORMALIZED PLOT OF ACCELERATION RESPONSE TIME HISTORIE
     .S... ,I3 /)
 2010 FORMAT (57H   NODE     ACCELERATION    MAXIMUM       TIME AT    PLO
     .T       /58H  NUMBER    COMPONENT       VALUES        MAXIMUM    SYM
     .BOL  )
 2011 FORMAT (I6,I13,1PE18.3,E12.3,I6)
 3001 FORMAT (46H1TIME HISTORIES FOR SELECTED STRESS COMPONENTS ,5H.....
     .    I3,41X,8HFILE NO.,I3 //
     .           20X,48HELEMENT TYPE - ELEMENT NUMBER - STRESS COMPONENT )
 3002 FORMAT (8H    TIME ,2X,8(I4,2H -,I3,1H-,I2))
 3003 FORMAT (53H1MAXIMUM STRESS VALUES FROM DYNAMIC RESPONSE ANALYSIS
     .  //)
 3007 FORMAT (I6,I6,I10,1PE18.3,E12.3,5X,2HNA)
 3008 FORMAT (53H1NORMALIZED PLOT OF STRESS RESPONSE TIME HISTORIES...
     .           I3/)
 3010 FORMAT (13H ELEMENT     2X 6HSTRESS 10X 7HMAXIMUM 6X 7HTIME AT 4X
     .4HPLOT /13H TYPE  NUMBER 2X 9HCOMPONENT 7X 7HVALUES  6X 7HMAXIMUM
     .4X 6HSYMBOL )
 3011 FORMAT (I6,I6,I10,1PE18.3,E12.3,I6)
 4001 FORMAT (47H1TIME HISTORIES FOR SELECTED NONLINEAR STRESSES  /
     . 6X,48H AND CORRESPONDING NONLINEAR DEFORMATIONS  .....  I3,
     . 38X,8HFILE NO.,I3 //
     .20X,48HELEMENT TYPE - ELEMENT NUMBER - STRESS COMPONENT  )
 4002 FORMAT (12X,4(12H STRESS      ,12HDEFORMATION )/
     .          8H    TIME,2X,8(I4,2H -,I3,1H-,I2))
 4003 FORMAT (68H1MAXIMUM NONLINEAR STRESSES AND CORRESPONDING NONLINEAR
     . DEFORMATIONS //)
 4007 FORMAT (2I6,I10,1PE18.3,E12.3,2X,6HSTRESS )
 4008 FORMAT (22X,1PE18.3,E12.3,2X,11HDEFORMATION )
 4009 FORMAT (60H1NORMALIZED PLOT OF NONLINEAR STRESS RESPONSE TIME HIST
     .ORIES /58H AND CORRESPONDING NONLINEAR DEFORMATION TIME HISTORIES.
     ...  I3/)
 4011 FORMAT (I6,I6,I10,1PE18.3,E12.3,5X,A1)
 4012 FORMAT (22X,1PE18.3,E12.3,5X,A1)
      END
```

```
*DECK PLOT
      SUBROUTINE PLOT (X,XM,L,DT,NDS,ISP,ISD)
C
      DIMENSION X(8,1),XM(8),PM(8),QM(8),SM(8),IP(8)
      COMMON/EMTX/ PP(101)
      DATA PM /1H1,1H2,1H3,1H4,1H5,1H6,1H7,1H8/
      DATA QM /1H1,1HA,1H2,1HB,1H3,1HC,1H4,1HD/
      DATA BL,V,P /1H ,1H.,1H+/
C
C     NORMALIZED PLOT OF TIME HISTORIES OF TIME FUNCTIONS
C
      DO 30 I=1,L
      GO TO (10,20) ISD
   10 SM(I)=PM(I)
      GO TO 30
   20 SM(I)=QM(I)
   30 CONTINUE
C
      DO 100 I=1,L
      IF (XM(I)) 50,100,50
   50 XM(I)=50./XM(I)
  100 CONTINUE
      TT=0.
      WRITE(6,2000)
      WRITE(6,2001)
      WRITE(6,2002) TT,P,(V,I=1,24),P,(V,I=1,24),P,(V,I=1,24),P,
     .                (V,I=1,24),P,TT
C
      K=1
      DO 200 I=2,100
  200 PP(I)=BL
      NDS1=NDS-1
      DO 500 N=1,NDS1
      PP(  1)=V
      PP( 51)=V
      PP(101)=V
      II=ISP
  210 IF (II.LE.0) GO TO 250
      WRITE(6,2003) PP
      II=II-1
      GO TO 210
  250 TT=TT+DT
      DO 300 I=1,L
      XX=XM(I)*X(I,N)
      M=XX
      M=M+51
      IP(I)=M
  300 PP(M)=SM(I)
      IF (K.LT.10) GO TO 320
      PP(  1)=P
      PP( 51)=P
      PP(101)=P
      K=1
      WRITE(6,2002) TT,PP,TT
      GO TO 340
  320 WRITE(6,2003) PP
      K=K+1
C
C     RESET PP(101)
C
  340 DO 360 I=1,L
      M=IP(I)
  360 PP(M)=BL
  500 CONTINUE
C
      TT=TT+DT
      WRITE(6,2002) TT,P,(V,I=1,24),P,(V,I=1,24),P,(V,I=1,24),P,
     .                (V,I=1,24),P,TT
      WRITE(6,2001)
      RETURN
C
C     *CARRIAGE CONTROL CHACTER Z SURPRESS SKIP OVER PAGE FOLDS
C
 2000 FORMAT (/56X,8HORDINATE )
 2001 FORMAT (/12HZ  TIME -1.0,21X,4H-0.5,22X,3H0.0,22X,3H0.5,22X,3H1.0,
     .        X,4HTIME )
 2002 FORMAT (1HZ,F7.2,2X,101A1,F7.2)
 2003 FORMAT (1HZ,9X,101A1)
      END
```

```
*DECK SBEAM
      SUBROUTINE SBEAM
C
      COMMON A(1)
      COMMON/EPAR/ NPAR(14),NUMNP,NELTYP,NUMEL,NUMNEL,NEQ,MBAND,MTOT,
     .             N1,N2,N3,N4,N5,N6
      COMMON/JUNK/ STR(4),MM,L,K,NTAG,NDYN,SIG(12),EXRA(184)
C
      N7=N6+NPAR(5)
      N8=N7+NPAR(5)
      N9=N8+NPAR(5)
      N10=N9+NPAR(4)*12
      N11=N10+NPAR(3)*6
      N12=N11+NPAR(6)*12
      IF (N12.GT.MTOT) CALL ERROR (1,N12-MTOT,7HBEAM   )
      CALL TEAM (NPAR(2),NPAR(3),NPAR(4),NPAR(5),NPAR(6),
     .           A(N1),A(N2),A(N3),A(N4),A(N5),A(N6),A(N7),A(N8),
     .           A(N9),A(N10),A(N11),NUMNP,MBAND,NUMEL)
C
      RETURN
      END
```

```
*OECK TEAM
      SUBROUTINE TEAM (NBEAM,NUMETP,NUMFIX,NUMMAT,NUMNPAR,ID,X,Y,Z,INO,
     .                 E,G,RC,SFT,CCPROP,ENPRCP,NUMNP,MBANO,NUMEL)
C
      CIMENSION IC(NUMNP,1),X(1),Y(1),Z(1),INC(1),E(1),G(1),RO(1),
     .          SFT(NUMFIX,1),COPROP(NUMETP,1),ENPROP(NUMNPAR,1),
     .          STIF(722),LMS(12),EC(12),T(3,3)
      COMMCN/EMTX/ LM(24),NC,NS,ASA(24,24),RF(24,4),XM(24),SA(12,24),
     .             SF(12,4),ENPAR(24),S(12,12),F(48),TTT(72)
      COMMCN/JUNK/ LC(4),JK(6),MELTYP,OL,MATTYP,ILC(4),TS(2,2),LS(4),
     .             EMUL(3,4)
      ECUIVALENCE (STIF,LM),(LMS,TTT(1)),(EC,TTT(13)),(T,TTT(25))
C
C     FCRMS 3-O BEAM STIFFNESS ANO STRESS ARRAYS
C
      WRITE (6,2005) NBEAM,NUMETP,NUMFIX,NUMMAT,NUMNPAR
      DC 5 I=1,1346
    5 STIF(I)=0.
C
C     REAC ANC PRINT MATERIAL PROPERTY DATA
C
      WRITE (6,2001)
      DO 10 I=1,NUMMAT
      REAC  (5,1001) N,E(N),G(N),RO(N)
      WRITE (6,2002) N,E(N),G(N),RO(N)
   1C G(N)=0.5*E(N)/(1.+G(N))
C
C     READ ANO PRINT GEOMETRIC PROPERTIES OF COMMON ELEMENTS.
C
      WRITE (6,2003)
      OO 30 I=1,NUMETP
      REAC  (5,1002) N,(CCPROP(N,J),J=1,6)
      IF((CCPROP(N,1).NE.C.0).ANC.(CCPROP(N,4).NE.0.0).ANC.
     1   (CCPROP(N,5).NE.C.0).ANC.(CCPROP(N,6).NE.0.0))  GO TO 20
      WRITE (6,2013)
      CALL EXIT
   20 WRITE (6,2004) N,(CCPROP(N,J),J=1,6)
   30 CONTINUE
C
C     ELEMENT LOAO MULTIPLIERS
C
      REAC  (5,1006) ((EMUL(I,J),J=1,4),I=1,3)
      WRITE (6,2006) ((EMUL(I,J),J=1,4),I=1,3)
C
C     REAC ANC PRINT FIXEC ENO FORCES IN LOCAL COOROINATES
C
      IF(NUMFIX .EQ. O) GO TO 56
      WRITE (6,2010)
      OO 55 I=1,NUMFIX
      REAO  (5,1005) N,(SFT(N,J),J=1,12)
   55 WRITE (6,2011) N,(SFT(N,J),J=1,12)
   56 CONTINUE
C
C     REAC ANC PRINT ELEMENT NONLINEAR PARAMETERS
C
      IF (NUMNPAR.EQ.0) GO TO 59
      WRITE(6,2020)
      CC 58 I=1,NUMNPAR
   58 REAC (5,1007) N,(ENPROP(N,J),J=1,12)
      WRITE(6,2021) (N,(ENPROP(N,J),J=1,12),N=1,NUMNPAR)
   59 CCNTINUE
C
C     REAC ANC PRINT ELEMENT CATA. GENERATE MISSING INPUT.
C
      WRITE (6,4000)
      L=0
   60 KKK=0
      REAC (5,3000) INEL,INI,INJ,INK,IMAT,IMEL,ILC,INELKI,INELKJ,INC,IOO
      IF (IOO.GT.NUMNPAR) CALL ERROR (3,INEL,7HBEAM    )
      IF (INEL.NE.1) GO TC 15
      NI=INI
      NJ=INJ
      NK=INK
   15 IF (INC.EC.0) INC=1
   65 L=L+1
      KKK=KKK+1
      ML=(NEL-L
      IF (ML)  66,67,68
   66 CALL ERROR (4,INEL,7HBEAM    )
   67 NEL=INEL
      NI=INI
      NJ=INJ
      NK=INK
      MATTYP=IMAT
      MELTYP=IMEL
      OO 90 I=1,4
   90 LC(I)=ILC(I)
      NEKCD(=INELKI
      NEKCCJ=INELKJ
      NINO=IDO
      GO TC 69
   68 NEL=INEL-ML
      NI=IN+KKK*INCR
      NJ=JN+KKK*INCR
   69 CONTINUE
      WRITE (6,4001) NEL,NI,NJ,NK,MATTYP,MELTYP,LC,NEKOOI,NEKOOJ,NINO
C
   74 OX=X(NJ)-X(NI)
      OY=Y(NJ)-Y(NI)
      DZ=Z(NJ)-Z(NI)
      DL=SCRT(DX*OX+OY*OY+OZ*OZ)
      IF(OL)  75,75,76
   75 CALL ERROR (5,NEL,7HBEAM    )
C
C     FORM GLOBAL TO LOCAL COORDINATE TRANSFORMATION.
C
   76 T(1,1)=OX/OL
      T(1,2)=DY/OL
      T(1,3)=OZ/OL
C
      A1=X(NJ)-X(NI)
      A2=Y(NJ)-Y(NI)
```

```
      A3=Z(NJ)-Z(NI)
      B1=X(NK)-X(NI)
      B2=Y(NK)-Y(NI)
      B3=Z(NK)-Z(NI)
      AA=A1*A1+A2*A2+A3*A3
      AB=A1*B1+A2*B2+A3*B3
      U1=AA*B1-AB*A1
      U2=AA*B2-AB*A2
      U3=AA*B3-AB*A3
      UU=U1*U1+U2*U2+U3*U3
      UU=SQRT(UU)
      IF (UU.GT.0.) GO TO 77
      CALL ERROR (6,INEL,7H BEAM   )
   77 T(2,1)=U1/UU
      T(2,2)=U2/UU
      T(2,3)=U3/UU
      T(3,1)=T(1,2)*T(2,3)-T(1,3)*T(2,2)
      T(3,2)=T(1,3)*T(2,1)-T(1,1)*T(2,3)
      T(3,3)=T(1,1)*T(2,2)-T(1,2)*T(2,1)
C
C     CHECK IF NEW STIFFNESS NEEDED
C
      IF (NFL.EQ.1) GO TO 80
      IF  (ABS(OS-OL).GT.OL/100.)  GO TO 80
      IF ((MT.NE.MATTYP).OR.(ME.NE.MELTYP)) GO TO 80
      IF ((JK(1).NE.NEKODI).OR.(JK(2).NE.NEKODJ)) GO TO 80
      DO 78 I=1,4
      IF (LS(I).NE.LC(I)) GO TO 80
   78 CONTINUE
      DO 79 I=1,2
      DO 79 J=1,2
      IF (ABS(TS(I,J)-T(I,J)).GT.ABS(T(I,J)/100.)) GO TO 80
   79 CONTINUE
      GO TO 150
C
   80 OS=OL
      MT=MATTYP
      ME=MELTYP
      DO 81 I=1,2
      DO 81 J=1,2
   81 TS(I,J)=T(I,J)
      DO 82 I=1,4
   82 LS(I)=LC(I)
      JK(1)=NEKODI
      JK(2)=NEKODJ
C
C     FORM NEW STIFFNESS
C
      CALL NEWBM (E,G,RO,COPROP,SFT,NUMFIX,NUMETP)
C
C     FORM ELEMENT LOCATION MATRIX
C
  150 DO 170 M=1,6
      LM(M)=ID(NI,M)
      LM(M+12)=0
      LM(M+18)=0
  170 LM(M+6)=ID(NJ,M)
      NS=12
      NO=12
C
C     TRANSFORM TO MASTER DEGREES OF FREEDOM
C
      CALL SLAVE (X,Y,Z,ID,NUMNP,NI,NJ)
C
C     WRITE ELEMENT INFORMATION ON TAPE
C
      CALL WRITET (MBANC,NDIF)
C
C     SET NONLINEAR ELEMENT INDICATOR AND STORE NONLINEAR INFORMATION
C
      NN=NUMEL+NEL
      IF (NINC.LE.0) GO TO 200
      INC(NN)=2
      DO 190 I=1,12
  190 ENPAR(I)=ENPROP(NINC,I)
      MTYPE=2
      WRITE (3) MTYPE,LM,NO,NS,ASA,SA,S,ENPAR,TTT
      GO TO 250
  200 INO(NN)=-2
C
C     CHECK FOR LAST ELEMENT
C
  250 IF (NBEAM-NEL) 66,500,260
  260 IF (ML.GT.0)  GO TO 65
      IN=INI
      JN=INJ
      INCR=INC
      GO TO 60
  500 RETURN
C
 1001 FORMAT(I5,3F10.0)
 1002 FORMAT(I5,6F10.0)
 1005 FORMAT(I5,6F10.0/F15.0,5F10.0)
 1006 FORMAT (4F10.0)
 1007 FORMAT (I5,4F10.0/8F10.0)
 2001 FORMAT (24H1MATERIAL PROPERTIES.... ///
     .        54H MATERIAL    YOUNG S      POISSON S             MASS      /
     .        54H  NUMBER     MODULUS         RATIO              DENSITY     /)
 2002 FORMAT(1H ,I5,3X,F12.0,F14.5,F14.5)
 2003 FORMAT (////30H BEAM GEOMETRIC PROPERTIES....  //
    1   48H ELEMENT         AREA          AREA          AREA
    2  60H INERTIA      INERTIA      INERTIA
    3 / 48H  TYPE             X             Y             Z
    4                  30H     X             Y             Z                  )
 2004 FORMAT(1H ,I5,2X,6F12.3)
 2005 FORMAT(39H1.......THREE DIMENSIONAL BEAM ELEMENTS///
     .   36H  NUMBER OF BEAMS                   =,I5//
     .   36H  NUMBER OF GEOMETRIC PROPERTY SETS=,I5//
     .   36H  NUMBER OF FIXED END FORCE SETS   =,I5//
     .   36H  NUMBER OF MATERIALS               =,I5//
     .   36H  NUMBER OF BEAM N/L PROPERTY SETS =,I5)
 2006 FORMAT(///30H ELEMENT LOAD MULTIPLIERS...../12X,1HA,14X,1HB,14X,
```

```
     .  1HC,14X,1HO/6H X-DIR 4E15.6/6H Y-DIR 4E15.6/6H Z-DIR 4E15.6/ )
 2010 FORMAT (1H1
     1  30X40H FIXED END FORCES IN LOCAL COORDINATES
     2//53H TYPE   NODE        FORCE X      FORCE Y      FORCE Z
     3                   35H MOMENT X     MOMENT Y     MOMENT Z          )
 2011 FORMAT(1H ,I3,6X,1HI,3X,6F12.3/1H ,9X,1HJ,3X,6F12.3/)
 2013 FORMAT(1H0/
     1  60H SECTION PROPERTIES OTHER THAN SHEAR AREAS MAY NOT BE SPECIF
     2  34HIED AS ZERO. EXECUTION TERMINATED.)
 2020 FORMAT (1H1/30X 33HBEAM ELEMENT NONLINEAR PARAMETERS //
     1  8H    NPAR  4X 8HAXIAL    4X 8HMOMENT    4X 8HMOMENT    4X
     2  8H AXIAL   20X 24HYIELD FUNCTION CONSTANTS /
     3  8H     NC    6X 2HPU 9X 4HMU/Y 8X 4HMU/Z 9X 2HTU 8X 2HA0 6X 2HA1
     4  6X 2HA2 6X 2HA3 6X 2HB0 6X 2HB1 6X 2HB2 6X 2HB3  /)
 2021 FORMAT (I5,3X,4E12.3,8F8.3)
 3000 FORMAT (10I5,2I6,I8,I5)
 4000 FORMAT (23H1BEAM ELEMENT DATA.....  //
     . 5HOBEAM 5X 5HNODES 5X 5H MATL 5H GEOM 5X 10HELEM LOADS 4X    10X
     . 12H END CODES    5X 5H L/NL /
     .                    5H  NC       4X 1HI 4X 1HJ 4X 1HK 5H  NO  5H  NC
     .  4X 1HA 4X 1HB 4X 1HC 4X 1HD 9X 1HI 9X 1HJ 5X 5H  IND )
 4001 FORMAT (10I5,3I10)
 4004 FORMAT(1H ,31HNODAL POINT NUMBERS FOR ELEMENT,I5,36HARE IDENTICAL.
     1 EXECUTION TERMINATED.)
C
      END
```

```
*DECK NEWBM
      SUBROUTINE NEWBM(E,G,RO,COPROP,SFT,NUMFIX,NUMETP)
C
      DIMENSION E(1),G(1),RO(1),COPROP(NUMETP,1),SFT(NUMFIX,1)
      COMMON/EMTX/ LM(24),NC,NS,ASA(24,24),RF(24,4),XM(24),SA(12,24),
     .    SF(12,4),ENPAR(24),S(12,12),F(48),LMS(12),EC(12),T(3,3)
      COMMON/JUNK/ LC(4),JK(6),MELTYP,OL,MATTYP,ILC(4),TS(2,2),LS(4),
     .               EMUL(3,4),R(12),C(12),EL(3,4)
C
C     FORM NEW BEAM STIFFNESS
C
      DO 5 I=1,144
    5 S(I)=0.
      AX=COPROP(MELTYP,1)
      AY=COPROP(MELTYP,2)
      AZ=COPROP(MELTYP,3)
      AAX=COPROP(MELTYP,4)
      AAY=COPROP(MELTYP,5)
      AAZ=COPROP(MELTYP,6)
      SHFY=0.0
      SHFZ=0.0
      ZY=E(MATTYP)/(OL*OL)
      EIY=ZY*AAY
      EIZ=ZY*AAZ
      IF(AY.NE.0.0) SHFY=6.*EIZ/(G(MATTYP)*AY)
      IF(AZ.NE.0.0) SHFZ=6.*EIY/(G(MATTYP)*AZ)
      COMMY=EIY/(1.+2.*SHFZ)
      COMMZ=EIZ/(1.+2.*SHFY)
C
C     FIXED END FORCES IN LOCAL COORDS
C
      DO 73 N=1,4
      M=LC(N)
      IF (M.GT.0)  GO TO 71
      DO 70 I=1,12
   70 SF(I,N)=0.
      GO TO 73
   71 DO 72 I=1,12
   72 SF(I,N)=SFT(M,I)
   73 CONTINUE
C
C     ELEMENT LOCAL FORCES DUE TO GRAVITIES IN 3 DIRECTIONS
C
      DO 75 I=1,12
   75 EL(I)=0.
      ROM=RO(MATTYP)*AX
      DO 80 J=1,4
      DO 80 I=1,3
      XX=0.0
      DO 77 K=1,3
   77 XX=XX+ROM*T(I,K)*EMUL(K,J)
   80 EL(I,J)=XX
C
      DO 100 J=1,4
      K=1
      DO 100 I=1,12,6
      K=-1*K
      SF(I  ,J)=SF(I  ,J)-EL(1,J)*OL/2.0
      SF(I+1,J)=SF(I+1,J)-EL(2,J)*DL/2.0
      SF(I+2,J)=SF(I+2,J)-EL(3,J)*DL/2.0
      SF(I+4,J)=SF(I+4,J)-K*EL(3,J)*CL*OL/12.0
      SF(I+5,J)=SF(I+5,J)+K*EL(3,J)*CL*OL/12.0
  100 CONTINUE
C
C     FORM ELEMENT STIFFNESS IN LOCAL COORDINATES
C
      S(1,1)= E(MATTYP)* AX/OL
      S(4,4)= G(MATTYP)*AAX/OL
      S(2,2)= COMMZ*12./DL
      S(3,3)= COMMY*12./OL
      S(5,5)= COMMY* 4.*CL*(1.+0.5*SHFZ)
      S(6,6)= COMMZ* 4.*CL*(1.+0.5*SHFY)
      S(2,6)= COMMZ* 6.
      S(3,5)=-COMMY* 6.
      DO 102 I=1,6
```

```
      J=I+6
  102 S(J,J)=S(I,I)
      DO 104 I=1,4
      J=I+6
  104 S(I,J)=-S(I,I)
      S(6,12)= S(6,6)*(1.-SHFY)/(2.+SHFY)
      S(5,11)= S(5,5)*(1.-SHFZ)/(2.+SHFZ)
      S(2,12)= S(2,6)
      S(6, 8)=-S(2,6)
      S(8,12)=-S(2,6)
      S(3,11)= S(3,5)
      S(5, 9)=-S(3,5)
      S(9,11)=-S(3,5)
      DO 106 I=2,12
      K=I-1
      DO 106 J=1,K
  106 S(I,J)=S(J,I)
C
C     MODIFY STIFFNESS AND FIXED END FORCES FOR ZERO END CONDITIONS
C
      IF ((JK(1)+JK(2)).EQ.0) GO TO 145
      DO 140 K=1,2
      KK=JK(K)
      KD=100000
      I1=6*(K-1)+1
      I2=I1+5
      DO 140 I=I1,I2
      IF (KK.LT.KD)  GO TO 140
      SII=S(I,I)
      DO 125 N=1,12
  125 R(N)=S(I,N)
      DO 130 M=1,12
      C(M)=S(M,I)/SII
      DO 130 N=1,12
  130 S(M,N)=S(M,N)-C(M)*R(N)
      DO 135 N=1,4
      SFI=SF(I,N)
      DO 135 M=1,12
  135 SF(M,N)=SF(M,N)-C(M)*SFI
  136 KK=KK-KD
  140 KD=KD/10
  145 CONTINUE
C
C     PERFORM LOCAL TO GLOBAL TRANSFORMATION
C
      DO 31 I=1,288
   31 SA(I)=0.
      DO 150 LA=1,10,3
      LB=LA+2
      DO 150 MA=1,10,3
      MB=MA-1
      DO 150 I=LA,LB
      DO 150 JM=1,3
      J=JM+MB
      XX=0.
      DO 151 K=1,3
  151 XX=XX+S(I,K+MB)*T(K,JM)
  150 SA(I,J)=XX
C
C     ELEM STIFF ASA(12,12) AND FIXED END FORCES RF(12) IN GLOBAL COORDS
C
      DO 32 I=1,576
   32 ASA(I)=0.
      DO 160 LA=1,10,3
      LB=LA-1
      DO 160 MA=1,10,3
      MB=MA+2
      DO 160 IL=1,3
      I=IL+LB
      DO 160 J=MA,MB
      XX=0.
      DO 161 K=1,3
  161 XX=XX+T(K,IL)*SA(K+LB,J)
  160 ASA(I,J)=XX
C
      DO 165 LA=1,10,3
      LB=LA-1
      DO 165 IL=1,3
      I=IL+LB
      DO 165 N=1,4
      XX=0.
      DO 162 K=1,3
  162 XX=XX-T(K,IL)*SF(K+LB,N)
  165 RF(I,N)=XX
C
C     FORM MASS MATRIX
C
      XXM =ROM*DL/2.0
      XXMX=XXM*(AAX/AX)
      XXMY=XXM*(DL**2/210.+AAY/(AX*5.0))
      XXMZ=XXM*(DL**2/210.+AAZ/(AX*5.0))
      DO 180 M=1,3
      RXM=XXMX*T(1,M)**2+XXMY*T(2,M)**2+XXMZ*T(3,M)**2
      XM(M   )=XXM
      XM(M+3)=RXM
      XM(M+6)=XXM
  180 XM(M+9)=RXM
      RETURN
      END
```

```
*DECK TRANSFM
      SUBROUTINE TRANSFM (RO,COPROP,NUMETP)
C
      DIMENSION RO(1),COPROP(NUMETP,1)
      COMMON/EMTX/ LM(24),NC,NS,ASA(24,24),RF(24,4),XM(24),SA(12,24),
     .  SF(12,4),ENPAR(24),S(12,12),F(48),LMS(12),EC(12),TI(3,3),TJ(3,3)
      COMMON/JUNK/ LC(4),JK(6),MELTYP,DL,MATTYP,BETA,B,CP,O,RA,AX,
     .                 EMUL(3,4),ILC(4),LS(4),R(12),C(12),EL(3,4)
C
C     PERFORM LOCAL TO GLOBAL TRANSFORMATION
C
      DO 31 I=1,288
   31 SA(I)=0.
      DO 150 LA=1,10,3
      LB=LA+2
      DO 150 MA=1,10,3
      MB=MA-1
      DO 150 I=LA,LB
      DO 150 JM=1,3
      J=JM+MB
      XX=0.
      IF (J.GT.6) GO TO 152
      DO 151 K=1,3
  151 XX=XX+S(I,K+MB)*TI(K,JM)
      GO TO 150
  152 DO 153 K=1,3
  153 XX=XX+S(I,K+MB)*TJ(K,JM)
  150 SA(I,J)=XX
C
      DO 32 I=1,576
   32 ASA(I)=0.
C
      DO 160 LA=1,10,3
      LB=LA-1
      DO 160 MA=1,10,3
      MB=MA+2
      DO 160 IL=1,3
      I=IL+LB
      DO 160 J=MA,MB
      XX=0.
      IF (I.GT.6) GO TO 162
      DO 161 K=1,3
  161 XX=XX+TI(K,IL)*SA(K+LB,J)
      GO TO 160
  162 DO 163 K=1,3
  163 XX=XX+TJ(K,IL)*SA(K+LB,J)
  160 ASA(I,J)=XX
C
      DO 170 LA=1,10,3
      LB=LA-1
      DO 170 IL=1,3
      I=IL+LB
      DO 170 N=1,4
      XX=0.
      IF (I.GT.6) GO TO 172
      DO 171 K=1,3
  171 XX=XX-TI(K,IL)*SF(K+LB,N)
      GO TO 170
  172 DO 173 K=1,3
  173 XX=XX-TJ(K,IL)*SF(K+LB,N)
  170 RF(I,N)=XX
C
C     FORM MASS MATRIX
C
      XL  =RA*BETA
      XXM =RO(MATTYP)*AX*XL/2.0
      XXMX=XXM*(COPROP(MATTYP,4)/AX)
      XXMY=XXM*(XL**2/210.+COPROP(MATTYP,5)/(5.C*AX))
      XXMZ=XXM*(XL**2/210.+COPROP(MATTYP,6)/(5.C*AX))
      DO 180 M=1,3
      XM(M   )=XXM
      XM(M+6)=XXM
      XM(M+3)=XXMX*TI(1,M)**2+XXMY*TI(2,M)**2+XXMZ*TI(3,M)**2
  180 XM(M+9)=XXMX*TJ(1,M)**2+XXMY*TJ(2,M)**2+XXMZ*TJ(3,M)**2
      RETURN
      END
```

```
*DECK CBEAM
      SUBROUTINE CBEAM
C
      COMMON A(1)
      COMMON/EPAR/ NPAR(14),NUMNP,NELTYP,NUMEL,NUMNEL,NEQ,MBAND,MTOT,
     .             N1,N2,N3,N4,N5,N6
      COMMON/JUNK/ STR(4),PP,L,K,NTAG,NDYN,SIG(12),EXRA(184)
C
C
      N7=N6+NPAR(5)
      N8=N7+NPAR(5)
      N9=N8+NPAR(5)
      N10=N9+NPAR(4)*12
      N11=N10+NPAR(3)*6
      N12=N11+NPAR(6)
      N13=N12+NPAR(7)*12
      IF (N13.GT.MTOT) CALL ERROR (1,N13-MTOT,7HCBEAM  )
      CALL CTEAM (NPAR(2),NPAR(3),NPAR(4),NPAR(5),NPAR(6),NPAR(7),
     .             A(N1),A(N2),A(N3),A(N4),A(N5),A(N6),A(N7),A(N8),
     .             A(N9),A(N10),A(N11),A(N12),NUMNP,MBAND,NUMEL)
      RETURN
      END
```

```
*DECK CBEAM
      SUBROUTINE CBEAM (NCBEAM,NUMETP,NUMFIX,NUMMAT,NUMRAD,NUMNPAR,
     .                  ID,X,Y,Z,INC,E,G,RO,SFT,CCPROP,RAD,ENPROP,
     .                  NUMNP,MBAND,NUMEL)
C
C     FORM 3-D CURVED BEAM STIFFNESS AND STRESS-DISP. ARRAYS
C
      DIMENSION ID(NUMNP,1),X(1),Y(1),Z(1),INC(1),E(1),G(1),RO(1),
     .          SFT(NUMFIX,1),CCPROP(NUMETP,1),RAD(1),ENPROP(NUMNPAR,1),
     .          STIF(722),LMS(12),EC(12),TI(3,3),TJ(3,3)
      COMMON/EMTX/ LM(24),ND,NS,ASA(24,24),RF(24,4),XM(24),SA(12,24),
     .             SF(12,4),ENPAR(24),S(12,12),F(48),TTT(72)
      COMMON/JUNK/ LC(4),JK(6),MELTYP,DL,MATTYP,BETA,B,OP,O,RA,AREA,
     .             EMUL(3,4),ILC(4),LS(4)
      EQUIVALENCE (STIF,LM),(LMS,TTT(1)),(EC,TTT(13)),(TI,TTT(25)),
     .            (TJ,TTT(34))
C
      WRITE (6,2005) NCBEAM,NUMETP,NUMFIX,NUMMAT,NUMRAD,NUMNPAR
      DO 5 I=1,1346
    5 STIF(I)=0.
C
C     READ AND PRINT RADIUS OF CURVATURE DATA
C
      WRITE (6,2000)
      DO 8 I=1,NUMRAD
      READ (5,1000) N,RAD(N)
      IF (RAD(N).NE.0.0) GO TO 7
      WRITE (6,2014)
      CALL EXIT
    7 WRITE (6,2015) N,RAD(N)
    8 CONTINUE
C
C     READ AND PRINT MATERIAL PROPERTY DATA
C
      WRITE (6,2001)
      DO 10 I=1,NUMMAT
      READ  (5,1001) N,E(N),G(N),RO(N)
      WRITE (6,2002) N,E(N),G(N),RO(N)
   10 G(N)=0.5*E(N)/(1.+G(N))
C
C     READ AND PRINT CROSS SECTIONAL PROPERTIES
C
      WRITE (6,2003)
      DO 30 I=1,NUMETP
      READ  (5,1002) N,(CCPROP(N,J),J=1,6)
      IF((CCPROP(N,1).NE.0.0).AND.(CCPROP(N,4).NE.0.0).AND.
     1   (CCPROP(N,5).NE.0.0).AND.(CCPROP(N,6).NE.0.0))  GO TO 20
      WRITE (6,2013)
      CALL EXIT
   20 WRITE (6,2004) N,(CCPROP(N,J),J=1,6)
   30 CONTINUE
C
C     ELEMENT LOAD MULTIPLIERS
C
      READ  (5,1006) ((EMUL(I,J),J=1,4),I=1,3)
      WRITE (6,2006) ((EMUL(I,J),J=1,4),I=1,3)
C
C     READ AND PRINT FIXED END FORCES IN LOCAL COORDINATES
C
      IF(NUMFIX .EQ. 0) GO TO 56
      WRITE (6,2010)
      DO 55 I=1,NUMFIX
      READ  (5,1005) N,(SFT(N,J),J=1,12)
   55 WRITE (6,2011) N,(SFT(N,J),J=1,12)
   56 CONTINUE
C
C     READ AND PRINT ELEMENT NONLINEAR PARAMETERS
C
      IF (NUMNPAR.EQ.0) GO TO 59
      WRITE(6,2020)
      DO 58 I=1,NUMNPAR
   58 READ (5,1007) N,(ENPROP(N,J),J=1,12)
      WRITE(6,2021) (N,(ENPROP(N,J),J=1,12),N=1,NUMNPAR)
   59 CONTINUE
C
C     READ AND PRINT ELEMENT DATA FOR EACH ELEMENT
C
      WRITE (6,4000)
      L=0
   60 READ (5,3000) INEL,INI,INJ,INK,IMAT,IMEL,ILC,INELKI,INELKJ,IRAD,IQ
      IF (IQ.GT.NUMNPAR) CALL ERROR (3,INEL,7HCBEAM  )
      L=L+1
      ML=INEL-L
      IF (ML)  66,67,66
   66 CALL ERROR (4,INEL,7HCBEAM  )
   67 NEL=INEL
      NI=INI
      NJ=INJ
      NK=INK
      MATTYP=IMAT
      MELTYP=IMEL
      DO 68 I=1,4
   68 LC(I)=ILC(I)
      NEKODI=INELKI
      NEKODJ=INELKJ
      NR=IRAD
      NINO=IQ
      WRITE (6,4001) NEL,NI,NJ,NK,MATTYP,MELTYP,LC,NEKODI,NEKODJ,NR,NINO
C
C     FORM GLOBAL TO LOCAL COORDINATE TRANSFORMATION.
C
   74 DX=X(NJ)-X(NI)
      DY=Y(NJ)-Y(NI)
      DZ=Z(NJ)-Z(NI)
      DL=SQRT(DX*DX+DY*DY+DZ*DZ)
      IF(DL) 75,75,76
   75 CALL ERROR (5,NEL,7HCBEAM  )
   76 RA=RAD(NR)
      ARGU=DL/(2.0*RA)
      BETA=2.0*ASIN(ARGU)
      B =SIN(BETA)
      CP=COS(BETA)
```

```
      O =1.0-OP
      BX=X(NI)-X(NK)
      BY=Y(NI)-Y(NK)
      BZ=Z(NI)-Z(NK)
      BB=BX*BX+BY*BY+BZ*BZ
      BB=SCRT(BB)
      IF (BB.GT.0.0) GO TO 77
      CALL ERROR (6,NEL,7HCBEAM  )
   77 CX=CY*BZ-CZ*BY
      CY=CZ*BX-CX*BZ
      CZ=OX*BY-CY*BX
      CC=CX*CX+CY*CY+CZ*CZ
      CC=SCRT(CC)
      BX=BX/BB
      BY=BY/BB
      BZ=BZ/BB
      CX=CX/CC
      CY=CY/CC
      CZ=CZ/CC
      AX=BY*CZ-BZ*CY
      AY=BZ*CX-BX*CZ
      AZ=BX*CY-BY*CX
C
      TI(1,1)=AX
      TI(1,2)=AY
      TI(1,3)=AZ
      TI(2,1)=BX
      TI(2,2)=BY
      TI(2,3)=BZ
      TI(3,1)=CX
      TI(3,2)=CY
      TI(3,3)=CZ
C
      TJ(1,1)=AX*CP-BX*B
      TJ(1,2)=AY*CP-BY*B
      TJ(1,3)=AZ*CP-BZ*B
      TJ(2,1)=AX*B+BX*OP
      TJ(2,2)=AY*B+BY*CP
      TJ(2,3)=AZ*B+BZ*CP
      TJ(3,1)=CX
      TJ(3,2)=CY
      TJ(3,3)=CZ
C
C     CHECK IF NEW STIFFNESS NEEOEO
C
      IF (NEL.EC.1) GO TO 80
      IF (MK.NE.NR)  GO TC 80
      IF  (ABS(DS-DL).GT.DL/100.)  GC TO 80
      IF ((MT.NE.MATTYP).CR.(ME.NE.MELTYP)) GC TO 80
      IF ((JK(1).NE.NEKCCI).CR.(JK(2).NE.NEKOCJ)) GO TO BC
      DO 79 I=1,4
      IF (LS(I).NE.LC(I)) GO TO 80
   79 CONTINUE
      GC TC 100
C
   80 DS=DL
      MT=MATTYP
      ME=MELTYP
      MR=NR
      DO 85 I=1,4
   85 LS(I)=LC(I)
      JK(1)=NEKODI
      JK(2)=NEKODJ
C
C     FORM NEW CURVEO BEAM STIFFNESS
C
      CALL NEWCBM (E,G,RC,COPROP,SFT,RAO,NUMFIX,NUMETP)
C
  100 CALL TRANSFM (RC,COPROP,NUMETP)
C
C     FORM ELEMENT LOCATION MATRIX
C
      DO 170 M=1,6
      LM(M)=IO(NI,M)
      LM(M+12)=0
      LM(M+18)=0
  170 LM(M+6)=ID(NJ,M)
      NS=12
      NO=12
C
C     TRANSFORM TO MASTER OEGREES OF FREEDOM
C
      CALL SLAVE (X,Y,Z,IC,NUMNP,NI,NJ)
C
C     WRITE ELEMENT INFORMATION ON TAPE
C
      CALL WRITEF (MBANO,NDIF)
C
C     SET NONLINEAR ELEMENT INOICATOR AND STORE NONLINEAR PARAMETERS
C
      NN=NUMEL+NEL
      IF (NINC.LE.0) GO TO 200
      INC(NN)=3
      DC 190 I=1,12
  190 ENPAR(I)=ENPROP(NINC,I)
      MTYPE=3
      WRITE (3) MTYPE,LM,NC,NS,ASA,SA,S,ENPAR,TTT
      GC TC 250
  200 INC(NN)=-3
C
C     CHECK FOR LAST ELEMENT
C
  250 IF (NCBEAM-NEL) 66,500,60
  500 RETLRN
C
 1000 FORMAT(I5,F10.0)
 1001 FORMAT(I5,3F10.0)
 1002 FORMAT(I5,6F10.C)
 1005 FORMAT(I5,6F10.C/F15.0,5F10.0)
 1006 FORMAT (4F10.0)
 1007 FORMAT (I5,4F10.0/8F10.0)
 2000 FORMAT (26H1RADII OF CURVED BEAMS....  //
```

76.

```
     .        27H RADIUS         RADIUS OF       /
     .        27H NUMBER         CURVATURE      /)
2001 FORMAT (////24H MATERIAL PROPERTIES....  //
     .        54H MATERIAL    YOUNG S      POISSON S            MASS       /
     .        54H NUMBER      MODULUS       RATIO            DENSITY      /)
2002 FORMAT(1H ,I5,3X,F12.0,F14.5,F14.5)
2003 FORMAT (38H1CURVED BEAM GEOMETRIC PROPERTIES.....  //
    1   48H ELEMENT       AREA         AREA         AREA
    2  60H INERTIA      INERTIA     INERTIA
    3 / 48H  TYPE          X            Y            Z
    4                30H    X            Y            Z               /)
2004 FORMAT(1H ,I5,2X,6F12.3)
2005 FORMAT(39H1.......THREE DIM. CURVED BEAM ELEMENTS///
    .  36H  NUMBER OF CURVED BEAMS             =,I5//
    .  36H  NUMBER OF SECTIONAL PROPERTY SETS=,I5//
    .  36H  NUMBER OF FIXED END FORCE SETS    =,I5//
    .  36H  NUMBER OF MATERIALS               =,I5//
    .  36H  NUMBER OF RADII                   =,I5//
    .  36H  NUMBER OF N/L PARAMETER SETS      =,I5)
2006 FORMAT (///30H ELEMENT LOAD MULTIPLIERS...../12X,1HA,14X,1HB,14X,
    .  1HC,14X,1HD/6H X-DIR 4E15.6/6H Y-DIR 4E15.6/6H Z-DIR 4E15.6/  )
2010 FORMAT (1H1
    1  30X40H FIXED END FORCES IN LOCAL COORDINATES
    2//53H TYPE   NODE        FORCE X      FORCE Y      FORCE Z
    3                     35H MOMENT X     MOMENT Y     MOMENT Z          //)
2011 FORMAT(1H ,I3,6X,1HI,3X,6F12.3/1H ,9X,1HJ,3X,6F12.3/)
2013 FORMAT(1H0/
    1  60H SECTION PROPERTIES OTHER THAN SHEAR AREAS MAY NOT BE SPECIF
    2  34HIED AS ZERO. EXECUTION TERMINATED.)
2014 FORMAT(1H0/
    1  60H RADIUS OF CURVATURE MAY NOT BE SPECIFIED
    2  34H     AS ZERO. EXECUTION TERMINATED.)
2015 FORMAT (I5,F20.5)
2020 FORMAT (1H1/30X 40HCURVED BEAM ELEMENT NONLINEAR PARAMETERS  //
    .  8H NL PAR  4X 8HAXIAL     4X 8HMOMENT   4X 8HMOMENT   4X
    .  8HTORSION  20X 24HYIELD FUNCTION CONSTANTS /
    .  8H     NC    6X 2HPL 9X 4HMU/Y 8X 4HMU/Z 9X 2HTU 8X 2HA0 6X 2HA1
    .  6X 2HA2 6X 2HA3 6X 2HB0 6X 2HB1 6X 2HB2 6X 2HB3  /)
2021 FORMAT (I5,3X,4E12.3,8F8.3)
3000 FORMAT (10I5,2I6,I8,I5)
4000 FORMAT (30H1CURVED BEAM ELEMENT DATA.....  //
    . 5HBEAM 5X 5HNODES 5X 5H MATL 5H GEOM 5X 10HELEM LOADS 4X    10X
    . 12H  END CODES   3X 6HRADIUS 3X 5H NINO /
    .                      5H  NO      4X 1HI 4X 1HJ 4X 1HK 5H  NC  5H  NC
    .  4X 1HA 4X 1HB 4X 1HC 4X 1HD 9X 1HI 9X 1HJ   8X 2HNO 8H     NC /)
4001 FORMAT (10I5,2I10,I10,I8)
4004 FORMAT(1H ,31HNODAL POINT NUMBERS FOR ELEMENT,I5,36HARE IDENTICAL.
    1 EXECUTION TERMINATED.)
C
      END
```

77.

```
*DECK NEWCBM
      SUBROUTINE NEWCBM (E,G,RC,COPROP,SFT,RAC,NUMFIX,NUMETP)
C
      DIMENSION E(1),G(1),RC(1),COPROP(NUMETP,1),SFT(NUMFIX,1),RAC(1)
      COMMON/EMTX/ LM(24),NC,NS,ASA(24,24),RF(24,4),XM(24),SA(12,24),
     . SF(12,4),ENPAR(24),S(12,12),F(48),LMS(12),EC(12),TI(3,3),TJ(3,3)
      COMMON/JUNK/ LC(4),JK(6),MELTYP,OL,MATTYP,BETA,B,OP,D,RA,AX,
     .              EMUL(3,4),ILC(4),LS(4),R(12),C(12),EL(3,4),V(12,4)
C
C     FORM NEW CURVED BEAM STIFFNESS
C
      DO 5 I=1,144
    5 S(I)=0.
      AX=COPROP(MELTYP,1)
      AY=COPROP(MELTYP,2)
      AZ=COPROP(MELTYP,3)
      AAX=COPROP(MELTYP,4)
      AAY=COPROP(MELTYP,5)
      AAZ=COPROP(MELTYP,6)
C
      RA2=RA*RA
      RA3=RA2*RA
      EIY=E(MATTYP)*AAY
      EIZ=E(MATTYP)*AAZ
      PHIZ=AAZ/(AX*RA2)
      PHIY=EIY/(G(MATTYP)*AAX)
C
      IF (AY.LE.0.) GO TO 20
      ZETAZ=EIZ/(AY*G(MATTYP)*RA2)
      GO TO 21
   20 ZETAZ=0.
   21 IF (AZ.LE.0.) GO TO 30
      ZETAY=EIY/(AZ*G(MATTYP)*RA2)
      GO TO 31
   30 ZETAY=0.
   31 CONTINUE
      COMMY=RA3/EIY
      COMMZ=RA3/EIZ
C
C     FIXED END FORCES IN LOCAL COORDINATES
C
      DO 73 N=1,4
      M=LC(N)
      IF (M.GT.0)  GO TO 71
      DO 70 I=1,12
   70 SF(I,N)=0.
      GO TO 73
   71 DO 72 I=1,12
   72 SF(I,N)=SFT(M,I)
   73 CONTINUE
C
C     FORM ELEMENT STIFFNESS IN LOCAL COORDINATES
C
      AA=BETA*0.5-0.5*B*OP
      CC=BETA*0.5+0.5*B*OP
      EE=0.5*B*B
```

```
C
      F11=COMMZ*(BETA+CC-2.C*B+PHIZ*CC+ZETAZ*AA)
      F12=COMMZ*(C-EE-PHIZ*EE+ZETAZ*EE)
      F16=(COMMZ/RA)*(B-BETA)
      F22=COMMZ*(AA+PHIZ*AA+ZETAZ*CC)
      F26=(COMMZ/RA)*(-D)
C
      F33=COMMY*(AA+PHIY*(BETA+CC-2.C*B)+ZETAY*BETA)
      F34=(COMMY/RA)*(AA-PHIY*(B-CC))
      F35=(COMMY/RA)*(EE+PHIY*(D-EE))
      F44=(COMMY/RA2)*(AA+PHIY*CC)
      F45=(COMMY/RA2)*(EE-PHIY*EE)
      F55=(COMMY/RA2)*(CC+PHIY*AA)
      F66=(COMMZ/RA2)*BETA
C
      U=F11*F22*F66+2.0*F12*F16*F26-F22*F16*F16-F11*F26*F26-F66*F12*F12
      W=F33*F44*F55+2.0*F34*F45*F35-F44*F35*F35-F33*F45*F45-F55*F34*F34
C
      S(1,1)= (F22*F66-F26*F26)/U
      S(1,2)=-(F12*F66-F16*F26)/U
      S(1,6)= (F12*F26-F22*F16)/U
      S(2,2)= (F11*F66-F16*F16)/U
      S(2,6)=-(F11*F26-F12*F16)/U
      S(6,6)= (F11*F22-F12*F12)/U
C
      S(3,3)= (F44*F55-F45*F45)/W
      S(3,4)=-(F34*F55-F35*F45)/W
      S(3,5)= (F34*F45-F44*F35)/W
      S(4,4)= (F33*F55-F35*F35)/W
      S(4,5)=-(F33*F45-F35*F34)/W
      S(5,5)= (F33*F44-F34*F34)/W
C
      S(1, 7)=-S(1,1)*DP+S(1,2)*B
      S(1, 8)=-S(1,1)*B-S(1,2)*DP
      S(1,12)= S(1,1)*RA*C+S(1,2)*RA*B-S(1,6)
      S(2, 7)=-S(1,2)*DP+S(2,2)*B
      S(2, 8)=-S(1,2)*B-S(2,2)*DP
      S(2,12)= S(1,2)*RA*C+S(2,2)*RA*B-S(2,6)
      S(3, 9)=-S(3,3)
      S(3,10)= S(3,3)*RA*C-S(3,4)*DP+S(3,5)*B
      S(3,11)=-S(3,3)*RA*B-S(3,4)*B-S(3,5)*DP
      S(4, 9)=-S(3,4)
      S(4,10)= S(3,4)*RA*C-S(4,4)*DP+S(4,5)*B
      S(4,11)=-S(3,4)*RA*B-S(4,4)*B -S(4,5)*DP
      S(5, 9)=-S(3,5)
      S(5,10)= S(3,5)*RA*C-S(4,5)*DP+S(5,5)*B
      S(5,11)=-S(3,5)*RA*B-S(4,5)*B-S(5,5)*DP
      S(6, 7)=-S(1,6)*DP+S(2,6)*B
      S(6, 8)=-S(1,6)*B-S(2,6)*DP
      S(6,12)= S(1,6)*RA*C+S(2,6)*RA*B-S(6,6)
C
      S( 7, 7)= S(1,1)
      S( 7, 8)=-S(1,2)
      S( 7,12)= S(1,6)
      S( 8, 8)= S(2,2)
      S( 8,12)=-S(2,6)
      S( 9, 9)= S(3,3)
      S( 9,10)= S(3,4)
      S( 9,11)=-S(3,5)
      S(10,10)= S(4,4)
      S(10,11)=-S(4,5)
      S(11,11)= S(5,5)
      S(12,12)= S(6,6)
C
      DO 106 I=2,12
      K=I-1
      DO 106 J=1,K
  106 S(I,J)=S(J,I)
C
C     ELEMENT LOCAL FORCES DUE TO GRAVITIES IN 3 DIRECTIONS
C
      DO 107 I=1,60
  107 EL(I)=0.
      RCM=RO(MATTYP)*AX
      DO 110 J=1,4
      DO 110 I=1,3
      XX=0.
      DO 109 K=1,3
  109 XX=XX+RCM*TI(I,K)*EMUL(K,J)
  110 EL(I,J)=XX
C
      V11=COMMZ*((2.0*D-0.75*B*B-BETA*B+0.5*BETA*B*DP+0.25*BETA*BETA)
     .             +PHIZ*(C.5*BETA*B*DP+0.25*BETA*BETA-0.25*B*B))
      V12=COMMZ*((3.0*B-BETA*DP-0.75*B*DP+0.5*BETA*DP*DP-0.75*BETA)
     .            -PHIZ*(0.5*BETA*B*B+0.25*B*DP))
      V21=COMMZ*((0.25*BETA-0.75*B*DP+0.5*BETA*DP*DP)
     .            -PHIZ*(0.5*BETA+0.25*B*DP-0.5*BETA*DP*DP))
      V22=COMMZ*((0.25*BETA*BETA-0.5*BETA*B*DP+C.5*B*B-0.25*DP*DP+DP
     .      -0.75)+PHIZ*(C.25*BETA*BETA-0.5*BETA*B*DP+0.25*B*B))
      V3 =COMMY*((1.0-DP-0.5*B*B)+PHIY*(C.5*BETA*BETA-BETA*B+0.5*B*B))
      V4 =(COMMY/RA)*((1.0-DP-0.5*B*B)-PHIY*(DP+BETA*B-0.5*B*B-1.0))
      V5 =(COMMY/RA)*((B-C.5*BETA-0.5*B*DP)
     .                +PHIY*(B-C.5*BETA-BETA*DP+0.5*B*DP))
      V61=(COMMZ/RA)*(BETA*B-2.0+2.C*DP)
      V62=(COMMZ/RA)*(BETA+BETA*DP-2.C*B)
C
      R71=-RA*BETA*DP
      R72= RA*BETA*B
      R81=-R72
      R82= R71
      R9 =-RA*BETA
      R10= RA2*(BETA-B)
      R11=-RA2*C
      R121=RA2*(B-BETA*DP)
      R122=RA2*(BETA*B+DP-1.0)
C
      DO 120 J=1,4
      V(1,J)=EL(1,J)*V11+EL(2,J)*V12
      V(2,J)=EL(1,J)*V21+EL(2,J)*V22
      V(3,J)=EL(3,J)*V3
      V(4,J)=EL(3,J)*V4
      V(5,J)=EL(3,J)*V5
```

```
      V(6,J)=FL(1,J)*V61+EL(2,J)*V62
C
      SF( 7,J)=SF( 7,J)+EL(1,J)*R71+EL(2,J)*R72
      SF( 8,J)=SF( 8,J)+EL(1,J)*R81+EL(2,J)*R82
      SF( 9,J)=SF( 9,J)+EL(3,J)*R9
      SF(10,J)=SF(10,J)+EL(3,J)*R10
      SF(11,J)=SF(11,J)+EL(3,J)*R11
      SF(12,J)=SF(12,J)+EL(1,J)*R121+EL(2,J)*R122
  120 CONTINUE
C
      DO 124 I=1,12
      DO 124 L=1,4
      XX=0.
      DO 123 K=1,6
  123 XX=XX-S(I,K)*V(K,L)
  124 SF(I,L)=SF(I,L)+XX
C
C     MODIFY STIFFNESS AND FIXED END FORCES FOR ZERO END CONDITIONS
C
      IF ((JK(1)+JK(2)).EQ.0) GO TO 145
      DO 140 K=1,2
      KK=JK(K)
      KD=100000
      I1=6*(K-1)+1
      I2=I1+5
      DO 140 I=I1,I2
      IF (KK.LT.KD)  GO TO 140
      SII=S(I,I)
      DO 125 N=1,12
  125 R(N)=S(I,N)
      DO 130 M=1,12
      C(M)=S(M,I)/SII
      DO 130 N=1,12
  130 S(M,N)=S(M,N)-C(M)*R(N)
      DO 135 N=1,4
      SFI=SF(I,N)
      DO 135 M=1,12
  135 SF(M,N)=SF(M,N)-C(M)*SFI
  136 KK=KK-KD
  140 KD=KD/10
  145 CONTINUE
C
      RETURN
      END
```

```
*DECK BOUND
      SUBROUTINE BOUND
C
      COMMON A(1)
      COMMON/EPAR/ NPAR(14),NUMNP,NELTYP,NUMEL,NUMNEL,NEQ,MBAND,MTOT,
     .             N1,N2,N3,N4,N5,N6
      COMMON/JUNK/ STR(4),MM,L,K,NTAG,NDYN,SIG(12),EXRA(184)
C
      N7=N6+NPAR(3)*6
      N8=N7+NPAR(4)*12
      IF (N8.GT.MTOT) CALL ERROR (1,N8-MTOT,7HBOUND  )
      CALL BIND (NPAR(2),NPAR(3),NPAR(4),A(N1),A(N2),A(N3),A(N4),A(N5),
     .           A(N6),A(N7),NUMNP,MBAND,NUMEL)
      RETURN
      END
```

```
*DECK BIND
      SUBROUTINE BIND (NBOUND,NSTIF,NUMNPAR,IC,X,Y,Z,IND,STIF,ENPROP,
     .                 NUMNP,MBAND,NUMEL)
C
      DIMENSION ID(NUMNP,1),X(1),Y(1),Z(1),IND(1),STIF(NSTIF,1),
     .          ENPROP(NUMNPAR,1),ENPAR(24),T(3,3)
      COMMON/EMTX/ LM(24),ND,NS,ASA(24,24),P(24,4),XM(24),SA(12,24),
     .             SF(12,4),SY(6),EP(6),UE(6),PAR(6),S(12,12),F(48),
     .             TTT(72)
      COMMON/JUNK/ DX,DY,DZ,DD,AX,AY,AZ,AA,BX,BY,BZ,BB,SPRING(6),NN
      EQUIVALENCE (ENPAR,SY),(T,TTT)
C
C     FORM ELEMENT STIFFNESS OF BOUNDARY SPRING ELEMENTS
C
      DO 5 I=1,1346
    5 LM(I)=0.
      ND=6
      NS=6
      NE=0
      WRITE(6,2000) NBOUND,NSTIF,NUMNPAR
C
C     READ AND PRINT SPRING STIFNESS SETS
C
      READ (5,1010) (N,(STIF(N,J),J=1,6),N=1,NSTIF)
      WRITE(6,2001)
      WRITE(6,2010) (N,(STIF(N,J),J=1,6),N=1,NSTIF)
C
C     READ AND PRINT NONLINEAR ELEMENT PARAMETERS
C
```

```
      IF (NUMNPAR.EQ.D) GO TO 9
      REAC (5,1C2D) IN,(ENPROPIN,J),J=1,12),N=1,NUMNPAR)
      WRITE(6,2002)
      WRITEI6,201D) IN,(ENPRCPIN,J),J=1,6 ),N=1,NUMNPAR)
      WRITE(6,2003)
      WRITEI6,2010) (N,IENPROPIN,J),J=7,12),N=1,NUMNPAR)
    9 CONTINUE
C
C     READ ANC PRINT ELEMENT DATA---CATA NEEC TC BE SUPPLIED FOR EACH
C
      WRITE(6,2004)
   1D NE=NE+1
      READI5,103D) INE,NI,NJ,NK,MS,NINO
      IF IINE.NE.NE) CALL ERRCR (4,INE,7HBOLNC  )
      IF ININC.GT.NUMNPAR) CALL ERRCR I3,INE,7HBCUNO  )
      WRITEI6,204D) NE,N1,NJ,NK,MS,NIND
C
C     FCRM LOCAL TO GLOBAL TRANSFORMATION
C
      DX=XINJ)-XINI)
      DY=YINJ)-YINI)
      CZ=Z(NJ)-ZINI)
      CC=SCRTIDX*CX+DY*DY+DZ*CZ)
      IF (CC.LE.D.) CALL ERROR I5,INE,7HBCUND  )
      AX=XINK)-XINI)
      AY=Y(NK)-Y(NI)
      AZ=Z(NK)-Z(NI)
      BX=CY*AZ-CZ*AY
      BY=CZ*AX-CX*AZ
      BZ=CX*AY-DY*AX
      BB=SCRTIBX*BX+BY*BY+BZ*BZ)
      IF (BB.LE.O.D) CALL ERROR I6,NE,7HBOUND  )
C
      T(3,1)=BX/BB
      T(3,2)=BY/BB
      T(3,3)=BZ/BB
      T(1,1)=CX/DD
      T(1,2)=DY/DD
      T(1,3)=DZ/DD
      T(2,1)=TI3,2)*T(1,3)-TI3,3)*T(1,2)
      T(2,2)=TI3,3)*T(1,1)-T(3,1)*T(1,3)
      T(2,3)=T(3,1)*T(1,2)-T(3,2)*TI1,1)
C
C     FCRM BOUNCARY STIFFNESSES IN LCCAL COORDINATE SYSTEM
C
      DO 100 I=1,144
  100 SII)=0.
      DO 110 I=1,6
      SPRING(I)=STIF(MS,I)
      S(I,I)=SPRING(I)
  110 CCNTINUE
C
C     FORM LUCAL TO GLOBAL STRESS ARRAY
C
      DO 120 I=1,288
  12D SA(I)=D.
      DO 15D LA=1,6,3
      LB=LA+2
      DD 150 MA=1,6,3
      MB=MA-1
      DO 150 I=LA,LB
      DD 150 JM=1,3
      J=JM+MB
      XX=D.
      DO 151 K=1,3
      YY=SII,K+MB)
      IF (YY.EQ.D.) GC TO 151
      XX=XX+YY*TIK,JM)
  151 CONTINUE
  15C SA(I,J)=XX
C
C     FCRM ELEMENT STIFFNESSES IN GLCBAL COORDINATE SYSTEM
C
      DO 155 I=1,576
  155 ASA(I)=0.
      DC 160 LA=1,6,3
      LB=LA-1
      DO 160 MA=1,6,3
      MB=MA+2
      DC 160 IL=1,3
      I=IL+LB
      DC 16D J=MA,MB
      XX=0.
      DO 161 K=1,3
      YY=SAIK+LB,J)
      IF (YY.EQ.0.) GC TO 161
      XX=XX+T(K,IL)*YY
  161 CONTINUE
  160 ASA(I,J)=XX
C
C     FCRM ELEMENT LOCATICN MATRIX
C
      DO 17D I=1,6
      LM(I)=IOINI,I)
      LM(I+6)=0
      LM(I+12)=0
  17D LM(I+18)=0
C
C     WRITE ELEMENT INFORMATION ON TAPE
C
      CALL WRITET (MBAND,NDIF)
C
C     SET NONLINEAR ELEMENT INDICATOR AND STORE NONLINEAR PARAMETERS
C
      NN=NUMEL+NE
      IF (NINC.EQ.O) GO TO 200
      INC(NN)=4
      DO 18D I=1,6
      II=I+6
      SY(I)=ENPROP(NINC,I)
      EP(I)=ENPROPININD,II)
      UE(I)=SYII)/SPRINGII)
```

```
  180 CONTINUE
      MTYPE=4
      WRITE (3) MTYPE,LM,NO,NS,ASA,SA,S,ENPAR,TTT
      GO TO 250
  200 IND(NN)=-4
C
  250 IF (NC.LT.NBOUNC) GO TO 10
      RETURN
C
 1010 FORMAT (I5,6F10.0)
 1020 FORMAT (I5,6F10.0/5X,6F10.0)
 1030 FORMAT (6I5)
C
 2000 FORMAT (24H1......BOUNDARY ELEMENTS   ///
     .  28H NUMBER OF ELEMENTS          =,I5//
     .  28H NUMBER OF STIFFNESS SETS   =,I5//
     .  28H NUMBER OF N/L PAR. SETS    =,I5)
 2001 FORMAT (4H1SET 20X 31HSTIFFNESSES OF BOUNDARY SPRINGS /
     .  4H NC  4X 2HR1 10X 2HR2 10X 2HR3 10X 2HM1 10X 2HM2 10X 2HM3 /)
 2002 FORMAT (4H1SET 20X 35HYIELDING FORCES OF BOUNDARY SPRINGS /
     .  4H NC  4X 2HR1 10X 2HR2 10X 2HR3 10X 2HM1 10X 2HM2 10X 2HM3 /)
 2003 FORMAT (4H1SET 20X 39HPLASTIC STIFFNESSES OF BOUNDARY SPRINGS /
     .  4H NC  4X 2HR1 10X 2HR2 10X 2HR3 10X 2HM1 10X 2HM2 10X 2HM3 /)
 2004 FORMAT (5H1ELE. 5X 5HNODES 5X 5H MATL 5X 5H NINO /
     .  5H  NO  4X 1HI 4X 2HJ 4X 1HK 5H  NO  5X 5H  NO  /)
 2010 FORMAT (I4,6E12.3)
 2040 FORMAT (5I5,I10)
C
      END


*DECK EXPJT
      SUBROUTINE EXPJT
C
      COMMON/EPAR/ NPAR(14),NUMNP,NELTYP,NUMEL,NUMNEL,NEQ,MBAND,MTOT,
     .             N1,N2,N3,N4,N5,N6
      COMMON/JUNK/ STR(4),MM,L,K,NTAC,NCYN,SIG(12),EXRA(184)
      COMMON A(1)
C
      N7=N6+NPAR(4)*7
      N8=N7+NPAR(4)
      N9=N8+NPAR(4)*6
      N10=N9+NPAR(3)*6
      IF(N10.GT.MTOT) CALL ERROR (1,N10-MTOT,7HEXPJB    )
      CALL XPJT (NPAR(2),NPAR(3),NPAR(4),A(N1),A(N2),A(N3),A(N4),A(N5),
     .           A(N6),A(N7),A(N8),A(N9),NUMNP,MBAND,NUMEL)
C
      RETURN
      END
```

```
*DECK XPJT
      SUBROUTINE XPJT (NEXPJ ,NSTIF,NUMNPAR,ID,X,Y,Z,INO,ENPRCP,NT,XT,
     .                 STIF,NUMNP,MBAND,NUMEL)
      DIMENSION  ID(NUMNP,1),X(1),Y(1),Z(1),INC(1),ENPRCP(NUMNPAR,1),
     .           NT(1),XT(NUMNPAR,1),STIF(NSTIF,1),ENPAR(24),AT(6,6),
     .           T(3,3)
      COMMON/EMTX/ LM(24),NC,NS,ASA(24,24),P(24,4),XM(24),SA(12,24),
     .             SF(12,4),CCF,SCF,CAP,TG,STIE,SYTIE,SIMP,NTIE,XTIE(6),
     .             TRACE,C,DETIE,SJ,KO(6),S(12,12),F(48),TTT(72)
      COMMON/JUNK/ SQ,TSC,CSC,SSQ,A(6,6),DA(12,12)
      EQUIVALENCE (ENPAR,COF),(AT,TTT),(T,TTT(37))
C
C     FORM 3-D STIFFNESSES FOR EXPANSION JOINT ELEMENTS
C
      DO 5 I=1,1346
    5 LM(I)=0.
      NC=12
      NS=12
      NE=0
      WRITE(6,2000) NEXPJ ,NSTIF,NUMNPAR
C
C     READ AND PRINT LINEAR SPRING STIFFNESS SETS
C
      READ(5,1040) (N,(STIF(N,J),J=1,6),N=1,NSTIF)
      WRITE(6,2030)
      WRITE(6,2040) (N,(STIF(N,J),J=1,6),N=1,NSTIF)
C
C     READ AND PRINT NONLINEAR ELEMENT PARAMETERS
C
      IF (NUMNPAR.EQ.0) GO TO 9
      READ(5,1010) (N,(ENPRCP(N,J),J=1,7),NT(N),(XT(N,J),J=1,6),
     .             N=1,NUMNPAR)
      WRITE(6,2001)
      WRITE(6,2002) (N,(ENPRCP(N,J),J=1,7),N=1,NUMNPAR)
      WRITE(6,2003)
      WRITE(6,2004) (N,NT(N),(XT(N,J),J=1,6),N=1,NUMNPAR)
    9 CONTINUE
C
C     READ AND PRINT ELEMENT DATA---DATA NEED TO BE SUPPLIED FOR EACH
C
      WRITE(6,2010)
   10 NE=NE+1
      READ(5,1030) INE,NI,NJ,NK,NL,KC,JS,MS,NINC,D,SQ,TRACE
      IF (NINC.GT.NUMNPAR) CALL ERROR (3,INE,7HEXPLB   )
      IF (INC.NE.NE) CALL ERROR (4,INE,7HEXPJB   )
      IF (TRACE.EQ.0.) TRACE=1.0E+10
      WRITE(6,2020) NE,NI,NJ,NK,NL,KC,JS,MS,NINC,D,SQ,TRACE
C
C     FORM EXPANSION JOINT TO LOCAL COORDINATE
C
      IF (SQ.EQ.0.) GO TO 20
      SQ=SQ*3.1415927/180.
      TSC=TAN(SQ)
      CSC=COS(SQ)
      SSC=SIN(SQ)
      GO TO 21
```

```
   20 SC=0.
      TSC=0.0
      CSC=1.0
      SSC=0.0
   21 DO 25 I=1,6
      DO 25 J=1,6
   25 A(I,J)=0.
C
      A(1,1)=1.
      A(1,6)=0.5*D
      A(2,2)=1.
      A(3,3)=1.
      A(3,4)=-A(1,6)
      A(3,5)=0.5*C*TSQ
      A(4,1)=1.
      A(4,6)=-A(1,6)
      A(5,5)=1.0/CSQ
      A(6,3)=1.0
      A(6,4)=A(1,6)
      A(6,5)=-A(3,5)
C
C     FORM LOCAL TO GLOBAL TRANSFORMATION
C
      DX=X(NL)-X(NI)
      DY=Y(NL)-Y(NI)
      DZ=Z(NL)-Z(NI)
      CL=SQRT(DX*DX+DY*DY+DZ*DZ)
      IF (CL) 55,55,60
   55 CALL ERROR (5,NE,7HEXPJB   )
C
   60 AX=X(NK)-X(NI)
      AY=Y(NK)-Y(NI)
      AZ=Z(NK)-Z(NI)
      BX=AY*DZ-AZ*DY
      BY=AZ*DX-AX*DZ
      BZ=AX*DY-AY*DX
      BB=SQRT(BX*BX+BY*BY+BZ*BZ)
      IF (BB) 65,65,70
   65 CALL ERROR (6,NE,7HEXPJB   )
C
   70 T(3,1)=BX/BB
      T(3,2)=BY/BB
      T(3,3)=BZ/BB
      AA=SQRT(AX*AX+AY*AY+AZ*AZ)
      IF (AA) 65,65,80
   80 T(2,1)=-AX/AA
      T(2,2)=-AY/AA
      T(2,3)=-AZ/AA
      T(1,1)=T(2,2)*T(3,3)-T(2,3)*T(3,2)
      T(1,2)=T(2,3)*T(3,1)-T(2,1)*T(3,3)
      T(1,3)=T(2,1)*T(3,2)-T(2,2)*T(3,1)
C
C     FORM JOINT TO GLOBAL TRANSFORMATION
C
      DO 90 I=1,36
   90 AT(I)=0.
      DO 100 LA=1,6,3
      LB=LA+2
      DO 100 MA=1,6,3
      MB=MA-1
      DO 100 I=LA,LB
      DO 100 JM=1,3
      J=JM+MB
      XX=0.
      DO 95 K=1,3
      XX=XX+A(I,K+MB)*T(K,JM)
   95 CONTINUE
  100 AT(I,J)=XX
C
C     FORM LOCAL TO EXPANSION JOINT COORDINATE
C
      DO 56 I=1,36
   56 A(I)=0.0
      A(1,1)=0.5
      A(1,6)=1.0/D
      A(2,2)=1.0
      A(3,3)=0.5
      A(3,4)=-1.0/D
      A(4,1)=0.5
      A(4,6)=-1.0/D
      A(5,4)=SSC
      A(5,5)=CSC
      A(6,3)=0.5
      A(6,4)=1.0/D
C
C     FORM JOINT STIFFNESS MATRIX IN LOCAL COORDINATE SYSTEM
C
      DO 101 I=1,144
  101 S( )=0.0
      DO 110 I=1,6
      J=KD(I)+1
      GO TO (110,111,112) J
  111 S( ,I)=TRACE
      S(I+6,I)=-TRACE
      S(I,I+6)=-TRACE
      S(I+6,I+6)=TRACE
      GO TO 110
  112 S(I,I)=STIF(MS,I)
      S(I+6,I)=-STIF(MS,I)
      S(I,I+6)=-STIF(MS,I)
      S(I+6,I+6)=STIF(MS,I)
  110 CONTINUE
C
C     FORM JOINT GLOBAL STRESS MATRIX
C
      DO 120 I=1,144
  120 DA(I)=0.0
      DO 150 LA=1,10,3
      LB=LA+2
      DO 150 MA=1,10,3
      MB=MA-1
      DO 150 I=LA,LB
```

```
      DO 150 JM=1,3
      J=JM+MB
      XX=0.0
      DO 151 K=1,3
  151 XX=XX+S(I,K+MB)*T(K,JM)
  150 DA(I,J)=XX
C
      DO 149 I=1,288
  149 SA(I)=0.0
      DO 130 LA=1,12,6
      LB=LA-1
      DO 130 MA=1,12,6
      MB=MA+5
      DO 130 IL=1,6
      I=IL+LB
      DO 130 J=MA,MB
      XX=0.0
      DO 135 K=1,6
  135 XX=XX+A(IL,K)*DA(K+LB,J)
  130 SA(I,J)=XX
C
C     FORM JOINT STIFFNESS MATRIX IN GLOBAL COORDINATE
C
      DO 161 I=1,576
  161 ASA(I)=0.0
      DO 162 LA=1,10,3
      LB=LA-1
      DO 162 MA=1,10,3
      MB=MA+2
      DO 162 IL=1,3
      I=IL+LB
      DO 162 J=MA,MB
      XX=0.0
      DO 163 K=1,3
  163 XX=XX+T(K,IL)*DA(K+LB,J)
  162 ASA(I,J)=XX
C
C     FORM ELEMENT LOCATION MATRIX
C
      DO 170 I=1,6
      LM(I)=ID(NI,I)
      LM(I+6)=ID(NJ,I)
      LM(I+12)=0
  170 LM(I+18)=0
C
C     WRITE ELEMENT INFORMATION ON TAPE
C
      CALL WRITET (MBAND,NDIF)
C
C     SET NONLINEAR ELEMENT INDICATOR AND STORE NONLINEAR PARAMETERS
C
      NN=NUMEL+NE
      IF (NINO.EQ.0) GO TO 200
      INC(NN)=5
      DO 180 I=1,7
  180 ENPAR(I)=ENPROP(NINC,I)
      NTIE=NT(NINO)
      DO 190 I=1,6
  190 XTIE(I)=XT(NINO,I)
      UETIE=SYTIE/STIE
      SJ=JS
      MTYPE=5
      WRITE (3) MTYPE,LM,ND,NS,ASA,SA,S,ENPAR,TTT
      GO TO 250
  200 INC(NN)=-5
C
  250 IF (NE.LT.NEXPJ) GO TO 10
      RETURN
C
 1010 FORMAT (I5,7F10.0,I5/ 6F10.0)
 1030 FORMAT (5I5,4X,6I1,3I5,3F10.0)
 1040 FORMAT (I5,6F10.0)
 2000 FORMAT (31H1.....EXPANSION JOINT ELEMENTS    ///
     .  29H NUMBER OF ELEMENTS           =  I5//
     .  29H NUMBER OF STIFFNESS SETS     =   I5 //
     .  29H NUMBER OF N/L PAR. SETS      =  I5)
 2001 FORMAT (53H1NONLINEAR PARAMETERS OF EXPANSION JOINT ELEMENTS....//
     .  4HNPAR 6X 8HFRICTION 4X 8HFRICTION 5X 4HSEAT 7X 3HTIE 7X 3HTIE
     .  8X 9HTIE YIELD 6X 6HIMPACT / 3HNO. 7X 6HCOEFF. 6X 9HSTIFFNESS
     .  4X 3HCAP 8X 3HGAP 8X 5HSTIFF 6X 5HFORCE 10X 6HSPRING )
 2002 FORMAT (I5,7E12.3)
 2003 FORMAT (////20H JOINT TIE BARS.....  //
     .  56H NPAR  NUMBER      TIE POSITIONS RELATIVE TO JOINT CENTER    /
     .  59H  NO.  OF TIES    1         2         3         4         5         6  )
 2004 FORMAT (I5,I5,3X,6F8.3)
 2010 FORMAT (////34H EXPANSION JOINT ELEMENT DATA.....  //
     .  5H ELEM 8X 4HNODE 11X 6H JOINT 3X 5HJOINT 3X 6HSPRING 2X 3HN/L
     .  8H    JOINT 8H     SKEW 8H    JOINT /
     .  5H  NO. 4X 1HI,4X 1HJ 4X 1HK 4X 1HL 3X 5H CODE 5X 4HSIGN 3X
     .  6HSET NO 5H   INC 8H     WIDTH 5H     ANGLE 2X 9HSTIFFNESS  /)
 2020 FORMAT (5I5,4X,6I1,2X ,3I6,2F9.3,E12.3)
 2030 FORMAT (4H1SET 20X 32HSTIFFNESSES OF EXPANSION SPRINGS /
     .  4H  NO   4X 2HR1 10X 2HR2 10X 2HR3 10X 2HM1 10X 2HM2 10X 2HM3 /)
 2040 FORMAT (I4,6E12.3)
      END




*DECK NEXPJT
      SUBROUTINE NEXPJT (NEL,NINO)
C
      COMMON/EMTX/ MTYPE,LM(24),ND,NS,ASA(24,24),SA(12,24),S(12,12),
     .              COF,SCF,CAP,TG,STIE,SYTIE,SIMP,NTIE,XTIE(6),TRACE,C,
     .              UETIE,SJ,KD(6),A(6,6),T(3,3),PTIE,KKO(6),TTT(20),
     .              ASSA(24,24),SSA(12,24),OF(24),F(6),FT(6),U(6),
     .              UPTIE(6)
```

```
      CCMMCN/NEM / EX(24),EX1(24),OEX(24),DFF(12),OP(12),EXJ(12),
     .             EXJ1(12),SS(12,12),U1(6),TK(6),EFI(12)
      CCMMCN/COLB/ USP(10,2),USPF(1C,2),KF(6),LPSLIP(2)
      DIMENSICN EFL(12)
C
      DO  2 I=1,NO
      OP(I)=0.
      DF(I)=0.
      EFL(I)=0.
    2 EFI(I)=0.
      DC 5 I=1,2
    5 UPSLIP(I)=USP(NEL,I)
C
C     COMPUTE RELATIVE DISPLACEMENT IN JCINT CCCRDINATE
C
      DC 20 LA=1,12,6
      LB=LA+5
      MB=LA-1
      DO 20 I=LA,LB
      II=I-MB
      EXJ(I)=0.
      DC 15 KK=1,6
      K=KK+MB
   15 EXJ(I)=EXJ(I)+A(II,KK)*EX(K)
   20 CONTINUE
      DO 50 I=1,6
   50 U(I)=EXJ(I+6)-EXJ(I)
      WRITE(6,9000) (U (I),I=1,6)
 9000 FORMAT(1H ,25X,6E15.6)
C
C     CCMPLTE JOINT FORCE IN JOINT CCORDINATE
C
      DC 80 I=1,6
      XX=0.
      DO 75 J=1,ND
   75 XX=XX+SA(I,J)*CEX(J)
   80 F(I)=F(I)+XX
C
C     CCMPUTE NEW JOINT STIFFNESS MATRIX IN GLCBAL CCCRDINATE
C
      CALL NXPJT (NIND)
C
C     CCMPUTE NCNLINEAR RESTORING FORCE
C
      IF (NINC.EQ.D) GO TC 185
      K=D
      DO 175 I=1,6,3
      KK=KKD(I)+2
      GO TC (170,175,16C,175) KK
  160 IF (NTIE.EQ.0) GO TC 175
      IF (K.NE.D) GO TO 175
      K=1
      FAX=0.
      FBX=0.
      DO 165 J=1,NTIE
      FAX=FAX+FT(J)*(0.5-XTIE(J)/D)
  165 FBX=FBX+FT(J)*(0.5+XTIE(J)/D)
      EFL(1)=EFL(1)-FAX
      EFL(4)=EFL(4)-FBX
      GO TC 175
  170 EFL(I)=EFL(I)-SIMP*(U(I)+GAP)
  175 CONTINUE
      DO 180 I=1,6,3
  180 EFL(I+6)=-EFL(I)
  185 CONTINUE
C
C     CCMPLTE COULOMB FRICTICNAL FORCE
C
      IF (CCF.LE.0.) GO TO 250
      DC 230 I=1,6,3
      J=I+2
      IF (SJ*F(J).LE.D.) GO TO 230
      UESLIP=COF*ABS(F(J))/SCF
      II=I/3+1
      KK=KF(I)+2
      GO TC (200,205,210) KK
  200 CP(I)= COF*ABS(F(J))
      USP(NEL,II)=U(I)+UESLIP
      GO TC 230
  205 CP(I)=-SCF*(U(I)-UPSLIP(II))
      GC TC 230
  210 DP(I)=-COF*ABS(F(J))
      USP(NEL,II)=U(I)-UESLIP
  230 CONTINUE
      DO 240 I=1,6,3
  240 CP(I+6)=-OP(I)
  250 CONTINUE
C
C     TRANSFCRM RESTORING AND FRICTICNAL FORCE TO GLOBAL COORDINATE
C
      DO 300 LA=1,12,6
      LB=LA-1
      DC 300 IL=1,6
      I=IL+LB
      XX=0.
      YY=0.
      DO 255 K=1,6
      IF (A(K,IL).EQ.0.) GO TO 255
      XX=XX+A(K,IL)*CP(K+LB)
      YY=YY+A(K,IL)*EFL(K+LB)
  255 CONTINUE
      OF(I)=XX
  300 EFI(I)=YY
C
      RETURN
      END
```

```
*DECK NXPJT
      SUBROUTINE NXPJT (NIND)
C
      COMMON/EMTX/ MTYPE,LP(24),NC,NS,ASA(24,24),SA(12,24),S(12,12),
     .             COF,SCF,GAP,TG,STIE,SYTIE,SIMP,NTIE,XTIE(6),TRACE,D,
     .             UETIE,SJ,KD(6),A(6,6),T(3,3),PTIE,KKD(6),TTT(20),
     .             ASSA(24,24),SSA(12,24),OF(24),F(6),FT(6),U(6),
     .             UPTIE(6)
      COMMON/NEW / EEEE(72),CFF(12),CP(12),EXJ(12),EXJ1(12),SS(12,12),
     .             U1(6),TK(6)
      COMMON/COLB/ USP(10,2),USPF(10,2),KF(6),UPSLIP(2)
C
      DO 10 I=1,6
      FT(I)=0.
      KF(I)=0
   10 TK(I)=0.
C
C     CHECK JOINT CONDITION
C
      PTIE=1000.
      IF (NTIE.EQ.0) GO TO 25
      DO 20 I=1,NTIE
      IF (PTIE.GT.UPTIE(I)) PTIE=UPTIE(I)
   20 CONTINUE
   25 PTIE=PTIE+TG
C
      KKD(1)=KD(1)
      KKD(4)=KD(1)
C
      DO 30 I=1,6,3
      II=I/3+1
      IF (U(I).LT.-GAP) KKD(I)=-1
      IF (U(I).GT.PTIE) KKD(I)= 1
      UESLIP=COF*ABS(F(I+2))/SCF
      XX=UPSLIP(II)+UESLIP
      YY=UPSLIP(II)-UESLIP
      IF (U(I).GT.XX) KF(I)=1
      IF (U(I).LT.YY) KF(I)=-1
   30 CONTINUE
C
C     COMPUTE TIE STIFFNESSES
C
      TAA=0.
      TAB=0.
      TBB=0.
      IF (NTIE.EQ.0) GO TO 60
      DO 50 I=1,NTIE
      XX=(U(1)+U(4))*0.5+XTIE(I)*(U(1)-U(4))/D
      XX=XX-TG
      IF (XX.LT.UPTIE(I)) GO TO 45
      IF (XX-UPTIE(I)-UETIE) 40,40,35
   35 UPTIE(I)=XX-UETIE
      TK(I)=0.
      FT(I)=SYTIE
      GO TO 50
   40 TK(I)=1.0
      FT(I)=STIE*(XX-UPTIE(I))
      GO TO 50
   45 FT(I)=0.
   50 CONTINUE
C
      DO 55 I=1,NTIE
      TKS=TK(I)*STIE
      IF (TKS.EQ.0.) GO TO 55
      TAA=TAA+TKS*(0.5*D-XTIE(I))**2/D**2
      TAB=TAB+TKS*(0.5*D+XTIE(I))*(0.5*D-XTIE(I))/D**2
      TBB=TBB+TKS*(0.5*D+XTIE(I))**2/D**2
   55 CONTINUE
   60 CONTINUE
C
C     FORM NEW NONLINEAR STIFFNESS MATRIX IN JOINT COORDINATE
C
      DO 65 I=1,144
   65 SS(I)=0.
C
C     1. CONTRIBUTION FROM COULOMB FRICTIONAL FORCE
C
      NINF=0
      IF (COF.LE.0.) GO TO 85
      DO 80 I=1,6,3
      IF (SJ*F(I+2).LE.0.) GO TO 80
      IF (KF(I)) 80,75,80
   75 SS(I,I)=SS(I,I)+SCF
      NINF=1
   80 CONTINUE
   85 CONTINUE
C
C     2. CONTRIBUTION FROM TIE BAR AND/OR IMPACT SPRING
C
      DO 90 I=1,6,3
      IF (KKD(I).NE.KD(1)) GO TO 100
   90 CONTINUE
      NIND=0
      GO TO 130
  100 K=0
      NIND=1
      DO 120 I=1,6,3
      KK=KKD(I)+2
      GO TO (110,120,115,120) KK
  110 SS(I,I)=SS(I,I)+SIMP
      GO TO 120
  115 IF (K.NE.0) GO TO 120
      K=1
      SS(1,1)=SS(1,1)+TAA
      SS(1,4)=SS(1,4)+TAB
      SS(4,1)=SS(4,1)+TAB
      SS(4,4)=SS(4,4)+TBB
  120 CONTINUE
  130 CONTINUE
C
      IF (NIND.EQ.1.OR.NINF.EQ.1) GO TO 200
      DO 150 I=1,576
```

```
  150 ASSA(I)=ASA(I)
      DO 160 I=1,288
  160 SSA(I)=SA(I)
      RETURN
  200 CONTINUE
C
      DO 250 LA=1,12,6
      LB=LA+5
      DO 250 MA=1,12,6
      MB=MA+5
      IF (LA.EQ.1.AND.MA.EQ.1) GO TO 250
      SIGN=-1.
      IF (LA.EQ.7.AND.MA.EQ.7) SIGN=1.
      DO 240 I=LA,LB
      II=I-LA+1
      DO 240 J=MA,MB
      JJ=J-MA+1
      SS(I,J)=SIGN*SS(II,JJ)
  240 CONTINUE
  250 CONTINUE
C
C     TRANSFORM TO GLOBAL COORDINATE SYSTEM
C
      DO 310 I=1,288
  310 SSA(I)=0.
      DO 330 LA=1,12,6
      LB=LA+5
      DO 330 MA=1,12,6
      MB=MA-1
      DO 330 I=LA,LB
      DO 330 JM=1,6
      J=JM+MB
      XX=0.
      DO 325 K=1,6
      IF (SS(I,K+MB).EQ.0..OR.A(K,JM).EQ.0.) GO TO 325
      XX=XX+SS(I,K+MB)*A(K,JM)
  325 CONTINUE
  330 SSA(I,J)=XX
C
      DO 351 I=1,576
  351 ASSA(I)=0.
      DO 360 LA=1,12,6
      LB=LA-1
      DO 360 MA=1,12,6
      MB=MA+5
      DO 360 IL=1,6
      I=IL+LB
      DO 360 J=MA,MB
      XX=0.
      DO 355 K=1,6
      IF (A(K,IL).EQ.0..OR.SSA(K+LB,J).EQ.0.) GO TO 355
      XX=XX+A(K,IL)*SSA(K+LB,J)
  355 CONTINUE
  360 ASSA(I,J)=XX
C
C     COMBINE LINEAR AND NONLINEAR STIFFNESS MATRIX
C
      DO 400 I=1,24
      DO 400 J=1,24
      IF (ASA(I,J).EQ.0.) GO TO 400
      ASSA(I,J)=ASSA(I,J)+ASA(I,J)
  400 CONTINUE
      DO 410 I=1,12
      DO 410 J=1,24
      IF (SA(I,J).EQ.0.) GO TO 410
      SSA(I,J)=SSA(I,J)+SA(I,J)
  410 CONTINUE
C
      RETURN
      END
```


☆U.S. GOVERNMENT PRINTING OFFICE: 1977 728-327/1202 1-3

FHWA
R&D